Towards vaccines and therapeutic antibodies against *Clostridium difficile* based on synthetic glycans

Inaugural-Dissertation
to obtain the academic degree
Doctor rerum naturalium (Dr. rer. nat.)

submitted to the Department of Biology, Chemistry and Pharmacy
of Freie Universität Berlin

by

Felix Bröcker

from Berlin, Germany

June 2016

This work was performed between January 2012 and June 2016 under the guidance of Prof. Dr. Peter H. Seeberger in the Department of Biomolecular Systems, Max Planck Institute of Colloids and Interfaces Potsdam, and the Institute of Chemistry, Biochemistry and Pharmacy, Freie Universität Berlin.

1. Reviewer: Prof. Dr. Peter H. Seeberger

2. Reviewer: Prof. Dr. Rudolf Tauber

Date of the oral defense: 06.10.2016

Acknowledgements

First and foremost I like to express my gratitude to Prof. Peter H. Seeberger for providing the opportunity to perform my PhD studies in the inspirational and challenging research environment of the Biomolecular Systems Department, for his continuous generous support, excitement and invaluable input. I furthermore like to thank Dr. Chakkumkal Anish for his ideas and his kind supervision during the first three years of my PhD work.

I am grateful to Prof. Rudolf Tauber for kindly agreeing to review this thesis.

This thesis would not have come into being without the synthetic *Clostridium difficile* glycans that were kindly supplied by Dr. Christopher Martin and Dr. Ju Yuel Baek. I also like to acknowledge the great support of Annette Wahlbrink in generating the monoclonal antibodies that were crucial for this work.

I would like to thank present and former colleagues of the Max Planck Institute of Colloids and Interfaces (MPICI) for fruitful collaborations and valuable scientific input, especially Dr. Claney L. Pereira for coordinating and guiding glycan synthesis and vaccine projects, Prof. Laura Hartmann and Dr. Felix Wojcik for the synthesis of oligo(amidoamine)s, Dr. Christoph Rademacher, Jonas Aretz und Jonas Hanske for the NMR studies with monoclonal antibodies, Dr. Daniel Kolarich and Uwe Möginger for helpful advice on mass spectrometry and an exciting collaboration on glycoconjugate analysis, Dr. You Yang for providing *Yersinia pestis* oligosaccharides, Prof. Bernd Lepenies for helpful advice on animal ethics, Dr. Benjamin Schumann for kind help with glycoconjugate synthesis, Dr. Sharavathi Guddehali Parameswarappa and Dr. Adam Calow for supplying synthetic antigens of *Streptococcus pneumoniae* and Dr. Jonathan Hudon for a fascinating project on fully synthetic vaccines.

The efforts and input by my collaborators of other institutes are gratefully acknowledged; Prof. Jochen Mattner, Julia Komor and Erik Wegner of the Unversität Erlangen for providing clinical specimens of *C. difficile* patients, for performing the challenge studies and for kindly assisting in the *in vitro* assays with viable *C. difficile* bacteria, Dr. Karl Andersson of Ridgeview Diagnostics, Uppsala, Sweden, for performing Interaction Map analyses, Dr. Uwe Bierfreund and Dr. Vanya Uzunova of GE Healthcare, Uppsala, Sweden, for kind support with surface plasmon resonance measurements, Prof. Markus Wahl and Nicole Holton of the Freie Universität Berlin for providing access to and help with their isothermal titration calorimetry device, Prof. Regine Heilbronn and Dr. Mario Mietzsch of Charité Medical School, Berlin, for an exciting collaboration on adeno-associated viruses, Prof. Roland Brock and Rike Wallbrecher of the Radboud University Nijmengen, The Netherlands, for a fruitful cooperative work on cell-penetrating peptides, Prof. Liise-anne Pirofski and Prof. Johanna Rivera, Albert Einstein College of Medicine, New York, USA, as well as Dr. Leif Sander of Charité Medical

School for fascinating collaborations on *S. pneumoniae*, Dr. Ulrich Nübel of the Robert-Koch-Institut, Wernigerode, and Dr. Jochen Klumpp of the ETH Zurich, Switzerland, for providing various bacterial strains, the staff of Octapharma AG, Berlin, especially Dr. Guido Kohla, for kindly providing access to their MALDI-TOF mass spectrometer and the coworkers of Vaxxilon GmbH, Berlin, for on-going cooperations on vaccines against *C. difficile*. I would like to express my deepest gratitute to Prof. Werner Reutter of the Freie Universität Berlin who sadly passed away in May of 2016. His passion of science and generous spirit have been truly inspiring and will stay remembered. I also thank the members of his group, Paul Robin Wratil, Yujing Yao, Dr. Long Duc Nguyen and Hoang Giang Nguyen for exciting cooperations and valuable scientific input.

I would like to thank all my present and former colleagues of the Department of Biomolecular Systems not only for valuable advice on scientific questions but also for contributing to a highly enjoyable working atmosphere, especially Dr. Anika Reinhardt, Andreas Geissner, Dr. Reka Kurucz, Dr. Sebastian Götze, Dr. Stefan Matthies, Dr. Markus Weishaupt, Dr. Nahid Azzouz, Eike Wamhoff, Stephanie Zimmermann, Timo Johannssen, Dr. Julia Hütter, Theresa Wagner, Uwe Vogel, Melanie Leddermann, Dr. Bopanna Monnanda Ponnappa, Katrin Sellrie, Jonnel Jaurigue, Paulina Kaplonek, Dr. Chian-Hui Lai, Dr. Chien-Fu Liang and Dr. Ursula Neu.

The kind organizational assistance of Dorothee Böhme is gratefully acknowledged.

I highly appreciate the valuable input on animal ethics and practical work by Dr. Uwe Klemm and Dr. Gesa Rausch of the Max Planck Institute for Infection Biology, Berlin, as well as by Susanne Eisenschmidt of the MPICI.

I am indebted to Prof. Karin Moelling for being an outstanding and generous mentor, for exciting and inspirational discussions and for her continuous invaluable help with scientific and non-scientific issues.

The generous financial support by the Max Planck Society is gratefully acknowledged.

Finally, I would like to thank my family and friends for the faith and support during this most fascinating and instructive period of my life.

List of Publications

A. Scientific Publications and Reviews

1. Broecker F, Seeberger PH. 2016. Synthetic glycan microarrays. *Methods Mol Biol* (accepted manuscript).
2. Broecker F, Martin CE, Wegner E, Mattner J, Baek JY, Pereira CL, Anish C, Seeberger PH. 2016. Synthetic lipoteichoic acid glycans are potential vaccine candidates to protect from *Clostridium difficile* infections. *Cell Chem Biol* **23:** 1014–1022. DOI: http://dx.doi.org/10.1016/j.chembiol.2016.07.009
3. Broecker F, Hanske J, Martin CE, Baek JY, Wahlbrink A, Wojcik F, Hartmann L, Rademacher C, Anish C, Seeberger PH. 2016. Multivalent display of minimal *Clostridium difficile* glycan epitopes mimics antigenic properties of larger glycans. *Nat Commun* **7:** 11224. DOI: http://dx.doi.org/10.1038/ncomms11224
4. Möginger U, Resemann A, Martin C, Parameswarappa S, Govindan S, Wamhoff E, Broecker F, Suckau D, Pereira CL, Anish C, Seeberger PH, Kolarich D. 2016. Cross Reactive Material 197 glycoconjugate vaccines contain privileged conjugation sites. *Sci Rep* **6:** 20488. DOI: http://dx.doi.org/10.1038/srep20488
5. Broecker F, Anish C, Seeberger PH. 2015. Generation of monoclonal antibodies against defined oligosaccharide antigens. *Methods Mol Biol* **1331:** 57–80. DOI: http://dx.doi.org/10.1007/978-1-4939-2874-3_5
6. Wallbrecher R, Verdurmen WPR, Schmidt S, Bovee-Geurts PH, Broecker F, Reinhardt A, Seeberger PH, van Kuppevelt TH, Brock R. 2014. The stoichiometry of peptide-heparan sulfate binding as a determinant of uptake efficiency of cell-penetrating peptides. *Cell Mol Life Sci* **71:** 2717–2729. DOI: http://dx.doi.org/10.1007/s00018-013-1517-8
7. Broecker F, Aretz J, Yang Y, Hanske J, Guo X, Reinhardt A, Wahlbrink A, Anish C, Seeberger PH. 2014. Epitope recognition of antibodies against a *Yersinia pestis* lipopolysaccharide trisaccharide component. *ACS Chem Biol* **9:** 867–873. DOI: http://dx.doi.org/10.1021/cb400925k
8. Mietzsch M, Broecker F, Reinhardt A, Seeberger PH, Heilbronn R. 2014. Differential adeno-associated virus serotype-specific interaction patterns with synthetic heparins and other glycans. *J Virol* **88:** 2991–3003. DOI: http://dx.doi.org/10.1128/JVI.03371-13

9. Martin CE, Broecker F, Eller S, Oberli MA, Anish C, Pereira CL, Seeberger PH. 2013. Glycan arrays containing synthetic *Clostridium difficile* lipoteichoic acid oligomers as tools toward a carbohydrate vaccine. *Chem Commun* **49:** 7159-7161. DOI: http://dx.doi.org/10.1039/c3cc43545h

10. Martin CE,* Broecker F,* Oberli MA, Komor J, Mattner J, Anish C, Seeberger PH. 2013. Immunological evaluation of a synthetic *Clostridium difficile* oligosaccharide conjugate vaccine candidate and identification of a minimal epitope. *J Am Chem Soc* **135:** 9713–9722. DOI: http://dx.doi.org/10.1021/ja401410y (*equal contribution)

B. Patents

1. Rathwell D, Parameswarappa SG, Govindan S, Broecker F, Anish C, Pereira CL, Seeberger PH. Protein and peptide-free synthetic vaccines against Streptococcus pneumoniae type 3. PCT number: PCT/EP2014/069947.

2. Seeberger PH, Martin CE, Broecker F, Anish C. Oligosaccharides and oligosaccharide-protein conjugates derived from Clostridium difficile polysaccharide PS-I, methods of synthesis and uses thereof, in particular as vaccines and diagnostic tools. PCT number: PCT/EP2012/003240.

C. Scientific Conferences and Symposia

1. Vaccine potential of synthetic *Clostridium difficile* glycans (Poster). GLYCO^{23} 23rd International Symposium on Glycoconjugates, Split, Croatia, 2015.

2. Synthetic glycan antigens as vaccine candidates against *Clostridium difficile* (Oral presentation). The Fourth Symposium – RIKEN-Max Planck Joint Research Center, Kobe, Japan, 2015.

3. Immune responses to surface carbohydrates from *Clostridium difficile* (Oral presentation). Ringberg Conference on Chemistry and Biology of Carbohydrate Vaccines, Ringberg Castle, Rottach-Egern, Germany, 2013.

4. Synthetic glycans as vaccine candidates against *Clostridium difficile* (Poster and oral presentation). 24th Joint Glycobiology Meeting, Wittenberg, Germany, 2013.

5. Epitope mapping of synthetic carbohydrate antigens from *Clostridium difficile* and immunological evaluation of oligosaccharide conjugate vaccines (Poster). 9th Molecular Interactions Workshop Next Generation Biotechnology, Berlin, Germany, 2013.

6. Immunological evaluation of a synthetic *Clostridium difficile* oligosaccharide conjugate vaccine candidate and identification of a minimal epitope (Poster). The 7th Glycan Forum, Berlin, Germany, 2013.

Contents

List of Abbreviations

Alum	Aluminum hydroxide gel adjuvant
APC	Allophycocyanin dye or antigen-presenting cell
APS	Ammonium persulfate
ATCC	American Type Culture Collection
BCA	Bicinchoninic acid
BCR	B cell receptor
BM	Bone marrow
BMDC	Bone marrow-derived dendritic cell
BSA	Bovine serum albumin
CD	Cluster of differentiation
CDI	*Clostridium difficile* infection
CDT	*Clostridium difficile* binary toxin
CFA	Complete Freund's adjuvant
CFUs	Colony-forming units
COSY	Correlation spectroscopy
CRM_{197}	Cross-reactive material-197
Da	Dalton
DC	Dendritic cell
DHAP	2,5-Dihydroxyacetophenone
DMEM	Dulbecco's Modified Eagle Medium
DMF	*N*,*N*-Dimethylformamide
DMSO	Dimethylsulfoxide
DNAP	Di-*p*-nitrophenyl adipate
DPBS	Dulbecco's Phosphate-Buffered Saline
DSAP	Di-*N*-succinimidyl adipate
DSMZ	Deutsche Sammlung von Mikroorganismen und Zellkulturen
DT	Diphtheria toxin
ECM	Extracellular matrix
EDTA	Ethylenediaminetetraacetic acid
ELISA	Enzyme-linked immunosorbent assay
ExoA	Exotoxin A
FA	Freund's adjuvant
FBS	Fetal bovine serum
Fc	Fragment crystallizable
FcRn	Neonatal Fc receptor
FDA	Food and Drug Administration
FITC	Fluorescein isothiocyanate
FMT	Fecal microbiota transplantation
FPLC	Fast protein liquid chromatography
GM-CSF	Granulocyte macrophage colony-stimulating factor
Gro	Glycerol
GroA	Glyceric acid
GroP	Glycerol phosphate
GSL	Glycosphingolipid
HAT	Hypoxanthine, aminopterin and thymidine

HRP	Horseradish peroxidase
HSA	Human serum albumin
ICFA	Incomplete Freund's adjuvant
IgA, IgG, IgM	Immunoglobulin A, G, M
IL	Interleukin
IM	Interaction Map
i. p.	Intraperitoneal(ly)
i. r.	Intrarectal(ly)
ITC	Isothermal titration calorimetry
IVC	Individually ventilated cage
IVIG	Intravenous Immunoglobulins
k_a	Association constant
k_d	Dissociation constant
K_D	Equilibrium constant
kDa	Kilodalton
Kdo	3-Deoxy-D-*manno*-oct-2-ulosonic acid
LPS	Lipopolysaccharide
LTA	Lipoteichoic acid
LTB	Heat-labile enterotoxin
mAb	Monoclonal antibody
mAU	Milli absorbance units
MALDI-TOF MS	Matrix-assisted laser desorption/ionization with time-of-flight mass spectrometry
MBL	Mannan-binding lectin
MenA, -C, -W, -Y	*Neisseria meningitidis* serogroup A, C, W, Y
MFI	Mean fluorescence intensity
MHC	Major histocompatibility complex
MPICI	Max Planck Institute of Colloids and Interfaces
MRSA	Methicillin-resistant *Staphylococcus aureus*
NEAA	Non-essential amino acids
NHS	*N*-hydroxysuccinimide
NKT cell	Natural killer T cell
NMR	Nuclear magnetic resonance
NOE	Nuclear Overhauser Effect
NOESY	Nuclear Overhause Enhancement Spectroscopy
OAA	Oligo(amidoamine)
OD_{600}	Optical density at 600 nm
OPA	Opsonophagocytosis assay
PBMC	Peripheral blood mononuclear cell
PBS	Phosphate-buffered saline
PE	Phycoerythrin
PEG	Polyethylene glycol
Pen/Strep	Penicillin/Streptomycin
pIgR	Polymeric imunoglobulin receptor
PMT	Photomultiplier tube
ppm	Parts per million
PS-I/-II/-III	Polysaccharide-I/-II/-III
PTFE	Polytetrafluoroethylene
PVDF	Polyvinylidene difluoride

ROS	Reactive oxygen species
RPMI	Roswell Park Memorial Institute
RT	Ribotype
RU	Response units
s. c.	Subcutaneous(ly)
SD	Standard deviation
SDS-PAGE	Sodium dodecyl sulfate polyacrylamide gel electrophoresis
SEM	Standard error of the mean
SLP	S-layer protein
sIGA	Secreted Immunoglobulin A
SPF	Specific pathogen-free
SPR	Surface plasmon resonance
STD-NMR	Saturation transfer difference-NMR
TA	Teichoic acid
TBS	Tris-buffered saline
TcdA	*Clostridium difficile* toxin A
TcdB	*Clostridium difficile* toxin B
TCR	T cell receptor
TEMED	*N*,*N*,*N'*,*N'*-Tetramethylethylenediamine
TFA	Trifluoroacetic acid
Th cell	T helper cell
THF	Tetrahydrofuran
TLC	Thin-layer chromatography
TLR	Toll-like receptor
TMB	3,3',5,5'-Tetramethylbenzidine
TNF-α	Tumor necrosis factor-alpha
wk	Week
zTOCSY	Total correlation spectroscopy with z filter

List of Monosaccharides

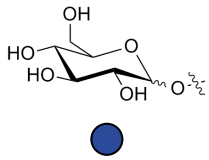

D-Glucose
(D-Glc)

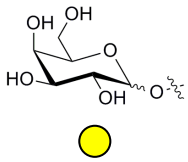

D-Galactose
(D-Gal)

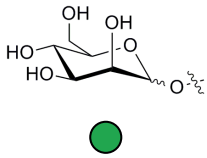

D-Mannose
(D-Man)

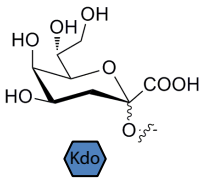

3-Deoxy-D-*manno*-oct-2-ulosonic acid (Kdo)

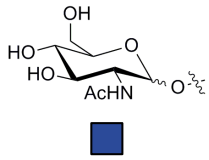

D-*N*-Acetylglucosamine
(D-GlcNAc)

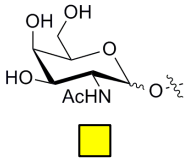

D-*N*-Acetylgalactosamine
(D-GalNAc)

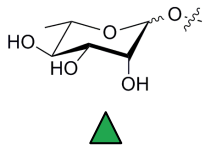

L-Rhamnose
(L-Rha)

Summary

Clostridium difficile is a leading cause of infectious diarrhea and mortality worldwide. Emerging antibiotic resistance has fostered studies on toxin-neutralizing vaccines and therapeutic monoclonal antibodies (mAbs) that limit symptoms but not intestinal colonization by *C. difficile*. Bacterial surface glycans are promising targets for colonization-inhibiting vaccines but are weakly and inconsistently expressed by *C. difficile in vitro*. Their study has recently been facilitated by chemically synthesized glycans. This thesis describes detailed immunological examinations of synthetic glycans of *C. difficile* polysaccharide-I (PS-I) and lipoteichoic acid (LTA) *en route* towards novel vaccines and therapeutic mAbs.

Efforts to ascertain the vaccine potential of the PS-I pentasaccharide repeat unit are described in **Section 1.1**. Microarray-assisted screening of clinical specimens revealed a correlation of pentasaccharide-specific antibody levels with reduced symptoms of *C. difficile* disease, indicative of protective effects. The pentasaccharide elicited T cell-dependent antibody responses in mice when formulated as glycoconjugate with the CRM_{197} protein. Anti-pentasaccharide antibodies localized to the intestine *in vivo* and bound to *C. difficile* bacteria *in vitro*. Vaccination with the glycoconjugate significantly protected mice from experimental *C. difficile* infection.

Section 1.2 describes the identification of a minimal epitope of PS-I. A disaccharide of rhamnose and glucose emerged as the smallest epitope recognized by pentasaccharide-raised murine antibodies, as shown by microarray and surface plasmon resonance (SPR). When formulated as CRM_{197} glycoconjugate, the disaccharide elicited antibodies of comparable quality as the pentasaccharide did. This provided a crucial step towards anti-clostridial vaccines with limited synthetic effort.

In **Section 1.3**, the generation and analysis of anti-PS-I mAbs is described. They were obtained *via* the hybdridoma technique from mice immunized with the pentasaccharide-CRM_{197} glycoconjugate. SPR studies demonstrated nanomolar affinity binding to the pentasaccharide and low-affinity recognition of the disaccharide. Isothermal titration calorimetry revealed that enhanced binding to the pentasaccharide was the result of an entropic gain likely mediated by hydrophobic interactions with rhamnoses. The mAbs recognized *C. difficile* and could protect mice from bacterial disease.

Section 1.4 focuses on efforts towards a fully synthetic vaccine based on oligovalent PS-I disaccharides. Insights gained from glycan-antibody interaction studies allowed for the rational design of a PS-I glycan mimetic intended to elicit protective antibodies. Five disaccharides presented on a synthetic scaffold were highly antigenic and bound by antibodies with five orders of magnitude stronger avidity than monovalent glycans, as shown by SPR. Equipped

with a CRM_{197} T cell epitope, the fully synthetic vaccine candidate elicited antibodies highly specific for the PS-I pentasaccharide in mice. These findings provided proof-of-concept that immunological properties of larger glycans can be resembled by oligovalent display of minimal epitopes.

Section 1.5 describes studies on the vaccine potential of synthetic LTA oligomers. Microarray-assisted screening of patient-derived sera showed that synthetic LTA glycans represent natural epitopes that are likely immunogenic during *C. difficile* infection. Based on these findings, a CRM_{197} glycoconjugate displaying a tetrasaccharide of LTA was synthesized that was immunogenic in mice. *In vivo* challenge studies demonstrated that vaccination with the LTA glycoconjugate could significantly protect mice from *C. difficile* colonization.

In conclusion, this study shows that synthetic PS-I and LTA glycans are promising antigens for colonization-inhibiting vaccines and therapeutic antibodies against *C. difficile*.

Zusammenfassung

Clostridium difficile ist weltweit eine Hauptursache infektiöser Diarrhö und Sterblichkeit. Antibiotikaresistenzen führten zur Untersuchung gegen bakterielle Toxine gerichteter Impfstoffe und monoklonaler Antikörper. Diese lindern Symptome, verhindern aber nicht die intestinale Besiedlung durch *C. difficile*. Bakterielle Oberflächenglykane sind vielversprechende Angriffspunkte für Besiedlungs-inhibierende Impfstoffe, werden vom Erreger *in vitro* jedoch nur schwach produziert. Ihre Untersuchung wurde kürzlich durch chemisch synthetisierte Glykane vereinfacht. Diese Arbeit beschreibt immunologische Untersuchungen synthetischer Glykane des *C. difficile* Polysaccharids PS-I und Lipoteichonsäure (LTA), welche zu neuen Impfstoffen und therapeutischen Antikörpern führen können.

Arbeiten hinsichtlich des Impfstoffpotenzials der Pentasaccharid-Wiederholungseinheit von PS-I sind in Abschnitt 1.1 beschrieben. Mikroarray-basierte Screenings klinischer Proben zeigten eine Korrelation Pentasaccharid-spezifischer Antikörper mit schwächeren Symptomen, was auf eine Schutzwirkung hindeutet. Das Pentasaccharid erzeugte T-Zell-abhängige Antikörperantworten in Mäusen, wenn dieses als Glykokonjugat mit dem CRM_{197}-Protein formuliert wurde. Anti-Pentasaccharid-Antikörper wurden *in vivo* in den Intestinaltrakt transportiert und banden an *C. difficile in vitro*. Impfung mit dem Glykokonjugat schützte Mäuse signifikant vor experimenteller *C. difficile*-Infektion.

Abschnitt 1.2 beschreibt die Identifizierung eines minimalen Epitops von PS-I. Ein Disaccharid aus Rhamnose und Glukose wurde mittels Mikroarray und Oberflächenplasmonresonanzspetroskopie (SPR)-Messungen als kleinstes Epitop, das von Pentasaccharid-erzeugten Mausantikörpern erkannt wird, identifiziert. Das als CRM_{197}-Glykokonjugat formulierte Disaccharid erzeugte in Mäusen Antikörper, die denen gegen das Pentasaccha-rid ähnelten. Dies ist ein wichtiger Schritt hinsichtlich der Entwicklung von Impfstoffen mit limitiertem synthetischen Aufwand.

Abschnitt 1.3 umfasst die Erzeugung und Analyse monoklonaler Antikörper gegen PS-I, die durch die Hybridom-Technik aus mit Pentasaccharid-CRM_{197}-Glykokonjugat immunisierten Mäusen erhalten wurden. SPR-Studien zeigten, dass die Antikörper mit nanomolarer Affinität das Pentasaccharid und mit niedrigerer Affinität das Disaccharid erkennen. Isothermale Titrationskalorimetrie-Messungen ließen eine entropisch bevorzugt Bindung an das Pentasaccharid erkennen, vermutlich erzeugt durch hydrophobe Interaktionen mit Rhamnosen. Die Antikörper erkannten *C. difficile* und schützten Mäuse vor bakterieller Krankheit.

Abschnitt 1.4 legt den Fokus auf Bestrebungen in Richtung eines komplett synthetischen Impfstoffs basierend auf oligovalenten PS-I-Disacchariden. Durch Glykan-Antikörper-

Interaktionsstudien gewonnene Einblicke ermöglichten das rationale Design von PS-I-Glykanmimetika, welche protektive Antikörper hervorrufen sollen. SPR-Studien zeigten, dass fünf auf einem synthetischen Träger präsentierte Disaccharide stark antigen wirksam waren und von Antikörpern mit fünf Größenordnungen stärkerer Avidität als monovalente Glykane gebunden wurden. Mit einem CRM_{197}-T-Zell-Epitop versehen erzeugte der komplett synthetische Impfstoffkandidat in Mäusen Antikörper mit hoher Spezifität gegen das Pentasaccharid. Dies lieferte den Machbarkeitsnachweis, dass immunologische Eigenschaften größerer Glykane durch oligovalente Präsentation minimaler Epitope nachgeahmt werden können.

Abschnitt 1.5 beschreibt Studien hinsichtlich des Impfstoffpotenzials synthetischer LTA-Oligomere. Mikroarray-basiertes Screening von Patientenseren zeigte, dass synthetische LTA-Glykane natürlichen Epitopen entsprechen, die vermutlich während der *C. difficile*-Infektion immunogen wirksam sind. Basierend darauf wurde ein CRM_{197}-Glykokonjugat mit einem LTA-Tetrasaccharid synthetisiert, das in Mäusen immunogen war. *In vivo*-Infektionsversuche zeigten, dass eine Impfung mit dem LTA-Glykokonjugat die *C. difficile*-Besiedlung in Mäusen signifikant verminderte.

Zusammenfassend zeigt diese Studie, dass synthetische PS-I- und LTA-Glykane vielversprechende Antigene für Besiedlungs-inhibierende Impfstoffe und therapeutische Antikörper gegen *C. difficile* sind.

Chapter 1

Introduction

1.1 *Clostridium difficile*

Clostridium difficile is a Gram-positive, obligate anaerobic, rod-shaped and spore-forming bacterium that was first identified in the stool of healthy newborns in 1935.[1–3] Initially labeled *Bacillus difficilis* since isolation and culture was difficult, it was renamed to *Clostridium difficile* in 1960 based on morphologic similarities to other clostridial species.[4] In 1962, *C. difficile* was first described as a pathogen.[5] The bacterium was identified in wounds, abscesses, blood and other body fluids of patients with various diseases. The *C. difficile* isolates were resistant to several antibiotics and highly virulent when injected into guinea pigs that died within few days. Since no bacterial growth was observed in the animals, death was concluded to have been the consequence of yet uncharacterized *C. difficile* toxins.[5]

1.1.1 Disease Epidemiology

In 1978, toxin-producing (toxigenic) *C. difficile* was discovered as causative agent of pseudomembranous colitis, a severe form of colonic inflammation that frequently follows antibiotic treatment.[6–8] Today, toxigenic *C. difficile* is the leading cause of antibiotic-induced, hospital-acquired (nosocomial) colitis and diarrhea in the developed countries.[9] The disease burden now even surpasses that attributed to methicillin-resistant *Staphylococcus aureus* (MRSA).[10] Infection with *C. difficile*, termed CDI, can be asymptomatic but frequently causes symptoms from mild fever to diarrheal colitis and death in severe cases.[2] The main risk factors are comorbidities, use of broad-spectrum antibiotics, hospitalization, immune suppression and advanced age ($>$65 years).[11] In 2013, *C. difficile* caused 250,000 infections, 14,000 deaths and $1 billion in excess medical costs in the US.[12] The total burden to the US economy amounts to

about $8.2 billion annually.[13] Presently, an estimated 5 % of hospitalized patients will acquire CDI, and while most other nosocomial infections such as MRSA are decreasing, *C. difficile* rises continuously.[10] From 2000 to 2007, *C. difficile*-related deaths increased by 400 %.[12] The recent gain in incidence and case-fatality rates of CDI has been attributed to newly emerging hypervirulent *C. difficile* strains characterized by elevated toxin secretion and antibiotic resistance, such as ribotype 027.[14,15] Ribotype 027 has recently caused recent severe epidemics in North America, Europe, Asia and Oceania.[16,17] Other strains contribute to morbidity and mortality worldwide, including ribotypes 001, 017, 046 and 078 that have been responsible for outbreaks in Europe, the Americas and Asia, and have developed drug resistance as well.[18–22] A number of widely used antibiotics, especially clindamycin, cephalosporines, penicillins and fluoroquinolones, are becoming increasingly ineffective against *C. difficile*.[23,24] In addition to hospitalized elderly patients that are at main risk, children[25], adolescents[16] and pregnant women[26] are now acquiring CDI also outside of healthcare facilities[17], further exacerbating the social and economic burden.

1.1.2 Life Cycle

C. difficile passes through a life cycle in which the dividing vegetative cells produce metabolically inactive spores [Fig. 1.1].[27] The vegetative cells can only thrive in the anaerobic intestinal tract, in humans preferrably the colon.[28] Outside of this environment, vegetative cells are killed within minutes when oxygen is present.[29] In contrast, spores survive exposure to oxygen for five months or longer and are resistant to desiccation, alcohol-based disinfectants, UV radiation and temperatures of up to 71 °C.[30–33] Both asymptomatic carriers and CDI patients shed *C. difficile* spores that are the main vehicle of transmission through the fecal-oral route.[27] Viable spores are detected abundantly in hospitals on the hands of healthcare personnel, on medical equipment, floors, bedsheets and bathroom surfaces.[30,34] Spores are also found in wild and domesticated animals, fresh water and soil.[4,35] Infants provide a particularly important reservoir, since up to 70 % carry *C. difficile*.[36–38] Despite frequent colonization also with toxigenic strains, infants rarely develop CDI, likely because they lack the cellular receptors for clostridial toxins.[39] Up to 15 % of the adult population asymptomatically carry *C. difficile*, including toxigenic strains.[40]

Ingested spores that survive stomach passage (pH 1.5-3.5) germinate in the small intestine to form vegetative cells.[27] Fewer than ten spores may be sufficient for infection, depending on the *C. difficile* strain and host parameters.[41] Patients receiving proton pump

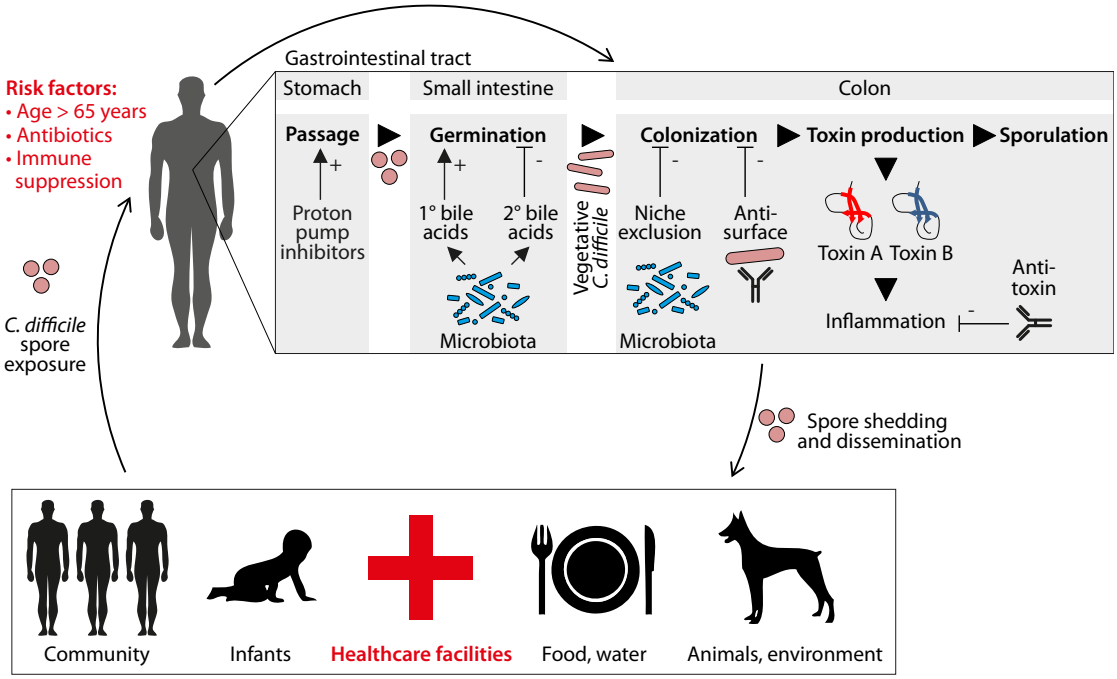

Figure 1.1: Life cycle of *C. difficile*. Spores from various sources, mainly healthcare facilities, are ingested and survive stomach passage. Germination to vegetative cells occurs in the small intestine. The cells colonize the colon, followed by secretion of toxins that cause inflammation and disease. Sporulation occurs and spores are defecated. Outside of the intestine, spores remain viable for long time periods and can infect humans and other mammalian species. Interventions and host factors that eiher inhibit or favor *C. difficile* at different steps of the life cycle are indicated. Figure adapted from Seekatz and Young[27].

inhibitors for gastric diseases provide a stomach milieu (pH > 4) that favors spore survival, which may explain their increased risk of acquiring CDI.[29] Germination in the small intestine is triggered by specific metabolites of the gut microbiota, especially primary bile acids such as taurocholate.[42,43] Conversely, secondary bile acids like chenodeoxycholate inhibit germination.[44] Vegetative cells migrate to the colon where they attach to the epithelium that is covered by a dense and viscous mucus layer.[45] Colonization is mediated by bacterial adhesins that either bind to the epithelial cell surface or to mucus-associated extracellular matrix (ECM) proteins. Various *C. difficile* adhesins have been characterized, including S-layer proteins (SLPs) P36 and P47[46–48], cell wall protein Cwp66[49], heat shock protein GroEL[50], the Fbp68 fibronectin-binding protein[51] as well as flagellar proteins FliC and FliD[52]. In addition, the ECM-degrading surface cysteine protease Cwp84 contributes to adherence.[53,54] Small animal immunization studies and human serum analyses indicated that antibodies to the bacterial adhesins are capable of limiting colonization of *C. difficile*.[49,50,55–66] Therefore, the immunosenescent elderly[67], immunosuppressed HIV-positive individuals[68,69] and organ transplant receivers[70,71] are at increased risk of contracting CDI. Another factor that influ-

ences colonization is the composition of the gut microbiota.[27] The healthy adult intestine harbors 10^{14} bacteria of about one thousand different species that provide colonization resistance to *C. difficile* by occupying ecological niches and competing for nutrients.[72,73] Reduced microbial complexity that is a consequence of antibiotic use or of advanced age favors acquisition of *C. difficile*.[74,75]

Following colonization, *C. difficile* multiplies and produces toxins.[45] The main virulence factors are clostridial toxins A and B (TcdA and TcdB) that share 63 % sequence homology and have glucosyltransferase activity.[76] TcdA and TcdB are large secreted proteins of about 300 kDa that enter epithelial cells *via* receptor-mediated endocytosis.[77,78] The uptake involves binding to glycan or glycoprotein receptors including α-Gal*p*-(1→3)-β-Gal*p*-(1→4)-GlcNAc, Lewis blood group antigens, heat shock glycoprotein gp96, sucrase-isomaltase (TcdA)[79–82], chondroitin sulfate proteoglycan 4 and poliovirus receptor-like 3 (toxin B)[83,84]. Inside the host cell, both toxins transfer glucose from UDP-glucose to Rho familiy GTPases, which triggers rearrangement of the actin cytoskeleton and, in turn, apoptotic or necrotic cell death.[85–88] The resulting tissue damage activates local inflammation, leading to CDI symptoms.[45] Most disease-causing *C. difficile* strains express both TcdA and TcdB that act in concert.[83] A third toxin termed binary toxin CDT, composed of CDTa and CDTb subunits, is found in about 6 % of clinical *C. difficile* isolates.[89,90] CDT uses lipolysis-stimulated lipoprotein receptor to enter cells and triggers cytoskeletal disorganization through actin-specific ADP ribosyltransferase activity.[91,92] Binary toxin potentiates pathogenic effects of TcdA and TcdB, leading to more severe disease associated with ribotype 027 and other highly virulent strains.[93,94] About 50 to 70 % of the human population harbor systemic and/or mucosal antibodies to clostridial toxins that can alleviate CDI symptoms through toxin-neutralizing activity.[45,95]

Finally, muliplying *C. difficile* cells produce spores that are shed by CDI patients in quantities of up to 10^7 spores per gram of feces.[2,27,45] Elevated spore formation (sporulation) characteristic of ribotype 027 and other hypervirulent strains may increase environmental survival and dissemination.[45,96]

1.2 Therapy against *C. difficile*: Current Guidelines and Investigational Approaches

Antibiotics are currently the only therapy against CDI approved by the US Food and Drug Administration (FDA) and other health agencies worldwide.[97] The evidence-based recommenda-

tion is treatment with metronidazole, vancomycin or fidaxomicin that are active against most *C. difficile* strains. Although resistance to these antibiotics has recently been identified in some clinical isolates[98], the majority of CDI cases can be successfully cured[97]. Patients with complicated, life-threatening disease that often require long-lasting and combined antibiotic treatment, however, frequently experience recurrent infections.[99–102] Recurrence is the result of antibiotic-induced damage to the gut microbiota, a condition that favors re-emergence of the same *C. difficile* strain or re-infection by spores from the environment.[100–102] This affects up to 30 % of patients after initial antibiotic treatment and almost two thirds following treatment for a second episode.[100–104] Recurrence rates are increasing, partly attributed to emerging hypervirulent strains.[14,15,105–107] Antibiotic treatment involves significant medical costs of an estimated $25,000 per patient and recurrent disease episode.[108] Other antibiotics such as nitazoxanide and rifaximin may be efficacious against drug-resistant *C. difficile* strains but are currently not approved for CDI treatment.[109–113]

The fact that depressed antibody levels, especially low anti-toxin IgG, predispose for the acquisition of *C. difficile* provided a rationale to investigate passive immunotherapy as treatment against recurrent CDI.[114,115] Intravenous polyclonal immunoglobulins[116] (IVIG) or toxin-neutralizing monoconal antibodies[117] (mAbs) are efficiently transported to the intestinal lumen by transcytosis[118–120] and have been shown to significantly limit recurrence[109]. Anti-toxin mAb therapy is further discussed in **Section 1.3.3**.

Other investigational therapies target the dysbiotic gut microbiota of CDI patients by means of probiotics or fecal microbiota transplantation (FMT).[109,110,121,122] Probiotics are orally administered microorganisms that thrive in the intestine and may thereby limit growth of *C. difficile*. A promising probiotic is the yeast *Saccharomyces boulardii* that significantly reduced recurrence of CDI in two placebo-controlled clinical trials.[123,124] In addition, probiotic use of a non-toxigenic *C. difficile* strain has been shown to efficiently limit recurrence in small animal models and is presently subject to clinical investigation.[125] FMT, the transfer of fecal microbiota from a healthy donor, has recently emerged as the most effective treatment option with impressive cure rates of about 90 % against recurrent CDI.[97,103,126–130] Fecal material is applied directly to the patient's intestine as a suspension[128] or orally administered *via* frozen capsules that dissolve in the small intestine[129]. The procedure restores the dysbiotic gut microbiota and thereby precludes colonization by *C. difficile*.[74,75] Due to safety concerns and the non-characterizable nature of human feces[131–133], FMT is presently not generally approved by the FDA and other health agencies and considered a rescue therapy only after

antibiotics have failed repeatedly[97]. To overcome safety concerns of FMT, combinations of defined enteric bacterial species are currently investigated as substitute for human stool.[134]

1.3 Vaccines against *C. difficile*: Current Status and Future Directions

The limitations of antibiotic treatment have recently solicited the search for a protective vaccine against CDI, a disease generally considered to be vaccine-preventable.[135] Vaccines provide the most effective and cost-saving measure to prevent infectious diseases.[136] To date, however, no vaccine against *C. difficile* is commercially available.[135] Currently investigated vaccine candidates either aim at inducing toxin-neutralizing antibodies or at preventing colonization by targeting surface antigens. In addition to preventive vaccines, passive immunization approaches with mAbs against toxins or surface antigens provide a promising therapeutic option against recurrent CDI.

1.3.1 Vaccination with Clostridial Toxins

The toxin-neutralizing vaccine candidates utilize TcdA and TcdB, the major virulence factors of *C. difficile*, as immunogens.[7–9] Toxins were identified as auspicious vaccine targets in the 1980s when levels of toxin-neutralizing serum and mucosal antibodies were found to correlate with protection from clinical manifestations of CDI.[137–139] Soon after these discoveries, immunization with formalin-inactivated toxins (toxoids) isolated from *C. difficile* culture was shown to completely protect hamsters and mice from experimental disease.[140–145] Since the 1990s, recombinant DNA technology made nontoxic derivatives of the clostridial toxins from easy to handle bacteria like *Escherichia coli* available, circumventing the process of formalin inactivation and the laborious culture of *C. difficile*.[135] Immunization with toxin fragments[146–149] as well as chimeric toxin A/B constructs[150–152] have been shown similarly efficacious as toxoids in preventing CDI disease manifestations in small animals. While early studies suggested that anti-TcdA antibodies alone sufficiently protect humans from CDI symptoms, today's consensus is that an effective toxin-neutralizing vaccine needs to induce antibodies to both TcdA and TcdB.[153–155] Such a vaccine would also limit symptoms caused by TcdA-negative, TcdB-positive *C. difficile* strains associated with severe disease.[156–158]

Following the promising results in small animals, three toxin-based *C. difficile* vaccine candidates have been forwarded to clinical investigation [Table 1.1]. The first one is ACAM-

Table 1.1: Anti-toxin vaccine candidates tested in clinical studies. i. m., intramuscular. [a]References include either the original publication or the trial details provided at clinicaltrials.gov. Table modified from Leuzzi *et al.*[135]

Antigens (manufacturer)	Development stage	Formulation	Subjects	Ref.[a]
Toxoids A and B (ACAM-CDIFF by Acambis)	Phase I	4 doses i. m., ± Alum	Healthy adults	159,160
	Pilot study	4 doses i. m., no adjuvant	Patients	161
Toxoids A and B (Sanofi Pasteur)	Phase I	3 doses i. m., with Alum	Healthy adults and elderly	162,163
	Phase II	3 doses i. m., ± Alum	Adults at risk for CDI	164
Mutant toxoids A and B (Pfizer)	Phase I	3 doses i. m., ± Alum	Healthy adults and elderly	168
Toxin A/B fusion protein (VLA84 by Valneva)	Phase I	3 doses i. m., ± Alum	Healthy adults and elderly	171
	Phase II	3 doses i. m., ± Alum	Healthy adults and elderly	172

CDIFF by Acambis.[159] This two-component vaccine contains formalin-inactivated, partially purified toxoids (∼44 %) obtained from *C. difficile* culture and ammonium sulfate fractionation of TcdA and TcdB. A phase I trial demonstrated the safety and immunogenicity of ACAM-CDIFF that was administered intramuscularly with or without aluminum hydroxide (Alum) adjuvant to healthy adults.[159] All vaccinated participants mounted neutralizing serum antibodies to both toxins.[160] This encouraged a pilot trial in three patients with recurrent CDI that received the non-adjuvanted toxoid vaccine.[161] Two of the participants developed neutralizing antibodies to both TcdA and TcdB, and all three experienced resolution of diarrhea. Following acquisition of Acambis by Sanofi Pasteur in 2008, the production process has been optimized to obtain toxoids of higher purity (>90 %).[145] The Alum-adsorbed vaccine showed a good safety and tolerability profile and induced 100 % (TcdA) and 75 % (TcdB) seroconversion in healthy adults and elderly volunteers in a phase I trial.[162,163] A recently completed phase II trial with over 600 hospitalized adults at risk for CDI confirmed the safety and found seroconversion rates of 97 % and 92 % for toxins A and B, respectively, after three intramuscular injections of the Alum-adsorbed vaccine.[164] Another phase II trial with CDI patients investigating the prevention of recurrence has been completed, but results have not been reported.[165] A phase III interventional trial is currently recruiting participants.[166]

Pfizer is investigating a vaccine composed of genetically modified toxoids A and B produced in a non-sporulating *C. difficile* strain that lacks native toxin genes.[167] This production process limits the safety issues associated with large-scale fermentation, such as exposure

to spores and toxins.[135] Despite site-directed mutations at the glucosyltransferase domains that are responsible for cytopathic effects, residual toxicity was observed that is abrogated by formalin treatment.[167] A phase I trial found the vaccine that was administered intramuscularly with or without Alum to be safe and well-tolerated in healthy adult (50-64 years) and elderly (65-85 years) subjects.[168] Both cohorts showed similar magnitudes of neutralizing anti-TcdA/B IgG responses and seroconversion rates above 90 %. The non-adjuvanted vaccine was more immunogenic than the Alum-adsorbed proteins[168], in contrast to the Acambis/Sanofi Pasteur toxoids[164]. Phase II trials testing different adjuvant-free vaccination regimes in healthy adults and elderly volunteers are ongoing.[169,170]

A recombinant toxin A/B fusion protein that lacks glucosyltransferase activity termed VLA84 is investigated by Valneva, with opt-in rights by GlaxoSmithKline.[171–173] Phase I and II trials showed favorable safety and tolerability, with or without Alum, and induction of functional antibodies to both toxins in healthy adult and elderly subjects.[171,172] Similar to the Pfizer vaccine[168], immunogenicity of the non-adjuvanted fusion protein was superior to Alum-adsorbed VLA84[174]. Phase III investigation is expected to start by mid-2016. With overall good safety and immunogenicity profiles, the first toxin-neutralizing vaccines are expected to obtain licensure around the year of 2020.[135]

1.3.2 Vaccination with Surface Antigens

An inherent limitation of toxin-neutralizing vaccines is their inability to prevent bacterial colonization that precedes toxin production.[135] Although tetanus and diphtheria toxoid vaccines have successfully limited infections with *Clostridium tetani* and *Corynebacterium diphtheriae*, respectively, these bacteria may be more susceptible to toxin immunity than *C. difficile* due to their different infectious routes.[175] *C. tetani* is not transmitted between individuals, in spite of a significant human reservoir.[176] *C. diphtheriae* spreads from person to person, but epidemics can easily be contained due to the lack of spore production.[177] Contrarily, *C. difficile* infections frequently originate from spores shed by aymptomatic carriers of toxigenic strains, including infants[36–38,178] and adults[40]. The human reservoir may further increase upon introduction of toxin-neutralizing vaccines, as high anti-toxin antibody levels correlate with asymptomatic carriage.[154,179] Increased risk of infection imposed on non-vaccinated, immunocompromised and elderly populations and the evolution of more virulent and drug-resistant strains may result. Due to these potential drawbacks, colonization-preventing vaccination approaches that could limit the human reservoir are intensely investigated.[135]

Early evidence that vaccination with surface antigens can limit disease was gained from hamsters immunized with crude protein extracts of bacterial cultures.[65] It was shown that the levels of *C. difficile*-agglutinating antibodies correlated with protection from lethal challenge. The molecular characterization of surface proteins that mediate bacterial adherence spawned more targeted immunization studies.[135] S-layer proteins (SLPs) are the most abundant proteins on the surface of *C. difficile*.[58] Partially purified SLPs obtained from bacterial culture were capable of elicing SLP-specific antibodies in mice and hamsters that, however, did not confer significant protection from lethal *C. difficile* challenge.[57] Immunization with recombinant SLP produced in *E. coli* only weakly reduced colonization and lethality of challenged mice and hamsters, respectively.[58] Several studies testing the vaccine potential of GroEL protein[62], flagellar proteins FliC[63] and FliD[180] as well as the cysteine protease Cwp84[64,181] confirmed that immunity to surface proteins only partially prevents colonization and death in small animal models. With conflicting results concerning the administration route, it is still debated whether parenteral or mucosal immunization, inducing predominantly systemic IgG or mucosal IgA, respectively, is favorable to deliver surface antigens.[135] Recently, immunization with spore-associated proteins has been shown to completely prevent *C. difficile* colonization in mice.[182] However, long-lasting protection may be difficult to achieve since high levels of circulating antibodies are required to entirely block spore germination.

A potential drawback of using proteins for a vaccine is their predisposition to antigenic variation. Protective efficacy may decrease over time due to selection of escape mutants that display different antigen repertoires than those represented in the vaccine. Escape mutants of *Mycobacterium tuberculosis*, *Bordetella pertussis* and other bacterial pathogens cause on-going infections despite area-wide vaccination.[183] In the case of *C. difficile*, significant sequence variability within immunodominant epitopes of TcdB[184] and surface proteins such as SLPs[185,186] contribute to virulence and immune evasion. Protein-based vaccines may therefore not confer broad and sustainable protection from the various circulating clinical *C. difficile* strains. Surface glycans provide appealing alternative vaccine targets. Glycans are less prone to escape mutations, since unlike proteins they are not directly encoded in the bacterial genome but arise from multi-enzyme assembly machineries.[187] Currently investigated glycan-based vaccine approaches against *C. difficile* are described in **Section 1.4**.

1.3.3 Passive Immunization with Monoclonal Antibodies

The discovery of toxin-neutralizing antibodies whose presence correlates with protection from disease has spawned the investigation of anti-toxin mAbs for CDI treatment.[45,95,117] Passive immunization is an attractive therapeutic option especially for the elderly and immunocompromised individuals that do not produce sufficient levels of *C. difficile*-specific antibodies to contain the disease.[67–71] First evidence for the therapeutic efficacy of passive immunization was obtained in hamsters that were protected from lethal *C. difficile* challenge by intravenous or oral administration of polyclonal anti-toxin antibodies in both prophylactic and therapeutic settings.[188-190] While antibodies to TcdA alone only conferred partial protection, combined anti-toxin A and B completely prevented death.[190] Likewise, anti-toxin mAbs are effective in animals. Oral administration of a lethal dose of TcdA together with a murine anti-TcdA mAb completely prevented death of hamsters.[191] The same mAb protected mice from *C. difficile* disease and lethality when administered intravenously prior to challenge.[192]

The first fully human anti-toxin mAbs were generated by immunizing transgenic mice carrying human immunoglobulin genes with inactivated toxins A and B.[193] Intraperitoneal injection of these mAbs partially protected hamsters from lethal *C. difficile* challenge in both prophylactic and therapeutic settings. Combined use of anti-toxin A and B offered enhanced protection over either mAb alone. These human mAbs, termed GS-CDA1 (anti-TcdA) and MDX-1388 (anti-TcdB) have recently entered clinical investigation [Table 1.2].[117] A phase II trial sponsored by Medarex investigated their therapeutic efficacy in hospitalized CDI patients.[194] Combined with antibiotics, intravenous administration of GS-CDA1 and MDX-1388 significantly reduced the recurrence rate to 7 % as compared to antibiotics alone with 25 %. Merck has completed the MODIFY I/II phase III studies that investigated the clinical efficacy of intravenous anti-TcdA (actoxumab) and anti-TcdB (bezlotoxumab) in hospitalized CDI patients.[195,196] In both MODIFY I and MODIFY II, bezlotoxumab reduced recurrence rates from 27.6 % and 25.7 % (antibiotics alone) to 15.9 % and 14.9 % (antibiotics combined with bezlotoxumab), but did not improve diarrheal symptoms or the duration of hospitalization.[197] Actoxumab did not provide any clinical benefits. Bezlotoxumab was selected for marketing authorization application, with an FDA decision expected by July of 2016.[197]

Table 1.2: Human anti-toxin mAbs tested in clinical studies. i. v., intravenous. [a]References include either the original publication or the trial details provided at clinicaltrials.gov. Table modified from Zhao *et al.*[188]

mAbs (manufacturer)	Development stage	Formulation	Subjects	Ref.[a]
Anti-TcdA GS-CDA1 and anti-TcdB MDX-1388 (Medarex)	Phase II	1 dose i. v., GS-CDA1 + MDX-1388	Patients	117,194
Anti-TcdA actoxumab and anti-TcdB bezlotoxumab (Merck)	Phase III	1 dose i. v., actoxumab or bezlotoxumab or both combined	Patients	195,196

1.4 The Prospects of Glycan-based Vaccines against *C. difficile*

The cell wall of Gram-positive bacteria including *C. difficile* contains a number of immunologically active surface-exposed glycopolymers that provide attractive targets for both active and passive vaccination approaches.

1.4.1 The Cell Wall of Gram-positive Bacteria

Gram-positive bacteria have a single lipid membrane surrounded by a cell wall containing peptidoglycan as main structural component [Fig. 1.2].[198–200] Peptidoglycan (also known as murein) is a polymer of alternating β-(1→4)-linked D-GlcNAc and D-*N*-Acetylmuramic acid (D-MurNAc) subunits that is cross-linked by species-specific oligopeptides *via* the 3-position of D-MurNAc. In contrast to Gram-negatives with a single peptidoglycan layer of 7-8 nm, Gram-positive bacteria express multi-layered peptidoglycan of 20-80 nm thickness that confer their species-specific shape, e. g., rod or coccal. The cell wall is densely functionalized with glycopolymers that are either covalently attached to peptidoglycan or membrane-anchored, termed teichoic acids (TA) and lipoteichoic acids (LTA), respectively.[201–209]

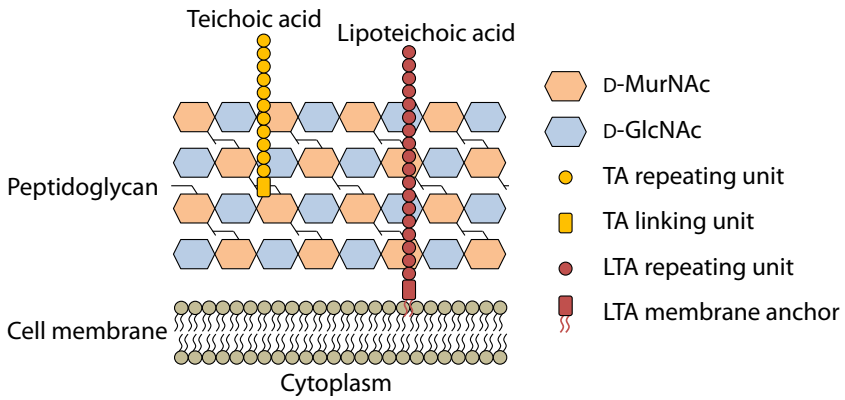

Figure 1.2: Cell wall of Gram-positive bacteria. Figure adapted from Brown *et al.*[200]

TAs comprise a disaccharide linking unit and a polymer of phosphodiester-linked polyol repeating units that can be functionalized with glycan moieties [Fig. 1.3].[201–203] The conserved linking disaccharide is composed of D-*N*-Acetylmannosamine (D-ManNAc) that is β-(1→4)-linked to D-GlcNAc-1-phosphate with up to three glycerol-3-phosphate (GroP) units attached to the 4-position of D-ManNAc.[201,202] The anomeric phosphate group of the disaccharide is linked to peptidoglycan *via* a phosphodiester bond to the C-6 hydroxyl of D-MurNAc. The repeating units extend from the GroP end of the linking unit.[201,202] TA repeating units exhibit substantial inter-species variation and are classified as types I-IV based on their composition [Fig. 1.3]. The common structural feature is a GroP moiety functionalized with various amino acids and/or glycans.[201] The typical size of TAs is 5-10 kDa, corresponding to about 15 to 40 repeating units.[203] TAs maintain ion homeostasis of Gram-positive bacteria due to their net negative charge that attracts cations such as Mg^{2+} or K^{+}.[202] Networks of TA-coordinated cations are also critical for the porosity and rigidity of the cell wall and support the overall bacterial shape.[202] In addition, TAs have been shown to mediate adhesion of pathogenic Gram-positive bacteria to host tissues.[210,211] Being recognized by the adaptive immune system, TAs provide attractive targets for vaccination approaches.[212]

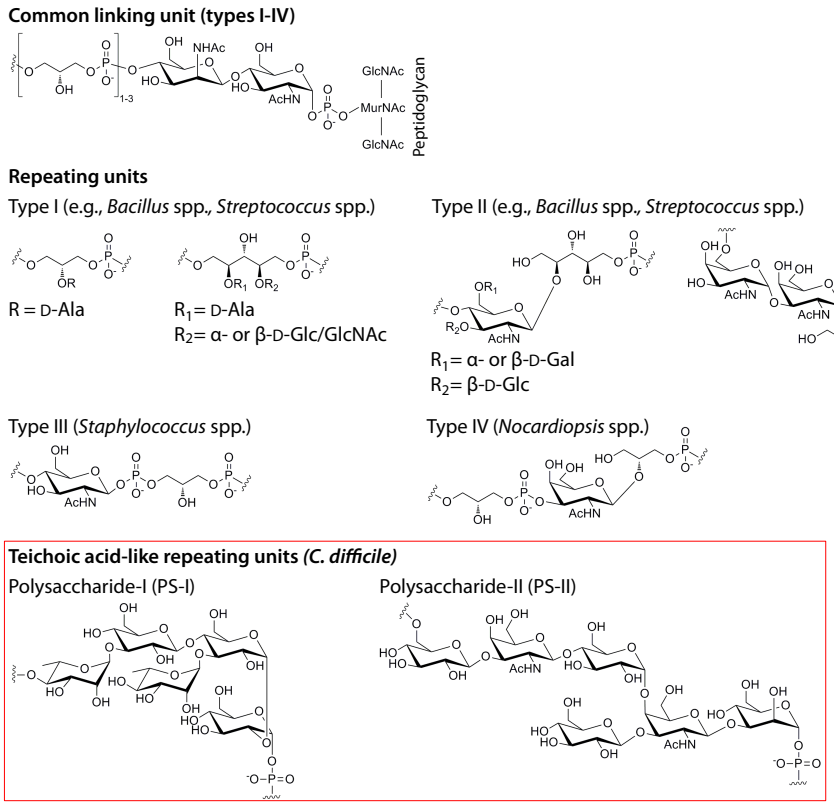

Figure 1.3: Structural diversity of teichoic acids. *C. difficile* teichoic-acid like repeating units are highlighted. Figure adapted from Brown *et al.*[201] and Ganeshapillai *et al.*[205]

LTAs consist of an anchoring unit that is linked to a polymer of phosphodiester-linked polyol repeating units of high inter-species variability. Five LTA structures termed types I-V have been identified [Fig. 1.4]. The anchoring unit is a glycerol molecule functionalized with two fatty acid esters and a mono- to trisaccharide in most cases composed of D-Glc. The repeating units are connected to the terminal glycan moiety of the anchor *via* a phosphodiester linkage (types I, II, III and V) or a glycosidic bond (type IV). The common structural feature of LTA type I-IV repeating units is a GroP moiety that is functionalized with amino acids and/or glycans. Type V LTA, in contrast, does not contain GroP but glyceric acid (GroA). The typical size of LTAs is 10 kDa that corresponds to about 25 type I repeating units.[204] Being negatively charged, LTAs bind cations, support ion homeostasis and cell wall integrity similar to TAs.[204] Human pathogens such as *Listeria monocytogenes* and group A *Streptococcus* utilize LTAs to attach to host epithelium.[213,214] Like TAs, LTAs are immunogenic and therefore auspicious targets for antibacterial vaccines.[204]

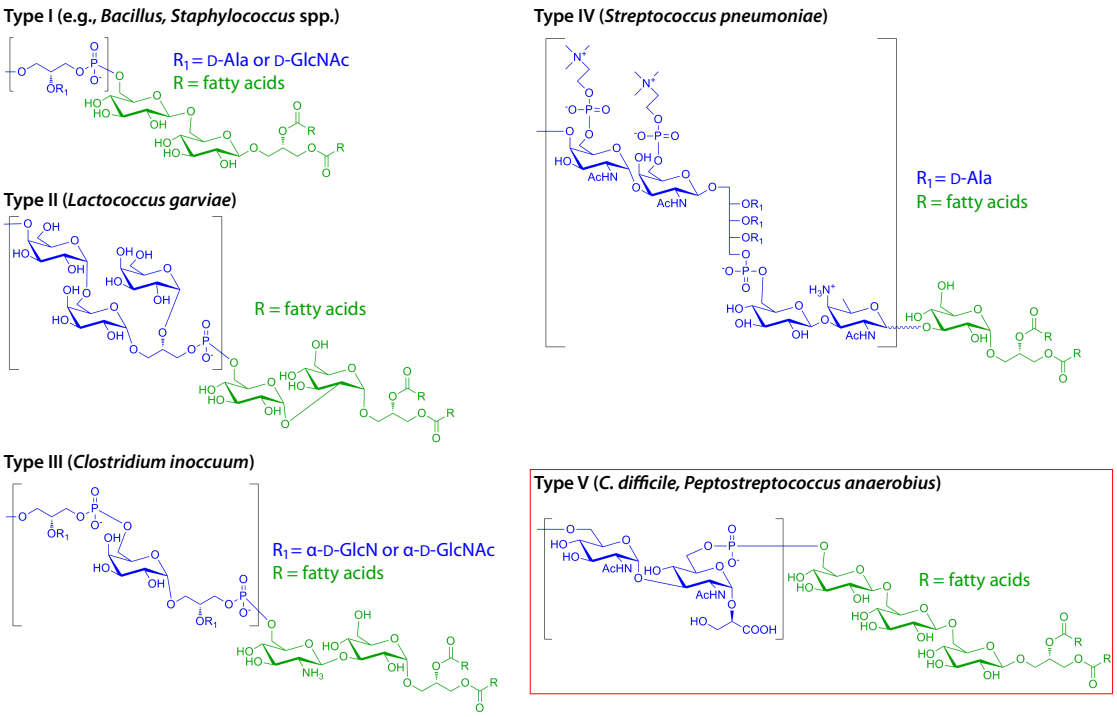

Figure 1.4: Structural diversity of lipoteichoic acids. The repeating units are depicted blue and the anchoring units green. Fatty acids (R) usually are saturated or mono-unsaturated C14 to C18 species.[207] The wavy bond in type IV represents *alpha* linkage between repeating units and *beta* linkage to the anchoring unit.[204] *C. difficile* LTA is highlighted. Figure adapted from Percy and Gründling[204] and Reid *et al.*[207]

1.4.2 Structure and Function of *C. difficile* Cell Wall Glycans

While the presence of phosphate-containing surface carbohydrates was already reported in the early 1980s[215,216], it was not until 2008 that the structures of two *C. difficile* cell wall glycans designated as Polysaccharide-I (PS-I) and Polysaccharide-II (PS-II) have been determined[205].

PS-II constitutes about 40 % by weight of the cell wall.[216] The polysaccharide consists of phosphodiester-linked branched hexasaccharide repeating units containing D-Glc, D-Man and D-GalNAc moieties as shown in [Fig. 1.3].[205,216] PS-II has an average size of about 10 kDa corresponding to six to eight repeating units and to date has been identified on all investigated *C. difficile* isolates *in vitro*.[205,206] PS-I is composed of phosphodiester-linked branched D-Glc and L-Rha-containing pentasaccharide repeating units [Fig. 1.3].[205,206] Originally identified solely on an isolate of *C. difficile* ribotype 027, PS-I was suggested to be a strain-specific polysaccharide.[205] The subsequent detection on other, non-ribotype 027 strains[206] and the frequent presence of PS-I-specific serum antibodies in horses[217], however, indicated that PS-I is likely commonly expressed *in vivo*. Due to their structural similarities with TAs, PS-I and PS-II have been designated as teichoic acid-like polysaccharides.[205] PS-II is in part also present as a membrane-anchored low molecular weight species of two repeating units.[206] To date, both polysaccharides have been uniquely identified on *C. difficile*.

A third surface glycan, termed PS-III or LTA, has recently been characterized.[207] The membrane-anchored polymer of phosphodiester-bridged disaccharide repeating units containing D-Glc, D-GlcNAc and GroA is classified as type V LTA [Fig. 1.4].[204] This polysaccharide has been identified also on three other *C. difficile*-related bacterial species; *Clostridium sordellii*, *Clostridium bifermentans* and *Peptostreptococcus anaerobius*.[208,215]

The functions of *C. difficile* cell wall glycans remain largely unknown, but roles in promoting cation homeostasis, wall integrity and adherence to host tissue similar to other TAs and LTAs are likely.[202,204] They may also contribute to the shape of *C. difficile*, since PS-I, PS-II and LTA are present in the rod-like vegetative form, but not in the ovoid spores.[206] In addition, PS-II anchors surface proteins to the cell wall *via* non-covalent interactions.[218] The anchored proteins, in turn, mediate bacterial adherence to intestinal epithelium.[46–48,219]

Extending from the cell wall, some *C. difficile* strains harbor lowly abundant capsule-like glycans under culture conditions.[220] However, these are not associated with virulence[220] and probably have limited biological function *in vivo* compared to the cell wall glycans[205,207].

1.4.3 Glycan-based Antibacterial Vaccines: Current State of the Art

Anti-bacterial vaccines can be subdivided into whole-cell and subunit vaccines.[221] The latter class utilizes defined components of the target bacterium, an approach considered to be favorable over whole-bacteria vaccines that often induce only limited protection and cause adverse reactions.[222] Bacterial surface glycans provide formidable targets for anti-bacterial subunit vaccines since they are commonly targeted by the adaptive immune system during infections.[223]

First-generation glycan-based subunit vaccines contain free capsular polysaccharides isolated from cultured bacteria including *Streptococcus pneumoniae*, *Haemophilus influenzae* type B and *Neisseria meningitidis*.[224] Intradermal or intramuscular injection of these vaccines induces protective anti-glycan antibodies in immunocompetent healthy adults.[223] Their immunogenicity is largely attributed to B cell receptor (BCR) crosslinking through binding repetitive B cell epitopes of the polysaccharides [Fig. 1.5a].[225] BCR crosslinking leads to the activation of glycan-specific B cells independent of T cell help and induces differentiation to short-lived plasma cells that produce low-affinity antibodies mainly of the IgM class.[223,225] Due to their limited immunogenicity, polysaccharide vaccines do not induce protection in individuals with weak immune systems, such as young children, the elderly and HIV patients.[224]

The poor quality of antibody responses to free glycans can be overcome by covalent attachment to a carrier protein that requires chemical activation of the polysaccharide.[226] The resulting glycoconjugate is able to induce T cell-dependent immunity. Binding of the B cell epitope-containing polysaccharide portion to the BCR of a glycan-specific B cell triggers internalization and processing of the glycoconjugate to peptide or glycopeptide fragments [Fig. 1.5b]. Glycoconjugate-derived T cell (glyco)peptide epitopes are presented on MHC class II molecules and recognized by T helper (Th) cells *via* their T cell receptor (TCR).[225] This interaction triggers Th cells to release cytokines such as interleukin-4 (IL-4) that stimulate immunoglobulin class switching and affinity maturation in the B cell. The resulting glycan-specific plasma cells are long-lived and produce high-affinity antibodies mainly of the IgG class. In addition, Th involvement triggers B cell differentiation to memory B cells that generate accelerated antibody responses once the immune system re-encounters the respective glycan epitope. Thereby, glycoconjugate vaccines are superior to free polysaccharides in mediating long-term protection also in the elderly and young children.[224]

Commonly used FDA-approved carrier proteins are formalin-inactivated diphtheria and tetanus toxoids as well as the non-toxic diphtheria toxin mutant CRM_{197}.[223,224] All cur-

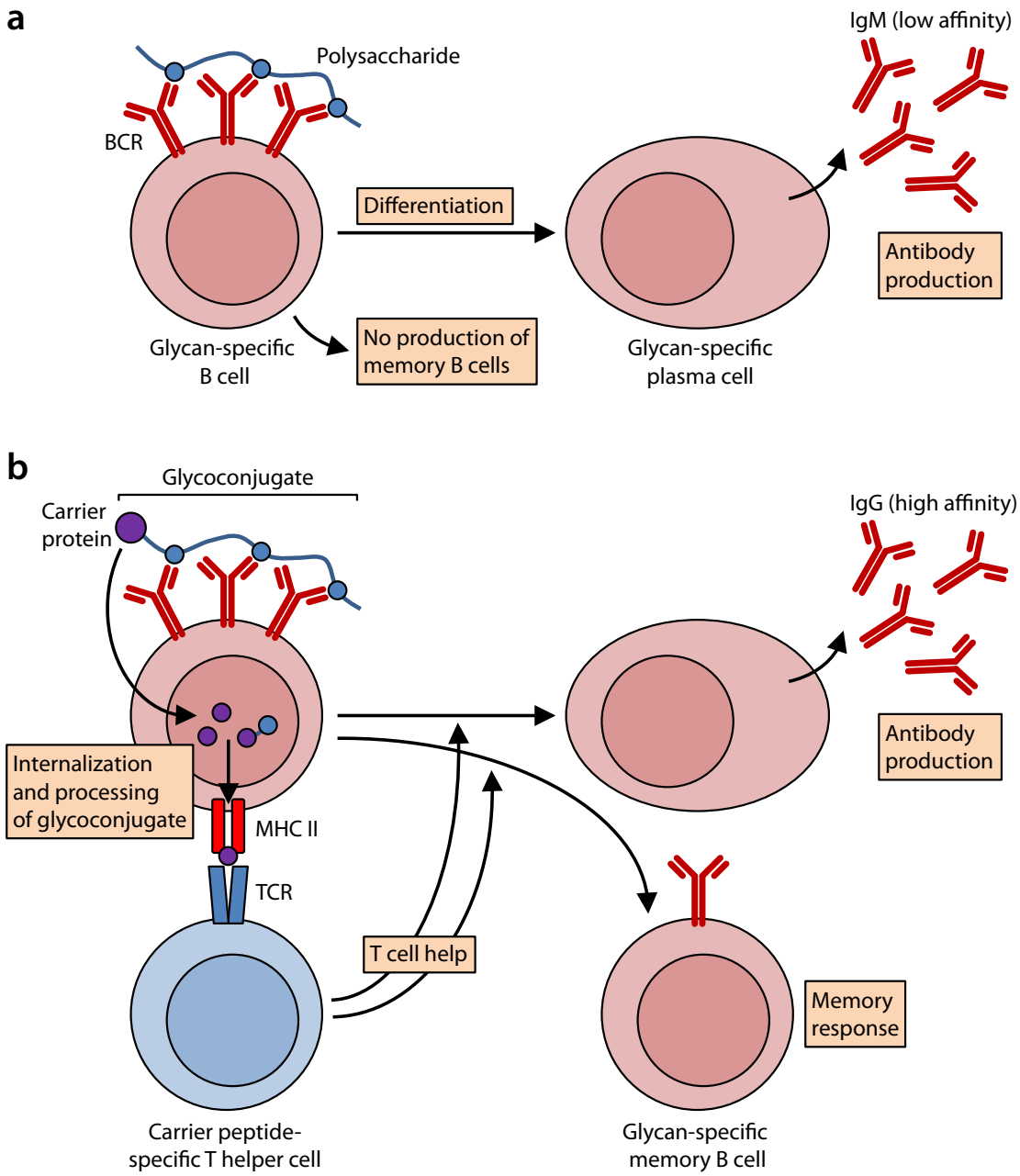

Figure 1.5: Mechanism of action of polysaccharide and glycoconjugate vaccines. (**a**) Polysaccharides induce BCR crosslinking through repetitive epitopes. This induces B cells differentiatiation into IgM-secreting plasma cells. (**b**) Glycoconjugates engage BCRs through the polysaccharide or oligosaccharide portion, thereby triggering internalization and processing to (glyco)peptides that are presented on MHC type II molecules to the TCR of carrier-specific Th cells. This induces differentiation of B cells to IgG-secreting plasma cells and to memory B cells. Figure adapted from Pollard *et al.*[204]

rently licensed glycoconjugate vaccines are adsorbed to aluminum salt adjuvants to increase their immunogenicity.[223,224] Aluminum salt particles act as a depot, whereby the adsorbed glycoconjugate antigen persists for up to three weeks at the site of injection.[227] This constantly attracts immune cells, including dendritic cells (DCs) and other professional antigen-presenting cells. The adsorbed, particulate antigens are subject to phagocytosis and are thereby more efficiently taken up DCs than soluble antigens.[227] After phagocytosis, DCs process the glycoconjugate to (glyco)peptides that are presented to naïve T cells in draining lymph nodes, which generates carrier-specific Th cells that help to differentiate B cells to antibody-producing plasma cells [Fig. 1.5b]. Furthermore, adsorption to aluminum salts partially denatures the (glyco)protein, which may facilitate its proteolytic processing and presentation by DCs.[228] The introduction of glycoconjugate vaccines against *S. pneumoniae*, *H. influenzae* type B, *N. meningitidis* and others has greatly reduced the incidence of the respective infectious diseases.[223]

Drawbacks of isolated polysaccharides are structural heterogeneity, batch-to-batch variation and contamination with undesired bacterial components.[229] The presence of impurities in polysaccharide-based vaccines has been associated with adverse reactions.[230] Thus, purification is a cumbersome process and multiple control steps are required to ensure that a polysaccharide preparation meets the quality for vaccine use.[231] Cost-efficient vaccine production may be further impeded for glycans that are inconsistently expressed *in vitro*, as is the case with both *C. difficile* PS-I and LTA.[206,217,232] These limitations can be overcome by using synthetic oligosaccharide antigens that are inherently free of contaminations and not restricted to *in vitro*-expressed polysaccharides.[233] Chemical synthesis furthermore allows for the installment of linker moieties usually containing nucleophiles such as thiols or primary amines for efficient, orientation-specific covalent attachment to lysine residues of carrier proteins.[229,233] Like polysaccharides, oligosaccharides are usually T cell-independent antigens whose immunogenicty benefits from conjugation to a protein and the use of an external adjuvant such as aluminum salt.[229,234] Such a semi-synthetic glycoconjugate vaccine has been brought into practice by Quimi-Hib, a vaccine against *H. influenzae* type B licensed in Cuba that contains tetanus toxoid-conjugated synthetic oligosaccharides of the capsular polysaccharide.[234]

1.4.4 *C. difficile* Cell Wall Glycans as Vaccine Candidates

Due to the absence of a genuine capsule[220], the cell wall-associated polysaccharides of *C. difficile* are surface-exposed and have been investigated as potential vaccine targets[232]. Studies on PS-II are most advanced due to consistent and high expression levels *in vitro*. The identification of polysaccharide-specific IgG in horse serum suggested that PS-II is immunogenic during natural exposure to *C. difficile*.[232] Pigs vaccinated with non-adjuvanted polysaccharide elicited anti-PS-II IgM antibodies.[206] Immunization of mice with a glycoconjugate composed of isolated PS-II and CRM_{197} formulated with MF59 adjuvant gave rise to high levels of anti-PS-II IgG.[235] The antibodies efficiently stained *C. difficile* bacteria, confirming that PS-II is a well-exposed antigen. PS-II polysaccharide conjugated to the heat-labile enterotoxin B (LTB) or bovine serum albumin (BSA) proved to be immunogenic in rabbits and mice, respectively.[232] Synthetically generated PS-II oligosaccharides have been studied as well. Seeberger and colleagues reported the first synthesis of the hexasaccharide repeating unit with an aminopentyl linker at the reducing end.[236] The identification of IgA to synthetic PS-II in the feces of CDI patients confirmed that the oligosaccharide shares one or more natural epitopes with the polysaccharide that are immunogenic during human infection. Immunization of mice with a glycoconjugate of the hexasaccharide and CRM_{197} formulated with Freund's adjuvant (FA) gave rise to anti-PS-II serum IgG and mAbs of high specificity.[236] An alternative synthetic route for the PS-II hexasaccharide, including a phosphorylated derivative, and a tetrasaccharide substructure with reducing end aminopentyl linkers was subsequently reported.[235] Corresponding CRM_{197} glycoconjugates formulated with MF59 were immunogenic in mice, but only IgGs raised by the hexasaccharide recognized *C. difficile* bacteria *in vitro*, more efficiently so when the phosphorylated compound was used.

Vaccine studies with PS-I has been hampered by inconsistent polysaccharide expression *in vitro*.[232] Seeberger and colleagues reported the first synthesis of the PS-I pentasaccharide repeating unit with reducing end aminopentyl linker.[237] An alternative synthetic route for the same molecule was later reported.[217] The consistent identification of IgGs in horse serum recognizing both natural and synthetic PS-I glycans confirmed the presence of shared epitopes that are immunogenic during CDI.[217]

Immunization of rabbits with whole *C. difficile* bacteria gave rise to IgGs binding to isolated LTA.[238] Purified and deacylated LTA was used to prepare glycoconjugates with the human serum albumin (HSA) and *Pseudomonas aeruginosa* exotoxin A (ExoA) carrier

proteins. IgGs raised with the FA-formulated glycoconjugates in mice and rabbits recognized vegetative *C. difficile* cells, showing that LTA is a surface-exposed antigen.[238] LTA is likely expressed ubiquitously, since the antibodies bound to a wide variety of *C. difficile* isolates and to some related clostridial species as well. A subset of *C. difficile* spores was also recognized, suggesting the presence of LTA in a maturation-specific manner.[238]

The currently available data supports that all three *C. difficile* glycans are surface-exposed antigens that are recognized by the adaptive immune system. Therefore, PS-I, PS-II and LTA are auspicious targets for colonization-preventing antibacterial vaccines.

1.5 Novel Developments in Glycan-Based Vaccines

Conventional glycoconugate vaccines contain rather ill-defined glycan epitopes and require constant cooling to prevent degradation and aggregation processes.[229] These limitations may be overcome by using rationally designed oligosaccharide epitopes instead of isolated polysaccharides and synthetic scaffolds to replace carrier proteins. In addition, mAbs directed against bacterial surface glycans provide an appealing alternative therapeutic option for antibiotic-resistant pathogens including *C. difficile*.

1.5.1 Rational Glycan Epitope Design

Oligosaccharide-based vaccines require the identification of epitopes that induce antibodies efficently recognizing the native bacterial surface glycan.[229] However, the structural determinants of oligosaccharides that guide specificity and affinity of anti-glycan antibodies remain poorly understood.[239,240] Therefore, epitopes that induce protective antibodies are conventionally discovered through time-consuming trial-and-error processes in which oligosaccharides are synthesized based on biological repeating units and immunologically evaluated in animals.[229,241,242] If an epitope proves to be non-immunogenic or the generated antibodies do not recognize the pathogen, different oligosaccharides are synthesized and tested.

A more rational approach to epitope selection and design that may help to reduce both synthetic effort and the number of animal experiments requires knowledge on how the adaptive immune system interacts with glycan antigens. One property that influences the immunogenicity of oligosaccharides is their size. Epitopes as small as disaccharides have been shown to induce protective antibodies against *S. pneumoniae* serotype 3 and the fungal pathogen *Candida albicans* in pre-clinical settings.[243,244] Larger glycans are usually more immunogenic

but come at the expense of synthetic complexity.[234,245–248] Therefore, the identification of a minimal epitope, the smallest oligosaccharide inducing antibodies to the larger glycan it is derived from, is a crucial step towards rationally designed vaccines with minimal synthetic effort.[242,243] The immunogenicity of small oligosaccharides strongly depends on how the epitope is presented. The terminal, non-reducing end of a glycan is most exposed to the immune system and consequently preferentially targeted by antibodies.[249] It is therefore conceivable that glycan epitopes exposing non-mammalian monosaccharide moieties at the non-reducing end represent highly immunogenic structures. Two recently reported examples are a tetrasaccharide of a *Bacillus anthracis* surface glycoprotein[240,250] and a trisaccharide component of *Yersinia pestis* lipopolysaccharide[239,251] (LPS). The *B. anthracis* tetrasaccharide contains an unusual terminal sugar named anthrose, 2-*O*-methyl-4-(3-hydroxy-3-methylbutanamido)-4,6-dideoxy-D-glucopyranose[240], and the *Y. pestis* trisaccharide has a non-reducing end L-*glycero*-D-*manno*-heptose moiety[239]. Two respective semi-synthetic glycoconjugates were highly immunogenic in mice and gave rise to antibodies efficiently recognizing the native glycans on *B. anthracis*[250] and *Y. pestis*[251], respectively. Molecular interaction studies with mAbs revealed that the terminal non-mammalian monosaccharides were crucial for antibody binding that was characterized by nanomolar affinity in both cases.[239,240]

Uncovering potential glycan epitopes greatly benefits from recent advances in oligosaccharide synthesis[233] as well as methods that enable detailed quantitative glycan-antibody interaction studies, of which glycan microarrays[229,252,253], surface plasmon resonance[239,240] (SPR) and isothermal titration calorimetry[254] (ITC) are important examples.

Glycan microarray technology is a powerful tool for multiplexed glycan-protein interaction studies in high throughput.[229,233,252,253] A large number of oligo- or polysaccharides can be immobilized on the same microarray slide either covalently or *via* non-covalent adsorption.[253] Oligosaccharides produced by chemical synthesis bearing reducing end linkers with primary amines can be covalently coupled to active ester-functionalized glass slides [Fig. 1.6a].[239,240] Incubation with antibody-containing samples such as serum of healthy and diseased individuals provides a useful starting point for discovering antigenic glycan epitopes whose levels of antibody recognition correlate with clinical parameters.[253] Glycan-antibody interactions are quantitatively detected by virtue of fluorescence-labeled detection antibodies. Microarrays can also be utilized to determine epitope recognition patterns of anti-glycan mAbs.[239,240]

Glycan microarrays are restricted to high-affinity interactions, as weakly bound antibodies are removed during washing procedures. In contrast, SPR allows for detecting low-affinity

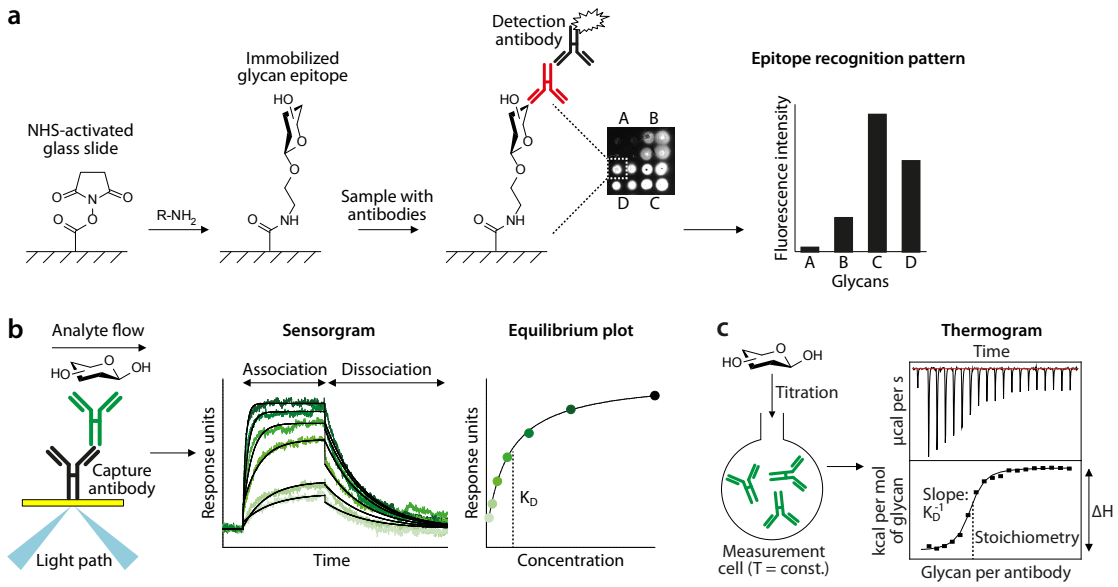

Figure 1.6: Methods to characterize glycan-antibody interactions. (**a**) Glycan microarray. Synthetic oligosaccharides are covalently immobilized *via* amino groups onto NHS ester-activated glass slides. Glycan-binding antibodies (red) are detected with a fluorescence-labeled antibody. Epitope recognition patterns to multiple glycans spotted onto the same slide are obtained. (**b**) SPR. A capture antibody is immobilized onto the sensor chip surface. Binding of glycans (analytes) to the captured anti-glycan mAb (green) is detected in real time by changes of intensity in the reflected light beam. The resulting sensorgram showing association and dissociation stages is used to infer binding kinetics by curve fitting (black overlaid lines). Alternatively, equilibrium constant K_D is determined with an equilibrium plot. (**c**) ITC. The glycan is titrated into an antibody solution (or *vice versa*) set to a constant temperature. Recorded heat changes yield a thermogram (top graph). An isotherm constructed by integration of injection peaks shows total enthalpy change (ΔH) over the glycan-to-antibody molar ratio (bottom graph). From the isotherm stoichiometry and K_D of the interaction is inferred. The depicted data is from experiments described in this thesis.

binding events down to the millimolar range and thereby represents a powerful complementary method. SPR can be employed to determine the affinity of mAb-glycan interactions and to map binding epitopes.[239,240,254] mAbs are either directly immobilized to the functionalized gold surface of the SPR sensor chip, or indirectly *via* capture antibodies recognizing the constant region of the mAb [Fig. 1.6b]. The latter approach is favorable since captured mAbs are not modified by the immobilization procedure and retain full binding activity. When glycans are passed over the sensor chip surface, their binding to the immobilized mAbs causes concentration-dependent changes in plasmon wavelength of the gold layer. These changes are detected by a beam of polychromatic light that is reflected from the gold surface. The wavelength that is in resonance with the surface plasmon is absorbed, which is detected in the reflected beam in real time and visualized as sensorgrams. From the sensorgrams, kinetic parameters of glycan-mAb interactions such as affinity, association and dissociation rate constants are inferred. SPR has been used, for instance, to study the

binding affinities and map the epitopes of mAbs against glycan antigens of *B. anthracis* and LPS structures of various Gram-negative bacteria.[239,240,254]

ITC is a useful technique for characterizing the thermodynamic parameters of glycan-mAb interactions in solution. Typically, the glycan antigen is titrated into a measurement cell that contains a solution of the mAb maintained at a constant temperature [Fig. 1.6c].[254] The heat released by glycan-mAb binding events is recorded by gradual glycan titrations as a function of time to yield a thermogram. By integration of the injection peak areas, an isotherm is calculated that is used to infer the affinity, stoichiometry, enthalpy (ΔH) and entropy (ΔS) of the interaction. Typical glycan-protein interactions are majorly enthalpy-driven through hydrogen bonding, van der Waals forces and electrostatic attractions when charged moieties are present.[256–262] Interactions involving hydrophobic groups can lead to favorable entropy by water displacement.[263] Thereby, recognition of methyl group-containing deoxy sugars such as rhamnose (6-deoxy-L-mannose) can contribute to antibody affinity, which may be harnessed for glycan epitope design.[249,264–266]

1.5.2 Fully Synthetic Glycan-based Vaccines

When conventionally displayed on glycoconjugates, small oligosaccharide antigens often induce only weak and inconsistent anti-glycan antibody responses due to immunodominance of the carrier protein.[267,268] Novel carrier strategies feature glycan antigens that are multivalently displayed on non-immunogenic synthetic backbones to enhance their immunogenicity.[269] Examples of synthetic carriers are cyclic[270] or dendrimeric[271] peptides that have shown favorable immunogenicity profiles in small animal studies, as well as oligo(amidoamine)s[272–276] (OAAs). Installment of a synthetic peptide T epitope can lead to T cell-dependent antibody responses.[269–271,277] Internal immunestimulatory molecules such as the toll-like receptor (TLR) agonist Pam_2CysSK_4[277] or glycosphingolipids (GSL) that activate natural killer T (NKT) cells[278,279] substitute for external adjuvants such as Alum [Fig. 1.7]. Fully synthetic vaccines would be less sensitive to temperature changes than conventional Alum-adsorbed glycoconjugates[280,281] and could thereby render cost-intensive cooling chains unneccessary.

1.5.3 Passive Vaccination with Monoclonal Antibodies against Antibiotic-Resistant Bacteria

Increasing drug resistance of *C. difficile* and many other bacterial pathogens has spawned the investigation of mAbs as therapeutic alternative to antibiotics.[282] Due to their surface-

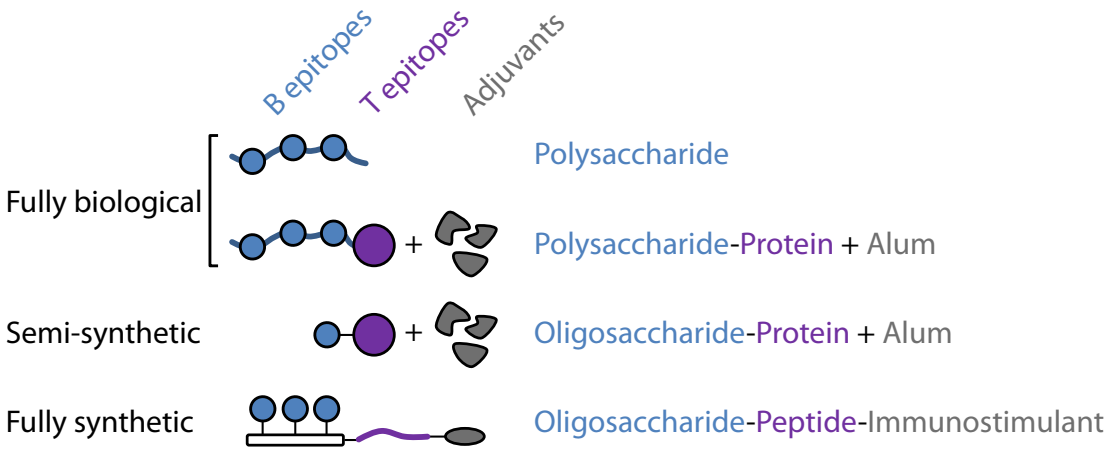

Figure 1.7: Evolution of glycan-based vaccines. First generation vaccines consist of free isolated polysaccharides that induce short-lived IgM responses to repetitive glycan B cell epitopes (blue circles).[224] By introduction of a carrier protein that contributes T cell epitopes and Alum as external adjuvant, long-lived and T cell-dependent IgG responses are generated.[224] Semi-synthetic vaccines contain carrier protein-linked synthetic oligosaccharide antigens and likewise require an external adjuvant.[234] Fully synthetic vaccines display one or multiple synthetic oligosaccharide antigens on a non-immunogenic carrier linked to a peptide T epitope and an immunostimulant serving as internal adjuvant, such as a TLR agonist or NKT-activating GSL.[277–279]

exposed nature and, compared to proteins, lower degree of antigenic variation, bacterial glycans provide formidable targets for anti-bacterial mAbs. As a recent example of this approach, mAbs directed against LPS of pathogenic *E. coli* significantly reduced the burden of bacterial disease in mice.[283] In the case of *C. difficile*, passive administration of mAbs against cell wall glycans could complement the comprehensively investigated toxin-neutralizing mAbs that are close to clinical implementation but only partially prevent recurrent disease (see **Section 1.3.3**).

1.6 Aims of this Thesis

Three known cell wall polysaccharides of *C. difficile* are promising targets for colonization-inhibiting antibacterial vaccines. Previous vaccine studies focusing on PS-II showed that this glycan antigen could efficiently induce the production of antibodies in small animals that recognized the bacterial surface. In contrast, little is known on the immunological properties of the other polysaccharides PS-I and LTA, as studies have been impeded by their low and inconsistent expression in cultured bacteria. To facilitate access to the latter glycans, Seeberger and coworkers have recently generated oligosaccharides of PS-I and LTA through chemical synthesis.[237,284,285]

This work aimed to evaluate the potential of synthetic oligosaccharides as anti-*C. difficile*

vaccine candidates through detailed studies on their immunological properties *in vitro* and *in vivo*. A comprehensive set of PS-I and LTA-derived oligosaccharides was kindly provided by Dr. Christopher Martin. Glycan microarray analyses were employed to reveal antigenic epitopes that served as a starting point for preclinical immunogenicity studies. The ability of CRM_{197} glycoconjugates displaying antigenic epitopes of PS-I and LTA to stimulate glycan-specific antibody responses was investigated in the mouse model. Anti-PS-I mAbs generated with the hybridoma technique helped to obtain comprehensive insights into glycan-antibody interactions using a combination of glycan microarray, SPR and ITC analyses. The interaction studies revealed a disaccharide minimal glycan epitope of PS-I that provided the basis of a fully synthetic vaccine candidate comprising five disaccharide copies and a CRM_{197} T cell epitope (kindly provided by Dr. Felix Wojcik). The ability of the synthetic construct to elicit anti-PS-I antibodies in mice was investigated. Cell culture-based *in vitro* assays were employed to assess whether polyclonal and monoclonal anti-glycan antibodies could reduce attachment of viable *C. difficile* bacteria to human colon epithelial cells. Finally, the *in vivo* protective efficacy of active vaccination with PS-I and LTA glycoconjugates and of passively administered anti-PS-I mAbs was studied in a murine model of *C. difficile* infection and disease.

Chapter 2

Materials & Methods

2.1 Materials

Instruments

Analytic balance XA205Du	Mettler Toledo; Urdorf, Switzerland
Autoclave Laboklav MV	SHP Steriltechnik; Detzel Schloss, Germany
Autoflex Speed MALDI-TOF system	Bruker Daltonics; Bremen, Germany
Balance M-prove	Sartorius AG; Göttingen, Germany
Biacore T100	GE Healthcare; Uppsala, Sweden
Biological safety cabinet Safe 2020	Thermo Scientific; Waltham, MA, USA
Centrifuge 5417R	Eppendorf; Hamburg, Germany
Centrifuge 5810R	Eppendorf; Hamburg, Germany
with swinging-bucket rotor, cat.no. A-4-81	
with microplate rotor, cat.no. A-2-DWP	
Centrifuge MiniSpin	Eppendorf; Hamburg, Germany
Centrifuge Multifuge 1 L-R	Thermo Scientific; Waltham, MA, USA
with swinging-bucket rotor, cat.no. 75002000	
with microplate rotor, cat.no. 75002010	
Centrifuge Sepatech Megafuge 1.0	Heraeus; Osterode, Germany
with swinging-bucket rotor, cat.no. 2150	
with microplate rotor, cat.no. 3471	
CO_2 cell culture incubator CB150	Binder; Tuttlingen, Germany
Flow cytometer FACS Canto II	BD Biosciences; Heidelberg, Germany
FPLC system Äkta Purifier UPC10	GE Healthcare; Uppsala, Sweden
Freezing container Nalgene	Sigma-Aldrich; St. Louis, MO, USA
Freeze dryer Alpha 2-4 LD Plus	Martin Christ; Osterode, Germany
Gel electrophoresis system Mini-Protein Tetra	Biorad; Munich, Germany
Horizontal shaker Yellow Line	IKA Werke; Staufen, Germany

continued on following page

Incubator hood TH 15	Edmund Bühler; Hechingen, Germany
LAS-4000 mini imager	Fujifilm; Tokyo, Japan
Light microscope Hund Wilovert	Wilovert; Buckinghamshire, UK
Light microscope Axiovert 40 C (inverted)	Zeiss; Oberkochen, Germany
Liquid nitrogen storage unit NRT 2010	Consarctic; Schoellkrippen, Germany
Magnetic stirrer RCT basic	IKA-Werke; Staufen, Germany
Microarray scanner 4300A	Molecular Devices; Sunnyvale, CA, USA
Microarray spotter sciFLEXARRAYER S3	Scienion; Berlin, Germany
Microcalorimeter MicroCal iTC200	GE Healthcare; Uppsala, Sweden
Microcentrifuge MiniStar silverline	VWR; Darmstadt, Germany
Micropipettes	Brandt; Wertheim, Germany
Microplate reader Infinite M200 PRO NanoQuant	Tecan Trading; Männedorf, Switzerland
NanoDrop ND-1000 Spectrophotometer	Thermo Scientific; Waltham, MA, USA
Neubauer cell counting chamber	Paul Marienfeld; Lauda Königshofen, Germany
pH-Meter 826 pH Mobile Meter	Metrohm Schweiz; Zofingen, Switzerland
Thermal shaker Thermomixer comfort	Eppendorf; Hamburg, Germany
Tissue homogenizer IKA T10	IKA-Werke; Staufen, Germany
Water bath TW8	Julabo; Seelbach, Germany

Consumables

Amicon Ultra centrifugal filters Ultracel	Merck Millipore; Tullagreen, Ireland
Bottle-top vacuum filters, 0.22 µm pore size	Corning; New York, NY, USA
Cell culture plates, 6-, 12-, 24-, 48- and 96-well	Corning; New York, NY, USA
Cell culture flasks, 25, 75, 150 and 300 cm^2	TPP; Trasadingen, Switzerland
Conical centrifuge tubes, 15 and 50 mL	Corning; New York, NY, USA
Cryogenic vials	Corning; New York, NY, USA
ELISA plates Nunc 96-well	Thermo Scientific; Waltham, MA, USA
Flow cytometry tubes	Sarstedt; Nürnberg, Germany
Injection needles, sterile	B. Braun; Melsungen, Germany
Microcentrifuge tubes, 0.5, 1.5 and 2 mL	Eppendorf; Hamburg, Germany
Microtiter plates, round-bottom, 96-well	Corning; New York, NY, USA
Microtiter plates, V-bottom, 384-well	Genetix; New Milton, UK
Pasteur pipettes, glass	Roth; Karlsruhe, Germany
Pipette tips	Greiner Bio One; Kremsmünster, Austria
Serological pipettes, 1, 5, 10 and 25 mL	Corning; New York, NY, USA
Syringes, sterile	B. Braun; Melsungen, Germany
Syringe filters, PVDF, 0.2 µm pore size	Roth; Karlsruhe, Germany

Kits, Reagents and Adjuvants

Acrylamide/bis-acrylamide, 30 % (29:1)	AppliChem; Darmstadt, Germany
Alum Alhydrogel gel adjuvant	Brenntag; Frederikssund, Denmark
Amersham ECL Prime Western Blotting Detection Reagent	GE Healthcare; Uppsala, Sweden
Amine Coupling Kit	GE Healthcare; Uppsala, Sweden
Bovine serum albumin (BSA), protease-free	VWR; Darmstadt, Germany
CodeLink-Activated Slides	SurModics; Eden Prairie, MN, USA
Complete Freund's adjuvant (CFA)	Sigma-Aldrich; St. Louis, MO, USA
2,5-Dihydroxyacetophenone (DHAP)	Bruker Daltonics; Bremen, Germany
Dulbecco's PBS buffer powder, 10 x	AppliChem; Darmstadt, Germany
Icomplete Freund's adjuvant (ICFA)	Sigma-Aldrich; St. Louis, MO, USA
Lipopolysaccharide (LPS), isolated from *E. coli*	Sigma-Aldrich; St. Louis, MO, USA
Micro BCA Protein Assay Kit	Thermo Scientific; Rockford, IL, USA
Mouse Antibody Capture Kit	GE Healthcare; Uppsala, Sweden
Mouse Antibody Isotyping Kit MMT1	AbD Serotec; Kidlington, UK
Mouse TNF-α Quantikine ELISA Kit	R&D Systems; Minneapolis, MN, USA
Murine IL-1β Standard ABTS ELISA Development Kit	Peprotech; Rocky Hill, NJ, USA
Murine IL-10 Standard ABTS ELISA Development Kit	Peprotech; Rocky Hill, NJ, USA
Murine IL-12 Standard ABTS ELISA Development Kit	Peprotech; Rocky Hill, NJ, USA
Murine IL-6 Standard ABTS ELISA Development Kit	Peprotech; Rocky Hill, NJ, USA
PageRuler Plus Prestained Protein Ladder	Thermo Scientific; Rockford, IL, USA
Polyethylene glycol (PEG) 1500	Roche; Mannheim, Germany
Protease Inhibitor Cocktail, EDTA-free, tablets	Sigma-Aldrich; St. Louis, MO, USA
Proteus Protein G Midi Purification Kit	AbD Serotec; Kidlington, UK
Recombinant Murine GM-CSF	Peprotech; Rocky Hill, NJ, USA
SPR sensor chips CM5	GE Healthcare; Uppsala, Sweden
3,3',5,5'-Tetramethylbenzidine (TMB)	Thermo Scientific; Rockford, IL, USA
N,*N*,*N'*,*N'*-Tetramethylethylenediamine (TEMED)	AppliChem; Darmstadt, Germany
Triethylamine	Sigma-Aldrich; St. Louis, MO, USA
Trypan Blue Solution, 0.4 %	Thermo Scientific; Rockford, IL, USA

Chemicals

Unless mentioned otherwise, all chemicals were analytical grade and purchased from Roth (Karlsruhe, Germany), Merck (Darmstadt, Germany) or Sigma-Aldrich (St. Louis, MO, USA). Deionized water in the following refers to water that was purified with a Milli-Q purification system (Merck Millipore; Billerica, MA, USA).

Antibodies

Flow cytometry	
Anti-mouse CD11c-APC (17-0114-81)	eBioscience; San Diego, CA, USA
Anti-mouse CD80-FITC (553768)	BD Biosciences; Heidelberg, Germany
Anti-mouse CD86-PE (553692)	BD Biosciences; Heidelberg, Germany
Anti-Mouse IgG (whole molecule)-FITC produced in goat (F0257)	Sigma-Aldrich; St. Louis, MO, USA
Goat anti-mouse IgG (H+L), AF 635 (A-31574)	Life Technologies; Carlsbad, CA, USA

Microarray	
AF 594 AffiniPure Donkey Anti-Mouse IgM, μ Chain Specific (715-585-140)	Dianova; Hamburg, Germany
Anti-Human IgA, (α-chain specific)-FITC produced in goat (F9637)	Sigma-Aldrich; St. Louis, MO, USA
Anti-Mouse IgA (α-chain specific)-FITC produced in goat (F9384)	Sigma-Aldrich; St. Louis, MO, USA
Goat anti-Human IgG (H+L), AF 647 (A-21445)	Life Technologies; Carlsbad, CA, USA
Goat anti-mouse IgG (H+L), AF 635 (A-31574)	Life Technologies; Carlsbad, CA, USA
Goat anti-mouse IgG1, AF 594 (A-21125)	Life Technologies; Carlsbad, CA, USA
Goat anti-mouse IgG2a, AF 647 (A-21241)	Life Technologies; Carlsbad, CA, USA
Goat anti-mouse IgG3, AF 488 (A-21151)	Life Technologies; Carlsbad, CA, USA

ELISA and western blot	
Anti-Diphtheria Toxin, goat (ab19950)	Abcam; Cambridge, UK
Anti-Goat IgG (whole molecule)-Peroxidase antibody produced in rabbit (A4174)	Sigma-Aldrich; St. Louis, MO, USA
Goat anti-Mouse IgG (H+L)-HRPO, MinX Hu,Bo,Ho, (115-032-062)	Dianova; Hamburg, Germany

Buffers and Solutions

Alum extraction buffer	0.6 M sodium citrate dihydrate, 0.55 M sodium phosphate dibasic, 30 mM sodium dodecyl sulfate, pH 8.5
Brine	Saturated aqueous solution of NaCl
Conjugation buffer for DSAP conjugation chemistry	100 mM sodium phosphate, pH 7.4
Conjugation buffer for *p*-nitrophenol chemistry	100 mM sodium phosphate, pH 8
Coomassie staining solution	0.5 % (w/v) Coomassie Brilliant Blue R-250, 50 % (v/v) methanol, 10 % (v/v) acetic acid
Coomassie destaining solution	50 % (v/v) methanol, 10 % (v/v) acetic acid
Coupling buffer	50 mM sodium phosphate, pH 8.5
Laemmli loading buffer, 4 x	40 % (v/v) glycerol, 0.25 M Tris-HCl, pH 6.8, with 4 % (w/v) SDS and 0.015 % (w/v) bromophenol blue
Phosphate-buffered saline (PBS)	137 mM NaCl, 2.9 mM KCl, 10 mM Na_2HPO_4, 1.8 mM KH_2PO_4, pH 7.4
PBS-T0.05	PBS with 0.05 % (v/v) Tween-20
PBS-T0.1	PBS with 0.1 % (v/v) Tween-20
PBS-BSA	PBS with 1 % (w/v) BSA
PBS-T-BSA	PBS with 0.01 % (v/v) Tween-20 and 1 % (w/v) BSA
Ponceau S staining solution	0.1 % (w/v) Ponceau S, 5 % (v/v) acetic acid
Protein A/G binding buffer	100 mM sodium phosphate, 150 mM NaCl, pH 7.4
Protein A/G elution buffer	200 mM glycine-HCl, pH 2.5
Protein A/G neutralization buffer	1 M Tris-HCl, pH 9
Quenching buffer for microarray	50 mM sodium phosphate, 50 mM ethanolamine, pH 9
Regeneration buffer for SPR	10 mM Tris-HCl, pH 1.7
SDS-PAGE running buffer	25 mM Tris, 192 mM glycine, pH 8.3, with 0.1 % SDS
SDS-PAGE separation buffer, 6 x	1.5 M Tris-HCl, pH 8.8
SDS-PAGE stacking buffer, 4 x	0.5 M Tris-HCl, pH 6.8
Silver stain fixing solution	50 % (v/v) ethanol, 12 % (v/v) acetic acid with 0.05 % (v/v) aqueous 37 % formaldehyde
Silver stain solution 1	1 mM $Na_2S_2O_3$
Silver stain solution 2	10 mM $AgNO_3$ with 0.08 % (v/v) aqueous 37 % formaldehyde
Silver stain solution 3	5 M Na_2CO_3, 1 mM $Na_2S_2O_3$ with 0.04 % (v/v) aqueous 37 % formaldehyde
Tris-buffered saline (TBS)	50 mM Tris-HCl, 150 mM NaCl, pH 7.5
TBS-T	TBS with 0.05 % (v/v) Tween-20
TBS-T-BSA	TBS with 0.05 % (v/v) Tween-20 and 1 % (w/v) BSA
Western blot transfer buffer	25 mM Tris, 192 mM glycine, 10 % (v/v) methanol, pH 8.3

Cell Culture Basal Media, Buffers and Supplements

BM Condimed H1 Hybridoma Supplement, 10 x	Roche; Mannheim, Germany
DPBS (Dulbecco's Phosphate-Buffered Saline)	PAN-Biotech; Aidenbach, Germany
DMEM (Dulbecco's Modified Eagle Medium)	PAN-Biotech; Aidenbach, Germany
DMSO cell culture grade	AppliChem; Darmstadt, Germany
Fetal bovine serum (FBS), South America 3302	PAN-Biotech; Aidenbach, Germany
Gentamycin, 50 mg/mL	Serva Electrophoresis; Heidelberg, Germany
L-Glutamine, stable, 200 mM	PAN-Biotech; Aidenbach, Germany
Hepes buffer solution, 1 mM	PAN-Biotech; Aidenbach, Germany
HT supplement, 50 x (5 mM hypoxanthine, 0.8 mM thymidine), Gibco	Life Technologies; Darmstadt, Germany
Hypoxanthine, aminopterin and thymidine (HAT) supplement, 50 x	Sigma-Aldrich; St. Louis, MO, USA
IMDM (Isocove's Modified Dulbecco's Medium), L-Glutamine and Hepes, with 3.024 g/L $NaHCO_3$	PAN-Biotech; Aidenbach, Germany
ISF-1 Medium, with 2.438 g/L $NaHCO_3$, L-Alanyl-L-Glutamine, Pluronic F68	Biochrom; Berlin, Germany
β-Mercaptoethanol, 50 mM in PBS	PAN-Biotech; Aidenbach, Germany
Non-essential amino acids (NEAA), 100 x	PAN-Biotech; Aidenbach, Germany
Pen/Strep (10,000 U/mL penicillin, 10 mg/mL streptomycin)	PAN-Biotech; Aidenbach, Germany
RPMI (Roswell Park Memorial Institute) 1640 medium, without L-Glutamine, with 2 g/L $NaHCO_3$	PAN-Biotech; Aidenbach, Germany
Sodium pyruvate, 100 mM	PAN-Biotech; Aidenbach, Germany
Trypsin/EDTA, 0.25 % / 0.02 % in PBS, without calcium and magnesium	PAN-Biotech; Aidenbach, Germany

Cell Culture Cultivation Media

All media were sterilized by filtering through bottle-top vacuum filters with 0.22 µm pore size before use. FBS was incubated at 56 °C for 45 min before use to inactivate complement proteins.

Complete IMDM	IMDM supplemented with 10 % FBS, 2 mM L-Glutamine, 1 mM sodium pyruvate, Pen/Strep (diluted 1:100), NEAA (diluted 1:100), 50 µM β-Mercaptoethanol and 50 µg/mL Gentamycin
Hybridoma selection	IMDM supplemented with 10 % FBS, 2 mM L-Glutamine, 1 mM sodium pyruvate, Pen/Strep (diluted 1:100), NEAA (diluted 1:100), 50 µM β-Mercaptoethanol, 50 µg/mL Gentamycin, BM Condimed H1 Hybridoma Supplement (diluted 1:10) and HAT (diluted 1:50)
Serum-free ISF-1	ISF-1 supplemented with Pen/Strep (diluted 1:100) and 50 µg/mL Gentamycin
Complete RPMI	RPMI supplemented with 10 % FBS, 2 mM L-Glutamine, 1 mM sodium pyruvate and Pen/Strep (diluted 1:100)
Bone marrow cell differentiation	RPMI supplemented with 10 % FBS, 2 mM L-Glutamine, Pen/Strep (diluted 1:100), 20 ng/mL recombinant murine GM-CSF
Complete MEM	MEM supplemented with 20 % FBS, 2 mM L-Glutamine and Pen/Strep (diluted 1:100)

Bacteria and Cell Lines

Clinical isolates of *C. difficile* ribotypes 001, 014, 027, 048 and 078 were kindly supplied by Dr. Ulrich Nübel of the Robert-Koch-Institut, Wernigerode, Germany. *C. difficile* ribotype 017 is a clinical isolate obtained by Prof. Jochen Mattner of the Universität Erlangen, Germany. *Clostridium bifermentans* was a kind gift of Dr. Jochen Klumpp of the ETH Zürich, Switzerland. The other bacteria were purchased from the Leibniz Institut DSMZ–Deutsche Sammlung von Mikroorganismen und Zellkulturen, Braunschweig, Germany. Mammalian cell lines were purchased from the American Type Culture Collection (ATCC), Manassas, VA, USA. Formalin-inactivated bacteria were stored in PBS at 4 °C. Mammalian cell lines were stored in liquid nitrogen (vapor phase) in appropriate culture medium supplemented with 10 % cell culture grade DMSO.

Bacteria	Source
Clostridium bifermentans	Environmental isolate, ETH Zurich
Clostridium perfringens	Environmental isolate, ETH Zurich
C. difficile reference strain DSM 1296	DSMZ
C. difficile ribotype 001	Clinical isolate, RKI Wernigerode
C. difficile ribotype 014	Clinical isolate, RKI Wernigerode
C. difficile ribotype 017	Clinical isolate, Universität Erlangen
C. difficile ribotype 027	Clinical isolate, RKI Wernigerode
C. difficile ribotype 046	Clinical isolate, RKI Wernigerode
C. difficile ribotype 078	Clinical isolate, RKI Wernigerode
Salmonella enterica DSM 17058	DSMZ
Streptococcus pneumoniae DSM 14377	DSMZ

Mammalian cell lines	Source
Caco-2 human colon adenocarcinoma (HTB-37)	ATCC
HL-60 human promyelocytic leukemia (CCL-240)	ATCC
P3X63Ag8.653 mouse myeloma (CRL-1580)	ATCC

Software

Biacore T100 Control and Evaluation Softwares	GE Healthcare; Uppsala, Sweden
Excel 2010	Microsoft; Redmond, Washington, USA
FACSDIVA Software 6.1.3	BD Biosciences; Heidelberg, Germany
FlexAnalysis Software	Bruker Daltonics; Bremen, Germany
FlowJo Analysis Software 7.6.5	Tree Star; Ashland, OR, USA
GenePix Pro 7	Molecular Devices; Sunnyvale, CA, USA
GraphPad Prism 6	GraphPad Software; La Jolla, CA, USA
OriginPro 8.6G Software	OriginLab; Northampton, MA, USA
sciFLEXARRAYER Software	Scienion; Berlin, Germany
Tecan i-control Software	Tecan Trading; Männedorf, Germany
UNICORN 5.11 Software	GE Healthcare; Uppsala, Sweden

2.2 Methods

Oligosaccharides

Oligosaccharides of *C. difficile* PS-I **1**-**6**[237,284] and **13**[286], the lipophosphoglycan capping tetrasaccharide of *Leishmania* species **8**[287-289] and oligomers of *C. difficile* LTA **17**-**19**[285] were synthesized by Dr. Christopher Martin according to published protocols. The hexasaccharide repeating unit of *C. difficile* PS-II **7**[236] was synthesized by Dr. Ju Yuel Baek, and 3-Deoxy-D-*manno*-oct-2-ulosonic acid (Kdo) **9**[290] was synthesized by Dr. You Yang, as described.

Preparation of Microarrays

Synthetic amine-functionalized oligosaccharides or proteins were immobilized on commercial *N*-hydroxysuccinimide (NHS) ester-activated microarray glass slides (CodeLink Activated Slides; SurModics; Eden Prairie, MN, USA) using a piezoelectric spotting device (S3; Scienion; Berlin, Germany) such that 64 identical subarrays were contained on each slide.[252] For spotting, oligosaccharides or proteins were diluted in coupling buffer (50 mM sodium phosphate, pH 8.5). Microarray slides were incubated in a humid chamber for 24 h at room temperature to complete coupling reactions. Remaining NHS ester groups were deactivated with quenching buffer (50 mM sodium phosphate, 50 mM ethanolamine, pH 9) for 1 h at 50 °C. Slides were rinsed three times with deionized water, dried by centrifugation (300 × *g*, 5 min) and stored desiccated until use.[252]

C. difficile Patients and Control Subjects

All clinical samples analyzed in this study were obtained from patients of the Universitätsklinikum Erlangen and were kindly provided by Prof. Jochen Mattner of the Universität Erlangen, Germany.[284] *C. difficile* infection (CDI) was diagnosed with a positive toxin ELISA and the growth of *C. difficile* from fecal material 5-25 days after the onset of clinical symptoms. The majority of CDI patients were hospitalized in intensive care units due to surgeries (e. g., abdominal, brain) or organ transplantation. The control groups reflect individuals whose fecal samples were sent in for microbial analysis as well as patients without diarrhea. Ten of the samples that were sent in for microbial analysis were not associated with gastrointestinal infections. In the remaining samples, *Salmonella enterica* (2 x), *Campylobacter jejuni* (1 x), *Citrobacter freundii* (4 x), *Pseudomonas aeruginosa* (2 x), *Proteus vulgaris* (1 x), *Providencia rettgeri* (1 x), *Enterobacter cloacae* (1 x) and *Candida albicans* (1 x) were identified. Most of the control subjects were ambulant patients, five suffered from malignant disease and eight were hospitalized in intensive care units. All CDI patients and controls were age- and sex-matched and between 10 and 92 years old.

Ethics Statement

Human serum and fecal samples: The study protocol (no. 4439) for the analysis of serum and fecal specimens of *C. difficile* patients and control individuals was approved by the Ethics Committee of the Universität Erlangen, Germany. ***Animal experiments:*** Mouse studies were

performed in strict accordance with the German regulations of the Society for Laboratory Animal Science and the European Health Law of the Federation of Laboratory Animal Science Associations. All efforts were made to minimize suffering. Experiments other than infection studies were performed at the Bundesinstitut für Risikobewertung, Berlin, Germany. Infection studies were performed by Prof. Jochen Mattner at the Universität Erlangen, Germany.

Processing of Blood Samples

Fresh mouse blood samples were transferred to 1.5 mL microcentrifuge tubes and incubated for at least 1 h at room temperature to induce blood clot formation. Blood was centrifuged for 10 min at 1,200 x *g* to separate erythrocytes from serum. Serum was carefully transferred from the supernatant into 0.5 mL microcentrifuge tubes and stored at -20 °C until use. Human serum samples were kindly provided by Prof. Jochen Mattner, Universität Erlangen, Germany.

Processing of Fecal Samples

Frozen human fecal samples were kindly provided by Prof. Jochen Mattner, Universität Erlangen, Germany. After thawing, stool samples were weighed in 1.5 mL microcentrifuge tubes. Two volumes of PBS supplemented with Protease Inhibitor Cocktail, EDTA-free (Sigma-Aldrich; St. Louis, MO, USA) per stool wet weight were added. Samples were vortexed vigorously, incubated on ice for 1 h, and centrifuged (10,000 x *g*, 20 min). Supernatants were carefully transferred into 0.5 mL microcentrifuge tubes and stored at -20 °C until use.

Microarray-assisted Binding Analysis of Antibodies

Spotted and quenched microarray slides were blocked using PBS with 1 % (w/v) BSA (PBS-BSA) for 1 h at room temperature, washed three times with PBS and dried by centrifugation. FlexWell 64 grids (Grace Bio-Labs; Bend, OR, USA) were applied to the slides to yield 64 wells for individual experiments.[252] Slides were incubated with fecal supernatant, serum or monoclonal antibodies (mAbs) diluted in PBS with 0.01 % (v/v) Tween-20 and 1 % (w/v) BSA (PBS-T-BSA). Fecal and serum samples were diluted 1:100 unless mentioned otherwise. mAbs were diluted at concentrations ranging from 0.001 to 50 $\mu g\,mL^{-1}$. Hybridoma supernatant was used undiluted. Slides were incubated with the respective samples for 1 h at room temperature in a humid chamber. Wells were washed three times using PBS with 0.1 % Tween-20 (PBS-T0.1). The grids were removed and slides were dried by centrifugation

(300 × *g*, 5 min). The dried microarrays were incubated with fluorescence-labeled detection antibodies diluted in PBS-T-BSA for 1 h at room temperature in a humid chamber. Equal distribution of the antibody solutions was achieved by application of coverslips, as described.[252] The following dilutions were used (detailed information on the antibodies can be found in the *Materials* section above): anti-human IgA (F9637), 1:100; anti-human IgG (A-21445), 1:400; anti-mouse IgA (F9384), 1:200; anti-mouse IgG (A-31574), 1:400; anti-mouse IgG1 (A-21125), 1:400; anti-mouse IgG2a (A-21241), 1:400; anti-mouse IgG3 (A-21151), 1:200; anti-mouse IgM (715-585-140), 1:200. After incubation with the detection antibodies, slides were washed three times with PBS-T0.1, rinsed once with deionized water and dried by centrifugation. The microarray slides were scanned with a GenePix 4300A scanner (Molecular Devices; Sunnyvale, CA, USA). The photomultiplier tube (PMT) voltage was adjusted to reveal scans free of saturated signals (usually, a value of 400). Image analysis was carried out with the GenePix Pro 7 software supplied with the 4300A instrument. Background-subtracted mean fluorescence intensity (MFI) values were exported to Microsoft Excel for further analyses. For competition microarray analyses, pooled sera of mice immunized with glycoconjugate **20** (Alum group, week 5, pooled, 1:1,500) was pre-incubated with adjuvant-extracted glycoconjugate **20** at 0.4 μg mL^{-1}, or CRM_{197} (50 μg mL^{-1}) as control, for 5 min before applying to blocked microarray slides. IgG antibody levels were detected and evaluated as above, using anti-mouse IgG (A-31574).

Synthesis of Di-*N*-Succinimidyl Adipate Spacer

2.3 g of *N*-hydroxysuccinimide and 2.79 mL of Et_3N were added to a solution of 1.453 mL adipoyl chloride in 90 mL tetrahydrofuran and reacted for 24 h while stirring. The solvent was evaporated *in vacuo* and the residue was partitioned between dilute aqueous hydrochloric acid and chloroform. The organic layer was separated and washed successively with water and brine, dried over sodium sulfate, filtered and evaporated to yield a white solid. The product was recrystallized from isopropanol. The structure and purity of the final product was confirmed by NMR spectroscopy with kind help of Dr. Stefan Matthies. DSAP spacer was stored in a desiccated environment to prevent hydrolysis.

Glycoconjugate Preparation with Di-*N*-Succinimidyl Adipate Spacer

In this procedure, di-*N*-succinimidyl adipate (DSAP) serves as crosslinking reagent between synthetic oligosaccharides bearing amine-functionalized linkers and lysine residues of the

carrier protein.[291] PS-I pentasaccharide **1** (3 mg) or PS-I disaccharide **3** (1.5 mg) were solubilized in 100 µL anhydrous dimethylsulfoxide (DMSO). LTA dimer **18** (2.6 mg) was dissolved in 200 µL anhydrous DMSO. Kdo **9** (2 mg) was dissolved in 190 µL anhydrous DMSO and 10 µL methanol. The respective solutions were added drop-wise, over a period of 30 min, to stirred solutions containing 10-fold molar excess of DSAP solubilized in 200 µL anhydrous DMSO with 10 µL Et_3N. The mixture was reacted for an additional 1.5 h at room temperature while stirring. After addition of 0.4 mL conjugation buffer (100 mM sodium phosphate, pH 7.4), non-reacted spacer was extracted twice with 10 mL of chloroform. The upper aqueous phase was recovered and immediately reacted with 1 mg of CRM_{197} (Pfénex; San Diego, CA, USA) that was solubilized in 1 mL of conjugation buffer. After 12 h of incubation at room temperature while stirring, the reaction product was desalted and concentrated with deionized water using 10 kDa centrifugal filter units (Merck Millipore; Tullagreen, Ireland). The protein concentration was determined with the Micro BCA Protein Assay Kit (Thermo Scientific; Rockford, IL, USA) according to the manufacturer's recommendations. Resulting glycoconjugates **10** (with pentasaccharide **1**), **11** (with Kdo **9**), **12** (with disaccharide **3**) and **20** (with LTA dimer **18**) were stored at 4 °C until use. A second preparation of the glycoconjugate with **1** termed **10'** was prepared using the same protocol with 2.9 mg **1** and 1 mg CRM_{197}. The GlcNAc-BSA glycoconjugate used to detect antibodies against the spacer moiety was prepared with this method and was a kind gift by Dr. Chakkumkal Anish.

Preparation of Sodium Dodecyl Sulfate Polyacrylamide Gels

Separation gels (10 %) were prepared by mixing 4.9 mL deionized water, 1.7 mL 6 x separation buffer (1.5 M Tris-HCl, pH 8.8), 3.3 mL acrylamide/bis-acrylamide 30 % (29:1) (AppliChem; Darmstadt, Germany), 100 µL of a 10 % (w/v) aqueous solution of ammonium persulfate (APS) and 10 µL of *N*,*N*,*N'*,*N'*-Tetramethylethylenediamine (TEMED) (AppliChem; Darmstadt, Germany). After application into a gel casting chamber (Mini-Protein Tetra; Biorad; Munich, Germany) the solution was gently overlaid with 50 % (v/v) isopropanol and the separation gel was allowed to polymerize for at least 30 min. The isopropanol layer was gently removed and the stacking gel solution composed of 3 mL deionized water, 1.25 mL 4 x stacking gel buffer (0.5 M Tris-HCl, pH 6.8), 0.65 mL acrylamide/bis-acrylamide, 100 µL of 10 % APS and 10 µL TEMED was added to the top of the polymerized separation gel. An appropriate comb was applied and the stacking gel was allowed to polymerize for at least 30 min. Gels were used directly or stored at 4 °C.

Sodium Dodecyl Sulfate Polyacrylamide Gel Electrophoresis

Protein samples were dissolved in Laemmli loading buffer (40 % (v/v) glycerol, 0.25 M Tris-HCl, pH 6.8 with 4 % (w/v) SDS and 0.015 % (w/v) bromophenol blue) and heated at 95 °C for 10 min. Samples were run on 10 % SDS-PAGE gels at 20 V cm^{-1} and stained with Coomassie staining solution (0.5 % (w/v) Coomassie Brilliant Blue R-250, 50 % (v/v) methanol, 10 % (v/v) acetic acid) for 30 min. Stained gels were destained with Coomassie destaining solution (50 % (v/v) methanol, 10 % (v/v) acetic acid). As an alternative to Coomassie staining, gels were stained by silver staining as follows. Gels were incubated in fixing solution (50 % (v/v) ethanol, 12 % (v/v) acetic acid with 0.05 % (v/v) aqueous 37 % formaldehyde) for 1 h. After washing twice with deionized water for 10 min, gels were incubated with silver stain solution 1 (1 mM $Na_2S_2O_3$) for 1 min and washed three times with deionized water for 20 s. Gels were incubated in silver stain solution 2 (10 mM $AgNO_3$ with 0.08 % (v/v) aqueous 37 % formaldehyde) for 12 min. After washing twice with deionized water for 20 s, gels were incubated silver stain solution 3 (5 M Na_2CO_3, 1 mM $Na_2S_2O_3$ with 0.04 % (v/v) aqueous 37 % formaldehyde) for 10-20 min until protein bands became visible. The reaction was stopped by washing twice with deionized water for 2 min.

Matrix-assisted Laser Desorption/Ionization with Time-of-Flight Mass Spectrometry

Mass spectra were acquired with an Autoflex Speed MALDI-TOF system (Bruker Daltonics; Bremen, Germany). Samples were spotted using the dried droplet technique with 2,5-dihydroxyacetophenone (DHAP) as matrix[292] on MTP 384 ground steel target plates (Bruker Daltonics). The matrix was prepared by dissolving 7.6 mg DHAP in 375 µL ethanol and addition of 125 µL of an 18 mg mL^{-1} aqueous solution of diammonium hydrogen citrate ($C_6H_8O_7 \cdot 2\,NH_3$). Samples were prepared by mixing 2 µL of desalted protein sample with 2 µL of DHAP matrix and 2 µL of 2 % (v/v) trifluoroacetic acid (TFA) prior to spotting. The mass spectrometer was operated in linear positive mode. Mass spectra were acquired over an m/z range from 30,000 to 210,000 and data was analyzed with the FlexAnalysis software provided with the instrument.

Glycan Determination with Anthrone Reagent

Anthrone reactions were performed in 96-well round-bottom plates following a published procedure[293] with modifications. 5 µL desalted solutions of **10**, **12***, **16** or CRM_{197} were added to 35 µL of a 0.1 % (w/v) solution of anthrone reagent in 98 % sulfuric acid. After incubation at 95 °C for 20 min, plates were cooled down for 10 min at room temperature and absorbance at 579 nm was determined in a spectrophotometric plate reader. Signals were compared to standard curves using D-Glucose and L-Rhamnose at a molar ratio of 3:2 (for **10**) or 1:1 (for **12*** and **16**). Such, total glycan content of the samples and average antigen-to-CRM_{197} molar ratios were calculated. For **12*** and **16**, this calculation yielded 20 molecules of disaccharide **3** and 1.3 molecules of pentavalent OAA **15** (equal to 6.5 molecules of the disaccharide **13**) per molecule of CRM_{197}, respectively.

Preparation of Intestinal Tissue Homogenates

A female C57BL/6 mouse immunized twice (at weeks 0 and 2) with **10** in the presence of Alum adjuvant as described below was sacrified at week 18 after initial immunization. An age-matched naïve mouse served as control. The intestinal tracts were surgically removed. Feces were obtained from the retrograde portion of the colon. The small intestine and the colon were separated from the remaining tissue and rinsed three times with ice-cold PBS supplemented with Protease Inhibitor Cocktail, EDTA-free (Sigma-Aldrich; St. Louis, MO, USA) to remove the luminal contents. Tissue was supplemented with 5 mL of ice-cold PBS with Protease Inhibitor and homogenized with an IKA T10 homogenizer (IKA-Werke; Staufen, Germany). After incubation on ice for 1 h, homogenates were centrifuged at 13,000 × *g* for 5 min. The supernatant was carefully removed and the protein content determined with the Micro BCA Protein Assay Kit (Thermo Scientific; Rockford, IL, USA) according to the manufacturer's recommendations. For microarray binding studies, the protein concentration was adjusted to 100 µg mL^{-1} with PBS.

Glycoconjugate Preparation with Di-*p*-Nitrophenyl Adipate Spacer

In this procedure, di-*p*-nitrophenyl adipate serves as crosslinker between synthetic oligosaccharides bearing amine-functionalized linkers and lysine residues of the carrier protein.[294] The crosslinking reagent was kindly provided by Dr. Sharavathi Guddehali Parameswarappa. To obtain glycoconjugate **12***, 2.2 mg (5.3 µmol) disaccharide **3** were reacted with 6-fold

molar excess of the crosslinking reagent in anhydrous DMSO/pyridine (2:1) in the presence of Et_3N for 2 h at room temperature. The reaction product was successively washed with dichloromethane/diethylether (1:1) until thin-layer chromatography (TLC) revealed complete removal of non-reacted crosslinking reagent. The reaction yielded 2.6 mg of the activated half ester as white solid (74 % yield). 1.4 mg (2.1 µmol) of the half ester were reacted with 2 mg (34.2 nmol) of CRM_{197} (Pfénex; San Diego, CA, USA) in 100 mM sodium phosphate buffer, pH 8, for 24 h at room temperature. To obtain glycoconjugate **16**, 380 µg (71.3 nmol) of pentavalent oligo(amidoamine) (OAA) **15** were reacted with 6-fold molar excess of the crosslinking reagent in anhydrous DMSO/pyridine (2:1) in the presence of Et_3N for 2 h at room temperature. The reaction product was successively washed with dichloromethane/diethylether (1:1) until TLC revealed complete removal of non-reacted crosslinking reagent. The reaction yielded 230 µg of the activated half ester as white solid (58 % yield). The complete reaction product was reacted with 0.5 mg of CRM_{197} in 100 mM sodium phosphate buffer, pH 8, for 24 h at room temperature. The resulting glycoconjugates were desalted and concentrated with deionized water using 10 kDa centrifugal filter units (Merck Millipore; Tullagreen, Ireland). The protein concentration was determined by measuring the absorbance at 280 nm in a Nanodrop ND-1000 spectrophotometer (Thermo Scientific; Waltham, MA, USA), using an extinction coefficient of 54,320 M^{-1} cm^{-1}. The extinction coefficient was calculated from the amino acid sequence of CRM_{197} retrieved from www.reagentproteins.com/product_detail/CRM197_Lyophilized.html with the ProtParam program on web.expasy.org/protparam/. The glycoconjugates were stored at 4 °C until use.

Western Blots

Proteins were separated by SDS-PAGE as described above and electroblotted in western blot transfer buffer (25 mM Tris, 192 mM glycine, 10 % (v/v) methanol, pH 8.3) onto polyvinylidene difluoride (PVDF) membranes using a tank blotting system. Ponceau S staining was performed to confirm successful protein transfer. After washing three times with TBS-T (Tris-buffered saline with 0.05 % (v/v) Tween-20) to remove the Ponceau stain, PVDF membranes were blocked with TBS-T containing 5 % (w/v) skimmed milk powder. The CRM_{197} protein was immunolabeled with goat anti-diphtheria toxin antibody (Abcam; Cambridge, UK) diluted 1:2500 in TBS-T with 1 % (w/v) BSA (TBS-T-BSA) and detected with anti-goat IgG horseradish peroxidase (HRP) conjugate antibody (Sigma-Aldrich; St. Louis, MO,

USA) diluted 1:5000 in TBS-T-BSA after three washing steps with TBS-T. PS-I glycans were immunolabeled with a mixture of mAbs 2C5, 10A1 and 10D6 (each at 2.5 μg mL^{-1} in TBS-T-BSA) and detected with anti-mouse IgG HRP conjugate antibody (Dianova; Hamburg, Germany) diluted 1:10,000 in TBS-T-BSA after three washing steps with TBS-T. Chemoluminescence was detected using the Amersham ECL Western Blotting Detection Reagent (GE Healthcare; Uppsala, Sweden) according to the manufacturer's recommendations, in a LAS-4000 mini imager (Fujifilm; Tokyo, Japan).

Alum Adsorption Studies

Two assays were performed to quantify the adsorption of glycoconjugate **20** or CRM_{197} (Pfénex; San Diego, CA, USA) to aluminum hydroxide gel adjuvant (Alum Alhydrogel; Brenntag; Frederikssund, Denmark). First, in a modified assay described by Skrastina *et al.*[295], Alum particles (3, 1.5, 0.3 or 0.03 μL) were incubated with 3 μg of glycoconjugate or CRM_{197} in PBS (final volume 20 μL) and briefly vortexed. Samples were incubated at 4 °C for 0.5, 1, 4 or 24 h while rotating or used directly after mixing. Samples were centrifuged at 3000 × *g* for 10 min. The protein concentration in the supernatant was determined with the Micro BCA Protein Assay Kit (Thermo Scientific; Rockford, IL, USA) modified such that it allowed for measuring small volume samples (5 μL) in a NanoDrop ND-1000 Spectrophotometer (Thermo Scientific; Waltham, MA, USA). Percent values were calculated by referencing to samples with Alum particles, but without protein set to 100 % and samples with protein, but without Alum set to 0 %. Second, a described flow cytometric assay[296] with modifications was performed. Different concentrations of the glycoconjugate or CRM_{197} (0.1, 1, 5 or 10 μg) were incubated with 10 μL of Alum in PBS (final volume 70 μL) at 4 °C while rotating for 24 h and subjected to flow cytometry, as described below.

Stability Studies of Glycoconjugates

To assess its long-term and temperature stability, glycoconjugate **20** was first filter-sterilized (0.22 μm pore size). The glycoconjugate was used either diluted in PBS, adsorbed to alum hydroxide gel adjuvant (Alum Alhydrogel; Brenntag; Frederikssund, Denmark) at a ratio of 1:1 (w/v), or formulated as 50 % (v/v) emulsion with Incomplete Freund's adjuvant (ICFA) (Sigma-Aldrich; St. Louis, MO, USA). All samples contained 15 μg of **20** in a final volume of 100 μL sterile PBS. The samples were incubated for one week at different temperature regimes (7 d at 4 °C, 6 d at 4 °C and 1 d at 37 °C, 4 d at 4 °C and 3 d at 37 °C, or 7 d at 37 °C).

The glycoconjugate was extracted from Alum particles with Alum extraction buffer (0.6 M sodium citrate dihydrate, 0.55 M sodium phosphate dibasic, 30 mM sodium dodecyl sulfate, pH 8.5), as described.[297] To 100 µL of the Alum-adsorbed glycoconjugate solution, 200 µL of Alum extraction buffer were added, mixed 10 times by inversion and incubated at 60 °C for 2.5 h with gently inverting the samples every 20 min. Samples were centrifuged at 425 x *g* for 2 min. The supernatant was directly used for analysis by SDS-PAGE or, after washing three times with deionized water using 10 kDa centrifugal filter units (Merck Millipore; Tullagreen, Ireland) to remove potentially detached glycans, to competition microarray studies. The glycoconjugate was extracted from ICFA emulsions by using a described procedure[298] with minor modifications. To the emulsions (100 µL), 50 µL of benzyl alcohol was added and vortexed for 20 min at maximum speed on a benchtop vortex. Samples were centrifuged at 16,100 x *g* for 10 min. Glycoconjugate was recovered from the aqueous (middle) phase that was used directly for SDS-PAGE or, after washing three times with deionized water using 10 kDa centrifugal filter units (Merck Millipore), to competition microarray studies.

Flow Cytometry

All flow cytometry measurements were performed with a FACS Canto II instrument (BD Biosciences; Heidelberg, Germany), counting at least 10,000 events per sample and using PBS with 1 % (w/v) BSA (PBS-BSA) as sample buffer. The acquired data was exported to the FlowJo Analysis Software 7.6.5 (Tree Star; Ashland, OR, USA) for further analysis. ***Bone marrow-derived dendritic cells:*** Bone marrow-derived dendritic cells (BMDCs) or bone marrow (BM) cells were incubated with anti-mouse CD11c-APC (eBioscience; San Diego, CA, USA), anti-mouse CD80-FITC and anti-mouse CD86-PE (both BD Biosciences; Heidelberg, Germany) antibodies, diluted 1:200 in PBS-BSA and incubated for 45 min at room temperature protected from light. Cells were washed once with PBS-BSA and subjected to flow cytometry. ***Opsonophagocytosis assay:*** Surface-bound bacteria were detected with anti-mouse IgG Alexa Fluor 635 antibody (Life Technologies; Carlsbad, CA, USA) diluted 1:200 in PBS-BSA and washed once with PBS-BSA prior to flow cytometric measurement. ***Alum adsorption assay:*** Alum particles that have been adsorbed with glycoconjugate **20** or CRM_{197} (Pfénex; San Diego, CA, USA) were blocked with 10 % (w/v) BSA in PBS for 30 min, washed once with PBS and incubated with undiluted hybridoma cell culture supernatant of a proprietary anti-CRM_{197} mouse IgG clone 8H6 (a kind gift by Dr. Chakkumkal Anish and Annette Wahlbrink) for 30 min. Particles were washed three times with PBS and incubated

with goat anti-mouse IgG (whole molecule)-FITC (Sigma-Aldrich; St. Louis, MO, USA) diluted 1:100 in PBS-BSA for 20 min. After washing once with PBS, particles were subjected to flow cytometry.

Animals

Mice were kept in individually ventilated cages (IVCs) in the animal facility of the Bundesinstitut für Risikobewertung, Berlin, Germany under specific pathogen-free (SPF) conditions. Mice were purchased from Charles River, Sulzfeld, Germany.

Immunizations

For all immunization studies, 6-8 weeks old, female C57BL/6 mice (Charles River; Sulzfeld, Germany) were used. Immunizations were performed *via* the subcutaneous (s. c.) route into the neck of mice using an injection volume of 100 µL and sterile needles with a length of 0.5 inches. Antigens were diluted in sterile PBS. Immunizations with Freund's adjuvant (FA) (Sigma-Aldrich; St. Louis, MO, USA) were performed as follows: For each first immunization (priming), the glycoconjugate or oligo(amidoamine) antigen (in PBS) was mixed with an equal volume of Complete Freund's adjuvant (CFA) with two 1 mL glass syringes connected through a polytetrafluoroethylene (PTFE) adapter to a homogeneous emulsion that was used for immunization. All subsequent immunizations were prepared with Incomplete Freund's adjuvant (ICFA) using the same procedure. For immunizations with Alum, glycoconjugate antigens (in PBS) were pre-adsorbed in 1.5 mL microcentrifuge tubes with 1 µL per µg protein of aluminum hydroxide gel adjuvant (Alum Alhydrogel; Brenntag; Frederikssund, Denmark) and rotated for 24 h at 4 °C. The glycan doses per injection were as follows: for glycoconjugates **10**, **12** and **20**, 3 µg; for oligo(amidoamine) **15**, 5 µg; for glycoconjugates **12*** and **16**, 1 µg.

Enzyme-linked Immunosorbent Assays

Cytokines: Commercial ELISA kits were used to determine concentrations of interleukins IL-1β, IL-6, IL-10 and IL-12 (Peprotech; Rocky Hill, NJ, USA) and tumor necrosis factor-alpha TNF-α (R&D Systems; Minneapolis, MN, USA) according to the manufacturer's recommendations. ***Whole cells and proteins:*** Formalin-inactivated bacteria at an optical density (OD_{600}) of 0.2 or proteins at a concentration of 2 or 10 µg mL^{-1} (all in PBS) were adsorbed to the surface of 96-well ELISA plates overnight at 4 °C. After washing once with

PBS, wells were blocked with PBS containing 1 % (w/v) BSA for 1 h at room temperature and washed once with PBS. Wells were incubated with pooled mouse sera diluted 1:300 (PS-I) or 1:500 (LTA/PS-III) or antibodies at the indicated concentrations in PBS with 0.01 % (v/v) Tween-20 and 1 % (w/v) BSA (PBS-T-BSA). After incubation for 1 h at room temperature, wells were washed three times with PBS containing 0.05 % (v/v) Tween-20 (PBS-T0.5). Wells were incubated with secondary antibodies, anti-mouse IgG HRP conjugate antibody (Dianova; Hamburg, Germany) diluted 1:10,000 or anti-goat IgG HRP conjugate antibody (Sigma-Aldrich; St. Louis, MO, USA) diluted 1:5000 (both in PBS-T-BSA) for 1 h at room temperature. After washing three times with PBS-T0.5, wells were incubated with 3,3',5,5'-Tetramethylbenzidine (TMB) substrate (Thermo Scientific; Rockford, IL, USA) and the color reaction was observed. After an appropriate incubation time at room temperature, the reaction was stopped with 2 % sulfuric acid. Absorbance at 450 nm was measured in a UV-Vis microplate reader (Tecan Trading; Männedorf, Germany).

Generation and Purification of Monoclonal Antibodies and Isotyping

The generation of mAbs to the pentasaccharide **1** followed our standard protocol[252] using glycoconjugate **10** composed of CRM_{197} (Pfénex; San Diego, CA, USA) and **1**. Six 6-8 weeks old, female C57BL/6 mice (Charles River; Sulzfeld, Germany) were subcutaneosly immunized with the glycoconjugate in the presence of aluminium hydroxide gel adjuvant (Alum Alhydrogel; Brenntag; Frederikssund, Denmark) three times in two-week intervals. Each immunization contained 3 µg of the immunogen **1**. The antibody response was followed weekly by glycan microarray-assisted analysis of sera for IgG antibodies to **1**, CRM_{197} and the generic spacer moiety composed of aminopentyl and adipoyl moieties, as well as control oligosaccharides. For serum IgG analysis, spotted and quenched microarray slides were blocked for 1 h using PBS with 1 % (w/v) bovine serum albumin (BSA) (PBS-BSA), washed three times with PBS and dried by centrifugation (300 x *g*, 5 min). Slides were then equipped with 64-well incubation chambers (FlexWell 64; Grace Bio-Labs, Bend, OR, USA), and incubated with mouse sera diluted 1:100 in PBS with 1 % (w/v) BSA and 0.01 % (v/v) Tween-20 for 1 h in a humid chamber. After washing three times using PBS with 0.1 % (v/v) Tween-20 (PBS-T0.1) and drying by centrifugation, the microarray slides were incubated for 1 h with anti-mouse IgG Alexa Fluor 635 antibody (A-31574) diluted 1:400 in PBS with 0.01 % Tween-20 (v/v) and 1 % BSA (w/v) (PBS-T-BSA) in a humid chamber. After washing three times using PBS-T0.1 and rinsing once with deionized water, microarray

slides were dried by centrifugation and scanned with a GenePix 4300A microarray scanner (Molecular Devices; Sunnyvale, CA, USA). The mouse with the highest IgG response to **1** was selected for splenocyte isolation one week after the third immunization. Splenocytes were fused with P3X63Ag8.653 myeloma cells (ATCC CRL-1580) that were grown in complete IMDM medium to obtain hybridomas using polyethylene glycol (PEG) 1500 (Roche; Mannheim, Germany).[252,299] The procedure followed the protocol of the BM Condimed H1 Hybridoma supplement (Roche; Mannheim, Germany). Fused hybridoma cells were seeded into ten 96-well cell culture plates using Hybridoma Selection medium and observed for clonal growth under a light microscope. Glycan microarray-assisted selection of hybridoma clones followed our standard protocol.[252] After the first subcloning step, Hybridoma Selection medium was replaced with complete IMDM containing BM Condimed H1 Hybridoma supplement and HT supplement (Life Technologies; Darmstadt, Germany) diluted 1:50. After three subsequent subcloning steps, three hybridoma clones, 2C5, 10A1, and 10D6, producing IgGs exclusively to **1** were recovered. To isolate mAbs, clonal hybridoma cells were gradually adapted to serum-free ISF-1 medium (Biochrom; Berlin, Germany) and expanded. IgGs from the supernatant medium were either isolated with the Proteus Protein G Midi Purification Kit (AbD Serotec; Kidlington, UK) or by fast protein liquid chromatography (FPLC). The isotypes of purified mAbs were determined with the Mouse Antibody Isotyping Kit MMT1 (AbD Serotec; Kidlington, UK) according to the manufacturer's recommendations.

Fast Protein Liquid Chromatography

FPLC was performed on an Äkta Purifier UPC10 System (GE Healthcare; Uppsala, Sweden) at 4 °C operated with the UNICORN 5.11 software supplied with the instrument. To purify monoclonal antibodies (mAbs) on large scale, up to 1 L of hybridoma supernatant was passed through 5 mL Pierce Protein A/G Chromatography cartridges (Thermo Scientific; Rockford, IL, USA) overnight at flow rates ranging from 0.5 to 1 mL min^{-1}. The next day, the following program was chosen to elute the resin-bound mAbs at a flow rate of 5 mL min^{-1}: 75 mL (15 column volumes) of 100 % Protein A/G binding buffer (100 mM sodium phosphate, 150 mM NaCl, pH 7.4) to wash the column, then 50 mL (10 column volumes) of 80 % Protein A/G binding buffer and 20 % Protein A/G elution buffer (200 mM glycine-HCl, pH 2.5) to remove non-specifically bound proteins, and finally 100 mL (20 column volumes) of 100 % Protein A/G elution buffer to elute IgGs. The flow-through was collected in 5 mL fractions in 15 mL conical tubes that contained an appropriate amount of Protein A/G neutralization

buffer (1 M Tris-HCl, pH 9) such that the final solutions attained approximately pH 7.4. The presence of protein within the fractions was followed by on-line UV absorption at 280 nm. The fractions that contained eluted IgG were concentrated using 10 kDa centrifugal filter units (Merck Millipore; Tullagreen, Ireland) with PBS. Protein concentration was determined with a NanoDrop ND-1000 Spectrophotometer (Thermo Scientific; Waltham, MA, USA). mAbs were stored at 4 °C in PBS. For long-term storage, 0.02 % (w/v) sodium azide was added.

Surface Plasmon Resonance

All SPR measurements were performed on a Biacore T100 instrument (GE Healthcare; Uppsala, Sweden) using CM5 sensor chips and PBS as running buffer. ***Polyclonal serum antibody analysis:*** Pentasaccharide **1** or disaccharide **3** were coupled to the sensor chip surface using the Amine Coupling Kit (GE Healthcare) and the standard parameters of the *Immobilization* procedure in the Biacore Control software provided with the instrument. Coupling conditions were the following: oligosaccharides diluted to 2 mM in 100 mM sodium phosphate buffer, pH 7.4, a flow rate of 10 μL min^{-1} and 420 s contact time, 25 °C. Binding runs were performed with the standard parameters of the *Binding* function, using serum diluted 1:50 in PBS, a flow rate of 30 μL min^{-1} and a temperature of 25 °C. To compensate for non-specific binding of serum components, samples were injected such that they passed through a flow cell functionalized with 10,000 response units (RU) of BSA. The binding responses were monitored as a function of time (sensorgram) and were double-referenced with PBS injections and BSA-functionalized flow cells. Regeneration buffer (10 mM glycine-HCl, pH 1.7) was passed through the flow cells for 30 s after each single measurement. Binding and stability values were assessed with the Biacore Evaluation software provided with the instrument. ***Analysis of mAbs:*** Affinities of mAbs were determined as described.[239] Measurement flow cells were functionalized with about 10,000 RU of mouse IgG capture antibody using Mouse Antibody Capture and Amine Coupling kits (both GE Healthcare) following the manufacturer's recommendations. Blank-immobilized flow cells were used as reference to compensate for non-specific binding of analytes to the sensor chip surface. Kinetic measurement runs were performed with the Biacore T100 Control software supplied with the instrument by using the *Kinetics* function. All measurements were performed at 25 °C and a flow rate of 30 μL min^{-1}. Approximately 500 RU of mAbs were captured at a concentration of 50 μg mL^{-1} in PBS. Then, oligosaccharides or oligo(amidoamine) (OAA) constructs (all diluted in PBS) were passed through both reference and measurement flow

cells at various concentrations. Standard parameters for association and dissociation times were applied unless mentioned otherwise. After each single measurement, flow cells were treated with regeneration buffer (10 mM glycine-HCl, pH 1.7) for 30 s. Kinetic evaluation of binding responses was performed with the Biacore T100 Evaluation software supplied with the instrument, using sensorgrams double-referenced to PBS injections and blank flow cells. Two kinetic models, a 1:1 binding Langmuir model and a two-state reaction model (the latter assuming a conformational change in the antibody-analyte complex) were evaluated for data fitting. The quality of fits was evaluated by inspecting residual plots, chi square and standard error values for association and dissociation rate constants (k_a and k_d, respectively). Both models yielded comparable fittings. The 1:1 binding model was chosen over the two-state reaction model to calculate k_a, k_d and equilibrium constant (K_D) values, as the former makes fewer assumptions. When k_a and/or k_d were outside of the measurable ranges of the instrument, a steady-state equilibrium model was used instead to infer K_D values. The kinetic 1:1 binding model was generally preferred over the steady-state model in cases where both were applicable since the former provides more information. Kinetic and steady-state fits yielded comparable K_D values. Fitting of the dissociation stage only was performed with a custom kinetic model kindly supplied by Dr. Uwe Bierfreund (GE Healthcare). Thermodynamic parameters were inferred by using the *Thermodynamics* function of the Biacore T100 Control software with the same experimental set-up described above but temperatures ranging from 13 to 37 °C. Values for the changes in Gibb's free energy (ΔG), enthalpy (ΔH) and entropy (ΔS) were inferred by van't Hoff analysis with the Biacore T100 Evaluation software. Interaction Map (IM) analysis from SPR binding traces was kindly carried out by Dr. Karl Andersson (Ridgeview Diagnostics; Uppsala, Sweden) according to published procedures.[300]

Isothermal Titration Calorimetry

All measurements were performed in a MicroCal ITC200 system (GE Healthcare; Uppsala, Sweden) that was provided by Prof. Markus Wahl of the Freie Universität Berlin, Germany with kind technical assistance of Nicole Holton. The temperature was 25 °C. Oligosaccharides **1** or **3** at 250 µM or 3 mM, respectively, were titrated into the measurement cell containing 7 µM of monoclonal antibodies 2C5 or 10A1 in PBS using an injection volume of 2 µL. The reference cell contained PBS only. Data analysis was performed with the OriginPro 8.6G software (OriginLab; Northampton, MA, USA) provided with the instrument. The *One Set of Sites* model was used to fit the data points to infer thermodynamic parameters and

stoichiometry values. Data for the low c value measurements in the case of disaccharide **3** were fitted with a constant stoichiometry of 2.

In vitro Differentiation of Mouse Bone Marrow Cells and Stimulation Assays

Bone marrow (BM) cells were isolated from femurs and tibias of six weeks old female BALB/c mice. Cell suspensions were adjusted to 10^6 cells mL^{-1} and seeded into 6-well cell culture plates (3 mL per well) in bone marrow cell differentiation medium (RPMI supplemented with 10 % FBS, 2 mM L-Glutamine, Pen/Strep (diluted 1:100) and 20 ng mL^{-1} recombinant murine GM-CSF (Peprotech; Rocky Hill, NJ, USA)). Cells were incubated for 8 days at 37 °C and 5 % CO_2 to induce differentiation into dendritic cells (DCs). Every 2-3 days, cells were fed by gently swirling the plates, aspirating 75 % of the medium and adding fresh bone marrow cell differentiation medium. Successful differentiation was assessed by flow cytometric determination of CD11c expression with non-differentiated BM cells serving as controls. For stimulation assays, BM-derived dendritic cells (BMDCs) were adjusted to 2.5×10^6 cells mL^{-1} in medium without GM-CSF and seeded into 96-well cell culture plates (200 µL per well) supplemented with different concentrations of LTA dimer **18** or *E. coli* lipopolysaccharide (LPS) (Sigma-Aldrich; St. Louis, MO, USA). BMDCs in medium alone served as control. Cells were incubated for 12 h at 37 °C and 5 % CO_2. Culture supernatants were recovered for cytokine determination by ELISA and cells for flow cytometric quantitation of DC activation markers.

Opsonophagocytosis Assay

The OPA followed published procedures[301] with modifications. The assay was performed with HL-60 cells (CCL-240; American Type Culture Collection; Manassas, VA, USA) that were differentiated to granulocyte-like cells with *N,N*-dimethylformamide (DMF), as described.[302] HL-60 cells (10^5 cells mL^{-1}) were incubated in RPMI-1640 with 10 % fetal calf serum, 100 U mL^{-1} penicillin, 100 µg mL^{-1} streptomycin, 2 mM L-Glutamine and 100 mM DMF for seven days at 37 °C and 5 % CO_2. Cell viability was confirmed by Trypan Blue exclusion assay. Cells with a viability of 80-90 % were used. All incubation and washing steps were performed with 1 % BSA in PBS. Formalin-inactivated bacteria (*C. difficile* ribotype 014) were incubated with pooled serum of mice immunized with glycoconjugate **20** in the presence of Alum (sera of weeks 0 and 5) diluted 1:50 for 30 min at 37 °C while shaking. Bacteria were washed three times. Bacterial adhesion was performed in 96-well round-bottom plates by adding 25 µL

bacterial suspension with an optical density (OD_{600}) of 1.2 to 10^6 differentiated HL-60 cells in a final volume of 125 µL per well and incubation at 4 °C for 30 min. Cells were washed three times with ice-cold buffer to remove unbound bacteria. Then, cells were incubated for 45 min at either 4 °C to measure adhesion or 37 °C to measure phagocytosis. After washing three times with ice-cold buffer, non-phagocytosed bacteria were detected by incubating cells with pooled serum (week 5) diluted 1:50 for 20 min and, after washing once, with goat anti-mouse IgG Alexa Fluor 635 antibody (Life Technologies; Carlsbad, CA, USA) diluted 1:500. The amount of surface-bound bacteria was determined by flow cytometry.

C. difficile Adhesion Inhibition Assay

This assay was performed with kind help of Prof. Jochen Mattner and Erik Wegner at the Universität Erlangen, Germany. The ability of antibodies to inhibit bacterial adhesion to intestinal surfaces was determined with an *in vitro* assay described before[303–305] with minor modifications. Caco-2 human colon epithelial cells (HTB-37; American Type Culture Collection; Manassas, VA, USA) were seeded into 96-well tissue culture plates (2×10^4 cells per well) in complete MEM (MEM supplemented with 20 % FBS, 2 mM L-Glutamine and Pen/Strep diluted 1:100) and grown for 2 days at 37 °C and 5 % CO_2 to obtain confluent monolayers. Cells were rinsed twice with serum- and antibiotics-free MEM and *C. difficile* bacteria obtained from liquid overnight cultures were washed twice with PBS. Cells and bacteria were pre-incubated at 37 °C and 5 % CO_2 with either pooled sera of mice immunized with glycoconjugate **20** (diluted 1:100 in MEM), 10 % xylitol solution in MEM, monoclonal antibody 2C5 (100 µg mL^{-1} in MEM) or MEM alone, cells for 45 min and bacteria for 10 min. Then, *C. difficile* suspensions were added to the Caco-2 monolayers (4×10^4 bacteria per well) and co-incubated at 37 °C and 5 % CO_2 for 1 h. Non-adherent bacteria were removed by washing three times with MEM. The monolayers were then treated with 1 % EDTA in PBS and detached by vigorous pipetting. Cell suspensions were vortexed, plated at appropriate dilutions onto blood agar plates and cultivated for at least 24 h at 37 °C under anaerobic conditions before counting of colony-forming units (CFUs).

C. difficile Challenge Studies

The challenge studies were performed with the kind help of Prof. Jochen Mattner and Erik Wegner at the Universität Erlangen, Germany. Female, 6-8 weeks old C57BL/6 mice were rendered susceptible to *C. difficile* infection and colitis with intraperitoneal (i. p.) injections

of clindamycin (20 mg per kg body weight) for one day.[306] The next day, mice were challenged *via* oral gavage with 10^7 (active immunization studies) or 10^8 (passive immunization studies) CFUs of the *C. difficile* strain M68.[307] M68 is a clindamycin-resistant ribotype 017 strain isolated from a hospital outbreak of *C. difficile* disease in Dublin, Ireland.[156] Intestinal colonization was quantified five or eight days after the infection by determining the *C. difficile* CFUs in fecal suspensions that were plated at limited dilutions on selective agar medium and cultivated for 24 h at 37 °C. The degree of colonization is diplayed as CFUs per g of feces. *Enterococcus* spp. CFUs served as control. Characteristic colonies were counted and identified at random by MALDI-TOF MS analysis. Histopathological analysis of colon samples was performed to determine the degree of colitis. For active immunization experiments, mice received Alum-adjuvanted glycoconjugates s. c. at doses corresponding to 3 µg glycan antigen. Glycoconjugates **10**' and **11** were administered two times at days -21 and -7 relative to the infection, **20** and CRM_{197} (a protein amount equal to **20**) were injected three times at days -35, -21 and -7. For passive immunization studies, mice received purified monoclonal antibodies i. p. and intrarectally (i. r.), both 100 µg, three times at days -7, -3 and 0 relative to bacterial challenge. Control groups contained non-infected and sham-immunized (with an equivolume of PBS) mice.

Chapter 3

Results

Parts of the results presented in this thesis have been published in the following articles:

Broecker F, Martin CE, Wegner E, Mattner J, Baek JY, Pereira CL, Anish C, Seeberger PH. 2016. Synthetic lipoteichoic acid glycans are potential vaccine candidates to protect from *Clostridium difficile* infections. *Cell Chem Biol* **23:** 1014–1022. DOI: http://dx.doi.org/10.1016/j.chembiol.2016.07.009

Broecker F, Hanske J, Martin CE, Baek JY, Wahlbrink A, Wojcik F, Hartmann L, Rademacher C, Anish C, Seeberger PH. 2016. Multivalent display of minimal *Clostridium difficile* glycan epitopes mimics antigenic properties of larger glycans. *Nat Commun* **7:** 11224. DOI: http://dx.doi.org/10.1038/ncomms11224

Martin CE, Broecker F, Eller S, Oberli MA, Anish C, Pereira CL, Seeberger PH. 2013. Glycan arrays containing synthetic *Clostridium difficile* lipoteichoic acid oligomers as tools toward a carbohydrate vaccine. *Chem Commun* **49:** 7159–7161. DOI: http://dx.doi.org/10.1039/c3cc43545h

Martin CE, Broecker F, Oberli MA, Komor J, Mattner J, Anish C, Seeberger PH. 2013. Immunological evaluation of a synthetic *Clostridium difficile* oligosaccharide conjugate vaccine candidate and identification of a minimal epitope. *J Am Chem Soc* **135:** 9713–9722. DOI: http://dx.doi.org/10.1021/ja401410y

A discussion and outlook of the results presented in this chapter is provided in **Chapter 4**.

3.1 Synthetic *C. difficile* Polysaccharide-I Glycans as Vaccine Candidates

The potential of synthetic *C. difficile* PS-I glycans as immunogens for preventive vaccines was investigated. The PS-I-derived oligosaccharides used in this study were kindly provided by Dr. Christopher Martin and obtained following published synthetic routes.[237,284] They comprised the pentasaccharide repeating unit, α-Rha*p*-(1→3)-β-Glc*p*-(1→4)-[α-Rha*p*-(1→3)]-α-Glc*p*-(1→2)-α-Glc*p* **1** and substructures thereof; trisaccharide Rha-(1→3)-Glc-(1→4)-Glc **2**, disaccharide Rha-(1→3)-Glc **3**, rhamnose **4**, tri-glucoside Glc-(1→4)-Glc-(1→2)-Glc **5** and di-glucoside Glc-(1→2)-Glc [Fig. 3.1]. The following three structurally nonrelated oligosaccharides served as controls. *C. difficile* PS-II hexasaccharide repeating unit **7** was kindly prepared by Dr. Ju Yuel Baek following reported synthesis protocols.[236] The lipophosphoglycan capping tetrasaccharide of *Leishmania* species **8** was synthesized by Dr. Christopher Martin, as described.[287–289] 3-Deoxy-D-*manno*-oct-2-ulosonic acid (Kdo) **9** was kindly supplied by Dr. You Yang.[290] All oligosaccharides were equipped with an aminopentyl linker moiety at the reducing end that allowed for orientation-specific covalent linkage to microarray surfaces and protein carriers to facilitate their immunological evaluation.

3.1.1 Synthetic PS-I Glycans Are Antigenic and Recognized by Antibodies of *C. difficile* Patients

One prerequisite for an oligosaccharide to act as candidate immunogen for a vaccine is its recognition by antibodies raised during natural human infection, referred to as antigenicity.[253] Precedence for this approach is provided by the identification of serum IgG antibodies to clostridial toxins in CDI patients by enzyme-linked immonosorbent assay (ELISA) that was the starting point to the successful use of toxins for vaccination.[135,137–139] The recent glycan microarray-assisted detection of secreted IgA (sIgA) antibodies to the synthetic PS-II repeating unit **7** in the feces of CDI patients by Seeberger and colleagues provided first experimental evidence for the antigenicity of *C. difficile* surface glycans.[236] Consequently, **7** proved to be immunogenic in mice. Glycan microarrays are a powerful tool to characterize the antigenic properties of oligosaccharides by enabling multiplexed binding studies with antibodies of diverse clinical specimens.[253] The recognition patterns of natural antibodies to a given set of oligosaccharides allows for the rational selection of the most promising glycan epitope(s) for subsequent immunological studies in small animal models.

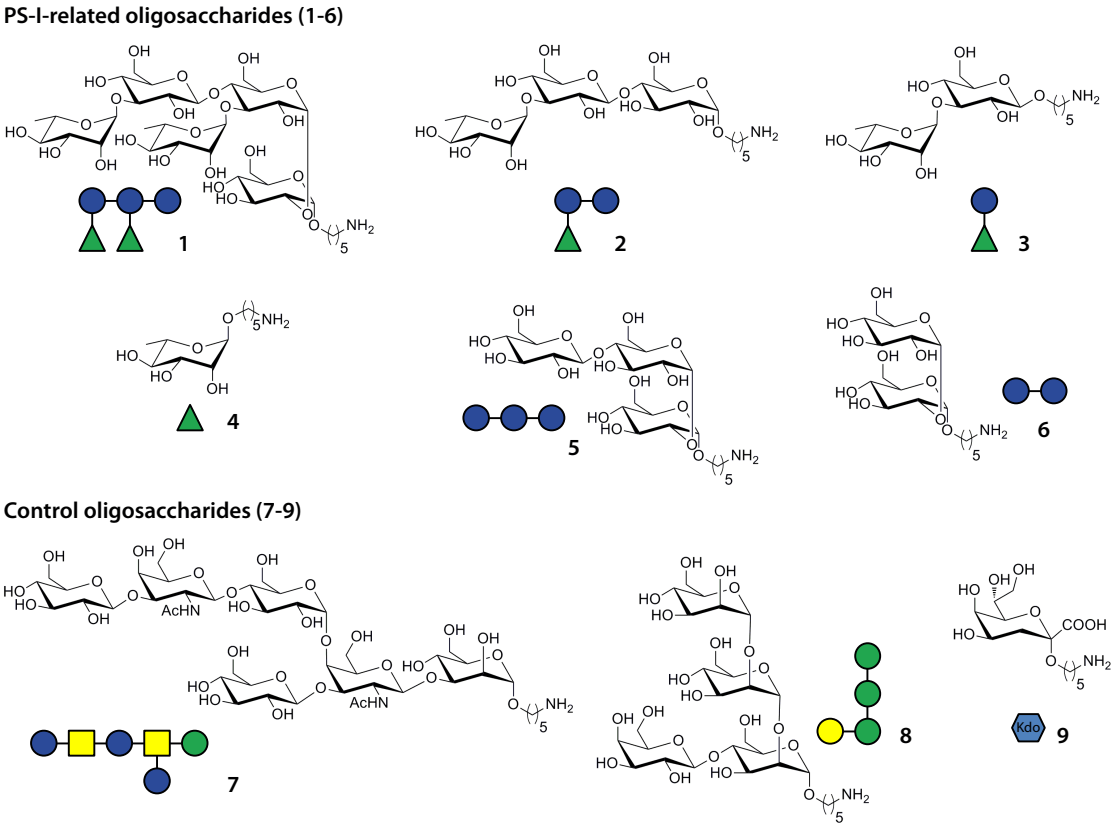

Figure 3.1: Synthetic oligosaccharides of *C. difficile* PS-I **1**-**6** and control glycans, *C. difficile* PS-II hexasaccharide **7**, *Leishmania* lipophosphoglycan capping tetrasaccharide **8** and Kdo **9**.

To investigate their antigenicity, PS-I oligosaccharides **1**-**6** were covalently coupled *via* the amine-functionalized linkers to the surface of *N*-hydroxysuccinimide (NHS) ester-activated microarray slides. This enabled the multiplexed screening for glycan-specific antibodies in human clinical specimens [Fig. 3.2a]. Oligosaccharides **7** and **8** as well as coupling buffer were spotted as controls [Fig. 3.2b]. The clinical samples used in this study were kindly provided by Prof. Jochen Mattner of the Universität Erlangen, Germany. First, sera obtained from 35 reconvalescent CDI patients (diagnosed with toxigenic *C. difficile* and recovered) were tested for the presence of IgG to **1**-**8**. 24 age- and sex-matched individuals without known history of CDI served as control group. Serum IgG to the *C. difficile* glycans **1**-**7** was detected in all individuals of both groups [Fig. 3.2b]. IgG to **8** was found in about 50 % of all individuals at generally low levels (data not shown). Quantitative analysis of serum IgG levels to **1**-**7** revealed a high degree of inter-individual variation in both groups [Fig. 3.2c]. The universal presence of IgG to rhamnose **4** confirmed reports by others.[308,309] There was no statistically significant difference in serum IgG levels between CDI patients and controls for any of the investigated glycans except for tri-glucoside **5**. Collectively, microarray-assisted serum IgG

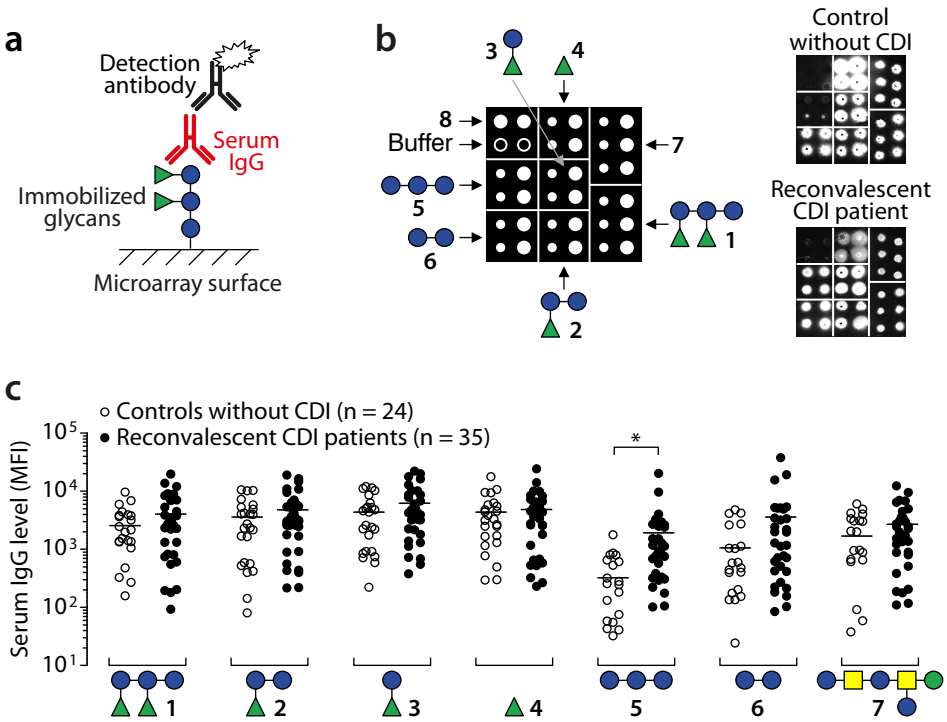

Figure 3.2: Microarray-assisted detection of IgG to PS-I glycans in human serum specimens. (**a**) Experimental setup. Oligosaccharides were coupled to microarray surfaces and probed with sera containing IgG that was detected by a fluorescence-labeled anti-IgG antibody. (**b**) The microarray spotting pattern is shown to the left. Oligosaccharides were spotted at 0.1 mM (small circles) or 1 mM (large circles). Representative microarray scans are shown to the right. (**c**) Serum IgG levels expressed as microarray-inferred mean fluorescence intensity (MFI) values obtained from the indicated oligosaccharides spotted at 1 mM. Circles represent single individuals (mean values of two experiments), horizontal lines the mean of each group. $^{*}P \leq 0.05$; unpaired two-tailed Student's *t*-Test. Figure modified from Martin *et al.*[284]

analysis demonstrated that synthetic PS-I glycans **1**-**6** are antigenic and represent naturally occurring epitopes recognized by systemic human antibodies.

sIgA serves as first line of defense against intestinal infections.[310] To investigate for the presence of sIgA to PS-I epitopes, fecal specimens obtained from 19 CDI patients and 23 age- and sex-matched controls without CDI were subjected to glycan microarray analysis [Fig. 3.3a]. The majority of samples of both groups contained detectable levels of sIgA to **1**-**6** and **7** [Fig. 3.3b]. sIgA to PS-II hexasaccharide **7** has been identified previously in feces of CDI patients.[236] Fewer than 50 % of all samples contained detectable amounts of sIgA to **8** (data not shown). Quantitative analysis revealed that levels of sIgA to **1**-**7** were highly variable inter-individually [Fig. 3.3c]. While there was no statistically significant difference between CDI and control individuals, the data verified the presence of mucosal antibodies to PS-I epitopes **1**-**6**. The presence of fecal sIgA and serum IgG to **1**-**7** in non-CDI control individuals may have been the result of previous asymptomatic exposure to *C. difficile*.[40]

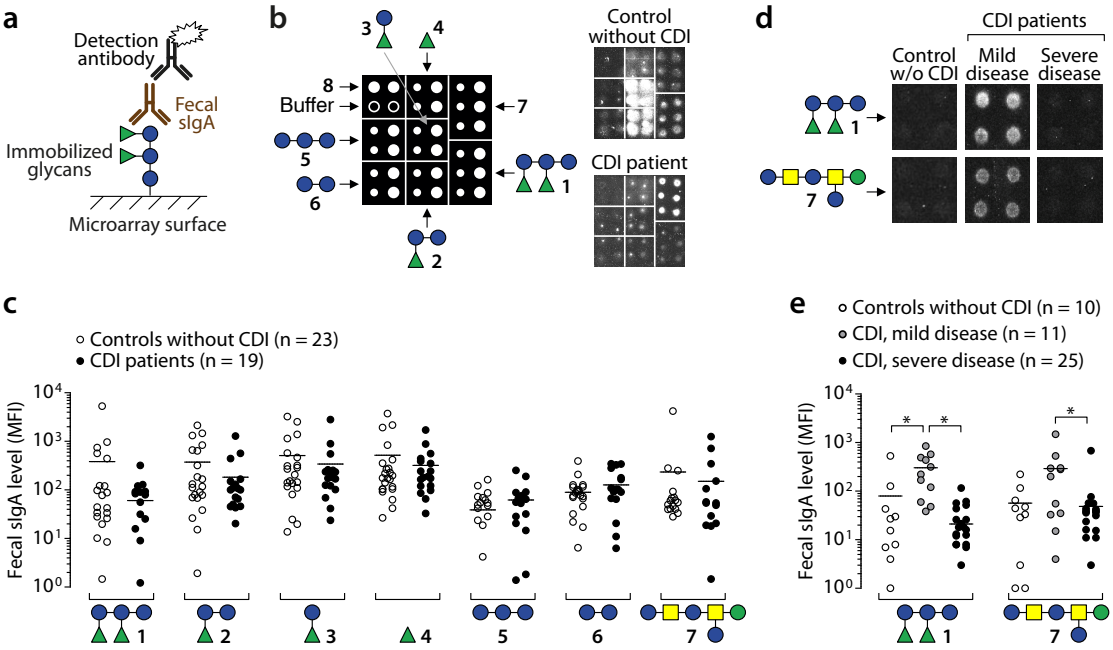

Figure 3.3: Microarray-assisted detection of sIgA to PS-I glycans in human fecal specimens. (**a**) Experimental setup. Oligosaccharides were coupled to microarray surfaces and probed with fecal supernatants containing sIgA that was detected with fluorescence-labeled anti-IgA antibody. (**b**) The microarray spotting pattern is shown to the left. Oligosaccharides were spotted at 0.1 mM (small circles) and 1 mM (large circles). Representative microarray scans are shown to the right. (**c**) Fecal sIgA levels of the indicated patient groups expressed as microarray-inferred MFI values obtained from the indicated oligosaccharides spotted at 1 mM. Circles represent single individuals (mean values of two experiments), horizontal lines the mean of each group. (**d**) Exemplary microarray scans representing fecal sIgA signals to the indicated glycans spotted at 1 mM in quadruplicate. (**e**) Fecal sIgA levels of the indicated patient groups depicted as in panel (**c**). $^*P \leq 0.05$; unpaired two-tailed Student's *t*-Test. Figure modified from Martin *et al.*[284]

High levels of fecal sIgA to TcdA in CDI patients have been shown to correlate with mild clinical symptoms, suggesting protective effects of these particular antibodies.[311] To determine whether glycan-specific fecal sIgA levels likewise correlate with disease symptoms, additional fecal specimens of CDI patients distinguished by clinical disease parameters were subjected to microarray-assisted antibody analysis. A group of eleven patients had self-limiting disease with watery diarrhea fewer than three times daily for less than five days associated with mild abdominal cramping and tenderness (mild disease). A second group comprising 25 patients presented with persisting watery diarrhea more than five times daily over ten days or longer and at least one of the following symptoms: fever, blood/pus in the stool, abdominal cramping/pain (severe disease). Ten individuals not diagnosed with CDI served as controls. Fecal sIgA levels were quantified using microarrays displaying PS-I pentasaccharide **1** and PS-II hexasaccharide **7** [Fig. 3.3d]. sIgA levels to **1** were significantly higher in CDI patients with mild disease than in the controls [Fig. 3.3e]. Most importantly,

patients with mild disease showed significantly higher sIgA levels to both **1** and **7** as compared to those with severe disease. This correlation raises the possibility that mucosal antibodies to **1** and **7** contribute to immune defense against *C. difficile* in the intestinal tract.

3.1.2 The PS-I Pentasaccharide Repeating Unit Is Immunogenic in Mice

PS-I pentasaccharide **1** was selected for further immunological evaluation in mice. The presence of anti-**1** IgG/sIgA in all investigated clinical specimens [Figs. 3.2 & 3.3] suggested that this epitope is commonly immunogenic during human exposure to *C. difficile*. Elevated sIgA levels correlated with milder clinical symptoms in CDI patients [Fig. 3.3], indicating protective effects. In addition, **1** contains two terminal rhamnose residues [Fig. 3.1]. As a non-mammalian sugar, rhamnose is foreign to the immune system and by itself highly immunogenic in humans and mice.[308,309,312,313] This suggested that immunogenicity of **1** may benefit from the two rhamnose units.

To study its immunogenicity in mice, **1** was first conjugated to the carrier protein CRM_{197}. Covalent linkage to a protein enhances the usually poor immunogenicity of carbohydrates and helps to induce T cell-dependent antibody responses.[226] CRM_{197}, a non-toxic mutant of the diphtheria toxin[314,315], is constituent of licensed conjugate vaccines against various bacterial pathogens[223–225] and a suitable carrier for synthetic oligosaccharides[316]. Reaction of **1** *via* the amine-functionalized linker to lysine side chains of CRM_{197} using di-*N*-succinimidyl adipate (DSAP) as crosslinker furnished glycoconjugate **10** [Fig. 3.4a]. Analysis by denaturing sodium dodecyl acrylamide gel electrophoresis (SDS-PAGE) showed that **10** ran at a higher mass than native CRM_{197} did [Fig. 3.4b]. This verified successful conjugation. There was no evidence of nonreacted protein. The mass shift between CRM_{197} and **10** was quantified by matrix-assisted laser desorption/ionization time-of-flight mass spectrometry (MALDI-TOF MS) to be about 9,500 Da [Fig. 3.4c]. The difference in mass corresponded to an average of 9.6 molecules **1** per CRM_{197}. Colorimetric carbohydrate quantification by anthrone assay[293] was in agreement with MALDI-TOF MS analysis and further verified incorporation of **1** into **10** [Fig. 3.4d].

To assess its capability of eliciting antibodies to immunogen **1**, mice were immunized with **10** in a prime-boost regime [Fig. 3.5a]. Three groups of six mice received **10** subcutaneously (s. c.) either non-adjuvanted, with aluminum hydroxide (Alum), or with Freund's adjuvant (FA). Alum was selected as a human-approved adjuvant for glycoconjugate vaccines[223–225] and FA due to its potent promotion of anti-glycan antibodies in mice[236]. Each injection

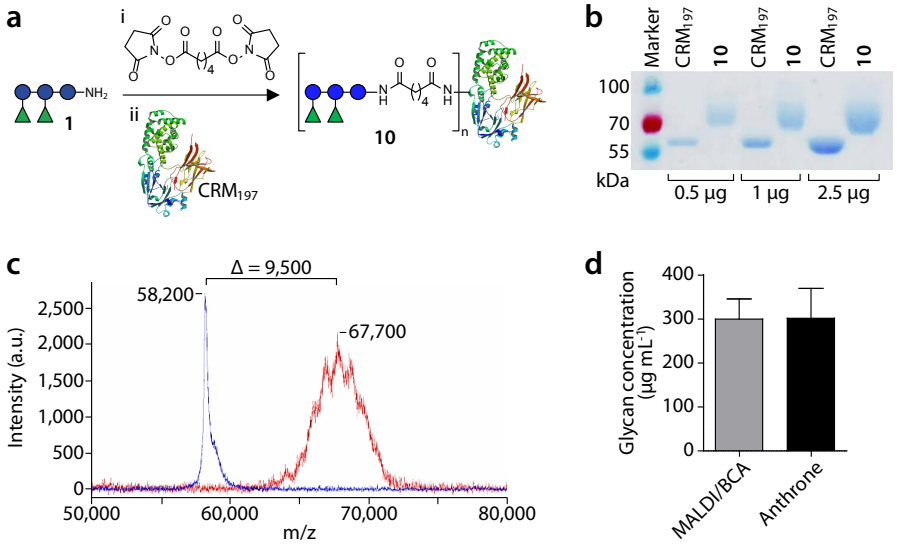

Figure 3.4: Preparation and characterization of glycoconjugate **10**. (**a**) Reaction scheme. *Reagents and conditions:* (i) di-*N*-succinimidyl adipate, Et_3N DMSO; (ii) CRM_{197}, 100 mM sodium phosphate, pH 7.4. Graphical representation of CRM_{197} was retrieved from the RCSB Protein Data Bank on www.rcsb.org. (**b**) Denaturing SDS-PAGE analysis of **10** and CRM_{197}. Protein was stained with Coomassie brilliant blue. Numbers to the left are marker protein sizes in kDa. (**c**) MALDI-TOF MS analysis of **10** (red) and CRM_{197} (blue). a.u., arbitrary units. (**d**) The glycan concentration of a solution of **10** was determined by two methods. Results obtained from MALDI-TOF MS analysis in combination with bicinchoninic acid (BCA) protein determination (gray) and from anthrone assay (black) are shown. Bars represent mean + SD of three independent experiments. Figure modified from Martin *et al.*[284]

contained an amount of **10** corresponding to 3 µg of immunogen **1**. Sera were retrieved at various time points up to 18 weeks after the initial immunization to follow the antibody responses over time. Microarray slides displaying immunogen **1**, CRM_{197} as well as control oligosaccharides **7** and **8** were employed to study antibody binding specificities [Fig. 3.5b]. A dummy glycoconjugate composed of GlcNAc monosaccharide and bovine serum albumin (BSA) that was synthesized with the same chemistry as **10** (a kind gift of Dr. Chakkumkal Anish) was also included. The GlcNAc-BSA conjugate allowed for detecting antibodies to the generic spacer moiety of aminopentyl and adipoyl groups. The spacers of glycoconjugates can be immunogenic and may in some cases suppress antibody responses to the glycan immunogen.[317] Microarray analysis revealed that immunization with **10** induced serum antibodies to all components of the glycoconjugate; the immunogen **1**, the carrier protein and the spacer [Fig. 3.5c]. Detectable quantities of anti-**1** antibodies were found in serum of four of six mice (no adjuvant), five of six mice (Alum) and six of six mice (FA). Antibodies to **7** and **8** remained undetectable throughout the observation period in any of the mice, demonstrating the high specificity of anti-glycan antibodies for **1**. Quantification of antibody levels revealed robust induction of anti-**1** IgM, IgG and IgA in all three groups of mice

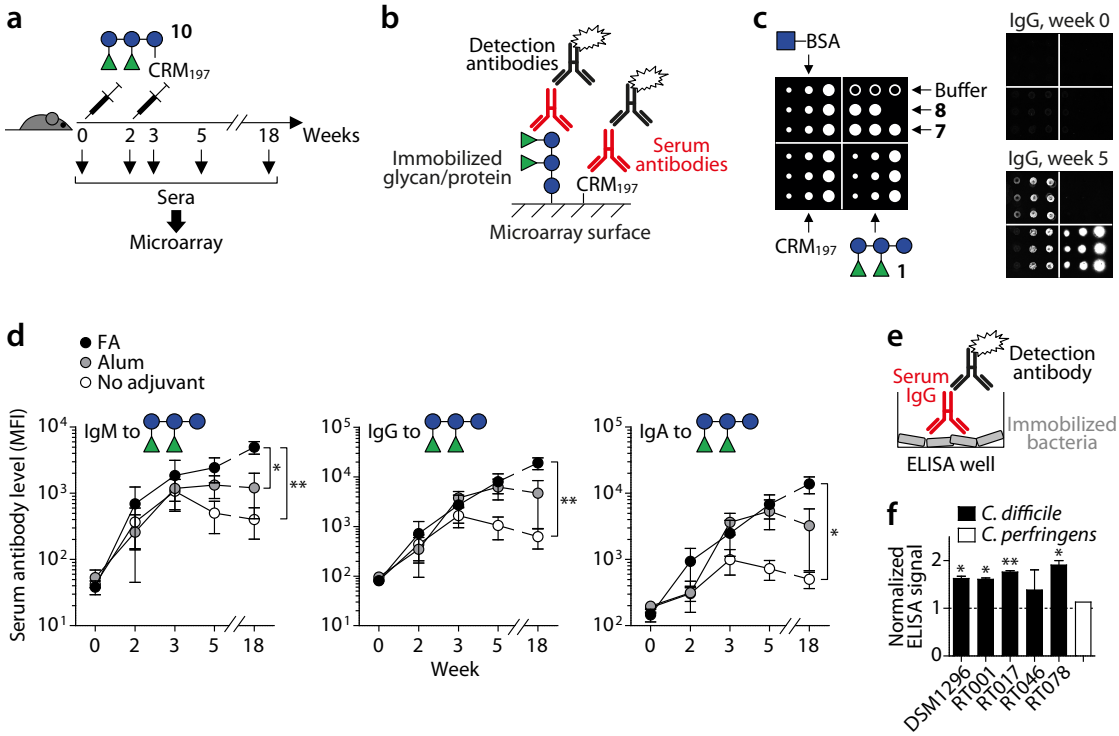

Figure 3.5: Immunogenicity of glycoconjugate **10** in mice. (**a**) Immunization regime. C57BL/6 mice were immunized s. c. with **10** at the indicated time points. Sera were retrieved and subjected to microarray-assisted antibody analysis. (**b**) Experimental setup applying to panels (**c**) and (**d**). (**c**) The microarray spotting pattern is shown to the left. GlcNAc-BSA glycoconjugate and CRM_{197} were spotted at 0.1, 0.5 and 1 µM, oligosaccharides at 0.1, 0.5 and 1 mM. Exemplary microarray scans representing IgG of one mouse immunized in the presence of Alum are shown to the right. (**d**) Serum antibody levels expressed as microarray-inferred MFI values obtained from **1** spotted at 1 mM. Data points show mean ± SEM of six mice. $*P \leq 0.05$, $**P \leq 0.01$; unpaired two-tailed Student's *t*-Test. (**e**) Experimental setup applying to panel (**f**). (**f**) IgG binding signals of pooled serum (Alum group) at week 5 to different bacteria as determined by whole cell ELISA. Signals were normalized to those of week 0 (dashed line). Bars show mean + SD of two independent experiments in duplicate. Statistical significance (week 5 vs week 0) is indicated as in panel (**d**). Figure modified from Martin *et al.*[284]

[Fig. 3.5d]. Long-lived antibody responses detectable 18 weeks after initial immunization and isotype switching from IgM to IgG and IgA indicated the involvement of T cell help. While **10** was immunogenic by itself, co-administration with an adjuvant further promoted anti-**1** antibodies. FA was more effective than Alum and helped to raise IgM, IgG and IgA levels that were significantly higher as compared to those elicited by non-adjuvanted **10**.

Alum was slightly less efficient than FA but is the more relevant adjuvant for potential clinical applications, as it is approved for human use and part of licensed glycoconjugate vaccines.[223–225] Therefore, the ability of antibodies elicited by **10** with Alum to recognize the native polysaccharide on the surface of *C. difficile* was investigated by whole cell ELISA. Formalin-inactivated bacteria were immobilized in ELISA plates, with *Clostridium perfringens*

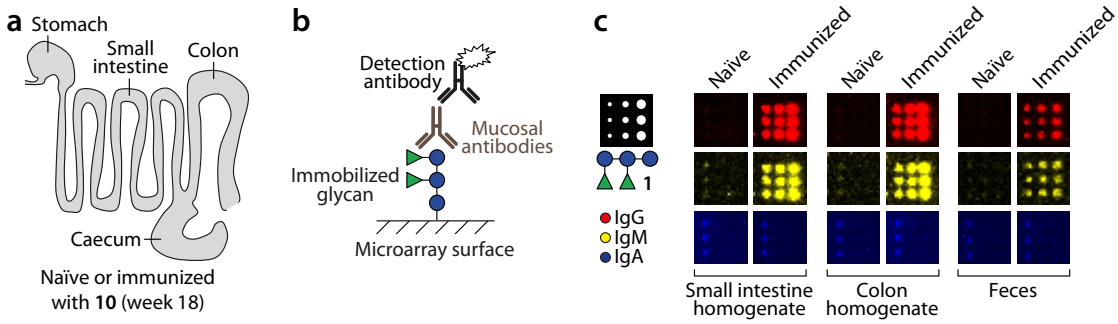

Figure 3.6: Detection of anti-**1** antibodies in the intestine of a mouse immunized with **10**. (**a**) The small intestine and colon of a mouse immunized with **10** in the presence of Alum (see Fig. 3.3a) were removed at week 18. An age-matched naïve mouse served as control. Supernatants of tissue homogenates and feces were subjected to microarray-assisted analysis of the mucosal antibodies. (**b**) Experimental setup. (**c**) The spotting pattern is shown to the left. Compound **1** was spotted in triplicate at 0.1, 0.5 and 1 mM. Exemplary microarray scans representing anti-**1** antibodies in both mice with the indicated color code are shown to the right.

serving as control [Fig. 3.5e]. *C. difficile* and *C. perfringens* are phylogenetically closely related species.[318] Yet, PS-I polysaccharide has been exclusively identified on *C. difficile* to date.[232] IgG of pooled serum at week 5 weakly but significantly bound to the *C. difficile* reference strain DSM1296 as well as to isolates representing the clinically relevant ribotypes 001, 017 and 078[19,156] [Fig. 3.5f]. No significant binding to *C. difficile* ribotype 046 or *C. perfringens* was observed. This demonstrated that anti-**1** antibodies specifically bound to the natural polysaccharide on the surface of *C. difficile*. The overall weak binding signals were likely the result of low and inconsistent expression levels of PS-I *in vitro*.[232]

In order to confer protection from *C. difficile* infection, the anti-**1** antibodies need to localize to the site of infection. Infection occurs *via* ingested *C. difficile* spores that germinate in the small intestine. Vegetative bacteria then migrate and adhere to colonic mucosa where they multiply and cause disease.[27] Mucosal antibodies that mediate resistance to intestinal infections comprise sIgA produced by tissue-resident B cells[310] as well as serum IgG[118,119] and IgM[120] transported into the intestinal lumen *via* receptor-mediated transcytosis. Consequently, the mammalian intestine harbors significant amounts of anti-bacterial IgG and IgM in addition to sIgA.[319] To test whether anti-**1** antibodies elicited by s. c. immunization with **10** localize to the intestine, one mouse of the Alum group was sacrificed at week 18 post-immunization. The intestinal tract was removed and homogenates of small intestine and colon tissues were subjected to glycan microarray-assisted antibody analysis [Fig. 3.6a,b]. Supernatants of the homogenates and feces of the same mice contained high amounts of anti-**1** IgG and IgM, but not IgA [Fig. 3.6c]. In contrast, there was no evidence for anti-**1** antibodies in corresponding samples of an age-matched naïve mouse. This showed that s. c.

immunization with **10** did not lead to signficant levels of mucosal sIgA, but the raised anti-**1** IgG and IgM antibodies were efficiently transported from the serum into the intestinal lumen and may thereby mediate protection from *C. difficile*.

3.1.3 Immunization with PS-I Pentasaccharide Limits *C. difficile* Colonization in Mice *In Vivo*

Next, the ability of a vaccine candidate with immunogen **1** to limit experimental *C. difficile* disease in mice was investigated. A new glycoconjugate of CRM_{197} and **1** termed **10'** was prepared with similar reaction conditions used to obtain **10** [Fig. 3.7a]. Kdo monosaccharide **9** expressed by Gram-negative bacteria[290,320] was coupled to the same carrier protein to furnish control glycoconjugate **11** [Fig. 3.7b]. Increased masses of both **10**' and **11** relative to native CRM_{197} observed by denaturing SDS-PAGE analysis verified successful conjugations [Fig. 3.7c]. The mass differences to CRM_{197} were determined to be 7,500 Da (**10'**) and 3,100 Da (**11**) by MALDI-TOF MS analysis [Fig. 3.7d]. For **10**' and **11**, respectively, this corresponded to an average of 7.5 molecules **1** and 7 molecules **9** per CRM_{197}. Having an almost similar antigen loading as compared to **10**', **11** provided a suitable control glycoconjugate for the intended challenge studies.

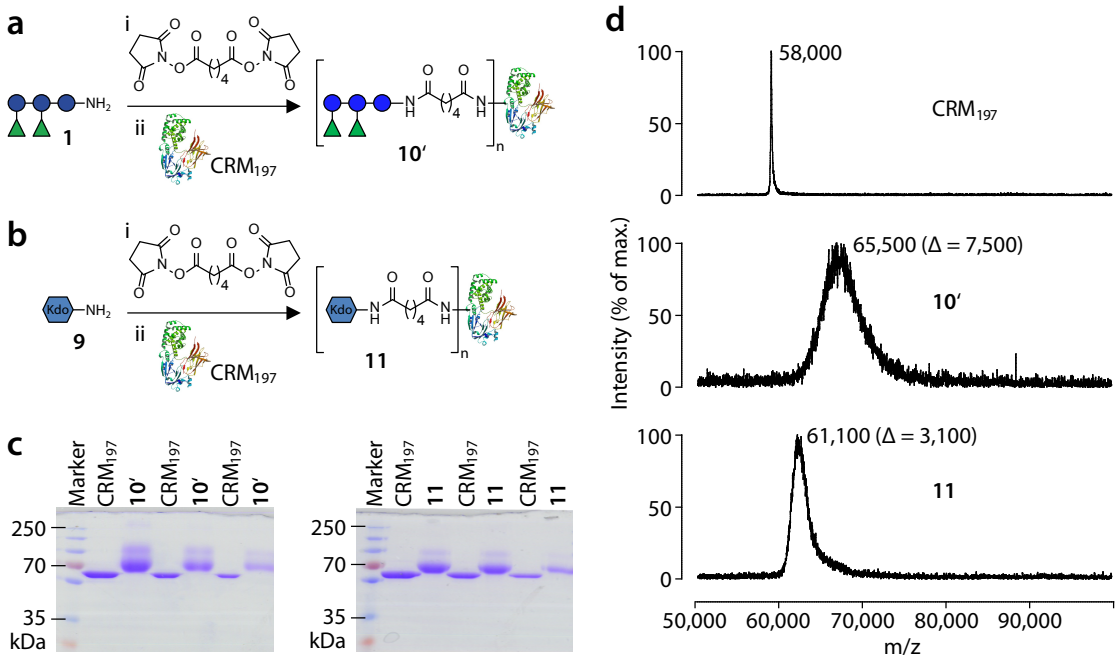

Figure 3.7: Preparation and characterization of glycoconjugates **10'** and **11**. (**a,b**) Reaction schemes. *Reagents and conditions:* (i) di-*N*-succinimidyl adipate, Et_3N DMSO; (ii) CRM_{197}, 100 mM sodium phosphate, pH 7.4. (**c**) Denaturing SDS-PAGE analysis of **10'** (left) and **11** (right) and CRM_{197}. Protein was stained with Coomassie brilliant blue. Numbers to the left of gels are marker protein sizes in kDa. (**d**) MALDI-TOF MS analysis of CRM_{197}, **10'** and **11**.

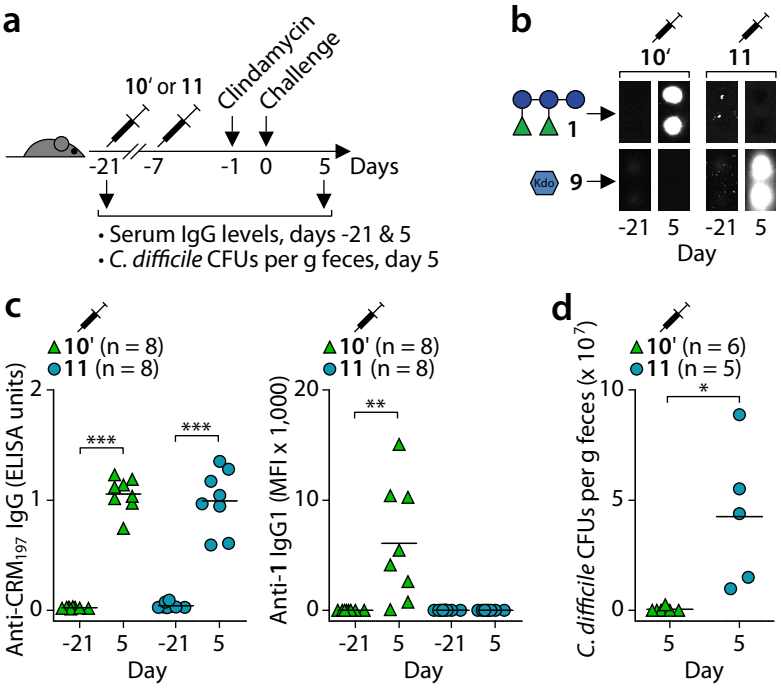

Figure 3.8: Immunogenicity of glycoconjugates **10**' and **11** and effects on intestinal *C. difficile* colonization. (**a**) Immunization regime. C57BL/6 mice were immunized s. c. with **10**' or **11** in the presence of Alum at the indicated time points. Serum and feces were retrieved to assess antibody responses and degrees of bacterial colonization, respectively. (**b**) Microarray scans representing IgG1 of two exemplary mice to the indicated glycans spotted in duplicate at 1 mM. (**c**) Antibody levels to the indicated antigens were inferred by ELISA (left) or microarray analysis (right). (**d**) The numbers of fecal *C. difficile* CFUs as a measure of bacterial colonization are shown. In panels (**c**) and (**d**), data points represent individual mice, horizontal lines the mean of each group. $^{*}P \leq 0.05$, $^{**}P \leq 0.01$, $^{***}P \leq 0.005$; unpaired two-tailed Student's *t*-Test.

Two groups of eight mice were immunized s. c. with either **10**' or **11** in a prime-boost regime [Fig. 3.8a]. Alum was used as adjuvant. Each injection comprised 3 µg of the respective glycan antigen. Six or five of the animals immunized with **10**' or **11**, respectively, were orally challenged with 10^7 colony-forming units (CFUs) of the *C. difficile* M68 strain that is known to colonize the murine intestine and to induce colitis.[307] The challenge studies were kindly performed by Prof. Jochen Mattner, Universität Erlangen, Germany. One day prior to the challenge, mice were rendered susceptible to *C. difficile* infection by intraperitoneal administration of the antibiotic clindamycin, as described.[306] The degree of intestinal colonization five days post-challenge was determined by counting the *C. dfficile* CFUs in fecal suspensions after culture at limited dilutions on selective agarose medium. Serum IgG responses at days -21 and 5 relative to the challenge were assessed with microarray slides presenting PS-I pentasaccharide **1** and Kdo **9** [Fig. 3.8b]. Expectedly, mice immunized with **10**' elicited IgG to **1** and injection of **11** promoted IgG to **9**. All mice mounted IgG to CRM_{197}, as inferred by ELISA [Fig. 3.8c], demonstrating that every animal was successfully

immunized. Comparison of the microarray-inferred IgG levels at days -21 and 5 revealed that seven of eight mice immunized with **10**' elicited detectable amounts anti-**1** antibodies. By contrast, neither mouse immunized with **11** had IgG to **1**. The mean level of *C. difficile* colonization determined as CFUs per gram of feces was lower by 99 % in mice immunized with **10**' than in the control group, with statistical significance [Fig. 3.8d]. Most notably, fecal *C. difficile* was indectable (CFU = 0) in five of six mice administered with **10**', whereas all five control mice immunized with **11** presented with high numbers of *C. difficile*. There was no difference in the extent of colitis between both groups, as determined by histopathological analysis of colon tissue at day 5 (personal communication by Jochen Mattner). This was likely attributed to the high infectious dose used for challenge that enabled some degree of bacterial colonization and toxin production before efficient clearance of *C. difficile* from the intestine at day 5. In conclusion, polyclonal anti-**1** IgG elicited by active immunization significantly and substantially limited intestinal *C. difficile* colonization in mice *in vivo*. PS-I pentasaccharide **1** is therefore an auspicious antigen for a colonization-inhibiting vaccine against CDI.

3.2 Identification of a Disaccharide Minimal Epitope of PS-I

Pentasaccharide **1** proved to be highly immunogenic and capable of eliciting protective antibodies. Yet, its synthesis is laborious, requires four differentially protected monosaccharide building blocks and multiple conversion and purification steps.[237,284] The antigenicity of the mono- to trisaccharide substructures of **1** in human serum and feces [Figs. 3.2 & 3.3] indicated that smaller glycans may be immunogenic as well. Finding the minimal epitope, referred to as the smallest oligosaccharide able to raise antibodies cross-reacting with **1**, is a key step *en route* towards PS-I-based vaccine candidates of reduced synthetic complexity.

3.2.1 Antibodies Raised with PS-I Pentasaccharide Recognize a Disaccharide Substructure

To reveal the epitope recognition pattern of polyclonal anti-**1** IgG, serum samples of mice immunized with glycoconjugate **10** were subjected to microarray analysis with slides containing **1** and its substructures **2**-**6** [Fig. 3.9a,b]. IgG raised without adjuvant not only recognized immunogen **1** but also, to a lower extent, trisaccharide **2**, disaccharide **3** and rhamnose **4** [Fig. 3.9c]. Co-administration with Alum promoted IgG to **1** and **4**, but barely to **2** and **3**. FA helped to elicit comparably high levels of IgG to **1**-**4**. IgG to oligoglucoses **5** and **6** were low or undetectable in all three groups. To characterize the kinetics of the antibody responses, IgG levels to **1**-**4** at various time points from week 0 to 5 after initial immunization were quantified [Fig. 3.9d]. Using no adjuvant, IgG levels to **1**-**3** transiently increased from week 0 to 3 but decreased again at week 5. The use of Alum led to a gradual increase of IgG to **1** from week 0 to 5, whereas levels to **2** and **3** increased up to week 3 and subsequently decreased. FA promoted continuously increasing IgG levels to **1**-**3** from week 0 to 5. In all three groups, IgG to **4** peaked at week 3 and decreased later on. Thus, the epitope recognition patterns and IgG kinetics markedly differed depending on the adjuvant used.

The antibody binding patterns and the observed differences between Alum and FA were further characterized by surface plasmon resonance (SPR). Pooled sera of these two mouse groups at various time points from week 0 to 5 were passed over sensor chip surfaces functionalized with **1** or **3** to obtain binding signals measured as changes in response units in real-time (sensorgrams) [Fig. 3.9e]. At week 5, comparable binding signals to **1** were obtained with serum of both Alum and FA groups [Fig. 3.9f]. Binding to **3** was only detected in the FA group serum. These observations confirmed the microarray results described above.

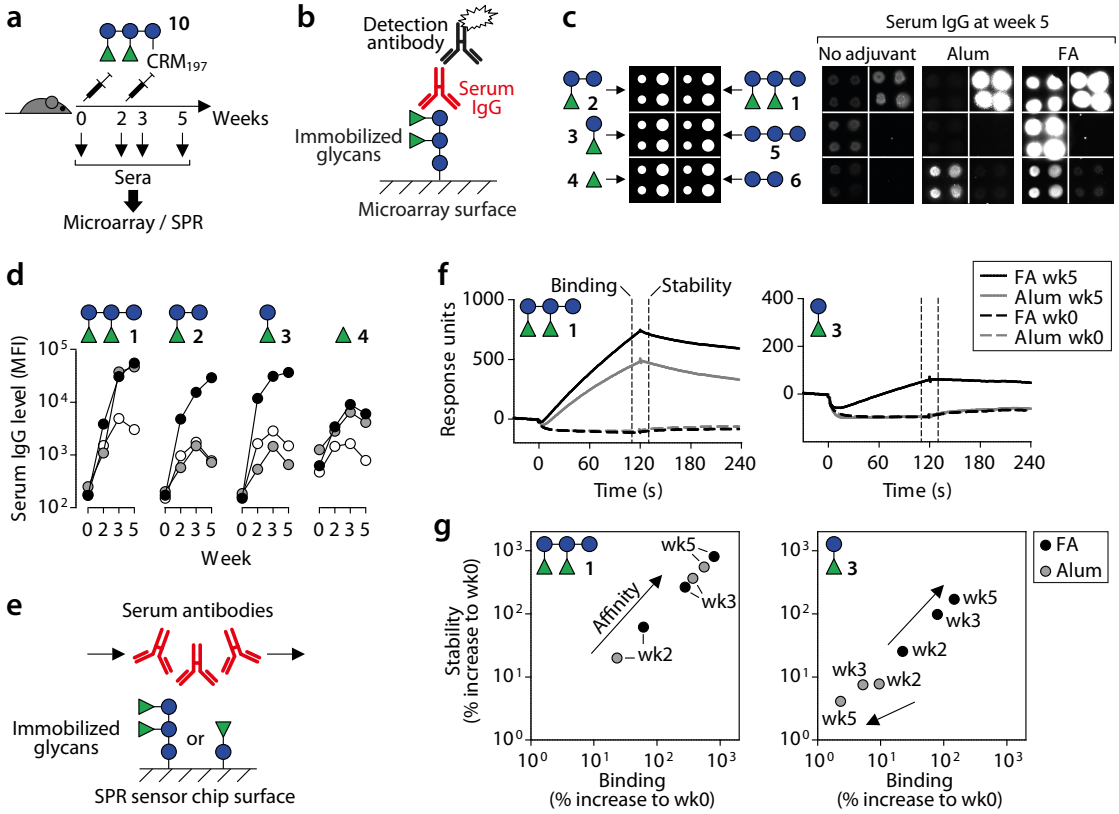

Figure 3.9: Recognition of oligosaccharide epitopes **1**-**6** by polyclonal anti-**1** serum antibodies. (**a**) Immunization regime. (**b**) Experimental setup applying to panels (**c**) and (**d**). (**c**) The microarray spotting pattern is shown to the left. Oligosaccharides were spotted at 0.5 and 1 mM (small and large spots, respectively). Exemplary microarray scans obtained with pooled serum of six mice (diluted 1:50) are shown to the right. (**d**) Microarray-inferred pooled serum IgG levels to the indicated oligosaccharides spotted at 1 mM expressed as MFI values. Data points show the mean of two experiments. (**e**) Experimental setup applying to panels (**f**) and (**g**). (**f**) Representative sensorgrams obtained with pooled serum that was passed over sensor chip surfaces functionalized with the indicated oligosaccharides. Dashed vertical lines indicate time points corresponding to binding and stability values. (**g**) SPR-inferred binding and stability values expressed as percent increase in response units to week 0 serum. Arrows highlight changes in affinity over time. Figure modified from Martin *et al.*[284]

The analysis of binding and stability values obtained from sensorgrams revealed increasing antibody affinity to **1** over time in serum of both groups [Fig. 3.9g]. Likewise, affinity to **3** continuously increased in serum of the FA group. Serum antibodies of the Alum group were characterized by overall lower affinity to **3** that decreased over time. Collectively, microarray and SPR studies with substructures of **1** unveiled disaccharide Rha-(1→3)-Glc **3** as the smallest epitope robustly recognized by polyclonal anti-**1** IgG. FA was required to promote affinity maturation to **3**.

3.2.2 The Disaccharide Substructure of PS-I Is Immunogenic in Mice and Elicits Antibodies Cross-reacting with the Pentasaccharide

Disaccharide **3** emerged as the smallest antigenic epitope of PS-I. To study its ability to raise antibodies cross-reactive to larger oligosaccharides, **3** was conjugated to CRM_{197} using DSAP as crosslinker [Fig. 3.10a]. Denaturing SDS-PAGE analysis of the resulting glycoconjugate **12** showed a shift towards higher masses as compared to native carrier protein, demonstrating successful incorporation of **3** [Fig. 3.10b]. The mass increase of **12** over CRM_{197} was quantified by MALDI-TOF MS analysis to be 5,100 Da [Fig. 3.10c], corresponding to an average of 9.8 molecules **3** per CRM_{197}.

To assess the immunogenicty of **3**, three mice were immunized s. c. with **12** in a prime-boost-boost regime [Fig. 3.11a]. As small oligosaccharides are frequently less immunogenic than more complex ones[234,245–248], **12** was administered with FA due to its potent promotion of anti-glycan antibodies [Fig. 3.5]. Serum IgG responses were followed by glycan microarray analysis [Fig. 3.11b]. After the second boosting immunization, two of three mice showed detectable amounts of IgG to **3** [Fig. 3.11c]. Serum of both mice also contained IgG cross-reactive to larger PS-I structures, trisaccharide **2** and pentasaccharide **1** [Fig. 3.11d]. An increase of IgG to rhamnose **4** was observed in one mouse. IgG to oligoglucoses **5** and **6** was

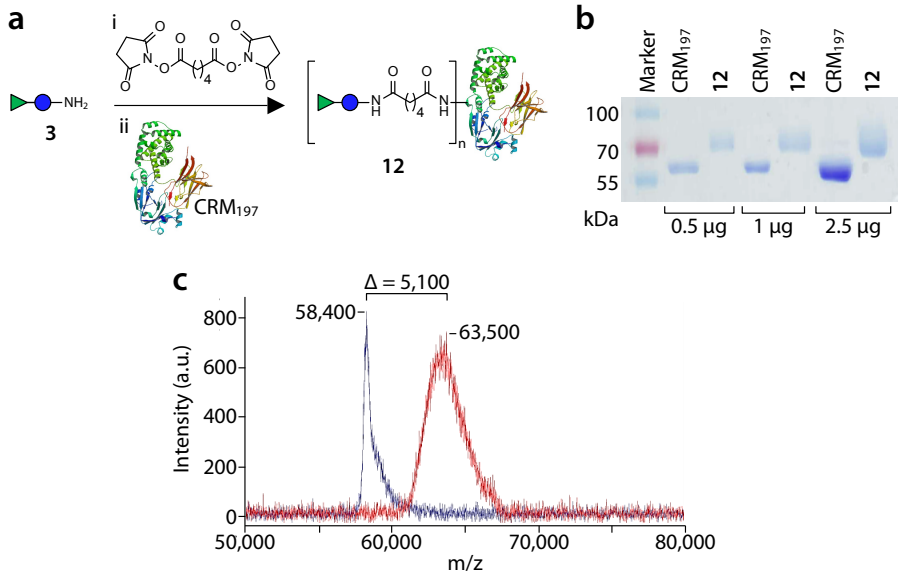

Figure 3.10: Preparation and characterization of glycoconjugate **12**. (**a**) Reaction scheme. *Reagents and conditions:* (i) di-*N*-succinimidyl adipate, Et_3N DMSO; (ii) CRM_{197}, 100 mM sodium phosphate, pH 7.4. (**b**) Denaturing SDS-PAGE analysis of **12** and CRM_{197}. Protein was stained with Coomassie brilliant blue. Numbers to the left are marker protein sizes in kDa. (**c**) MALDI-TOF MS analysis of **12** (red) and CRM_{197} (blue). a.u., arbitrary units. Figure modified from Martin *et al.*[284]

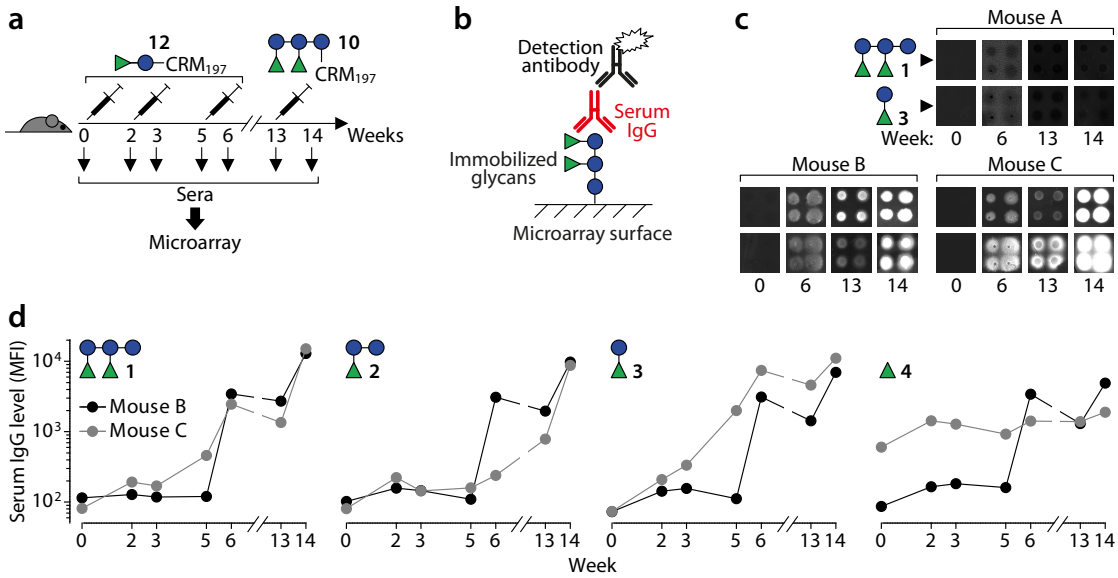

Figure 3.11: Immunogenicity of glycoconjugate **12**. (**a**) Immunization regime. (**b**) Experimental setup. (**c**) Representative microarray scans showing serum IgG to **1** and **3** of the three immunized mice. Glycans were spotted at 0.5 mM (two spots on the left side of the scans) and 1 mM (right). (**d**) Microarray-inferred serum IgG levels to **1**-**4** spotted at 1 mM expressed as MFI values. Data points show the mean of two experiments. Figure modified from Martin *et al.*[284]

not observed in any of the immunized animals (data not shown), as expected since these glycans are not part of the immunogen **3**. The IgG levels to **1**-**4** were further elevated by a third boosting immunization with FA-formulated glycoconjugate **10**, indicating the presence of B cells cross-reacting with **1** [Fig. 3.11d]. These findings demonstrated that **3** is immunogenic and constitutes the minimal epitope of **1**. The disaccharide is therefore a valid immunogen for vaccination approaches against *C. difficile*. However, **3** proved to be weakly immunogenic, as two boostings with glycoconjugate **12** were required to raise relatively low levels of anti-glycan antibodies in two of three mice.

3.3 Generation and Analysis of Monoclonal Antibodies to PS-I

Monoclonal antibodies (mAbs) are a useful tool to decipher the molecular basis of glycan-antibody interactions.[239,240,252,320–324] In the context of *C. difficile*, anti-PS-I mAbs may also be utilized for passive vaccination, an attractive therapeutic option especially for the elderly and immunocompromised individuals that may not respond sufficiently to active vaccines.[68–71] Toxin-neutralizing mAbs have been shown to reduce recurrence rates of CDI but suffer from limited efficacy since bacterial colonization is not affected.[188] The ability of polyclonal anti-**1** IgG to recognize the surface of *C. difficile* [Fig. 3.5] and to limit bacterial colonization in mice [Fig. 3.8] provided a rationale to produce mAbs specific for this antigen.

3.3.1 mAbs to PS-I Pentasaccharide Are Obtained from Immunized Mice

To obtain anti-**1** mAbs, six mice were immunized s. c. with glycoconjugate **10** in the presence of Alum three times in two-week intervals [Fig. 3.12a]. Alum was selected since this adjuvant promoted IgGs of high specificity to **1** and with lower cross-reactivity to smaller substructures as compared to FA [Fig. 3.9]. Highly specific mAbs may be advantageous for therapeutic applications since off-target effects on other bacteria with related antigens are less likely. Induction of IgG to immunogen **1**, the CRM_{197} carrier protein and the spacer moiety was confirmed by microarray-assisted analysis of serum obtained from the immunized mice [Fig. 3.12b,c,d]. One week after the second boosting immunization, splenocytes of one mouse

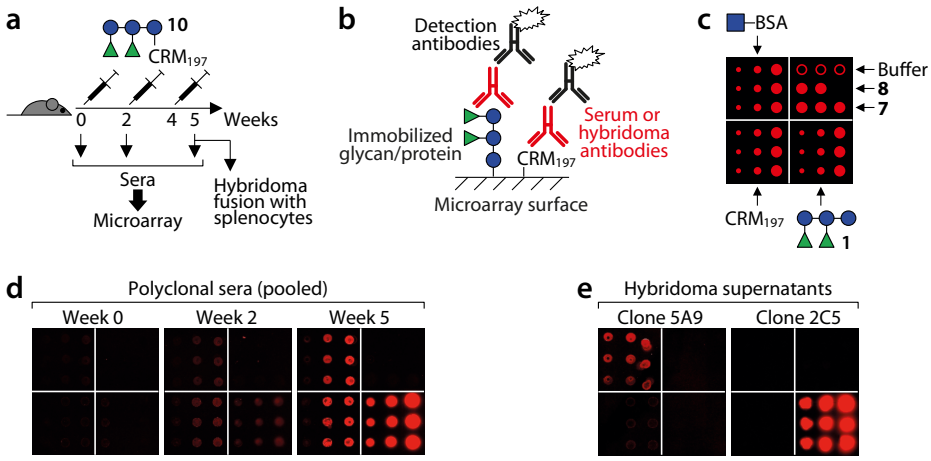

Figure 3.12: Generation of mAbs to **1**. (**a**) Immunization regime. (**b**) Experimental setup. (**c**) The microarray spotting pattern applying to panels (**d**) and (**e**) is shown. GlcNAc-BSA and CRM_{197} were spotted at 0.1, 0.5 and 1 µM, oligosaccharides at 0.1, 0.5 and 1 mM. (**d**) Exemplary microarray scans representing polyclonal serum IgG of the immunized mice. (**e**) Microarray scans showing binding profiles of IgG secreted by two representative hybridoma clones, 5A9 reacting to the spacer moiety and 2C5 to **1**. Figure modified from Broecker *et al.*[286]

with high IgG levels to **1** were fused *in vitro* with myeloma cells to obtain hybridomas, as described.[252,299] Hybridoma cells were selected *via* microarray analysis based on the binding profiles of their secreted antibodies [Fig. 3.12d]. Three types of antibodies were observed that either bound to CRM_{197}, the spacer moiety, or **1**, as expected from the reactivity of polyclonal serum. Hybridoma cells that produced anti-**1** IgG were subjected to three consecutive subcloning steps by limited dilution to establish monoclonality. This yielded three mAbs termed 2C5, 10A1 and 10D6 that uniquely recognized **1** without any reactivity to CRM_{197}, the spacer, or control oligosaccharides **7** and **8** [Fig. 3.12e].

3.3.2 mAbs Recognize the Pentasaccharide and Substructures Containing Rhamnose

The three mAbs were purified from supernatants of serum-free hybridoma cultures by fast protein liquid chromatography (FPLC) using protein A/G affinity columns [Fig. 3.13a]. The purified mAbs were subjected to denaturing SDS-PAGE analysis that revealed distinct bands

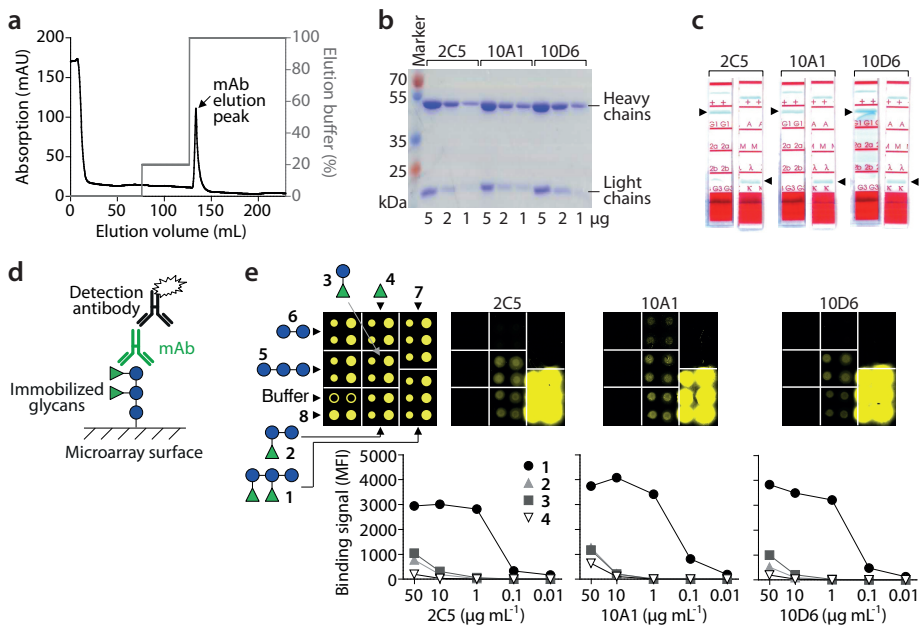

Figure 3.13: Purification and characterization of anti-**1** mAbs. (**a**) mAbs were purified from hybridoma supernatants by FPLC. A representative chromatogram of mAb 2C5 is shown. Absorption at 280 nm in mAU (milli absorbance units) is shown in black, the percentage of elution buffer in gray. (**b**) Denaturing SDS-PAGE analysis of the mAbs. Protein was stained with Coomassie brilliant blue. Marker band sizes in kDa are shown to the left. (**c**) Isotype analysis. (**d**) Experimental setup applying to panel (**e**). (**e**) Exemplary microarray scans showing binding patterns of mAbs at 10 µg mL^{-1}. The spotting pattern is shown to the left with oligosaccharides spotted at 0.5 mM (small circles) and 1 mM (large circles). Anti-mouse IgG1 was used for detection. Graphs show microarray-inferred binding signals (mean of two experiments) to the indicated glycans spotted at 1 mM. Figure modified from Broecker *et al.*[286]

of heavy and light immunoglobulin chains and no apparent protein impurity [Fig. 3.13b]. The mAbs were of the IgG1 subtype [Fig. 3.13c]. To reveal their epitope recognition patterns, mAbs 2C5, 10A1 and 10D6 were subjected to glycan microarray analysis with slides containing PS-I oligosaccharides **1**-**6** [Fig. 3.13d,e]. All three mAbs predominantly recognized pentasaccharide **1** but also rhamnose-containing substructures **2** and **3**. Weak binding to rhamnose **4** was observed at high concentrations of the mAbs (10 and 50 $\mu g\,mL^{-1}$). There was neither detectable binding to oligoglucoses **5** and **6** nor to control glycans **7** and **8**. The recognition pattern of the mAbs closely resembled that of polyclonal serum IgG obtained from mice immunized with Alum-adjuvanted **10** [Fig. 3.9].

3.3.3 mAbs Bind to the Pentasaccharide with Nanomolar Affinity and to Rhamnose-containing Substructures with Micromolar Affinity

To confirm the microarray-inferred recognition patterns and to measure binding affinities, mAbs 2C5, 10A1 and 10D6 were subjected to SPR analysis. Oligosaccharides **1**-**5**, at various concentrations, were passed through flow cells in which mAbs were captured with an anti-mouse IgG antibody [Fig. 3.14a].[239] Binding signals expressed as response units were double-referenced with blank-functionalized flow cells and cycles with running buffer (PBS) only. The resulting sensorgrams were utilized to derive equilibrium constants (K_D values) by fitting binding curves with a kinetic 1:1 Langmuir interaction model that also provided association and dissociation rate constants (k_a and k_d, respectively). Where rate constants were outside of the measurable range of the instrument, K_D values were calculated from steady-state equilibrium plots instead. Binding kinetics and K_D values are summarized in Table 3.1. The three mAbs recognized **1** with nanomolar affinities [Fig. 3.14b]. K_D values ranged from 163 nM (2C5) to 245 nM (10A1). The binding kinetics to **1** with respect to k_a and k_d were comparable for 2C5 and 10D6. Contrarily, 10A1 exhibited faster association and dissociation kinetics with both k_a and k_d outside of the measurable range. Affinities to trisaccharide **2** were similar for all three mAbs with micromolar K_D values ranging from 13.3 μM (10A1) to 18.8 μM (10D6) [Fig. 3.14c]. Likewise, disaccharide **3** was recognized by all three mAbs with micromolar K_D values between 5.9 μM (10A1) and 37.5 μM (10D6) [Fig. 3.14d]. Equilibrium constants to rhamnose **4** and triglucose **5** could not be determined for any of the mAbs since they by far exceeded 160 μM [Fig. 3.14e,f]. Overall, SPR studies confirmed binding patterns observed by microarray analysis and further verified that **3** is the minimal epitope of PS-I.

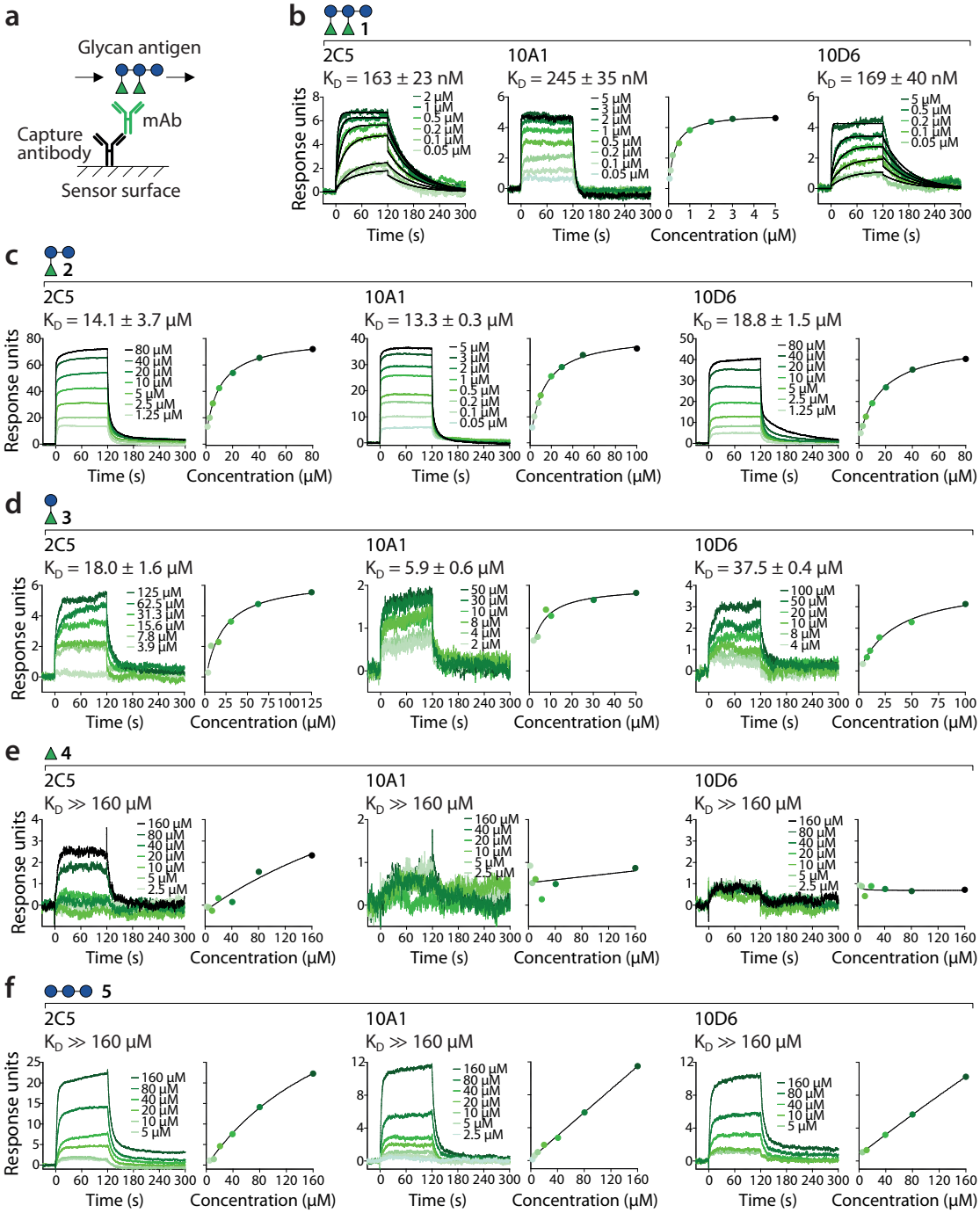

Figure 3.14: SPR-inferred binding affinities of mAbs 2C5, 10A1 and 10D6 to PS-I oligosaccharide epitopes. (**a**) Experimental setup. mAbs were captured with an anti-mouse IgG antibody immobilized on the sensor surface. Glycans were passed over the surface to monitor changes in response unit signals. (**b-f**) Representative sensorgrams resulting from interactions of the mAbs with the indicated oligosaccharides. Glycan concentrations are provided within the sensorgrams. If applicable, K_D values were inferred by curve fittings shown as black overlaid lines. In the other cases, representative equilibrium plots used to calculate K_D are shown to the right of the sensorgrams. The indicated K_D values are mean ± SEM of two or three independent experiments. Figure modified from Broecker *et al.*[286]

Table 3.1: SPR-inferred K_D values of anti-PS-I mAbs to different glycan epitopes. Association (k_a) and dissociation (k_d) rate constants are shown for interactions where kinetic modeling was applicable. The values are mean ± SEM of two or three independent experiments.

Epitope	mAb 2C5	mAb 10A1	mAb 10D6
1	163 ± 23 nM $k_a = 103 \pm 11 \times 10^3\ M^{-1}\ s^{-1}$ $k_d = 0.016 \pm 0.001\ s^{-1}$	245 ± 35 nM	169 ± 40 nM $k_a = 125 \pm 15 \times 10^3\ M^{-1}\ s^{-1}$ $k_d = 0.021 \pm 0.003\ s^{-1}$
2	14.1 ± 3.7 μM	13.3 ± 0.3 μM	18.8 ± 1.5 μM
3	18.0 ± 1.6 μM	5.9 ± 0.6 μM	37.5 ± 0.4 μM
4	» 160 μM	» 160 μM	» 160 μM
5	» 160 μM	» 160 μM	» 160 μM

3.3.4 Binding of mAbs to the Pentasaccharide Is Entropically Favored over the Disaccharide Minimal Epitope

SPR measurements confirmed that the anti-**1** mAbs also recognized the disaccharide minimal epitope **3**. However, binding affinity to **1** was about two orders of magnitude higher than to **3** [Table 3.1]. Since **3** is contained twice in the pentasaccharide [Fig. 3.1], enhanced affinity to **1** may be explained by re-binding of the mAbs to adjacent disaccharide copies. In this case, the mAb binding pocket would fit **3** only. Binding to **1** would be characterized by slower dissociation (smaller k_d) than to **3**, as well as interaction kinetics resulting from two consecutive binding events with the adjacent disaccharides. The components of complex interactions, however, cannot be differentiated *via* Langmuir modeling of sensorgrams. Instead, SPR binding curves of mAb 2C5 with **1** and **3** were subjected to Interaction Map (IM) analysis [Fig. 3.15a], kindly performed by Dr. Karl Andersson of Ridgeview Diagnostics, Uppsala, Sweden.[300] IM breaks down complex interactions into their underlying components that are represented as peaks in two-dimensional logarithmic scale heat maps.[300] The generated heat maps contained one dominant peak each, indicating that 2C5 interacted with both **1** and **3** in a 1:1-like manner [Fig. 3.15b]. The peak corresponding to **1** was approximately at $\log(k_a) = 5.1$ and $\log(k_d) = -1.34$. Interaction of 2C5 with **3** resulted in a dominant peak at around $\log(k_a) = 2.4$ and $\log(k_d) = -1.22$. A minor secondary peak was likely due to a neglegible buffer mismatch during the measurement. IM analysis showed that the enhanced affinity of 2C5 to **1** was mainly the result of faster association as compared to **3**, whereas k_d values were similar for both glycans. There was no indication for more than one binding event between 2C5 and **1**.

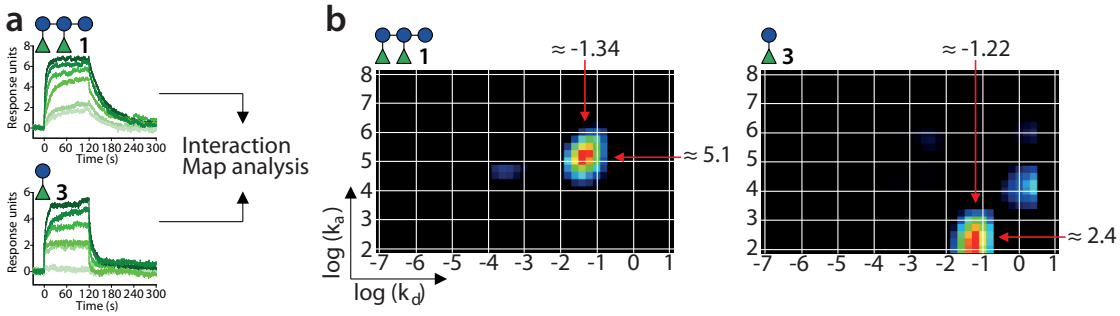

Figure 3.15: IM analysis of mAb 2C5 binding to **1** and **3**. (**a**) SPR sensorgram curves were subjected to IM analysis to yield the heat maps presented in panel (**b**), as described.[300] (**b**) Heat maps of 2C5 with **1** (left) and **3** (right). Approximated logarithmic rate constants that correspond to the major peaks are indicated. Figure modified from Broecker *et al.*[286]

IM analysis indicated that the mAb binding pocket encompasses not only **3** but a larger epitope present in **1**. In this case, both rhamnoses of **1** likely engage in the interaction, as terminal rhamnose is required for mAb binding [Fig. 3.14]. The methyl groups of rhamnose can participate in hydrophobic interactions with antibodies, leading to an entropic gain due to water displacement.[265,266,325] To test whether enhanced affinity to **1** over **3** can be explained by more favorable entropy, mAbs 2C5 and 10A1 were subjected to isothermal titration calorimetry (ITC) measurements with both glycans [Fig. 3.16a]. ITC allows for determining stoichiometries and thermodynamics of binding events. Interaction with **1** showed antibody-to-glycan stoichiometries of 2.2 and 2.6 for 2C5 and 10A1, respectively [Fig. 3.16b]. Small deviations from the expected value of two, the number of IgG antigen binding sites, may have been due to a low degree of antibody aggregation. For interactions with **3** the stoichiometry was set constant to two to enable data evaluation, a common requirement when analyzing weak interactions.[326] Antibody binding to both **1** and **3** was mainly enthalpy-driven [Fig. 3.16c]. For interactions with **1**, the enthalpy change was $\Delta H = -27.5\,kJ\,mol^{-1}$ (2C5) and $\Delta H = -22.2\,kJ\,mol^{-1}$ (10A1). Binding to **3** yielded comparable enthalpic terms of $\Delta H = -22.4\,kJ\,mol^{-1}$ and $\Delta H = -23.1\,kJ\,mol^{-1}$, respectively. By contrast, entropic contributions differed markedly between **1** and **3**. Favorable entropy was seen for both mAbs upon binding to **1**, with $-T\Delta S = -10\,kJ\,mol^{-1}$ (2C5) and $-T\Delta S = -13.3\,kJ\,mol^{-1}$ (10A1). For **3**, entropic terms were around zero with $-T\Delta S = -0.7\,kJ\,mol^{-1}$ and $-T\Delta S = 0.9\,kJ\,mol^{-1}$, respectively. The favorable entropy of the **1**-2C5 interaction was confirmed by SPR analysis at varying temperatures [Fig. 3.16d]. Affinity decreased as a function of temperature from $K_D = 165\,nM$ at 13 °C to $K_D = 385\,nM$ at 37 °C [Fig. 3.16d,e]. van't Hoff analysis of this data yielded similar thermodynamic terms as did ITC [Fig. 3.16f,g]. Overall, an entropic gain was

shown to be responsible for the higher antibody affinity to **1** over **3**. IM and thermodynamic analyses provided evidence that binding pockets of the anti-**1** mAbs encompass an epitope larger than **3**. Both rhamnoses of **1** likely participate in hydrophobic interactions with the mAbs. Implications on the design of PS-I glycan mimetics are described in **Section 3.4**.

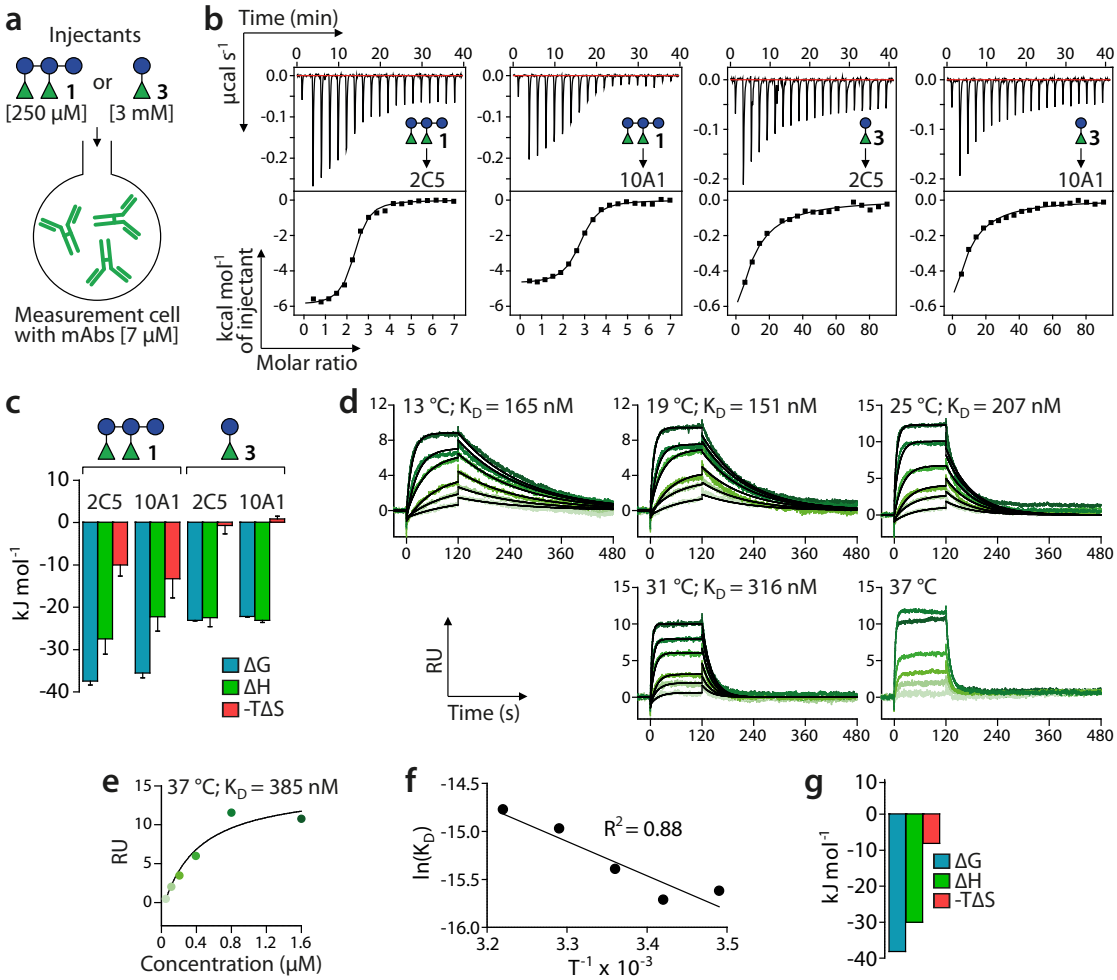

Figure 3.16: Thermodynamics of mAbs binding to **1** and **3**. (**a**) Setup of ITC experiments. (**b**) Representative ITC-derived thermograms. Thermodynamic terms were determined by non-linear least square fits of data points (black lines in the bottom diagrams). (**c**) ITC-inferred thermodynamic parameters. Bars show mean + SD of two independent experiments. (**d**) SPR sensorgrams of mAb 2C5 binding to **1** (experimental setup as in Fig. 3.14) at the indicated temperatures. Concentration of **1** ranged from 0.05 to 1.6 µM. Except for T = 37 °C, K_D was inferred by fitting curves with a 1:1 binding model (black overlaid lines). RU, response units. (**e**) K_D at T = 37 °C was determined from the depicted equilibrium plot. (**f**) van't Hoff plot with data shown in panels (**d**) and (**e**). (**g**) Thermodynamic parameters inferred by van't Hoff analysis. Figure modified from Broecker *et al.*[286]

3.3.5 Passively Administered mAbs Protect Mice from *C. difficile* Colitis

In order to confer protection against CDI, the anti-**1** mAbs need to recognize the natural polysaccharide on the surface of *C. difficile*. Therefore, binding of the mAbs to various

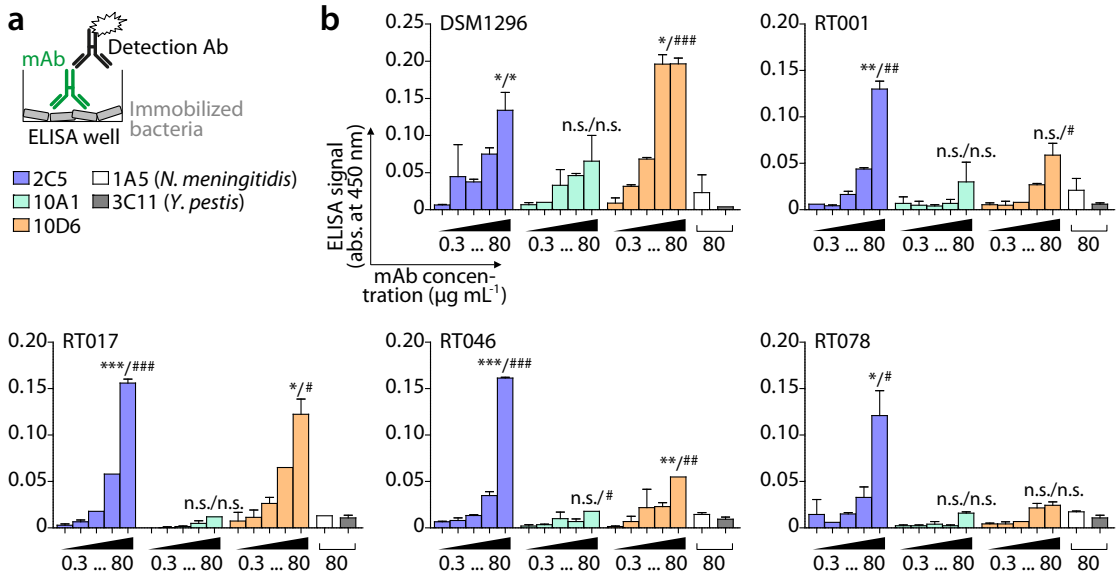

Figure 3.17: Binding of anti-**1** mAbs to various *C. difficile* strains *in vitro*. (**a**) Experimental setup. (**b**) Binding of the mAbs to the indicated bacteria expressed as ELISA signal (absorbance at 450 nm). Bars show mean ± SD of two experiments. Concentrations of the mAbs were 0.3, 1.3, 5, 20 and 80 µg mL^{-1} (from left to right). Statistical significance was inferred by comparing binding signals of mAbs at 80 µg mL^{-1}. $^{*}P \leq 0.05$, $^{**}P \leq 0.01$, $^{***}P \leq 0.005$ vs 1A5; $^{\#}P \leq 0.05$, $^{\#\#}P \leq 0.01$, $^{\#\#\#}P \leq 0.005$ vs 3C11; n.s., not significant; unpaired two-tailed Student's *t*-Test. RT, ribotype.

clinical isolates of *C. difficile* ribotypes 001, 017, 046 and 078 was tested. These ribotypes represent frequent disease-causing strains found in healthcare facilities worldwide.[18–22] Formalin-inactivated bacteria of the clinical isolates and of the *C. difficile* reference strain DSM1296 were immobilized on ELISA plates and probed with mAbs 2C5, 10A1 and 10D6 at concentrations ranging from 0.3 to 80 µg mL^{-1} [Fig. 3.17a]. Two irrelevant murine glycan-binding IgG mAbs at 80 µg mL^{-1} served as negative controls. mAb 1A5 recognizes LPS of *N. meningitidis* and was kindly supplied by Dr. Anika Reinhardt.[320] mAb 3C11, a kind gift by Dr. Chakkumkal Anish and Annette Wahlbrink, binds to *Y. pestis* LPS.[239,251] The two control mAbs did not recognize any of the *C. difficile* strains. 2C5 dose-dependently bound to all clinical *C. difficile* isolates and to DSM1296 with statistical significance against both control mAbs [Fig. 3.17b]. Dose-dependent and significant binding was also observed for 10D6 to all strains except for ribotype 078. 10A1 only recognized ribotype 046 significantly. This showed that the anti-**1** mAbs specifically recognized the native PS-I polysaccharide on the surface of *C. difficile*, with varying efficiencies depending on the mAb as well as on the bacterial strain. 2C5 was the only mAb binding to all investigated *C. difficile* strains, although epitope recognition patterns [Fig. 3.13] and affinities [Table 3.1] were similar to those of 10A1 and 10D6.

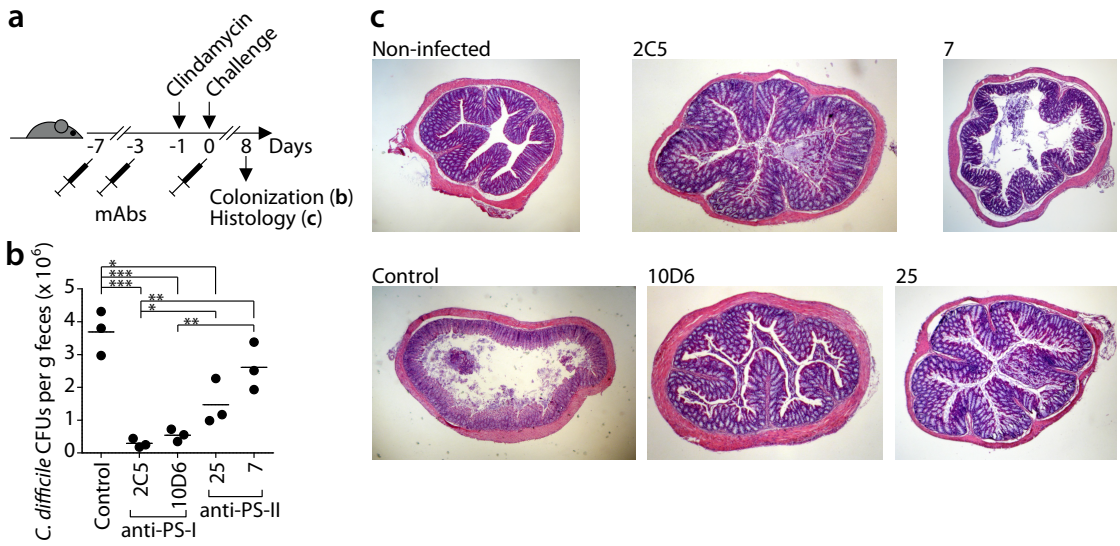

Figure 3.18: Effects of passive transfer of anti-**1** mAbs on experimental *C. difficile* disease. (**a**) Immunization and challenge regime. Mice received three injections of mAbs *via* the i. p. and i. r. routes, each injection contained 100 µg of purified antibody. Control mice received PBS only. (**b**) Comparison of intestinal colonization levels at day 8. Black dots represent individual mice, horizontal lines the mean of each group. $^{*}P \leq 0.05$, $^{**}P \leq 0.01$, $^{***}P \leq 0.005$; unpaired two-tailed Student's *t*-Test. (**c**) Histopathology of representative colon cross-sections. Tissue was stained with haematoxilin and eosin.

Next the ability of anti-**1** mAbs to limit experimental *C. difficile* disease *in vivo* was investigated in a murine challenge model. These studies were kindly performed by Prof. Jochen Mattner, Universität Erlangen, Germany. Groups of three mice each received three doses of 2C5 or 10D6 *via* the i. p. and intrarectal (i. r.) routes at days -7, -3 and 0 relative to the bacterial challenge [Fig. 3.18a]. Two mAbs against the PS-II hexasaccharide **7** termed 7 (IgG) and 25 (IgM) described previously[236] were also tested. Three control mice received sham injections with buffer (PBS). One day before the bacterial challenge, mice were rendered susceptible to *C. difficile* infection with the antibiotic clindamycin, as described.[306] The following day, mice orally received 10^8 CFUs of the clindamycin-resistant *C. difficile* strain M68 that is able to induce colitis in mice.[307] Eight days after bacterial challenge, colonic *C. difficile* CFUs were determined by plating limited dilutions of fecal suspensions on selective agar medium followed by overnight culture. The levels of *C. difficile* colonization determined as CFUs per gram of feces were significantly reduced by 92 % and 85 % in mice that have received 2C5 and 10D6, respectively, relative to the control group [Fig. 3.18b]. The difference in efficiency likely reflected better binding of 2C5 to *C. difficile* bacteria *in vitro* as compared to 10D6 [Fig. 3.17]. Anti-PS-II mAb 25 significantly reduced bacterial colonization by 60 %. A moderate, non-significant reduction by 29 % was observed for 7. These findings were

corroborated by histopathological analysis of colon cross-sections [Fig. 3.18c]. High levels of *C. difficile* colonization in the control mice led to severe morphologic alterations. Compared to healthy, non-infected mice, the luminal volume was increased and visible damage to the epithelium was characteristic of toxin-induced inflammation. Colons of mice treated with 2C5, 10D6 and 25 appeared similar to those of non-infected mice. Mice treated with the least efficient mAb 7 exhibited a morphology in-between that of healthy and control mice. Thus, the degree of colitis was inversely correlated with the level of bacterial colonization. In summary, mAbs 2C5, 10D6 and 25 significantly inhibited experimental *C. difficile* colonization and colitis in mice and thereby represent promising agents for passive immunotherapy against CDI.

3.4 Towards Fully Synthetic Vaccines Displaying Oligovalent Disaccharides

Based on the insights gained from antibody characterization and murine challenge studies, a rationally designed glycan mimetic of the PS-I polysaccharide able to elicit protective antibody responses was envisaged. The use of Alum promoted polyclonal and monoclonal antibodies with main reactivity to pentasaccharide **1** [Fig. 3.9 & Table 3.1] that both efficiently limited bacterial colonization in mice *in vivo* [Figs. 3.8 & 3.18]. Weak, micromolar affinity binding to single disaccharides **3** was likely dispensible for protective effects of the antibodies, but two connected copies of **3** were recognized with nanomolar affinity [Figs. 3.15 & 3.16]. The glucose moiety that is α-1→3-linked to rhamnose is required for binding as **3**, but not rhamnose **4** alone, was recognized by the mAbs [Table 3.1]. The glucoside backbone (oligoglucoses **5** and **6**) was neither bound by polyclonal nor monoclonal antibodies [Fig. 3.9 & Table 3.1]. Thus, terminal rhamnoses provided the major antigenic determinants with a minor but essential contribution of the linked glucoses. The additional glucose moiety at the reducing end of **1** was dispensible for antibody binding. The antibody interaction surface therefore likely encompasses the tetrasaccharide portion of **1** containing two adjacent copies of **3** [Fig. 3.19a].

Both polyclonal and monoclonal antibodies recognized the natural PS-I polysaccharide on the surface of *C. difficile* [Figs. 3.5 & 3.17]. In the polysaccharide, units of **1** are connected *via* glycosyl phosphate bridges between C-1 of the reducing end glucose and C-4 of terminal rhamnose [Fig. 3.19b].[205] Their binding patterns to synthetic glycans suggest that anti-**1** antibodies recognize two connected copies of **3** within each repeating unit of the polysaccharide, but neither the reducing end glucose nor the phosphodiester that is absent in **1**. A glycan mimetic of the polysaccharide therefore should include two or more connected units of **3**, and five disaccharide copies would constitute four overlapping antibody binding sites intended to generate avidity [Fig. 3.19c]. Such a glycan mimetic was expected to be highly antigenic and easily procured due to the straightforward synthesis of **3**.[284] To put these considerations into practice, disaccharides were covalentyl linked on oligo(amidoamine) (OAA) scaffolds. OAAs have been shown before to be non-toxic, non-immunogenic and suitable for oligovalent glycan presentation with comparably low synthetic effort.[272–276] The OAA compounds were kindly synthesized by Dr. Felix Wojcik. Thiol-ene coupling to conjugation-ready OAA backbones required the Rha-(1→3)-Glc disaccharide functionalized with a thiol group

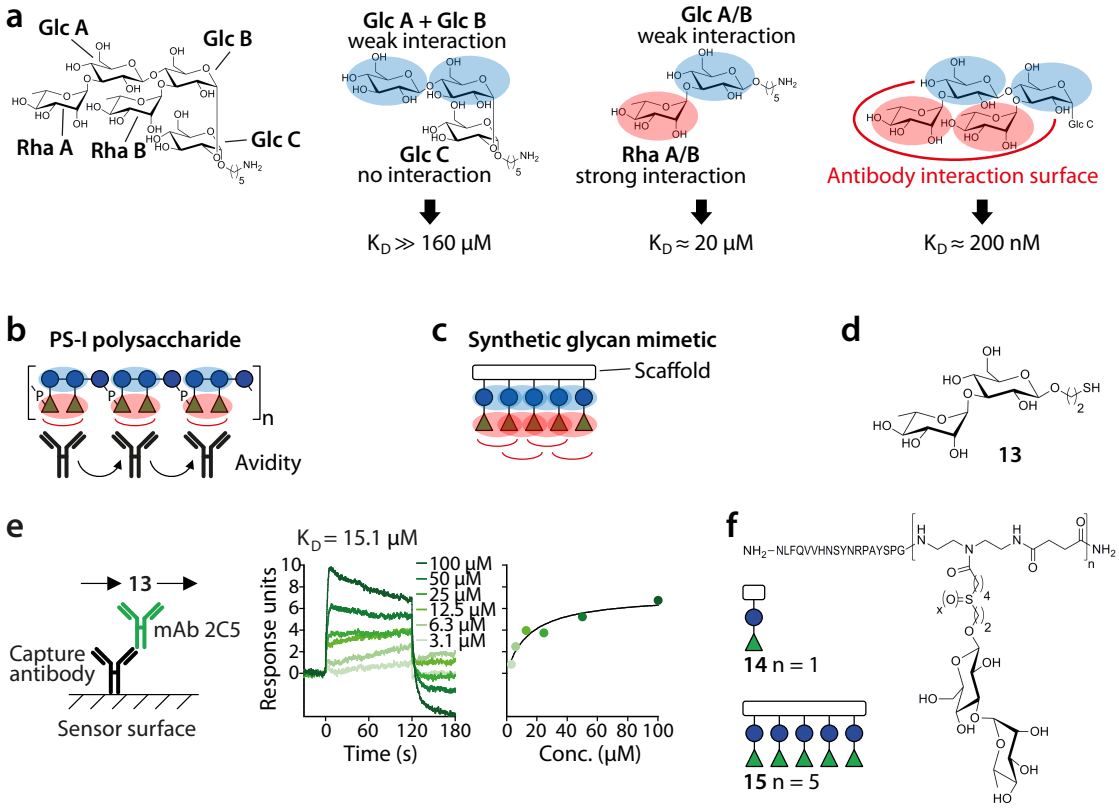

Figure 3.19: Rational design of synthetic glycan mimetics of the PS-I polysaccharide. (**a**) The proposed interaction surface of protective antibodies to PS-I (red line) was delineated from evidence of glycan-antibody interaction and *in vivo* challenge studies described in the previous sections. The indicated K_D values were obtained from SPR measurements of anti-**1** mAbs. Weak and strong mAb-antigen interactions are indicated blue and red, respectively. (**b**) Simplified structure of the PS-I polysaccharide indicating putative interaction surfaces with protective antibodies as red lines. Binding strength may be further enhanced by antibody re-binding (avidity) to neighboring epitopes. P indicates phosphodiester bridges. (**c**) Schematic of a pentavalent synthetic glycan mimetic with four overlapping antibody interaction surfaces. (**d**) Structure of disaccharide **13**. (**e**) Determination of the binding affinity of **13** to mAb 2C5 by SPR. (**f**) Structures of OAAs **14** (monovalent) and **15** (pentavalent). The peptide sequence of the T cell epitope is shown in one-letter code.

at the reducing end, compound **13** [Fig. 3.19d]. To test whether the thiol modification influenced antibody binding, the affinity of **13** to mAb 2C5 was determined by SPR [Fig. 3.19e]. The K_D value of 15.1 µM was similar to that of **3** (18.0 µM), and both interactions exhibited comparable association and dissociation kinetics [Table 3.1 & Fig. 3.14]. Thus, the thiol of **13** did not affect antibody binding. OAAs **14** (monovalent) and **15** (pentavalent) were obtained by thiol-ene coupling of **13** to activated OAA backbones. Solid-phase synthesis also allowed for the incorporation of a reported peptide T cell epitope, amino acids 366-383 of CRM_{197}[327], intended to recruit T cell help upon immunization. The synthesis of **13**-**15** is described elsewhere.[276,286]

3.4.1 A Pentavalent Glycan Mimetic of PS-I Is Strongly Antigenic

To test whether the disaccharide-functionalized OAAs were antigenic and if antibody binding strength benefited from oligovalent antigen display, **14** and **15** were subjected to SPR measurements with mAb 2C5 [Fig. 3.20a]. Oligosaccharides **3** and **1** served as additional controls representing monovalent interactions. It was expected that pentavalent display of the disaccharide in **15** would enhance antibody binding strength due to avidity effects. Binding of 2C5 to monovalent **14** was characterized by slow association rate constants that were below the measurable limit of the instrument, perhaps resulting from steric constraints imposed by the OAA scaffold [Fig. 3.20b]. Therefore, the dissocation rate constants k_d that are the major determinants of antibody binding strength were utilized to compare avidities.[328–334] The k_d values of **14**, **1** and **3** were comparable ($1.4 \times 10^{-3}\,s^{-1}$, $1.6 \times 10^{-3}\,s^{-1}$ and $1.9 \times 10^{-3}\,s^{-1}$, respectively), as expected since in all three cases re-binding of 2C5 could not occur. By contrast, dissociation of pentavalent **15** was five orders of magnitude slower ($k_d = 2.8 \times 10^{-8}\,s^{-1}$). Thus, **15** was highly antigenic and provided increased avidity over monovalent glycans through re-binding of the antibody. Whether increased affinity, i. e., faster association of **15** as compared to **14** also contributed to stronger binding could not be determined since k_a was below the measurable limit for both OAAs.

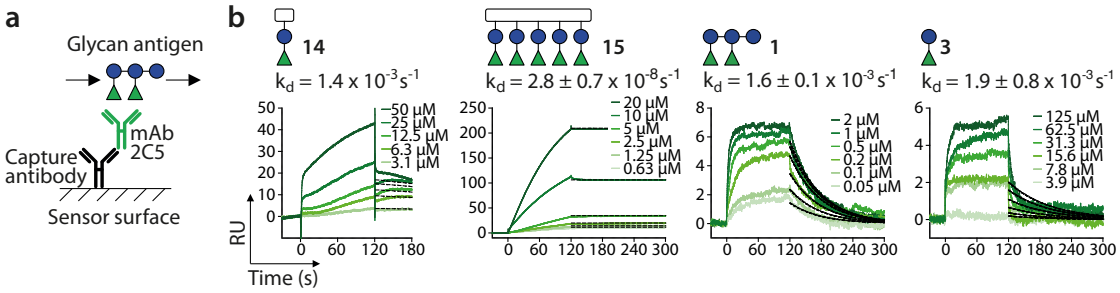

Figure 3.20: Antigenicity of synthetic glycan mimetics as determined by SPR. (**a**) Experimental setup. (**b**) Representative sensorgrams of the indicated antigens. The k_d values are mean ± SD of two or three experiments, except for **14** (one experiment). Dashed black lines show curve fittings with a dissociation stage model. Figure modified from Broecker *et al.*[286]

3.4.2 The Pentavalent Glycan Mimetic Elicits Highly Specific IgG in Mice

Knowing that it was highly antigenic raised the question whether **15** was immunogenic and able to elicit PS-I-specific antibodies in mice. Compound **15** represents a fully synthetic vaccine candidate comprising a peptide epitope intended to recruit T cell help [Fig. 3.19f]. Two semi-synthetic CRM_{197} glycoconjugate vaccine candidates served as controls. One was **12*** that comprised **3** and thereby represented monovalently displayed disaccharides [Fig. 3.21a].

The other one, **16**, contained **15** and was intended to determine if immunogenicity of the pentavalent OAA could be enhanced through presentation on a carrier protein [Fig. 3.21b]. Glycoconjugates were synthesized with di-*p*-nitrophenyl adipate[294] (DNAP) instead of the above used DSAP to facilitate the challenging conjugation reaction with **15**. DNAP is a more efficient crosslinking reagent since the half ester intermediates are less prone to hydrolysis during reaction with the carrier protein as compared to half esters of DSAP. Successful conjugation was verified by denaturing SDS-PAGE analysis of **12*** and **16** that were both shifted to higher masses relative to CRM_{197} [Fig. 3.21c]. Glycan incorporation was demonstrated by western blots using anti-**1** mAbs [Fig. 3.21d]. Stronger binding signals to **12*** indicated higher antigen loading as compared to **16**. A CRM_{197}-reactive anti-diphtheria toxin antibody bound to both glycoconjugates as well. Antigen loading was quantified using anthrone assay[293] [Fig. 3.21e]. For **12***, 140.6 µg carbohydrate per mg protein was equivalent to an average incorporation of 20 molecules **3** per CRM_{197}. Glycoconjugate **16** comprised 46.3 µg carbohydrate per mg protein, corresponding to an average of 1.3 molecules **15** (or 6.5 disaccharides) per CRM_{197}. Native CRM_{197} did not show detectable amounts of carbohydrate.

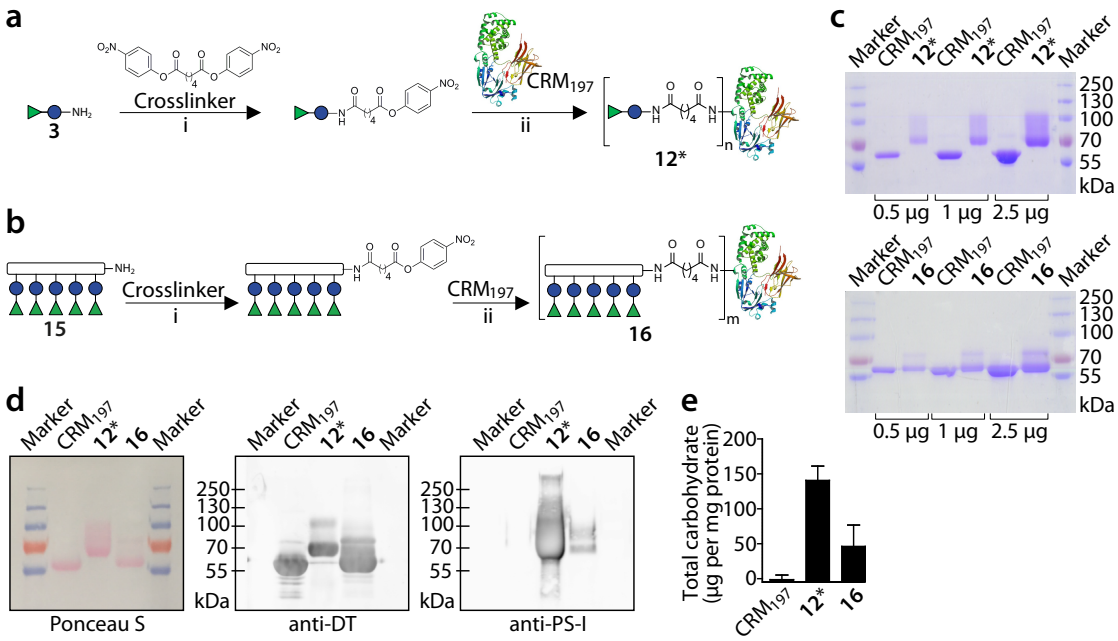

Figure 3.21: Preparation and characterization of glycoconjugates **12*** and **16**. (**a,b**) Reaction schemes for **12*** (**a**) and **16** (**b**). *Reagents and conditions:* (i) di-*p*-nitrophenyl adipate, Et_3N DMSO/pyridine (2:1); (ii) CRM_{197}, 100 mM sodium phosphate, pH 8. (**c**) Denaturing SDS-PAGE analysis of **12*** (top) and **16** (bottom) and CRM_{197}. Protein was stained with Coomassie brilliant blue. Numbers to the right are marker protein sizes in kDa. (**d**) Western blots. Protein transfer was verified by Ponceau S staining (left). CRM_{197} was detected with anti-DT (diphtheria toxin) antibody (center). PS-I glycans were detected with equimolar mAbs 2C5, 10A1 and 10D6 (right). (**e**) Total carbohydrate per mg protein as determined by anthrone assay. Bars show mean + SEM of two independent experiments. Figure modified from Broecker *et al.*[286]

Mice were immunized s. c. three times every two weeks either with **15**, **12*** or **16** (groups 1, 2 and 3, respectively) [Fig. 3.22a]. Two additional groups received **12*** twice and **16** once or *vice versa* (groups 4 and 5, respectively) to detect possible cross-reactive B cells. Each group comprised three mice. FA was selected for all immunizations since Alum requires adsorption of a (glyco)protein to exert its effect[227] and was therefore not applicable for **15**. Serum IgG responses of the immunized mice were followed by microarray analysis [Fig. 3.22b]. Glycoconjugate **15** (group 1) elicited IgGs to **1**, but not to **3**, even though **15** contains five copies of the disaccharide [Fig. 3.22c]. In contrast, **12*** (group 2) raised IgGs recognizing

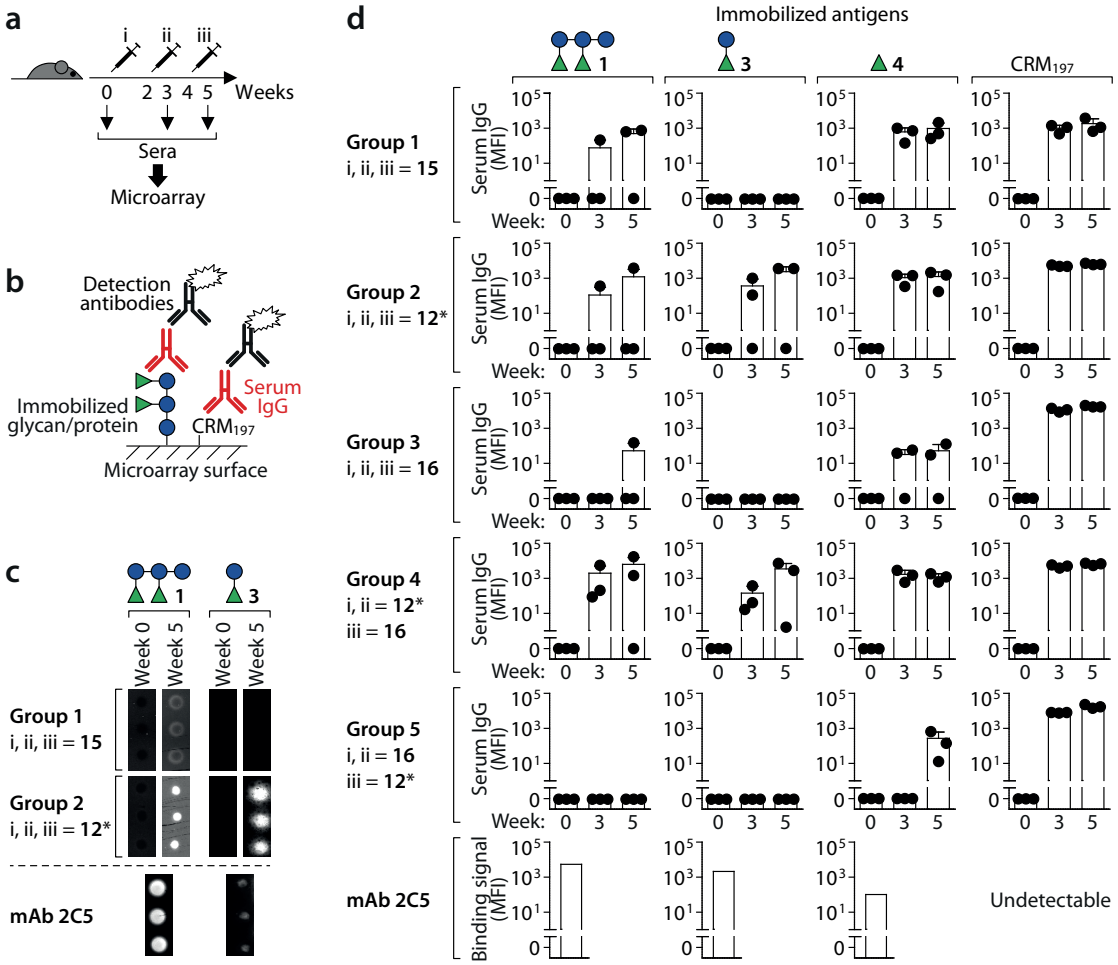

Figure 3.22: IgG responses to **15**, **12*** and **16** in mice inferred by microarray. (**a**) Immunization regime. Mice were immunized three times with **15**, **12*** or **16** (groups 1, 2 and 3, respectively), twice with **12*** and once with **16** or *vice versa* (groups 4 and 5, respectively). (**b**) Experimental setup. (**c**) Exemplary microarray scans representing serum IgG of one mouse of group 1 and one mouse of group 2. Oligosaccharides were spotted at 1 mM in triplicate. mAb 2C5 at 10 µg mL^{-1} served as positive control. (**d**) Serum IgG levels to the indicated glycans spotted at 1 mM or CRM_{197} at 1 µM expressed as MFI values. IgG to **1** was detected in serum diluted 1:20, IgG to the other antigens in 1:100-diluted serum. Black dots represent individual mice, bars mean + SD of each group. Figure modified from Broecker *et al.*[286]

both **1** and **3**. This was expected since glycoconjugate **12** that was similar in composition to **12*** but had lower antigen loading [Fig. 3.10] elicited IgGs of similar reactivity [Fig. 3.11]. Glycoconjugate **16** (group 3) did not elicit detectable amounts of IgG to the two glycan antigens except for one mouse with a weak response to **1** that was barely above the detection level [Fig. 3.22d]. However, **16** could boost an existing IgG response to both **1** and **3** elicited by **12*** (group 4), whereas the *vice versa* immunization regime did not yield detectable amounts of IgG (group 5). All mice produced IgG to CRM_{197}, demonstrating both successful immunizations and functionality of the synthetic T cell epitope of **15**. In addition, all **15**, **12*** and **16** elicited IgG to **4**, as observed before for glycoconjugates **10** and **12** that contained **1** and **3** as immunogens, respectively [Figs. 3.9 & 3.11]. IgG levels to **1** in groups 1-4 were low and only detectable in serum diluted 1:20, whereas antibodies to the other antigens were seen in 1:100 dilutions.

The antibody responses to **1** and **3** observed by microarray were verified by SPR measurements [Fig. 3.23a,b]. SPR is more sensitive than microarray and was expected to detect even lowly abundant serum antibodies. Measurement flow cells were functionalized with either **1** or **3**. BSA-functionalized flow cells served as references to compensate for non-specific binding of serum components. Sensorgrams obtained with mAb 2C5 that recognizes both **1** and **3** [Table 3.1] verified successful functionalization of the measurement flow cells [Fig. 3.23c]. Sensorgams obtained from pooled serum (diluted 1:100) of the five groups of mice described above were used to characterize antibody responses to **1** and **3** [Fig. 3.23d]. Binding signals of week 5 serum were subtracted by week 0 signals to minimize the background. Total antibody levels were estimated by determining the final response unit signals at the end of sample injection time at $t = 290\,s$ [Fig. 3.23e]. SPR measurements verified the presence of antibodies to **1**, but not to **3**, in mice immunized with **15** (group 1), whereas sera of mice immunized with **12*** (group 2) contained antibodies to both glycans. Antibodies to both **1** and **3** were furthermore seen in mice immunized twice with **12*** and once with **16** (group 4), but were undetectable in the remaining groups 3 and 5, further verifying that **16** did not induce measurable quantities of anti-PS-I antibodies. The SPR-inferred results were in good agreement with microarray data presented above. Collectively, murine immunization studies showed that the fully synthetic pentavalent vaccine candidate **15** elicited antibodies of high specificity to **1** at comparable levels to the semi-synthetic monovalent glycoconjugate **12***.

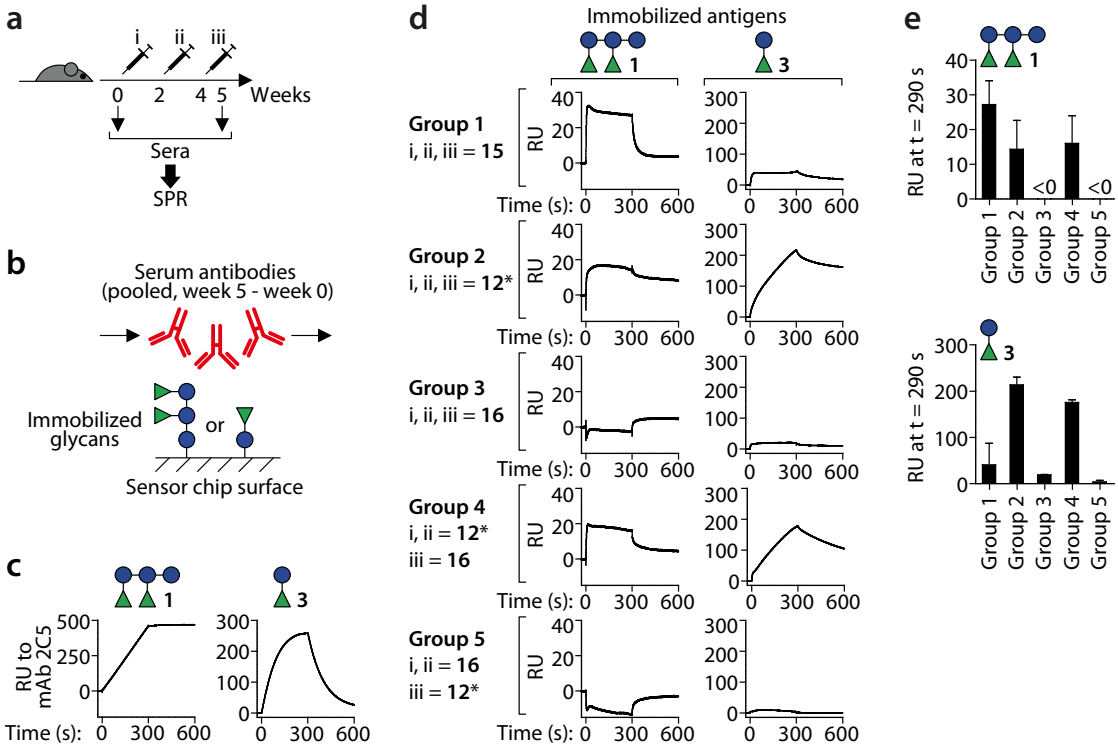

Figure 3.23: Antibody responses to **15**, **12*** and **16** inferred by SPR. (**a**) Immunization regime. Details are found in the caption of Fig. 3.22a. (**b**) Experimental setup. (**c**) Functionalization of the measurement flow cells was verified by injecting mAb 2C5 at 10 µg mL^{-1}. (**d**) Sensorgrams obtained from pooled serum of the indicated groups at week 5 at a dilution of 1:100. The curves are averaged from two independent experiments and were subtracted by the respective binding signals of week 0 serum. (**e**) The response units at t = 290 s obtained from sensorgrams shown in panel (**d**) served as an estimate of antibody levels. Bars show mean + SEM of two independent experiments. Figure modified from Broecker *et al.*[286]

3.5 Synthetic *C. difficile* Lipoteichoic Acid Glycans as Vaccine Candidates

In addition to PS-I and PS-II, a third *C. difficile* surface glycan termed lipoteichoic acid (LTA, also known as PS-III) has been recently described.[207] LTA is a polymer of disaccharide repeating units with the sequence α-Glc*p*NAc-(1→3)-(→*P*-6)-α-Glc*p*NAc-(1→2)-GroA (GroA being glyceric acid) that are connected *via* phosphodiester bridges between C-6 of the two GlcNAc residues (6-*P*-6) [Fig. 3.24]. Linked to the reducing end of this polymer, also through a 6-*P*-6 bridge, is a gentiotriosyl glycolipid β-Glc*p*-(1→6)-β-Glc*p*-(1→6)-β-Glc*p*-(1→1)-Gro, glycerol (Gro) being esterified with saturated or mono-unsaturated C_{14}-C_{18} fatty acids. This glycolipid serves as anchor to the bacterial cytoplasmic membrane. *C. difficile* LTA is classified as type V LTA that is structurally distinct from types I-IV of other Gram-positive bacteria [Fig. 1.4]. To date, type V LTA has been shown to be expressed by three other closely related species that are also pathogenic; *Clostridium sordellii*[215,335], *Clostridium bifermentans*[215,336] and *Peptostreptococcus anaerobius*[204,208,337].

Recently, glycoconjugates prepared with isolated *C. difficile* LTA polysaccharide were shown to elicit antibodies in rabbits and mice that bound to the surface of various *C. difficile* strains, suggesting that LTA is a ubiquitously expressed antigen.[238] The antisera also cross-reacted with the pathogenic clostridial species *C. bifermentans*[336], *C. butyricum*[338] and *C. subterminale*[339]. A broad range of clostridia are associated with infectious disease and sepsis[340], whereas non-pathogenic ones only represent a small fraction of the healthy intestinal microbiota[72,75]. Thus, *C. difficile* LTA represents an auspicious vaccine antigen, since cross-reactive antibodies may additionally target other pathogens but likely preserve the overall gut bacterial community.

Vaccine studies with *C. difficile* LTA have been hampered by low and inconsistent expression of the polysaccharide *in vitro*.[232] The availablity of synthetic oligosaccharide antigens may overcome these limitations. In 2013, Seeberger and colleagues reported the first synthesis of phosphodiester-bridged oligomers of *C. difficile* LTA, monomer **17**, dimer **18** and monomer flanked by two phosphodiesters **19** [Fig. 3.24].[285] Oligosaccharides **17**-**19** were used in this study and were kindly provided by Dr. Christopher Martin.

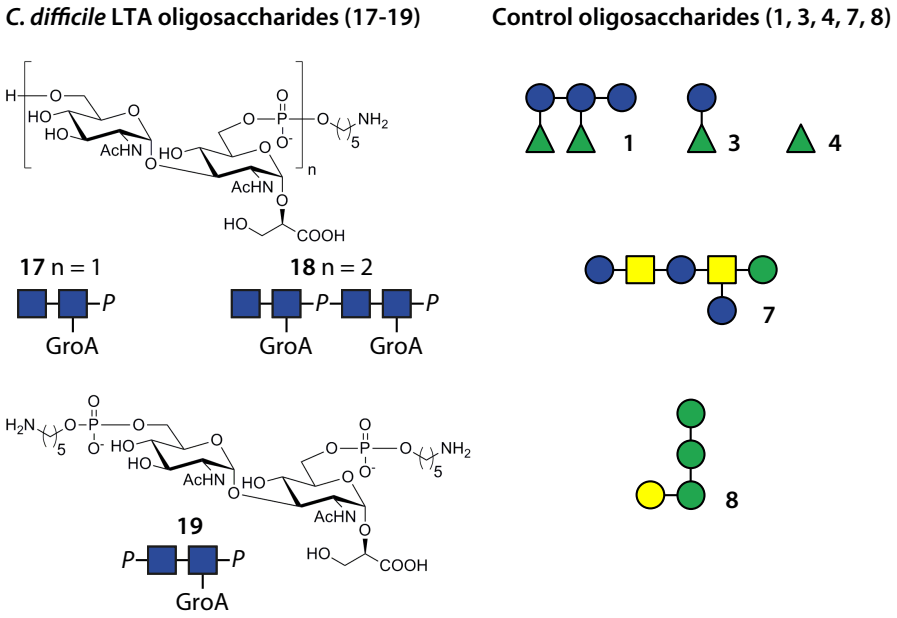

Figure 3.24: Synthetic oligosaccharides of *C. difficile* LTA **17**-**19** and control oligosaccharides, *C. difficile* PS-I pentasaccharide **1**, disaccharide **3**, rhamnose **4**, *C. difficile* PS-II hexasaccharide **7** and *Leishmania* lipophosphoglycan capping tetrasaccharide **8**. Detailed structures of the control oligosaccharides are provided in Fig. 3.1.

3.5.1 LTA Glycans do not Activate Innate Immunity *In Vitro*

LTA of various Gram-positive bacteria activate innate immune responses by engaging Toll-like receptor 2 (TLR2) on leukocytes, which leads to the release of immunestimulatory cytokines including interleukins (ILs) and tumor necrosis factor-alpha (TNF-α).[341] Contrarily, a recent study showed that stimulation with synthetic *C. difficile* LTA glycans did not activate cytokine release of peripheral blood mononuclear cells (PBMCs).[342] However, the major leukocyte population involved in the surveillance of intestinal mucosae are dendritic cells (DCs)[343] that only constitute fewer than 1 % of the PBMC population[344]. *C. difficile* being an intestinal pathogen provided a rationale to test whether synthetic LTA oligosaccharides activate innate immune responses specifically in DCs. To this end, murine bone marrow (BM) cells were differentiated into bone marrow-derived DCs (BMDCs) by *in vitro* stimulation with recombinant granulocyte macrophage-colony stimulating factor (GM-CSF) [Fig. 3.25a]. Successful differentiation was verified by flow cytometric detection of the murine DC marker CD11c[346] [Fig. 3.25b]. Both non-stimulated and stimulated BM cells showed similar scatter distributions, but CD11c expression was markedly increased in the GM-CSF-exposed as compared to naïve BM cells. The BMDCs were then stimulated *in vitro* with the largest available LTA glycan, dimer **18**. Concentrations from 0.1 to 10 µM of **18** were chosen since synthetic LTA molecules of other Gram-positive bacteria have been shown to exert stimulating activity

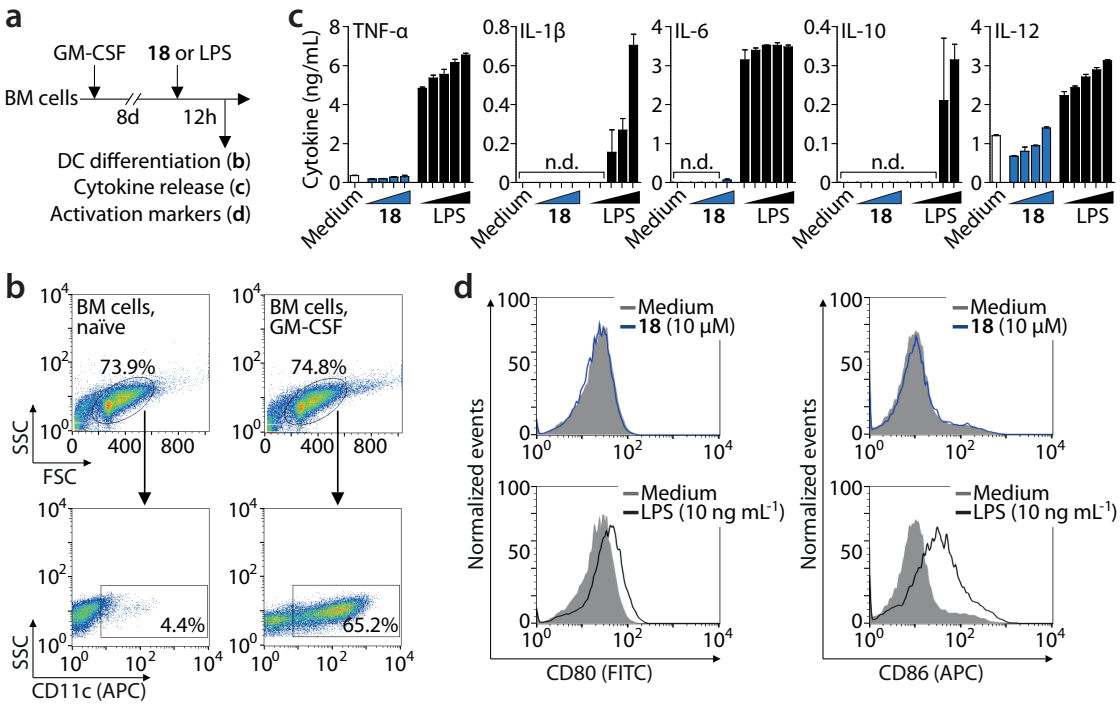

Figure 3.25: Synthetic *C. difficile* LTA does not activate innate immunity *in vitro*. (**a**) Murine BM cells were differentiated into BMDCs with GM-CSF. BMDCs were stimulated with **18** or *E. coli* LPS. Cytokine release and surface expression levels of CD11c, CD80 and CD86 were determined. (**b**) GM-CSF-induced differentiation was verified by flow cytometry. The gated scatter populations (top) were analyzed for CD11c expression (bottom). (**c**) ELISA-inferred cytokine release of BMDCs after stimulation with **18** or LPS. Bars show mean + SEM of two independent experiments. Medium represents non-stimulated BMDCs. n.d., not detectable. Concentrations from left to right: 0.1, 0.5, 1, 10 μM (**18**); 0.01, 0.05, 0.1, 1, 10 μg mL^{-1} (LPS). (**d**) Flow cytometric analysis of CD80 and CD86 surface expression levels. Histograms represent scatter populations gated as in panel (**b**). Figure adapted from Broecker *et al.*[345]

in this range.[347,348] Isolated LPS of *E. coli*, a known agonist of TLR4 that is expressed on DCs[349], served as positive control for activation of innate immunity. As expected, stimulating BMDCs with LPS triggered dose-dependent release of TNF-α and various ILs, all of which known to be secreted by activated DCs[350] [Fig. 3.25c]. By contrast, cytokine release was not affected by exposure to **18** even at the highest concentration of 10 μM. In addition, surface expression levels of the DC activation markers CD80 and CD86[350] were elevated on LPS-stimulated BMDCs but not on those exposed to **18** [Fig. 3.25d]. Taken together, **18** was unable to activate innate immune responses in DCs *in vitro*, in agreement with previous findings on synthetic *C. difficile* LTAs and PBMCs.[342]

3.5.2 LTA Glycans Are Antigenic and Recognized by Antibodies of *C. difficile* Patients

Next, the involvement of synthetic LTAs in adaptive immunity was investigated. To this end, feces obtained from eight CDI patients and eight control individuals without *C. difficile* disease were studied for the presence of anti-LTA secreted IgA (sIgA) with microarrays displaying **17**-**19** [Fig. 3.26a,b]. sIgA is involved in the immune defense against intestinal pathogens[310], and feces of CDI patients contain sIgA to both PS-I and PS-II antigens [Fig. 3.3]. Therefore, PS-I glycans **1**, **3**, **4** and PS-II hexasaccharide **7** were included on the microarrays as positive controls. In addition, clostridial toxin TcdA that is known to induce sIgA responses during CDI[311] was immobilized on the slides. *Leishmania* tetrasaccharide **8** served as negative control. In contrast to the PS-I, PS-II and TcdA antigens, sIgA to **17**-**19** was not or only barely detectable in fecal specimens of both patients and controls [Fig. 3.26c]. Some samples exhibited a low level of sIgA to **8**. In addition to mucosal sIgA, immunity to *C. difficile* can be conferred by systemic IgG to surface antigens.[135] Therefore, the presence of anti-LTA IgG was studied by microarray-assisted screening of serum samples obtained from eight reconvalescent CDI patients (diagnosed with *C. difficile* disease and recovered) and eight control individuals without a history of CDI [Fig. 3.26c]. In contrast to fecal sIgA, serum

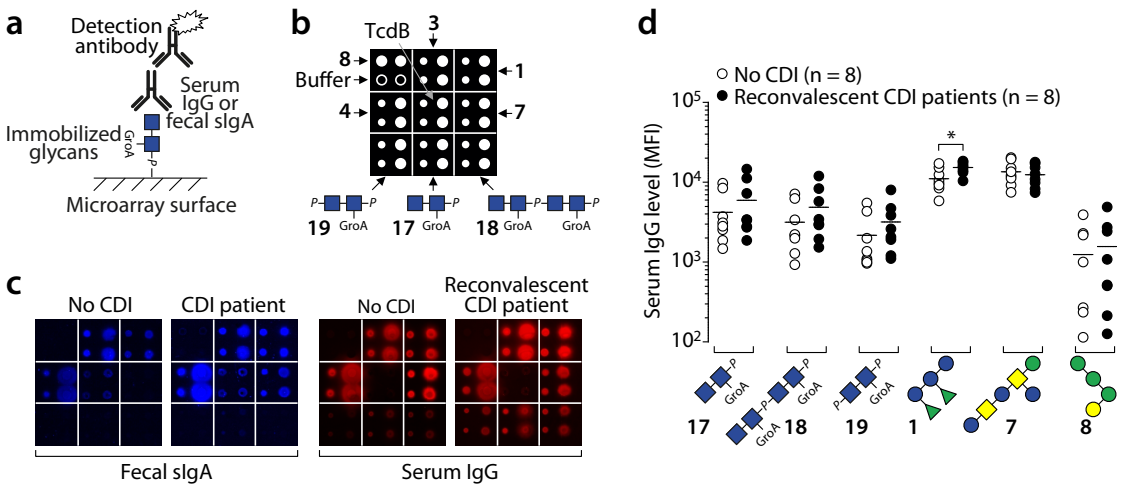

Figure 3.26: Microarray-assisted detection of antibodies to **17**-**19** in samples of *C. difficile* patients and healthy controls. (**a**) Experimental setup. (**b**) Spotting pattern of microarray scans presented in panel (**c**). Oligosaccharides were spotted at 0.5 mM (small circles) or 1 mM (large circles). TcdA was spotted at 0.5 µM (small circles) and 1 µM (large circles). (**c**) Exemplary microarray scans representing fecal sIgA (blue) and serum IgG (red) of one patient and one control individual. (**d**) Serum IgG levels expressed as microarray-inferred MFI values obtained from oligosaccharides spotted at 1 mM. Data points represent individual patients, horizontal lines the mean of each group. $^*P \leq 0.05$; unpaired two-tailed Student's *t*-Test. Figure adapted from Broecker *et al.*[345]

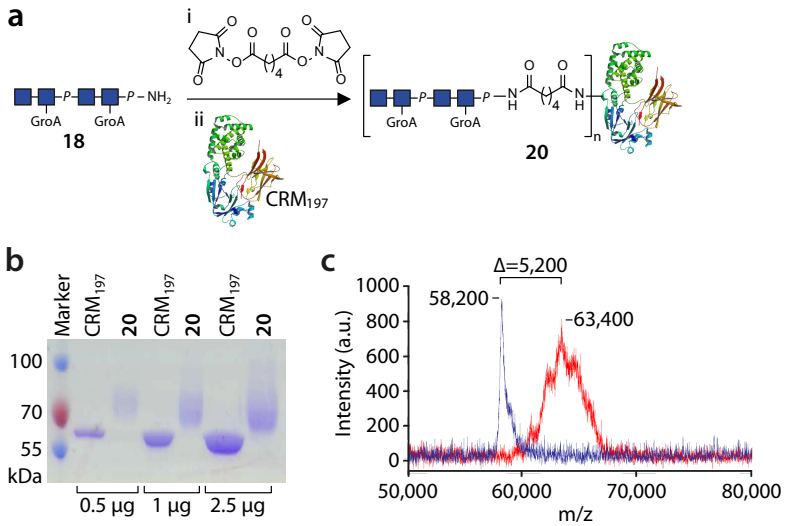

Figure 3.27: Preparation and characterization of glycoconjugate **20**. (**a**) Reaction scheme. *Reagents and conditions:* (i) di-*N*-succinimidyl adipate, Et_3N DMSO; (ii) CRM_{197}, 100 mM sodium phosphate, pH 7.4. (**b**) Denaturing SDS-PAGE analysis of **20** and CRM_{197}. Protein was stained with Coomassie brilliant blue. Numbers to the left are marker protein sizes in kDa. (**c**) MALDI-TOF MS analysis of **20** (red) and CRM_{197} (blue). a.u., arbitrary units. Figure adapted from Broecker *et al.*[345]

IgG to **17**-**19** was detected in all individuals of both cohorts. IgG to the PS-I and PS-II glycans, but not to TcdA, was also observed. Microarray-inferred serum IgG levels to **17**-**19** were slightly higher in the patients than in the controls, albeit without statistical significance likely due to the small sample sizes [Fig. 3.26d]. IgG to **1** was elevated in the patients relative to control individuals, as observed above [Fig. 3.2]. No differences in IgG levels to PS-II **7** and *Leishmania* antigen **8** between the two cohorts were observed. Collectively, microarray studies revealed that oligosaccharides **17**-**19** are antigenic and share epitopes with the natural LTA polysaccharide that likely elicits IgG responses during human exposure to *C. difficile*.

3.5.3 A Semisynthetic LTA Glycoconjugate Efficiently Adsorbs to Alum

LTA dimer **18** was selected for immunization studies in mice, as larger glycans are usually more immunogenic than smaller ones and more likely display protective epitopes of the natural polysaccharide.[234,245–248] A glycoconjugate composed of **18** and CRM_{197} was synthesized using DSAP crosslinker [Fig. 3.27a]. Successful conjugation was verified by denaturing SDS-PAGE analysis, in which the obtained glycoconjugate **20** migrated at higher masses relative to native CRM_{197} [Fig. 3.27b]. The mass shift was quantified by MALDI-TOF MS analysis to be 5,200 Da that corresponds to an average antigen loading of about four molecules **18** per CRM_{197} [Fig. 3.27c].

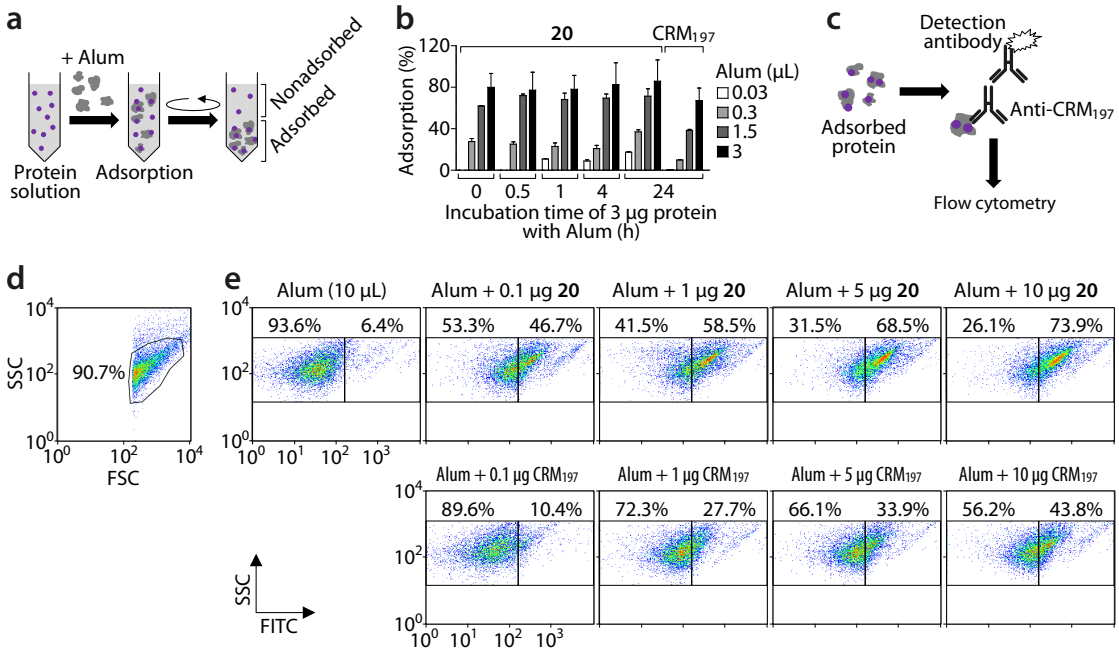

Figure 3.28: Adsorption of **20** and CRM_{197} to Alum. (**a**) Experimental flowchart applying to panel (**b**). (**b**) Adsorption efficiencies at various protein-to-Alum ratios and incubation times in percent. Bars show mean + SD of two or three independent experiments. (**c**) Experimental flowchart applying to panels (**d**) and (**e**). (**d**) Representative scatter plot of nonadsorbed Alum particles. The distribution did not change upon protein adsorption (data not shown). (**e**) Flow cytometric quantification of Alum-adsorbed **20** (top) or CRM_{197} (bottom) at various protein-to-Alum ratios. FITC signal intensity correlates with adsorption. The shown populations were gated within the respective scatter plots as in panel (**d**). Figure adapted from Broecker *et al.*[345]

Mice were intended to be immunized with **20** either in the absence of adjuvant, co-administered with FA or Alum. FA was selected due to its potent promotion of anti-glycan antibodies in mice [Figs. 3.5 & 3.11] and Alum as human-approved adjuvant[223]. To exert its immunogenicity-enhancing effects, Alum requires adsorption of (glyco)protein antigens that is mediated by electrostatic interactions.[281] Hence, presence of the negatively charged immunogen **18** [Fig. 3.24] was expected to influence the adsorption efficiency of **20** as compared to the non-conjugated carrier protein. Adsorption of **20** and CRM_{197} to Alum was quantitatively studied by two *in vitro* methods. In the first assay[295], Alum particles were incubated with **20** or CRM_{197} for up to 24 h at 4 °C. Then, the concentration of nonadsorbed protein was used to calculate adsorption efficiencies in percent [Fig. 3.28a]. Compound **20** was dose-dependently adsorbed to Alum more efficiently than CRM_{197} [Fig. 3.28b]. The efficiency did not majorly benefit from longer incubation times. Thus, the adsorption process was mostly completed within minutes, as reported previously for different proteins.[228] After 24 h of incubation and a 1:1 ratio of **20** (3 µg) to Alum (3 µL), 85.9 % of the glycoconjugate was adsorbed. Native CRM_{197} adsorbed less efficiently by 67.1 % under the same

conditions. To confirm these findings, adsorption was determined by flow cytometry, as described.[296] Following incubation with Alum, adsorbed **20** or CRM_{197} was quantitatively detected with an anti-CRM_{197} antibody (a kind gift by Dr. Chakkumkal Anish and Annette Wahlbrink) [Fig. 3.28c]. Alum particles that have a reported size of about 2-10 µm[351] showed a distinct scatter population that remained unchanged upon incubation with **20** or CRM_{197} [Fig. 3.29d]. Again, dose-dependent adsorption was observed with higher efficiency for **20** than for CRM_{197} [Fig. 3.29e]. When incubated at a 1:1 (w/v) protein-to-Alum ratio, the fraction of anti-CRM_{197}-labeled particles reached 73.9 % for **20** and 43.8 % for CRM_{197}. These conditions were used to prepare Alum-adsorbed **20** intended for immunizations.

3.5.4 The LTA Dimer Is Immunogenic in Mice and Raises IgG Recognizing the Natural Polysaccharide

Groups of three mice received **20** s. c. either without adjuvant, with Alum or with FA. The immunization regime included three injections each containing 3 µg of **18** in two-week intervals [Fig. 3.29a]. Anti-LTA serum IgG responses were followed by microarray analysis. Glycoconjugate **20** elicited IgG to **17**-**19** in all mice except for one of the Alum group [Fig. 3.29b]. The identification of IgG1, IgG2a and IgG3 subtypes indicated that class switching, a hallmark of T cell-dependent immunity, occurred [Fig. 3.29c]. Antibody levels increased over time. Post-immune (week 5) IgG1 and IgG2a levels were highest in mice immunized in the presence of FA, whereas Alum promoted strongest IgG3 responses. The differences, however, were not statistically significant due to the small group sizes. Effects of the adjuvants on anti-glycan antibody levels were less pronounced than observed before for glycoconjugate **10** with PS-I pentasaccharide **1** as immunogen [Fig. 3.5]. This also reflected in the ELISA-inferred post-immune anti-CRM_{197} IgG levels that were similar among the groups irrespective of the employed adjuvant [Fig. 3.29d].

Adjuvants can influence the epitope recognition pattern of anti-glycan antibodies, as observed above for PS-I pentasaccharide **1** [Fig. 3.9]. This provided a rationale to investigate whether antisera raised with **20** showed adjuvant-dependent binding patterns to LTA antigens as well. To this end, post-immune IgG1 levels to **17**-**19** were compared [Fig. 3.29e]. Levels to immunogen **18** and monomer substructures with one (**17**) or two (**19**) flanking phosphodiesters were comparable when no adjuvant or Alum was used, indicating that in these cases the minimal glycan epitope was monomer **17** or a substructure thereof. By contrast, **17** was only weakly recognized by FA-promoted IgG1 and efficient binding required

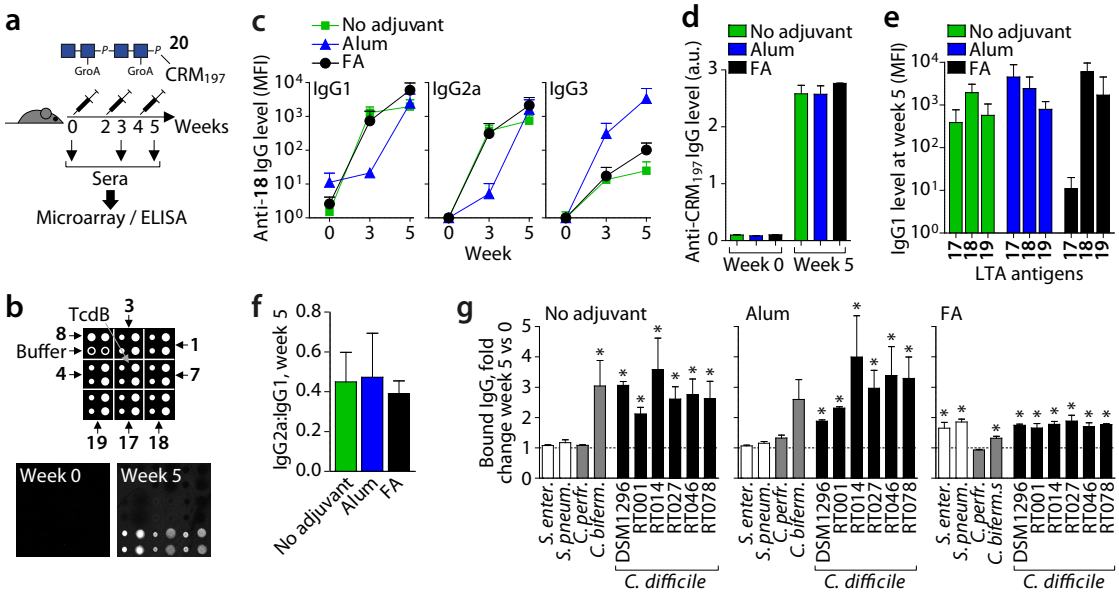

Figure 3.29: Immunogenicity of glycoconjugate **20**. (**a**) Immunization regime. (**b**) Exemplary microarray scans representing IgG1 of one mouse immunized with **20** and Alum. (**c**) Microarray-inferred serum IgG levels to **18** spotted at 1 mM expressed as MFI values. Data points show mean + SEM of three mice. (**d**) ELISA-inferred anti-CRM_{197} IgG levels of pooled sera. Bars show mean + SEM of two experiments. a.u., arbitrary units (absorption at 450 nm). (**e,f**) Epitope recognition patterns (**e**) and IgG2a:IgG1 ratios (**f**). Bars show mean + SEM of three (No adjuvant, FA) or two mice (Alum). (**g**) Serum IgG binding to various bacteria inferred by whole cell ELISA. Fold change is the ratio of week 5 to week 0 binding signals obtained with pooled serum. Bars show mean + SEM of two independent experiments in duplicate. $^*P \leq 0.05$, week 5 vs week 0; unpaired two-tailed Student's *t*-Test. *S. enter.*, *Salmonella enterica*; *S. pneum.*, *Streptococcus pneumoniae*; *C. perfr.*, *Clostridium perfringens*; *C. biferm.*, *Clostridium bifermentans*. Figure adapted from Broecker *et al.*[345]

the two phosphodiesters present in **19**. Adjuvants are also known to affect the activated T helper (Th) cell phenotype.[352] FA induces Th1-type responses predominated by IgG2a antibodies that mediate cellular immunity, whereas the Th2-directing Alum mainly promotes IgG1 important for antibody-mediated (humoral) immunity.[353] Therefore, as a readout for Th skewing and adjuvant activity, the IgG2a:IgG1 ratio in post-immune sera was compared [Fig. 3.29f]. There were no major differences in IgG2a:IgG1 ratios among the three groups of mice. This provided further credence to the notion that both FA and Alum had little influence on the immunogenicity of **20**.

Next, recognition of the natural polysaccharide on *C. difficile* by the anti-LTA antibodies was investigated. To this end, formalin-inactivated clinical isolates of ribotypes 001, 014, 027, 046 and 078 that represent frequent disease-causing strains in hospitals worldwide[18–22] and *C. difficile* reference strain DSM1296 were immobilized on ELISA plates. The related clostridia *C. bifermentans* and *C. perfringens* as well as two non-related bacterial species, *S. pneumoniae* (Gram-positive) and *Salmonella enterica* (Gram-negative), served as con-

trols. The immobilized bacteria were probed with pooled LTA antiserum. The level of bacteria-binding IgG was determined as post-immune (week 5) to pre-immune (week 0) ratios [Fig. 3.29g]. IgG raised without adjuvant or with Alum significantly bound to all investigated *C. difficile* strains. No binding was observed to the non-related control bacteria *S. enterica* and *S. pneumoniae*. The related *C. bifermentans*, but not *C. perfringens*, was recognized by post-immune IgG, similar to antibodies raised with isolated LTA polysaccharide.[238] This indicated that *C. difficile* and *C. bifermentans* share similar LTA epitopes. IgG raised in the presence of FA weakly bound to *C. difficile* but also to the other bacteria except for *C. perfringens*. The limited specificity of FA-promoted anti-LTA IgG for *C. difficile* may be explained by the epitope recognition pattern that was different from IgG raised without adjuvant or Alum [Fig. 3.29e]. This suggests that recognition of monomer **17** was crucial for efficient binding to the polysaccharide. FA proved not to be suitable as adjuvant for **20**.

3.5.5 The Semisynthetic LTA Glycoconjugate Is Stable when Formulated with Alum or Freund's Adjuvant

The weak efficacy of Alum and FA may have been due to reduced stability of **20** in the adjuvant-formulated as compared to the soluble form. Degradation may affect both the protein and the glycan part of the glycoconjugate. Some proteins have been shown to be less thermally stable when adsorbed to Alum.[228,354] Increased hydrolytic glycan degradation has been reported for a *H. influenzae* type b polysaccharide glycoconjugate vaccine following Alum adsorption.[355] FA is a water-in-oil adjuvant in which the water-soluble (glyco)protein is emulsified with mannide monooleate into paraffin oil.[356] It has been shown that emulsification in FA does not affect protein integrity within 24 h at 4 °C[357], but stability data on glycoconjugates is lacking.

To asses its stability in the adjuvant formulations, **20** was first adsorbed to Alum or emulsified with FA at similar conditions used for immunization studies. Non-formulated **20** that was diluted in phosphate-buffered saline (PBS) served as control. The three formulations were incubated for one week at various temperature regimes including 37 °C for up to seven days to simulate the conditions following injection into mice [Fig. 3.30a]. After the incubation period, Alum particles did not exhibit any visible changes. In contrast, FA emulsions exhibited some degree of phase separation that was most pronounced after seven days at 37 °C where a lower, less dense layer of about one third of the total volume was visible (data not shown), as described before.[358] Next, **20** was extracted from the adjuvant formulations following

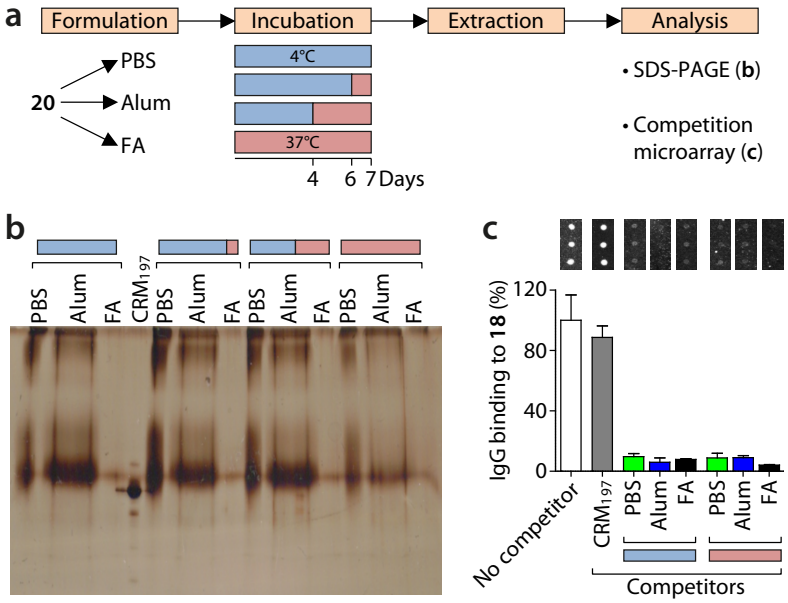

Figure 3.30: Stability of adjuvant-formulated **20** at various temperature regimes. (**a**) Experimental flowchart. (**b**) Denaturing SDS-PAGE analysis of adjuvant-extracted **20** following incubation at the indicated temperature regimes. CRM_{197} (100 µg) was loaded for comparison. Protein was visualized by silver staining. The amount of **20** varies as fixed volumes of crude extracts were used. (**c**) Competition microarray experiment with adjuvant-extracted and washed **20** following incubation at the indicated temperature regimes. The IgG binding signals of 1:1500-diluted pooled post-immune serum (week 5, mice immunized with **20** and Alum, see Fig. 3.29) to **18** spotted at 0.1 mM with or without competitors are shown. Bars represent mean + SD of three spots. Binding signals of serum without competitor were set to 100 %. The competitors, CRM_{197} at 50 µg mL^{-1}, or **20** at 0.4 µg mL^{-1}, were pre-incubated with the serum for 5 min before addition to the microarray slide. Microarray scans (**18** spotted in triplicate) are shown above the respective bars. Figure adapted from Broecker *et al.*[345]

published protocols. Extraction from Alum was achieved by 2.5 h of incubation in surfactant-containing, high ionic strength phosphate/citrate buffer at 60 °C.[297] The partially separated FA emulsions were vigorously mixed with 50 % (v/v) benzyl alcohol and **20** was retrieved from the distinct aqueous layer that formed upon high-speed centrifugation.[298] To study the integrity of **20**, crude extracts were separated by denaturing SDS-PAGE [Fig. 3.30b]. The extracted glycoconjugate, following the various incubation regimes, was shifted to similar masses above the native CRM_{197} protein that was loaded for comparison. There were no visible degradation products that would run at lower masses. To assess whether the glycan antigen **18** was still intact on **20**, the extracts were washed three times with deionized water using centrifugal filter devices with a cut-off size of 10 kDa. This would remove any detached glycan from the glycoconjugate. The washed extracts were used for a competition microarray experiment with pooled post-immune (week 5) serum of mice immunized with **20** and Alum [Fig. 3.29]. Pre-incubation of the serum with 0.4 µg mL^{-1} of extracted **20** reduced IgG binding signals to **18** by more than 90 %, similar to non-formulated **20** [Fig. 3.30c]. There were no

differences between adjuvant formulations or incubation temperatures. IgG inhibition was LTA-specific, since pre-incubating serum with native CRM_{197} at 50 µg mL^{-1} did not reduce IgG binding to **18**. This showed that the glycan antigen **18** remained present and intact in the extracts of **20**. Taken together, there was no evidence that limited adjuvanting efficacy of Alum or FA was due to impaired glycoconjugate stability.

3.5.6 Antisera Raised with LTA Dimer Show No Functional Activity *In Vitro* But Limit *C. difficile* Colonization *In Vivo*

The functionality of antisera raised with **20** was addressed *in vitro* using an opsonophagocytosis assay (OPA) that measures phagocytosis-promoting effects of bacteria-binding antibodies. This assay is commonly used to estimate the efficacy of *S. pneumoniae* vaccine candidates where opsonophagocytic activity correlates with protection.[301] OPA, however, is not established for *C. difficile*, as previous vaccine studies mainly focused on the secreted clostridial toxins as immunogens.[135] To investigate the phagocytosis-promoting activity of polyclonal serum antibodies raised with **20**, the assay reported for *S. pneumoniae* was modified. Pooled serum of the Alum group and inactivated *C. difficile* ribotype 014 bacteria were used, as this combination showed highest IgG binding signals [Fig. 3.29]. After binding of the polyclonal anti-LTA antibodies, bacteria were incubated with *in vitro*-differentiated HL-60 cells that served as phagocytes [Fig. 3.31a]. Antibody-laden bacteria were adhered to the cells at 4 °C. Then, phagocytosis was promoted at 37 °C, while control samples kept at 4 °C were used to measure bacterial adherence. Finally, the extent of phagocytosis was measured by flow cytometric quantification of cell surface-bound bacteria. There was no evidence that antibodies raised with **20** promoted uptake into phagocytes in this set-up, as the amount of surface-bound and therefore non-phagocytosed bacteria was identical for pre- (week 0) or post-immune (week 5) serum [Fig. 3.31b]. However, the OPA is not established for *C. difficile* and may require optimization, such as including complement.[359] Also this assay was performed with formalin-inactivated bacteria, since unlike *S. pneumoniae* that survives under aerobic conditions, *C. difficile* is a strict anaerobe. Formalin treatment may have altered the bacterial surface such that its recognition by phagocytes was impaired. Moreover, a positive control such as an antibody that is known to promote phagocytosis of *C. difficile* was not available.

A major activity of intestinal antibodies, including IgG, is physically preventing mucosal attachment of pathogens independent of phagocytes.[310,360] Therefore, the ability of LTA

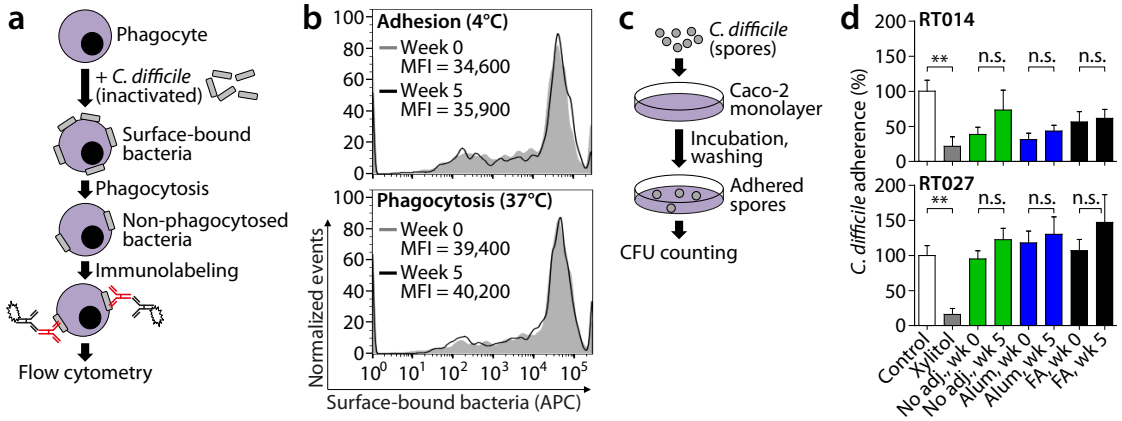

Figure 3.31: *In vitro* functional activity of LTA antiserum raised with **20**. (**a**) Experimental flowchart applying to panel (**b**). (**b**) Opsonophagocytic activity of LTA antiserum measured by flow cytometry. The results are representative of two independent experiments. (**c**) Experimental flowchart applying to panel (**d**). (**d**) Adherence of *C. difficile* spores following incubation with xylitol or pooled serum is shown. Bars represent mean + SEM of two or more experiments in triplicate. $^{**}P \leq 0.01$; n.s., not significant; unpaired two-tailed Student's *t*-Test.

antisera to inhibit colonization of *C. difficile* was tested with a reported *in vitro* assay.[303–305] The assay was performed at the Universität Erlangen with kind assistance of Prof. Jochen Mattner and Erik Wegner. Viable *C. difficile* suspensions obtained from liquid cultures of ribotype 014 and 027 strains that are both recognized by anti-LTA IgG [Fig. 3.29] were incubated with pooled sera. The antibody-laden bacteria were allowed to adhere to a monolayer of Caco-2 cells, a human colon adenocarcinoma-derived epithelial cell line[361] that served as a surrogate for colonic epithelium[305] [Fig. 3.31c]. After removal of any unbound bacteria, the monolayer was disrupted and plated at limited dilutions on blood agar medium that allows for growth of *C. difficile*. Up to this point, incubation and washing steps required about four hours under aerobic conditions, which inactivates the vast majority of vegetative *C. difficile* cells.[29] Therefore, any effect on bacterial adhesion determined by this assay is mainly targeted to the oxygen-resistant spores present in liquid cultures.[362] The agar plates were incubated for at least 24 h under anaerobic conditions and CFUs were counted to quantify the inhibition of spore adhesion. Xylitol that is known to block adhesion of *C. difficile* to Caco-2 cells[305] and was used as positive control significantly reduced adhesion of both ribotyoes 014 and 027 [Fig. 3.31d]. By contrast, LTA antisera had no significant effect on bacterial adhesion. This suggested that the LTA polysaccharide on *C. difficile* spores was either not surface-exposed or expressed at levels too low to bind sufficient amounts of anti-LTA antibodies. In support of this, expression of LTA polysaccharide in spores has been shown to be significantly lower than in vegetative cells *in vitro*.[206,238]

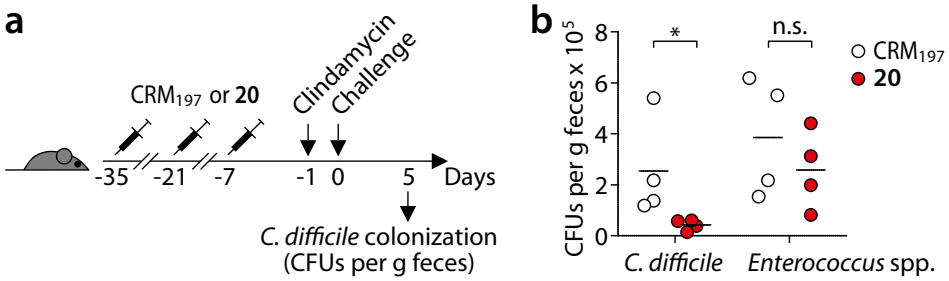

Figure 3.32: Levels of intestinal *C. difficile* colonization in mice immunized with **20** or CRM_{197}. (**a**) Immunization and challenge regime. (**b**) Comparison of intestinal colonization levels at day 5 determined as CFUs per gram feces. Data points represent individual mice, horizonzal lines the mean of each group. $^*P \leq 0.05$; n.s., not significant; unpaired one-tailed Student's *t*-Test. Figure adapted from Broecker *et al.*[345]

Finally, a murine challenge model was employed to assess whether immunization with **20** could limit *C. difficile* colonization *in vivo*. The challenge studies were kindly performed by Prof. Jochen Mattner at the Universität Erlangen, Germany. Two groups of four mice were immunized s. c. three times with either **20** or an equal amount of CRM_{197} as control in two-week intervals [Fig. 3.32a]. The human-approved Alum was selected as adjuvant since this formulation is closest to a potential clinical application.[223] Six days after the third immunization, mice were rendered susceptible to *C. difficile* infection with the antibiotic clindamycin, as described.[306] The next day, mice orally received 10^7 CFUs of the clindamycin-resistant *C. difficile* strain M68 that is able to induce colitis in mice.[307] Five days after the bacterial challenge, colonic CFUs of *C. difficile*, or of Gram-positive enterococci as control, were determined by plating limited dilutions of fecal suspensions on selective agar medium followed by overnight culture. The level of *C. difficile* colonization, determined as CFUs per gram of feces, was 83 % lower in mice immunized with **20** than in the CRM_{197} controls, with statistical significance [Fig. 3.32b]. There was no difference in *Enterococcus* levels. Both groups, however, exhibited similar degrees of enterocolitis that was assessed by histopathological analysis of colon tissue (personal communication by Jochen Mattner). Apparently, the remaining numbers of *C. difficile* bacteria that colonized the intestine of mice immunized with **20** were sufficient to induce disease symptoms in this experimental setting. However, the dose that was used for challenge (10^7 spores) by far exceeds the typical infectious dose causing human disease, which is likely ten spores or lower.[41,363,364] Therefore, LTA antisera may well prevent naturally acquired infection, rendering LTA dimer **18** a promising antigen for a vaccine against *C. difficile* colonization.

Chapter 4

Discussion

A discussion of the immunization and challenge experiments with PS-I pentasaccharide **1**, disaccharide **3** and LTA dimer **18** (**Sections 3.1, 3.2 and 3.5**, respectively) is provided in **Section 4.1**. The results related to the generation and analysis of mAbs against PS-I (**Section 3.3**) are discussed in **Section 4.2**. A discussion on the efforts towards a fully synthetic vaccine based on oligovalent disaccharides of PS-I (**Section 3.4**) is presented in **Section 4.3**. An outlook with respect to potential clinical applications of the vaccine candidates and mAbs is given at the end of each section.

4.1 Vaccine Potential of Synthetic PS-I and LTA Glycans

4.1.1 PS-I and LTA Oligosaccharides Are Antigenic

Glycan microarray-assisted screenings of serum and fecal specimens obtained from CDI patients and control individuals demonstrated that all herein investigated oligosaccharides of PS-I, **1**-**6**, were recognized by naturally circulating antibodies and thereby likely represent epitopes of the native polysaccharide [Figs. 3.2 & 3.3]. A tendency towards higher serum IgG levels in reconvalescent patients as compared to non-CDI control individuals suggested that exposure to the PS-I polysaccharide induces systemic antibodies during natural infection. A significant correlation of anti-**1** sIgA levels with milder disease symptoms was indicative of protective effects against CDI [Fig. 3.3]. Importantly, all studied clinical specimens contained detectable amounts of both serum IgG and fecal sIgA to pentasaccharide **1**, in agreement with a recent study that identified IgG to the synthetic pentasaccharide and to the isolated polysaccharide in all investigated horse serum samples.[217] These findings indicate that PS-I is likely a commonly expressed polysaccharide *in vivo* and thereby a vaild target for a vaccine

with potential activity against a broad variety of clinical *C. difficile* strains. Formal proof for the notion that PS-I is a ubiquitous antigen could be obtained through identifying the biosynthetic machinery required for the assembly of PS-I that is presently unknown. With the complete genome sequence of the *C. difficile* reference strain DSM1296 available[365], this information may soon be available. Knowing the sequence of the genome-encoded enzymatic complex could help to investigate clinical isolates for the presence of PS-I and to determine how its expression is regulated *in vivo*, i. e., which factors present in the intestine are responsible to induce expression. These factors could then be used to promote PS-I production *in vitro* in order to obtain larger amounts of the native polysaccharide for immunological interrogations.

Similar to the PS-I antigens, microarray-assisted screenings of human serum samples showed that LTA oligosaccharides **17**-**19** represented natural epitopes of the native LTA polysaccharide [Fig. 3.26]. A tendency towards higher serum IgG levels in reconvalescent patients as compared to non-CDI controls suggested that systemic antibody responses to LTA mediate immunity during infections with *C. difficile*. In contrast to PS-I, however, the absence of sIgA to LTA antigens in the majority of fecal specimens indicated that mucosal antibody responses play a less important role during exposure to *C. difficile* bacteria. Like PS-I, LTA polysaccharide is inconsistently and weakly expressed *in vitro*, and the biosynthetic machinery is unknown.[232] Therefore, the frequency of LTA expression among *C. difficile* strains *in vivo* remains elusive. In support of LTA being a ubiquitous antigen, anti-LTA IgG was identified in all herein investigated serum specimens [Fig. 3.26]. While PS-I appears to be unique to *C. difficile*[232], LTA has been identified also on other phylogenetically related species; *Peptostreptococcus anaerobius*, *Clostridium sordellii* and *Clostridium bifermentans*[204,208,215], all three being human pathogens[335-337]. An LTA-based vaccine may therefore not only confer protection against *C. difficile*, but also against related pathogens.

The ubiquitous presence of anti-PS-I and anti-LTA antibodies in the non-CDI control samples may have been the result of previous undiagnosed exposure to *C. difficile*, as up to 70 % of infants[36–38] and 15 % of adults[40] carry the bacterium without any apparent symptoms. The microarray screening data suggests that even asymptomatic *C. difficile* colonization can trigger long-lived antibody responses to both PS-I and LTA polysaccharides. This may be favorable for the envisaged vaccines, as the number of injections required to induce protective immunity could be reduced when memory B cells specific for PS-I/LTA are already present. The patients analyzed in this study only comprised adults, as CDI rarely develops in

infants and children.[16,17] Further screenings with samples of younger individuals could reveal at which age antibodies to PS-I and LTA polysaccharides start to emerge naturally and if the kinetics are comparable to antibody responses against capsular polysaccharides that are efficiently produced not before the age of two.[366]

4.1.2 Selected PS-I and LTA Oligosaccharides Are Highly Immunogenic and May Exert Intrinsic Adjuvanting Activity

Based on the finding that anti-**1** antibody levels correlate with protection from CDI symptoms, **1** was selected for immunological evaluation in mice. Conjugation to a protein was required to induce immunity, as administration of soluble **1** in the presence of FA did not elicit detectable amounts of serum antibodies (data not shown). When conjugated to CRM_{197} (glycoconjugate **10**), high levels of anti-**1** antibodies with T cell-mediated immunoglobulin class switch to IgG and IgA were generated even without external adjuvant [Fig. 3.5]. This indicated that **1** may exert intrinsic adjuvanting or immunestimulatory activity, whereby its two terminal rhamnoses may account for this effect. Rhamnose, a non-mammalian sugar[312], is by itself strongly immunogenic[313] and has been used as experimental adjuvant[367]. Its adjuvant activity has been proposed to rely on recognition by naturally circulating anti-rhamnose antibodies that promote uptake of rhamnose-containing vaccine constructs into antigen-presenting cells (APCs) *via* Fc receptor interactions.[367] Rhamnose-specific antibodies were present in some mice prior to immunization that, however, did not recognize **1** [Fig. 3.9]. Alternatively, **1** may engage pattern recognition receptors (PRRs) on APCs, such as CD14. This macrophage-expressed PRR binds to LPS, LTA and other bacterial glycans.[368,369] Most importantly, CD14 recognizes streptococcal rhamnose-glucose polymers, an interaction that triggers release of pro-inflammatory cytokines such as TNF-α.[370] This suggests that **1**, likewise composed of rhamnose and glucose [Fig. 3.1], may exert adjuvant effects through binding to CD14. Other PRRs that may recognize **1** include lectin receptors that trigger pro-inflammatory responses in immune cells upon glycan binding.[371] Their specificity is usually determined by terminal monosaccharide moieties, yet a genuine rhamnose-binding lectin has not been identified in mammals to date. Mannan-binding lectin (MBL), however, recognizes rhamnose-glucose glycans, despite its main eponymous reactivity to mannose.[370] Further studies are required to identify possible PRRs that interact with **1** and thereby promote its immunogenicity. These may well include CD14 and/or MBL.

Similar to **1**, the LTA dimer **18** may exert intrinsic immunestimulatory activity, as glycoconjugate **20** was highly immunogenic in mice in the absence of an external adjuvant [Fig. 3.29]. Co-administration with Alum or FA only marginally increased anti-**18** serum IgG levels. Of note, the limited efficacy of the adjuvants was neither due to a lack of adsorption to Alum [Fig. 3.28] nor the result of reduced stability after formulation with Alum or FA [Fig. 3.30]. A distinct feature of **18** that may be responsible for immunestimulatory effects is its highly negatively charged nature due to the presence of carboxylate and phosphate groups [Fig. 3.24]. The immunogenicity-enhancing effect of charged moieties of glycan antigens is well-established. Examples include the synthetic *C. difficile* PS-II hexasaccharide whose immunogenicity benefited from installment of a phosphate group[235], zwitterionic glycans that induce T cell-dependent immunity in the absence of a protein carrier[372,373] and Kdo-containing LPS structures that induce antibody responses in the non-conjugated form[320]. In the present study, the potent induction of anti-Kdo IgG in mice immunized with CRM_{197} glycoconjugate **11** was unexpected for a monosaccharide immunogen [Fig. 3.8]. A possible explanation for enhanced antibody responses to charged glycans including LTA **18** may be the general preference of B cell epitopes for charged structures.[374] In addition, **18** may engage PRRs. However, binding to TLR2 that is known to recognize LTA structures[341] can be ruled out since no activation of DCs upon *in vitro* stimulation with **18** was observed [Fig. 3.25]. This is likely a result of the unusual structure of *C. difficile* LTA that differs from LTA of most other Gram-positive bacteria bearing a conserved poly-1,3-(glycerolphosphate) backbone [Fig. 1.4].[204,207] Other PRRs that may recognize **18** include the macrophage-restricted CD14 known to bind LTA[369] or lectin receptors[371].

4.1.3 Alum but not FA Promotes Antibodies of High Specificity to the PS-I Pentasaccharide

The use of adjuvants further promoted anti-**1** antibody levels upon vaccination with **10** [Fig. 3.5]. FA promoted the highest levels of IgM, IgG and IgA to **1**, as expected since this adjuvant is known to be more potent than Alum.[375] Interestingly, the adjuvants not only influenced total antibody levels but also affected their reactivity. Alum mainly promoted IgG to the entire immunogen **1**, whereas with FA smaller substructures were also strongly recognized [Fig. 3.9]. This might be attributed to effects of the adjuvants on antigen processing. Glycoconjugates internalized by APCs are fragmented within endosomes into (glyco)peptides that are presented on MHC molecules to T cells.[225] Since glycosidases

are absent in endosomes, glycan degradation is mediated by the action of reactive oxygen species (ROS).[373,376] Alum mainly evokes Th2 responses characterized by anti-inflammatory cytokines such as IL-4 and IL-9 that suppress ROS production in APCs.[377–379] By contrast, FA elicits Th1 responses mediated by IFN-γ and other pro-inflammatory cytokines that activate ROS generation.[377,380] APCs not only present antigen-derived peptides on MHC proteins but also release partially fragmented antigens to the microenvironment that may be recognized by the BCR of B cells and thereby trigger differentiation into antibody-producing plasma cells.[381,382] The APC-secreted glycoconjugate fragments may differ as a result of adjuvant-dependent ROS activity, with Alum (low ROS induction) favoring those with intact **1** and FA (high ROS induction) those displaying degraded derivatives of **1** that become available as B cell epitopes. Another explanation for adjuvant-dependent antibody recognition patterns may be a direct influence of the adjuvants on B cell maturation in germinal centers. For example, it has been proposed that the Th1-directing MF59 adjuvant stimulates the process of somatic hypermutation, leading to antibodies with expanded epitope recognition repertoires.[330]

Alum emerged as favorable adjuvant for **10** as the more specific antibodies are less likely to cross-react with other bacteria of the intestine. With PS-I being a *C. difficile*-specific antigen, administration of Alum-formulated **10** is expected to preserve the overall gut bacterial community.[232] This aspect is particularly important in the context of CDI, as altered microbiota predispose for recurrent disease episodes.[100–102] Whether or not immunization with **10** alters the microbiota composition could be addressed by metagenomic sequencing of fecal samples obtained from vaccinated vs. naïve mice.[72,74,75]

Polyclonal serum anti-**1** antibodies raised with **10** in the presence of Alum recognized the native PS-I polysaccharide on *C. difficile* [Fig. 3.5]. Binding signals *in vitro* were weak, as expected since bacteria were obtained from liquid cultures that only allow for low expression levels of PS-I.[232] Importantly, serum antibodies induced by s. c. administration of **10** efficiently localized to the murine intestine, the site of *C. difficile* colonization, and were detectable at high levels in small intestine and colon tissue homogenates as well as in feces [Fig. 3.6]. The antibodies likely crossed the epithelial barrier *via* receptor-mediated transcytosis. Two receptors are known in mammals that shuttle antibodies from serum to the intestinal lumen and *vice versa*; the IgG-specific neonatal Fc receptor (FcRn) that despite its name is also expressed in adult tissue[118,119] and the polymeric immunoglobulin receptor (pIgR) specific for IgM and dimeric sIgA but not serum IgA that is a monomer[120]. Consistent

with these receptor specificities, the mouse intestinal tract harbored IgG and IgM, but not IgA, although the latter isotype was detected in serum of the same mice [Fig. 3.5]. The data indicates that s. c. immunization did not induce detectable levels of mucosal sIgA, a known characteristic of parenteral vaccination regimes.[383] Of note, however, both IgG and IgM have been shown to contribute to intestinal immunity against bacterial pathogens including *C. difficile*.[109,117,319]

4.1.4 Alum but not FA Promotes Antibodies Efficiently Binding to LTA Polysaccharide

Anti-LTA serum IgG raised with **20** exhibited adjuvant-dependent epitope recognition patterns, but distinct from those observed with PS-I glycoconjugate **10** [Fig. 3.29]. Alum, but not FA, promoted IgG strongly recognizing LTA monomer **17**. As described above, the observed differences may be due to ROS-mediated endosomal degradation of **18** within APCs and the release of partially fragmented forms of **20** that provide additional B cell epitopes.[381,382] Compared to the Th2 adjuvant Alum, the Th1-directing FA more potently induces ROS in APCs[378–380], which may promote fragmentation of **18** at the phosphodiester bonds that are prone to ROS-mediated cleavage[384]. Thereby, immunodominant B cell epitopes with terminally exposed phosphate as major antigenic determinant may become available. This could explain why FA-promoted IgG predominantly recognizes LTA glycans having two phosphodiesters (**18** and **19**) and only weakly **17** with one phosphodiester. By contrast, Alum-promoted anti-LTA IgG may more strongly recognize the glyceric acid (GroA) substituent. It has been reported that the substituents of native LTA are sterically more accessible to antibodies than the backbone[385], which may explain why antisera raised with Alum better reacted to *C difficile* bacteria *in vitro* [Fig. 3.29]. Overall, Alum proved to favorable over FA as adjuvant for **20**.

4.1.5 Vaccination with PS-I and LTA Glycoconjugates Limits *C. difficile* Colonization *In Vivo*

Both immunization with glycoconjugate **10**' of PS-I pentasaccharide **1** and **20** diplaying LTA dimer **18** significantly reduced intestinal bacterial colonization in mice upon oral *C. difficile* challenge [Figs. 3.8 & 3.32]. This provided further evidence that the two glycans are expressed *in vivo*. In addition, the data suggests that both PS-I and LTA polysaccharides mediate adherence of *C. difficile* to intestinal mucosae, a function that has been frequently attributed

to structurally related glycans of various human pathogens. For instance, teichoic acid of *Staphylococcus aureus* is required for colonization of the gastrointestinal tract in the mouse model[211] and LTA of *Listeria monocytogenes* has been shown to contribute to attachment to epithelial tisse[213].

Two preventive vaccinations (prime-boost) with PS-I glycoconjugate **10**' reduced colonization by 99 %, while three injections (prime-boost-boost) with LTA glycoconjugate **20** afforded 83 % reduction in challenged mice [Figs. 3.8 & 3.32]. Most strikingly, **10**' conferred complete clearance of *C. difficile* in 5/6 mice five days post-challenge, whereas with **20** some degree of colonization was observed in all challenged animals at the same time point. This suggests that the PS-I polysaccharide is either more important for bacterial adherence and/or more accessible to antibodies than LTA. However, a comparison of the efficacies has to be interpreted with caution, as two different control groups (immunized with Kdo glycoconjugate **11** or CRM_{197}, respectively) were used as reference. Parallel challenge studies that allow for direct comparison are therefore required. In both cases the disease burden with respect to the degree of colitis was was not reduced when compared to the control groups. This indicates that vaccination with neither **10**' nor **20** could entirely block infection, and the number of *C. difficile* bacteria that escaped antibody recognition were sufficient to cause disease. Noteworthy, intestinal pathology in mice manifests itself mainly during acute infection around day two post-challenge, followed by a phase of regeneration and natural bacterial clearance after about four weeks.[306,307] This course of disease significantly differs from that of human recurrent infections with later-onset symptoms and lack of natural bacterial eradication.[100–102] Moreover, the infectious dose used for the challenge studies, 10^7 spores, by far exceeds the typical number causing human infections that may be ten spores or lower, depending on the *C. difficile* strain and host parameters.[41,363,364] The high challenge dose was required since mice are inherently resistant to symptoms caused by clostridial toxins.[386] The more common and recognized model organism for *C. difficile* are hamsters that are more susceptible to toxin-mediated disease, require infectious doses as low as one or two spores and eventually succumb to infection.[363,386] Thus, hamsters better reflect human disease than mice. Further efforts at the MPICI will aim at investigating the protective efficacy of PS-I and LTA glycoconjugates in this model.

It remains to be elucidated whether the observed colonization-inhibiting effects conferred by the glycoconjugates were solely due to steric prevention of adherence or if other factors contributed as well. Antibody-mediated defense in the mammalian intestine involves complex

interactions of pathogens with immune cells and other mediators. For instance, antibody-opsonized bacteria that translocate through the epithelial barrier into the lamina propria are efficiently recognized by resident DCs *via* Fc receptor engagement and consequently are inactivated.[387,388] Moreover, intestinal epithelial cells secrete complement proteins into the lumen that contribute to antimicrobial activity and are activated by bacteria-bound antibodies.[389] The *in vitro* OPA studies described herein did not indicate that *C. difficile*-bound anti-LTA antibodies enhanced the process of phagocytosis [Fig. 3.31]. However, it has to be noted that the OPA, routinely performed to assess the efficacy of vaccines against the oxygen-tolerant *S. pneumoniae*[301], is not established for *C. difficile* or any other obligate anaerobe, as cell culture-based assays are not feasible under anaerobic conditions. The use of formalin-inactivated *C. difficile* bacteria was required, and formalin treatment may have altered the bacterial surface such that phagocytosis was limited. Moreover, the LTA polysaccharide is only weakly expressed by *C. difficile in vitro*[232], which may have impeded efficient opsonization by LTA-specific antibodies. The OPA for *C. difficile* requires further optimization such as including complement[359] that is required for antibody-mediated phagocytosis of *S. pneumoniae* as well[301]. Optimized conditions, however, will be difficult to achieve since a positive control by means of a phagocytosis-promoting *C. difficile*-binding antibody is presently not available.

A more established method to assess the *in vitro* activity of anti-*C. difficile* antibodies is an adhesion-inhibiting assay using a monolayer of Caco-2 cells as surrogate epithelium.[303–305] This assay did not indicate that anti-LTA antibodies prevented attachment of viable *C. difficile* bacteria [Fig. 3.31]. However, these experiments were performed under aerobic conditions, which effectively kills vegetative *C. difficile* bacteria.[29] Since the read-out of this assay is the number of colonies arising from monolayer-attached bacteria, any observed effects are predominantly those targeted to the oxygen-resistant spores.[362] It can be concluded that spore attachment is not affected by LTA-specific antibodies *in vitro*, which is likely due to the fact that LTA is expressed less by spores than by vegetative *C. difficle*.[206,238] To determine if vegetative cells are prevented from attachment, the assay will require modifications that allow for their culture-independent detection. For instance, fluorescence-labeled bacteria could be quantified microscopically[303] or by flow cytometry[390].

4.1.6 Considerations towards Clinical Application of Oligosaccharide-based Anti-*C. difficile* Vaccines

Forwarding the herein investigated vaccine candidates into clinical use may require enhancement of their *in vivo* protective efficacy. A number of variables influence the immunogenicity of glycoconjugates, including the adjuvant, glycan to protein ratio, conjugation chemistry, the choice of the carrier protein and the route of administration.

A number of investigational new adjuvants are mainly those promoting Th1-type responses, such as QS21 or MF59.[223,330] Changing the adjuvant for the herein described glycoconjugates of PS-I **1** and LTA **18** is likely not required as the *in vitro* data showed that Th2-directing Alum was more suitable than FA, a Th1 adjuvant, as discussed above. Alum provides the advantage of currently being the only adjuvant approved for human use in the United States.[223] However, glycoconjugates prepared with disaccharide **3** may require a strong Th1-directing adjvuvant to overcome its relatively weak immunogenicity [Fig. 3.11].

Alum promoted antibodies of favorable specificities, yet vaccination with Alum-formulated PS-I glycoconjugates **10** and **10'** only elicited detectable amounts of anti-**1** antibodies in 5/6 and 7/8 mice, respectively, and antibody levels were highly variable [Figs. 3.5 & 3.8]. Similarly, Alum-adjuvanted LTA glycoconjugate **20** only induced detectable levels of LTA-specific IgG in 2/3 mice [Fig. 3.29]. This indicates some degree of immunodominance of the CRM_{197} carrier protein in both cases. One factor that strongly influences the balance of immunogenicity between glycan and protein portions of glycoconjugates is the glycan to protein ratio.[247] Low glycan loading directs antibody responses the carrier protein, likely because fewer glycan-presenting B cell epitopes are exposed. By contrast, too high loadings reduce the immunogenicity of the entire glycoconjugate by inactivation of T cell epitopes.[247] Thus, there is a favorable glycan to protein ratio that, however, depends on both the carrier protein and the glycan antigen, and requires optimization for each combination. The present study allows for some conclusions to be drawn with respect to favorable glycan loading of CRM_{197} based on the ability of the different glycoconjugates in eliciting anti-glycan antibodies. The two glycoconjugates **12** and **12*** were obtained by different conjugation methods that afforded loadings of 9.8 and 20 copies of PS-I disaccharide **3** per CRM_{197}, respectively, but were otherwise identical in composition [Figs. 3.10 & 3.20]. While both elicited anti-PS-I IgG in 2/3 mice, **12*** induced lower levels of antibodies to **3** as well as CRM_{197} [Figs. 3.11 & 3.22]. This indicated that a loading of 20 destroyed T cell epitopes to an extent that significantly reduced the overall immunogenicity of **12***. Glycoconjugate **16** prepared with OAA **15** had

a low loading of 1.3 and did not induce any detectable anti-PS-I antibodies but higher responses to CRM_{197} than **12*** [Fig. 3.22]. Thus, in the case of **16** T cell epitopes were largely intact but **15**-displaying B cell epitopes were too sparsely distributed to induce significant antibody responses. Glycoconjugate **11** of Kdo **9** efficiently elicited anti-**9** antibodies in 8/8 mice, indicating that its loading of 7.5 was within the optimal range [Figs. 3.7 & 3.8]. This suggests that glycan immunogenicity of glycoconjugate **20** that contains the also negatively charged LTA **18** at a glycan to protein ratio of 4 [Fig. 3.27] may well benefit from higher loading, which could be afforded by the more efficient conjugation chemistry with DNAP crosslinker.[294] Glycoconjugates **10** and **10**' with PS-I **1** and loadings of 9.6 and 7, respectively, appeared to be already within the optimal range [Figs. 3.4 & 3.7]. The one mouse immunized with Alum-formulated **10** that did not mount antibodies to **1** instead elicited a strong response directed against the generic spacer moiety (data not shown), a known phenomenon observed especially for glycoconjugates of weakly immunogenic glycan antigens.[317] This may be circumvented by utilizing DNAP instead of DSAP crosslinker, as half ester intermediates of DNAP can be more efficiently separated from non-modified crosslinker, which prevents the attachment of potentially immunogenic glycan-free adipic acid molecules to the carrier protein.[294,316]

Another factor that governs the immunogenicity of glycan antigens is the choice of the carrier protein. For example, a recent study compared anti-glycan antibody levels raised in mice and rabbits in response to vaccination with glycoconjugates of either CRM_{197}, DT or TT toxoids and meningococcal capsular polysaccharides.[391] While CRM_{197} was shown to be favorable for meningococcal serogroup A (MenA), MenW and MenY polysaccharides, DT promoted higher anti-glycan antibody levels to MenC in both animal models. This shows that the optimal carrier protein is glycan antigen-dependent and thus remains to be identified for the synthetic PS-I and LTA glycans. For *C. difficile* glycans, clostridial toxins TcdA and/or TcdB (in the form of toxoids) or fragments thereof may be the most suitable carrier molecules, as such glycoconjugates could elicit both colonization-inhibiting and toxin-neutralizing antibodies simultaneously to act in concert. Of note, a recent study showed that a glycoconjugate composed of PS-II polysaccharide and a non-toxic TcdB fragment efficiently elicited anti-PS-II and toxin-neutralizing IgG in mice, providing proof-of-concept that this approach is feasible.[392] Clostridial toxoids have shown favorable safety and immunogenicity profiles in a number of clinical trials and toxoid-based vaccines are expected to obtain licensure within the next five years.[135] They may provide the additional advantage

that an adjuvant is likely dispensible, as the toxoid vaccines currently investigated clinically by Pfizer[168] and Valneva[174] were shown to be more immunogenic in the absence of Alum.

The route of administration may also influence vaccine efficacy of glycoconjugate vaccines against *C. difficile*. Small animal studies on vaccine candidates targeting *C. difficile* surface proteins showed that for some but not all antigens mucosal administration afforded better protection.[135] Thus, the optimal administration route appears to be antigen-specific and will require investigation for *C. difficile* surface glycans. Although serum IgG and IgM to **1** efficiently localized to the intestine of s. c.-immunized mice probably *via* receptor-mediated transcytosis[118–120] [Fig. 3.6] and *C. difficile* toxin-mediated tissue damage could further enhance the release of serum antibodies into the intestinal lumen in the case of disease[232], mucosal sIgA is recognized as the most important antibody isotype for mucosal immunity[310]. sIgA can be efficiently induced in small animals *via* rectal antigen administration.[64,180] Interestingly, transcutaneous injection of *C. difficile* protein antigens has been shown to potently induce both serum IgG and mucosal sIgA in mice that may act cooperatively.[143] Inducing sIgA may have the further advantage that unlike the largely all-or-none systemic antibody responses, IgA responses appear as a linear function of the total amount of antigen, which may be useful in designing vaccination schedules for *C. difficile*.[232,392]

Finally, co-administering glycoconjugates of *C. difficile* PS-I, PS-II and LTA antigens may confer enhanced levels of protection and would reduce the chance of escaping bacteria that do not express either one of the polysaccharides. This is subject of on-going research at the MPICI.

4.2 Generation and Analysis of mAbs to PS-I

mAbs to PS-I pentasaccharide **1** were generated to study glycan-antibody interactions and to investigate their potential as therapeutic agents against *C. difficile* disease. The mAbs were obtained from mice immunized with glycoconjugate **10** composed of CRM_{197} and **1** *via* the hybridoma technique [Fig. 3.12].[252,299] Alum was selected as adjuvant to generate mAbs that strongly bind to **1** but less to smaller substructures [Fig. 3.9]. Thereby, the resulting mAbs were expected to be of high specificity to *C. difficile* and to exert limited cross-reactivity to other bacteria. When used therapeutically the microbiota would be less damaged, which is especially important in the context of *C. difficile* infection where dysbiosis predisposes for recurrent infections.[72–75,100–102] Affinity purification by FPLC yielded highly

pure mAbs that were used for subsequent studies [Fig. 3.13]. Three mAbs 2C5, 10A1 and 10D6 were recovered that were all of the IgG1 subtype [Fig. 3.13], reflecting the fact that the Th2-directing Alum adjuvant mainly induces IgG1.[353]

4.2.1 Anti-1 mAbs Provide Detailed Insights into Glycan-antibody Interactions

To obtain insight into how antibodies interact with PS-I, glycan-mAb interactions were studied using various biochemical and biophysical methods. Microarray and SPR studies confirmed that disaccharide **3** is the minimal epitope of PS-I [Figs. 3.13 & 3.14]. However, mAb binding to the more antigenic pentasaccharide **1** was stronger with nanomolar K_D values than to **3** with micromolar K_D values [Table 3.1]. IM analysis revealed that both **1** and **3** interacted with mAbs in 1:1-like manner and that stronger binding to **1** was due to faster association but not slower dissociation [Fig. 3.15]. The binding stoichiometries and kinetics provided evidence that mAb re-binding to two adjacent units of **3** in **1** did not occur. ITC studies suggested that an epitope larger than **3** containing two rhamnose units is accommodated by the binding pockets of the mAbs, leading to entropically favored interactions [Fig. 3.16]. Taken together, SPR, IM and ITC studies led to the conclusion that rhamnoses were the major antigenic determinants with weak but essential contributions of the adjacent glucoses, as **3** but not rhamnose **1** was bound by the mAbs [Fig. 3.14]. The additional glucose of trisaccharide **2** likely did not participate, as **2** did not show enhanced affinity as compared to **3** [Table 3.1].

The considerations on epitope recognition were confirmed by saturation transfer difference (STD)-NMR measurements that were kindly performed by Dr. Christoph Rademacher and Jonas Hanske.[394] STD-NMR allows for determining binding epitopes of mAbs at atom-level detail.[239,240] As expected, STD effects imposed by mAb binding to disaccharide **3** showed that the main contact surface area was located around the terminal rhamnose, with highest STD effects at the indistinguishable methyl protons H6, H'6 and H"6 (100 % normalized STD effect), as well as H3 (99 %) and H2 (78 %) [Fig. 4.1a,b]. The glucose moiety in **3** contributed weakly to antibody binding around H3 (11 %). Despite the low saturation transfer, this interaction appears important for antibody binding, as rhamnose **4** was not recognized by the mAbs in SPR experiments [Fig. 3.14]. Comparison of STD-NMR spectra with **3** at a fixed saturation time indicated that all mAbs recognized a similar epitope [Fig. 4.1c]. In addition, trisaccharide **2**, which contains **3** and an additional glucose at the

reducing end, showed comparable STD effects with mAb 10A1. This observation indicated that the additional glucose did not participate in binding and explains similar binding affinities to **2** and **3** in the SPR experiments. STD effects for **1** could not be determined owing to its strong affinity to all three mAbs. However, competition experiments of trisaccharide **2** with **1** completely diminished any STD effects imposed by **2** [Fig. 4.1d], indicating identical binding sites and verifying high-affinity binding of **1**. Overall, STD-NMR data confirmed antibody binding to **1**-**3** and showed that interactions were mainly mediated by terminal rhamnoses with weak but essential participation of adjacent glucoses. These findings suggested that strong binding to **1** was likely achieved by linking two disaccharide **3** subunits *via* a glycosidic bond that does not interact directly with the antibodies.

IM analysis indicated that binding stoichiometries for **1** and **3** were identical, despite the fact that **1** contains two copies of **3**. Therefore, the mAb binding pockets probably do not provide two identical binding sites for **3**, but one binding site for **1** that may adopt a more complex conformation. To obtain structural insights into the conformation of **1**, two-dimensional (2D) NMR spectroscopy was employed [Fig. 4.1e]. Inter-residue nuclear Overhauser effects (NOEs) were all in agreement with a model of the solution structure of **1** based on calculations using the GLYCAM06 force field[396] [Fig. 4.1f]. The 2D NMR studies provided evidence that **1** adopts a conformation in which the two units of **3** are oriented in an angled position relative to each other. Taken together, IM, ITC and 2D NMR experiments indicated that the mAb binding pockets accommodate the tetrasaccharide portion of **1** without the reducing-end glucose. Disaccharide **3** made fewer contacts than **1**, resulting in lower binding affinity.

In a broader sense, the findings provide detailed insights into the nature of glycan-antibody interactions in general. Similar to lectins, antibody binding to glycans is mainly an enthalpy driven process often of low millimolar or micromolar affinity that in most cases is characterized by unfavorable entropy.[254,256–262,266,398–403] Enthalpy-entropy compensation often impedes high-affinity binding. Nanomolar affinities of antibodies to oligosaccharides are typically attributed to ionic interactions as for instance in the case of a trisaccharide antigen of *Chlamydia*[312,404] or to conformational rigidity of large polysaccharides that leads to favorable entropy resulting from lower entropic penalty upon antibody binding[255]. By contrast, the herein described mAbs bind with nanomolar affinity to **1**, a comparably small oligosaccharide antigen without any charged residues. Details on these interactions were revealed by STD-NMR. High-affinity binding to **1** likely results from nonpolar antibody interactions with

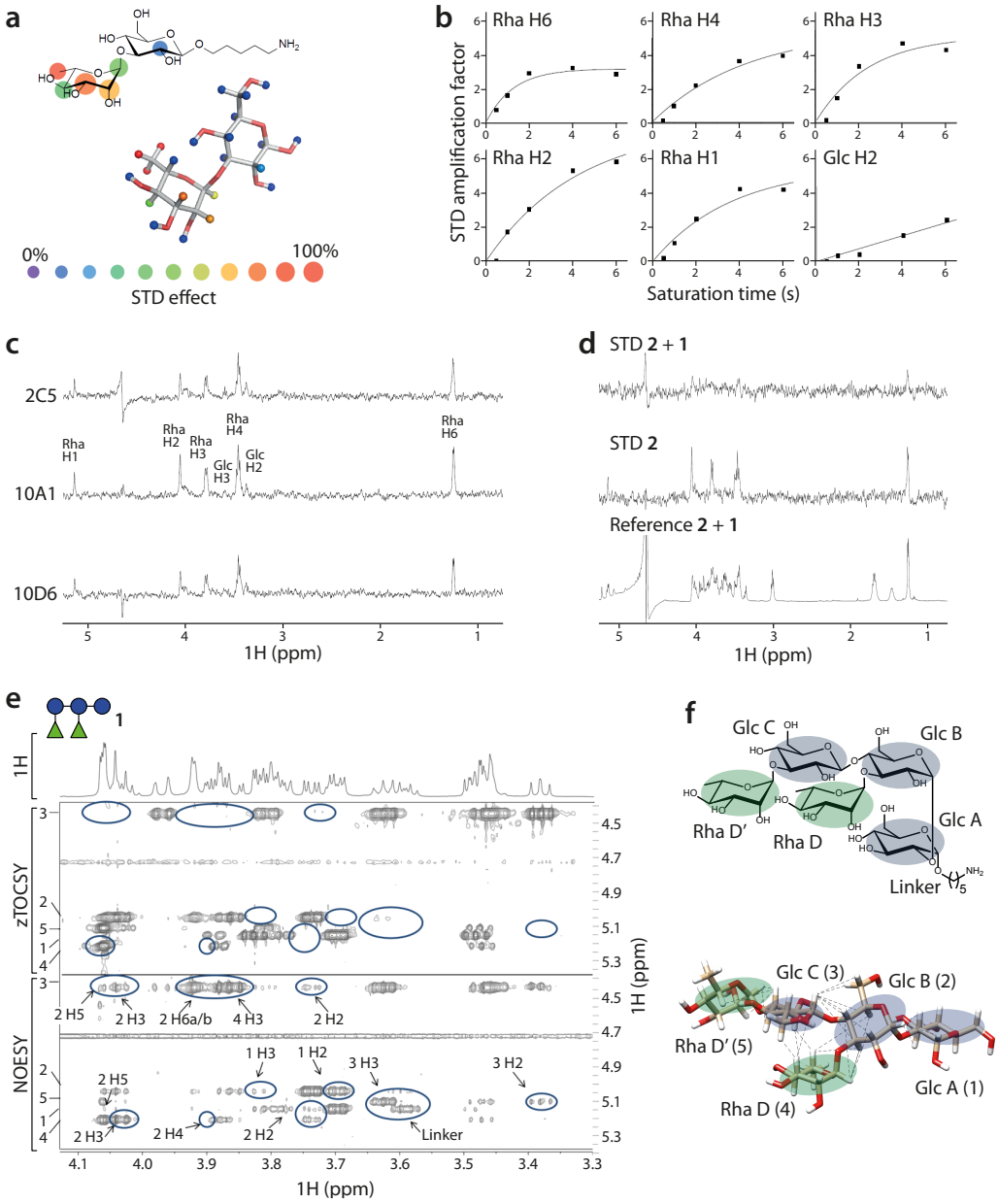

Figure 4.1: Epitope mapping of anti-**1** mAbs by STD-NMR and conformation of **1**. (**a,b**) Recognition of **3** by 10A1 shown as Lewis structure and 3D model calculated with Glycam[395]. Colors represent percent STD effects.[394] (**c**) Recognition patterns of **3** by three mAbs. STD spectra were acquired at 2 s saturation transfer time. (**d**) Competition of **2** by **1**. Trisaccharide **2** exerts STD effects at the same protons as **3** (center). Adding **1** led to disappearance of peaks imposed by **2**, indicating competition for the same binding site (top). The reference spectrum is shown at the bottom. (**e**) 1D proton NMR and 2D zTOCSY and NOESY spectra of **1** showing proton coupling to anomeric protons of the five residues numbered as in panel (**f**). Circles mark cross-peaks that appear in NOESY but do not show a corresponding peak in zTOCSY. These peaks were marked as inter-residue NOEs and labeled by residue number and proton name. (**f**) Chemical structure (top) and 3D model of **1** obtained with GLYCAM[396] and UCSF Chimera[397] (bottom). Glucose and rhamnose residues are highlighted blue and green, respectively. Dotted lines represent 23 inter-residue NOEs derived from comparing NOESY and zTOCSY spectra. All NOEs are within 5 Å distance in the model structure. Figure modified from Broecker *et al.*[286]

hydrophobic methyl groups that generate favorable entropy by water displacement. Interestingly, although the number of mAbs in this study was limited, all of them recognized the similar molecular epitope of PS-I with rhamnose as major antigenic determinant. The notion that affinity benefits from recognition of hydrophobic methyl groups of bacterial sugars is further supported by the recent observation that methyl groups of rhamnose and anthrose contribute significantly to nanomolar affinity antibody binding to an antigenic tetrasaccharide of *Bacillus anthracis*.[240]

The binding epitope could be further characterized by X-ray crystallography. This method is frequently used to decipher the molecular basis of glycan-antibody interactions and requires co-crystallization of mAb Fab fragments with the glycan antigen.[266,400,401] Unlike STD-NMR, crystallography allows for studying high-affinity interactions such as those with **1** and provides additional sequence information on the antibody binding pocket. Thereby, crystallography could confirm whether rhamnose indeed engages in favorable nonpolar interactions with the anti-**1** mAbs, as shown previously for *Shigella flexneri* glycan antigens whose rhamnose moieties interact *via* their methyl groups with hydrophobic pockets of an antibody constituted by tyrosine and histidine side chains.[266]

4.2.2 Anti-1 mAbs Prevent Experimental Colitis *In Vivo*

All three anti-**1** mAbs recognized the surface of *C. difficile* bacteria *in vitro*, as shown by whole-cell ELISA experiments [Fig. 3.17]. Yet, mAb 2C5 was the only one that significantly bound to all investigated *C. difficile* strains (5/5), followed by 10D6 (4/5) and 10A1 (1/5). 10A1 may not bind efficiently due to its faster dissociation kinetics compared to 2C5 and 10D6 [Table 3.1]. The reasons for the observed differences between 2C5 and 10D6 remain to be determined, as both mAbs recognized similar molecular epitopes of PS-I with association and dissociation kinetics in the same range. A slightly higher affinity of 2C5 to the minimal disaccharide epitope **3**, $K_D = 18.0\,\mu M$ as compared to $K_D = 37.5\,\mu M$ for 10D6, may be responsible for stronger recognition of natural PS-I. Thus, subtle differences in epitope recognition can have a significant impact on binding to the native PS-I polysaccharide. This aspect warrants further investigation, for instance, by more detailed characterization of binding epitopes by means of X-ray crystallography. Of note, the binding signals observed in the ELISA experiments were generally weak, likely because of the low *in vitro* expression levels of PS-I.[232] Overall the *in vitro* binding studies gave further credence to the notion that PS-I is a ubiquitous antigen and demonstrated that 2C5 is the mAb most efficiently recognizing

native PS-I on the surface of *C. difficile*.

mAbs 2C5 and 10D6 emerged as promising candidates for *in vivo* challenge studies in mice aming at assessing their ability to prevent *C. difficile* disease upon passive immunization. Two administrations with 100 µg of mAb *via* the intraperitoneal and intrarectal routes seven and three days prior to challenge and one at the day of infection significantly reduced both the degree of intestinal colonization and inflammation [Fig. 3.18]. 2C5 was moderately superior to 10D6, likely reflecting better *in vitro* binding to *C. difficile*. Two mAbs directed against PS-II also reduced *C. difficile* colonization and disease, but to a lower extent. This observation indicated that PS-I may be more important than PS-II for bacterial attachment *in vivo*. In line with this finding, it has been suggested that PS-I constitutes a virulence factor associated with aggressive behavior of *C. difficile*, as to date highest expression levels *in vitro* were found in an isolate of the hypervirulent ribotype 027 strain.[205,232] Of note, passive immunization with anti-**1** mAbs completely prevented colitis in mice, which was not achieved by active immunization as discussed above. The better efficacy of passive immunization may have been due to higher local concentrations of intrarectally administered mAbs as compared to serum antibodies raised by immunization that required transportation to the intestinal lumen. It remains to be elucidated whether intravenous administration is likewise able to confer protection against disease, since this route of administration is tyically applied in humans.[188,405] Challenge studies in hamster could reveal whether the anti-**1** mAbs also afford protection against lethal challenge and if co-administration of toxin-neutralizing mAbs[188] could afford synergistic protective efficacy.

4.2.3 Considerations towards Clinical Application of Anti-1 mAbs

Clinical application of the mAbs requires chimerization or humanization to prevent adverse reactions due to immunogenicity of the mouse protein.[405] Chimerized mAbs comprise the complete murine variable domains that are fused to human Fc domains *in vitro*.[406] This method allows for retaining full binding activity. Yet, chimeric mAbs are still about 30 % of mouse origin, which can generate undesired immune responses when introduced into humans. The murine fraction can be further decreased by replacing the hypervariable loops of variable domains with human ones.[407] Thereby, humanized mAbs of about 90 % human origin are generated that are less immunogenic than chimeric antibodies. However, exchanging hypervariable loops frequently reduces affinity compared to the parental murine mAb. The original binding strength can be restored by *in vitro* mutagenesis. Most mAbs currently

approved for human use are either chimeric or humanized.[405] The generation of humanized derivatives of the anti-**1** mAbs is subject of ongoing studies at the MPICI.

Fully human anti-**1** mAbs would be even less immunogenic.[405] They can be obtained by immunizing mice transgenic for the entire genetic repertoire of human IgG followed by clonal selection with the conventional hybridoma technique.[405] This method was applied, for instance, to obtain toxin-neutralizing mAbs against *C. difficile* disease that are subject to clinical investigation.[193] A powerful *in vitro* method to generate fully human mAbs is provided by phage display.[408] This technique relies on the generation of genetically modified M13 phages that display phage coat proteins fused to libraries of Fab fragments of human origin. Phage clones harboring Fab fragments on their surface that react with the antigen of interest are used to determine the corresponding gene sequence. The Fab-encoding genes are then fused *in vitro* to human Fc to generate fully human mAbs. The availability of large, universal Fab fragment gene libraries obtained from non-immunized individuals allows for rapid screening for desired binding specificities.[409] This is particularly appealing with respect to antibodies to *C. difficile* glycan antigens, since these are ubiquitously present in adult humans [Figs. 3.2 & 3.26].

Finally, antibody engineering allows for installing Fc portions with desired characteristics.[405] For anti-*C. difficile* mAbs it might be of interest to intall an Fc portion with modulated affinity to the FcRn receptor that shuttles IgG between serum and the intestine such that the mAb it is more efficiently transported to the luminal side after intravenous application.[410] Alternatively, antibody engineering could generate mAbs with increased resistance to gastrointestinal trypsin digestion that is characteristic of IgA.[411] This would allow for more efficient oral application to directly target the intestine. Moreover, this route of administration has been shown to cause fewer side effects than intravenous application.[412] Oral colon-specific delivery could be further enhanced by coating the mAbs on polystyrene nanocarriers, which has been shown to increase their resistance to degradation in the mouse model.[413] Alternatively, mAbs encapsulated in commercially available and human-approved hypromellose capsules that survive stomach passage and dissociate in the intestine provides an appealing option for oral delivery that has been successfully applied to treat recurrent *C. difficile* disease by means of FMT.[129]

4.3 Towards Fully Synthetic Vaccines Displaying Oligovalent Disaccharides

4.3.1 A Glycan Mimetic of Pentavalent Disaccharides Is Antigenic

Glycan microarray and SPR experiments revealed that anti-**1** mAb binding to PS-I glycans was primarily mediated by terminal rhamnoses and adjacent glucoses, but did not extend further into the antigens, as the additional glucose moiety at the reducing end of **2** did not enhance affinity as compared to **3** [Table 3.1]. This binding specificity was confirmed by STD-NMR measurements [Fig. 4.1]. The glycosidic bond that connects two units of **3** in pentasaccharide **1** does not directly participate in binding and may therefore be replaced by a linker to furnish structures mimicking immunologic properties of larger PS-I glycans [Fig. 3.19]. ITC and IM studies indicated that stronger mAb binding to **1** resulted from higher affinity, not avidity, despite the presence of two units of **3** in **1** [Figs. 3.15 & 3.16]. Two-dimensional NMR experiments showed that the pentasaccharide likely adopts a conformation with two units of **3** in an angled position [Fig. 4.1]. It was therefore reasoned that oligovalently displayed disaccharides **3** might afford enhanced antibody binding through increased affinity (faster association rates) when two adjacent disaccharides adopt a conformation similar to that of **1**, through increased avidity (slower dissociation rates) by re-binding events, or a combination of both.

To investigate whether adjacent disaccharide copies lead to increased mAb binding strength when compared to single disaccharides, OAAs were synthesized that oligovalently display **3**. The OAA backbone has been reported to be non-toxic, non-immunogenic and suitable for oligovalent glycan presentation with limited synthetic effort.[272–276] Straightforward solid-phase OAA synthesis furnished PS-I glycan mimetic **15** displaying five units of **3** [Fig. 3.19]. Five adjacent disaccharides correspond to 2.5 generic copies of the pentasaccharide, thereby enabling a combination of potential affinity- and avidity-enhancing effects. A comparably large construct was selected since larger PS-I glycans are more capable of eliciting antibodies than smaller ones [Figs. 3.5 & 3.9]. Tight mAb binding to **15** was shown by SPR [Fig. 3.20]. Owing to slow association rates that were below the measurable limit, potential increases in affinity could not be detected. However, the dissociation rates were about five orders of magnitude slower than for monovalent disaccharides, indicating strong avidity-enhancing effects. Thus, a PS-I glycan mimetic characterized by high-avidity antibody binding was successfully created. This is reminiscent of natural repetitive polysaccharides

that enable strong antibody binding through avidity effects despite typically low affinity to single epitopes.[223]

4.3.2 A Glycan Mimetic of Pentavalent Disaccharides Is Immunogenic

Immunization studies in mice were performed to investigate whether **15** is able to elicit PS-I-specific antibodies. Compound **15** was equipped with a CRM_{197} peptide epitope intended to recruit T-cell help[327], similar to previously described immunization efforts with multivalent tumor-associated carbohydrate antigens that included synthetic T-cell epitopes[269–271,277]. Antibody responses were compared to those elicited by the semisynthetic glycoconjugates **12*** and **16** obtained by covalently attaching **3** and **15**, respectively, to CRM_{197} [Fig. 3.21]. The glycoconjugates were synthesized with the DNAP spacer[294] to facilitate the challenging conjugation of **15** to CRM_{197}, as it allows for more efficient conjugation reactions than the DSAP spacer[291] used to obtain the other glycoconjugates in this study. Vaccinating mice with fully synthetic OAA **15** induced IgGs to pentasaccharide **1** at low but comparable levels to semi-synthetic glycoconjugate **12*** [Figs. 3.22 & 3.23]. Interestingly, in contrast to **12***, IgG to disaccharide **3** was not detectable after immunization with **15**. Therefore, the IgG response to **15** was more specific to larger PS-I glycans, which is desirable for a vaccine to limit cross-reaction with structurally related glycans. This also indicated that two adjacent disaccharides in **15** may have adopted a conformation that resembles **1** to some degree. Anti-CRM_{197} IgG raised with **15** indicated that the synthetic peptide epitope was recognized as a B cell epitope in addition to serving as T cell epitope that promoted immunoglobulin class switch to IgG [Fig. 3.22].

To investigate whether the immunogenicity of **15** could be further enhanced, the pentavalent OAA was conjugated to CRM_{197} [Fig. 3.21]. The resulting glycoconjugate **16**, however, was unable to generate anti-PS-I IgGs in mice, probably due to the low antigen loading of 1.3 molecules of **15** per CRM_{197} that resulted in too little B cell epitopes presented to the immune system. It has been noted previously that low antigen loading of glycoconjugates is associated with weaker antibody responses.[247] Compound **16**, however, was able to boost existing IgG responses to PS-I glycans elicited by **12***, suggesting a limited ability to raise anti-PS-I IgG that may be enhanced through higher antigen loading.

The anti-**1** IgG responses induced by **12***, displaying antigens at a high density of 20 molecules **3** per CRM_{197}, were relatively weak and only detectable at low serum dilutions (1:20) by glycan microarray [Fig. 3.22]. Glycoconjugate **12** that was similar in composition to

12* but had a lower antigen loading of 9.8 elicited higher levels of PS-I-specific IgGs in mice that were detectable at higher dilutions (1:100) [Fig. 3.11]. It has been suggested previously that excessive glycan loading of glycoconjugates may limit immunogenicity due to destruction of T cell epitopes, resulting in weak antibody responses.[247] Still, **12*** was suitable to compare antigen recognition patterns to mice immunized with **15**, as **12*** elicited IgGs cross-reacting to **1** and **3** similar to **12** [Figs. 3.11 & 3.22]. Collectively, the immunization data provided evidence that the fully synthetic vaccine candidate **15** elicited T cell-dependent IgG responses with main reactivity to **1**. This specifity is reminiscent of the Alum-promoted polyclonal and monoclonal antibodies induced by CRM_{197} glycoconjugates with **1** that conferred protection from *C. difficile* infection *in vivo* [Figs. 3.8 & 3.18].

4.3.3 Considerations towards Improving the Vaccine Potential of PS-I Glycan Mimetics

Further studies are required to increase the ability of oligovalently displayed disaccharides to elicit antibodies *in vivo*. As the carrier itself is not directly involved in antibody binding, it may be replaced to alter the distance of disaccharide copies, the biocompatibility and/or the flexibility of the vaccine construct. For instance, oligolysine backbones have been shown to be suitable carrier molecules for small oligosaccharide antigens to afford highly immunogenic synthetic vaccine candidates.[270,271,277] Comparative studies with constructs of different valencies may help to differentiate affinity from avidity effects. The antibody response to oligovalent glycan mimetics may also benefit from incorporation of immunestimulatory molecules such as the TLR agonist PAM_2CysSK_4[277] or NKT cell-activating GSL[278,279]. Exchanging the CRM_{197} T cell epitope, for instance, with the PADRE peptide that is known to efficiently promote anti-glycan IgG to synthetic vaccine constructs[277,414] may also help to increase anti-PS-I antibody responses. Once potently immunogenic synthetic vaccine constructs are identified, *in vivo* protective effects of the generated antibody responses could be assessed by challenge studies in mice or hamsters. A fully synthetic vaccine against *C. difficile* may benefit from enhanced stability as compared to the semi-synthetic glycoconjugates investigated herein or toxin-based vaccine candidates that are presently under clinical investigation.[135] The cold chain that is required for protein-containing vaccines and is responsible for up to 50 % of the total cost could thereby be avoided.[280,281] Thus, synthetic glycan mimetics of PS-I may pave the way towards more cost-efficient vaccines against *C. difficile*.

References

1. Hall IC, O'Toole E. 1935. Intestinal flora in new-born infants with a description of a new pathogenic anaerobe, *Bacillus difficilis*. *Am J Dis Child* **49:** 390–402.
2. Ghose C. 2013. *Clostridium difficile* infection in the twenty-first century. *Emerg Microbes Infect* **2:** e62.
3. Hunt JJ, Ballard JD. 2013. Variations in virulence and molecular biology among emerging strains of *Clostridium difficile*. *Microbiol Mol Biol Rev* **77:** 567–581.
4. McBee RH. 1960. Intestinal flora of some Antarctic birds and mammals. *J Bacteriol* **79:** 311–312.
5. Smith LD, King EO. 1962. Occurrence of *Clostridium difficile* in infections of man. *J Bacteriol* **84:** 65–67.
6. Tedesco FJ, Alpers DH. 1974. Editorial: pseudomembranous colitis. *West J Med* **121:** 499–500.
7. Bartlett JG, Chang TW, Moon N, Onderdonk AB. 1978. Antibiotic-induced lethal enterocolitis in hamsters: studies with eleven agents and evidence to support the pathogenic role of *Clostridia*. *Am J Vet Res* **39:** 1525–1530.
8. Bartlett JG, Moon N, Chang TW, Taylor N, Onderdonk AB. 1978. Role of *Clostridium difficile* in antibiotic-associated pseudomembraneous colitis. *Gastroenterology* **75:** 778–782.
9. Bartlett JG. 2006. Narrative review: the new epidemic of *Clostridium difficile*-associated enteric disease. *Ann Intern Med* **145:** 758–764.
10. Miller BA, Chen LF, Sexton DJ, Anderson DJ. 2011. Comparison of the burdens of hospital-onset, healthcare facility-associated *Clostridium difficile* infections and of healthcare-associated infection due to methicillin-resistant *Staphylococcus aureus* in community hospitals. *Infect Control Hosp Epidemiol* **32:** 387–390.
11. Kyne L, Sougioultzis S, McFarland LV, Kelly CP. 2002. Underlying disease severity as a major risk factor for nosocomial *Clostridium difficile* diarrhea. *Infect Control Hosp Epidemiol* **23:** 653–659.
12. Centers for Disease Control and Prevention. 2013. Antibiotic Resistance Threats in the United States, 2013. Accessed *via* http://www.cdc.gov/drugresistance/pdf/ar-threats-2013-508.pdf (2016-03-13).

13. Lucado J, Gould C, Elixhauser A. 2012. *Clostridium difficile* infetions (CDI) in hospital stays, 2009. HCUP statistical brief 124. Agency for Healthcare Research and Quality, Rockville, MD.

14. McDonald LC, Killgore GE, Thompson A, Owens RC Jr, Kazakova SV, Sambol SP, Johnson S, Gerding DN. 2005. An epidemic, toxin gene-variant strain of *Clostridium difficile*. *N Engl J Med* **353:** 2433–2441.

15. Warny M, Pepin J, Fang A, Killgore G, Thompson A, Brazier J, Frost E, McDonald LC. 2005. Toxin production by an emerging strain of *Clostridium difficile* associated with outbreaks of severe disease in North America and Europe. *Lancet* **366:** 1079–1084.

16. Zilberberg MD, Shorr AF, Kollef MH. 2008. Increase in adult *Clostridium difficile*-related hospitalizations and case-fatality rate, United States, 2000-2005. *Emerg Infect Dis* **14:** 929–931.

17. Freeman J, Bauer MP, Baines SD, Corver J, Fawley WN, Goorhuis B, Kuijper EJ, Wilcox MH. 2010. The changing epidemiology of *Clostridium difficile* infections. *Clin Microbiol Rev* **23:** 529–549.

18. Brazier JS, Raybould R, Patel B, Duckworth G, Pearson A, Charlett A, Duerden BI; HPA Regional Microbiology Network. 2008. Distribution and antimicrobial susceptibility patterns of *Clostridium difficile* PCR ribotypes in English hospitals, 2007-08. *Euro Surveill* **13:** pii: 19000.

19. Zaiss NH, Witte W, Nübel U. 2010. Fluoroquinolone resistance and *Clostridium difficile*, Germany. *Emerg Infect Dis* **16:** 675–677.

20. Plaza-Garrido Á, Barra-Carrasco J, Macias JH, Carman R, Fawley WN, Wilcox MH, Hernández-Rocha C, Guzmán-Durán AM, Alvarez-Lobos M, Paredes-Sabja D. 2015. Predominance of *Clostridium difficile* ribotypes 012, 027 and 046 in a university hospital in Chile, 2012. *Epidemiol Infect* **22:** 1–4.

21. Tenover FC, Akerlund T, Gerding DN, Goering RV, Boström T, Jonsson AM, Wong E, Wortman AT, Persing DH. 2011. Comparison of strain typing results for *Clostridium difficile* isolates from North America. *J Clin Microbiol* **49:** 1831–1837.

22. Hawkey PM, Marriott C, Liu WE, Jian ZJ, Gao Q, Ling TK, Chow V, So E, Chan R, Hardy K, Xu L, Manzoor S. 2013. Molecular epidemiology of *Clostridium difficile* infection in a major chinese hospital: an underrecognized problem in Asia? *J Clin Microbiol* **51:** 3308–3313.

23. Kelly CP. 2012. Can we identify patients at high risk of recurrent *Clostridium difficile* infection? *Clin Microbiol Infect* **18(Suppl 6):** 21–27.

24. Pépin J, Saheb N, Coulombe MA, Alary ME, Corriveau MP, Authier S, Leblanc M, Rivard G, Bettez M, Primeau V, Nguyen M, Jacob CE, Lanthier L. 2005. Emergence of fluoroquinolones as the predominant risk factor for *Clostridium difficile*-associated diarrhea: a cohort study during an epidemic in Quebec. *Clin Infect Dis* **41:** 1254–1260.

25. Nylund CM, Goudie A, Garza JM, Fairbrother G, Cohen MB. 2011. *Clostridium difficile* infection in hospitalized children in the United States. *Arch Pediatr Adolesc Med* **165:** 451–457.

26. Rouphael NG, O'Donnell JA, Bhatnagar J, Lewis F, Polgreen PM, Beekmann S, Guarner J, Killgore GE, Coffman B, Campbell J, Zaki SR, McDonald LC. 2008. *Clostridium difficile*-associated diarrhea: an emerging threat to pregnant women. *Am J Obstet Gynecol* **198:** 635.e1–635.e6.

27. Seekatz AM, Young VB. 2014. *Clostridium difficile* and the microbiota. *J Clin Invest* **124:** 4182–4189.

28. Keel MK, Songer JG. 2006. The comparative pathology of *Clostridium difficile*-associated diseases. *Vet Pathol* **43:** 225–240.

29. Jump RL, Pultz MJ, Donskey CJ. 2007. Vegetative *Clostridium difficile* survives in room air on moist surfaces and in gastric contents with reduced acidity: a potential mechanism to explain the association between proton pump inhibitors and *C. difficile*-associated diarrhea? *Antimicrob Agents Chemother* **51:** 2883–2887.

30. Gerding DN, Muto CA, Owens RC Jr. 2008. Measures to control and prevent *Clostridium difficile* infection. *Clin Infect Dis* **46(Suppl 1):** S43–49.

31. Macleod-Glover N, Sadowski C. 2010. Efficacy of cleaning products for *C. difficile*: environmental strategies to reduce the spread of *Clostridium difficile*-associated diarrhea in geriatric rehabilitation. *Can Fam Physician* **56:** 417–423.

32. Rodriguez-Palacios A, Lejeune JT. 2011. Moist-heat resistance, spore aging, and superdormancy in *Clostridium difficile*. *Appl Environ Microbiol* **77:** 3085–3091.

33. Setlow P. 2007. I will survive: DNA protection in bacterial spores. *Trends Microbiol* **15:** 172–180.

34. McFarland LV, Mulligan ME, Kwok RY, Stamm WE. 1989. Nosocomial acquisition of *Clostridium difficile* infection. *N Engl J Med* **320:** 2014–210.

35. al Saif N, Brazier JS. 1996. The distribution of *Clostridium difficile* in the environment of South Wales. *J Med Microbiol* **45:** 133–137.

36. Bolton RP, Tait SK, Dear PR, Losowsky MS. 1984. Asymptomatic neonatal colonisation by *Clostridium difficile*. *Arch Dis Child* **59:** 466–472.

37. Collignon A, Ticchi L, Depitre C, Gaudelus J, Delmée M, Corthier G. 1993. Heterogeneity of *Clostridium difficile* isolates from infants. *Eur J Pediatr* **152:** 319–322.

38. Rousseau C, Poilane I, De Pontual L, Maherault AC, Le Monnier A, Collignon A. 2012. *Clostridium difficile* carriage in healthy infants in the community: a potential reservoir for pathogenic strains. *Clin Infect Dis* **55:** 1209–1215.

39. Eglow R, Pothoulakis C, Itzkowitz S, Israel EJ, O'Keane CJ, Gong D, Gao N, Xu YL, Walker WA, LaMont JT. 1992. Diminished *Clostridium difficile* toxin A sensitivity in newborn rabbit ileum is associated with decreased toxin A receptor. *J Clin Invest* **90:** 822–829.

40. Furuya-Kanamori L, Marquess J, Yakob L, Riley TV, Paterson DL, Foster NF, Huber CA, Clements AC. 2015. Asymptomatic *Clostridium difficile* colonization: epidemiology and clinical implications. *BMC Infect Dis* **15:** 516.

41. Lawley TD, Croucher NJ, Yu L, Clare S, Sebaihia M, Goulding D, Pickard DJ, Parkhill J, Choudhary J, Dougan G. 2009. Proteomic and genomic characterization of highly infectious *Clostridium difficile* 630 spores. *J Bacteriol* **191:** 5377–5386.

42. Sorg JA, Sonenshein AL. 2010. Inhibiting the initiation of *Clostridium difficile* spore germination using analogs of chenodeoxycholic acid, a bile acid. *J Bacteriol* **192:** 4983–4990.

43. Heeg D, Burns DA, Cartman ST, Minton NP. 2012. Spores of *Clostridium difficile* clinical isolates display a diverse germination response to bile salts. *PLoS One* **7:** e32381.

44. Sorg JA, Sonenshein AL. 2009. Chenodeoxycholate is an inhibitor of *Clostridium difficile* spre germination. *J Bacteriol* **191:** 1115–1117.

45. Denève C, Janoir C, Poilane I, Fantinato C, Collignon A. 2009. New trends in *Clostridium difficile* virulence and pathogenesis. *Int J Antimicrob Agents* **33(Suppl 1):** S24–S28.

46. Calabi E, Ward S, Wren B, Paxton T, Panico M, Morris H, Dell A, Dougan D, Fairweather N. 2001. Molecular characterization of the surface layer proteins from *Clostridium difficile*. *Mol Microbiol* **40:** 1187–1199.

47. Calabi E, Calabi F, Phillips AD, Fairweather NF. 2002. Binding of *Clostridium difficile* surface layer proteins to gastrointestinal tissues. *Infect Immun* **70:** 5770–5778.

48. Cerquetti M, Molinari A, Sebastianelli A, Diociaiuti M, Petruzzelli R, Capo C, Mastrantonio P. 2000. Characterization of surface layer proteins from different *Clostridium difficile* clinical isolates. *Microb Pathog* **28:** 363–372.

49. Waligora AJ, Hennequin C, Mullany P, Bourlioux P, Collignon A, Karjalainen T. 2001. Characterization of a cell surface protein of *Clostridium difficile* with adhesive properties. *Infect Immun* **69:** 2144–2153.

50. Hennequin C, Porcheray F, Waligora-Dupriet A, Collignon A, Barc M, Bourlioux P, Bourlioux P, Karjalainen T. 2001. GroEL (Hsp60) of *Clostridium difficile* is involved in cell adherence. *Microbiology* **147:** 87–96.

51. Hennequin C, Janoir C, Barc MC, Collignon A, Karjalainen T. 2003. Identification and characterization of a fibronectin-binding protein from *Clostridium difficile*. *Microbiology* **149:** 2779–2287.

52. Tasteyre A, Barc MC, Collignon A, Boureau H, Karjalainen T. 2001. Role of FliC and FliD flagellar proteins of *Clostridium difficile* in adherence and gut colonization. *Infect Immun* **69:** 7937–7940.

53. Poilane I, Karjalainen T, Barc MC, Bourlioux P, Collignon A. 1998. Protease activity of *Clostridium difficile* strains. *Can J Microbiol* **44:** 157–161.

54. Janoir C, Péchiné S, Grosdidier C, Collignon A. 2007. Cwp84, a surface-associated protein of *Clostridium difficile* is a cysteine protease with degrading activity on extra cellular matrix proteins. *J Bacteriol* **189:** 7174–7180.

55. Drudy D, Calabi E, Kyne L, Sougioultzis S, Kelly E, Fairweather N, Kelly CP. 2004. Human antibody response to surface layer proteins in *Clostridium difficile* infection. *FEMS Immunol Med Microbiol* **41:** 237–242.

56. O'Brien JB, McCabe MS, Athié-Morales V, McDonald GS, Ní Eidhin DB, Kelleher DP. 2005. Passive immunisation of hamsters against *Clostridium difficile* infection using antibodies to surface layer proteins. *FEMS Microbiol Lett* **246:** 199–205.

57. Ní Eidhin DB, O'Brien JB, McCabe MS, Athié-Morales V, Kelleher DP. 2008. Active immunization of hamsters against *Clostridium difficile* infection using surface-layer protein. *FEMS Immunol Med Microbiol* **52:** 207–218.

58. Bruxelle JF, Mizrahi A, Hoys S, Collignon A, Janoir C, Péchiné S. 2016. Immunogenic properties of the surface layer precursor of *Clostridium difficile* and vaccination assays in animal models. *Anaerobe* **37:** 78–84.

59. Wright A, Drudy D, Kyne L, Brown K, Fairweather NF. 2008. Immunoreactive cell wall proteins of *Clostridium difficile* identified by human sera. *J Med Microbiol* **57(Pt 6):** 750–756.

60. Péchiné S, Gleizes A, Janoir C, Gorges-Kergot R, Barc MC, Delmée M, Collignon A. 2005. Immunological properties of surface proteins of *Clostridium difficile*. *J Med Microbiol* **54(Pt 2):** 193–196.

61. Péchiné S, Janoir C, Collignon A. 2005. Variability of *Clostridium difficile* surface proteins and specific serum antibody response in patients with *Clostridium difficile*-associated disease. *J Clin Microbiol* **43:** 5018–5025.

62. Péchiné S, Hennequin C, Boursier C, Hoys S, Collignon A. 2013. Immunization using GroEL decreases *Clostridium difficile* intestinal colonization. *PLoS One* **8:** e81112.

63. Ghose C, Eugenis I, Sun X, Edwards AN, McBride SM, Pride DT, Kelly CP, Ho DD. 2016. Immunogenicity and protective efficacy of recombinant *Clostridium difficile* flagellar protein FliC. *Emerg Microbes Infect* **5:** e8.

64. Péchiné S, Denève C, Le Monnier A, Hoys S, Janoir C, Collignon A. 2011. Immunization of hamsters against *Clostridium difficile* infection using the Cwp84 protease as an antigen. *FEMS Immunol Med Microbiol* **63:** 73–81.

65. Torres JF, Lyerly DM, Hill JE, Monath TP. 1995. Evaluation of formalin-inactivated *Clostridium difficile* vaccines administered by parenteral and mucosal routes of immunization in hamsters. *Infect Immun* **63:** 4619-4627.

66. Senoh M, Iwaki M, Yamamoto A, Kato H, Fukuda T, Shibayama K. 2015. Inhibition of adhesion of *Clostridium difficile* to human intestinal cells after treatment with serum and intestinal fluid isolated from mice immunized with nontoxigenic *C. difficile* membrane fraction. *Microb Pathog* **81:** 1–5.

67. Di Bella S, Capone A, Musso M, Giannella M, Tarasi A, Johnson E, Taglietti F, Campoli C, Petrosillo N. 2013. *Clostridium difficile* infection in the elderly. *Infez Med* **21:** 93–102.

68. Collini PJ, Bauer M, Kuijper E, Dockrell DH. 2012. *Clostridium difficile* infection in HIV-seropositive individuals and transplant recipients. *J Infect* **64:** 131–147.

69. Collini PJ, Kuijper E, Dockrell DH. 2013. *Clostridium difficile* infection in patients with HIV/AIDS. *Curr HIV/AIDS Rep* **10:** 273–282.

70. Alonso CD, Kamboj M. 2014. *Clostridium difficile* infection (CDI) in solid organ and hematopoietic stem cell transplant recipients. *Curr Infect Dis Rep* **16:** 414.

71. Alonso CD, Marr KA. 2013. *Clostridium difficile* infection among hematopoietic stem cell transplant recipients: beyond colitis. *Curr Opin Infect Dis* **26:** 326–331.

72. Qin J, Li R, Raes J, Arumugam M, Burgdorf KS, Manichanh C, Nielsen T, Pons N, Levenez F, Yamada T, Mende DR, Li J, Xu J, Li S, Li D, Cao J, Wang B, Liang H, Zheng H, Xie Y, Tap J, Lepage P, Bertalan M, Batto JM, Hansen T, Le Paslier D, Linneberg A, Nielsen HB, Pelletier E, Renault P, Sicheritz-Ponten T, Turner K, Zhu H, Yu C, Li S, Jian M, Zhou Y, Li Y, Zhang X, Li S, Qin N, Yang H, Wang J, Brunak S, Doré J, Guarner F, Kristiansen K, Pedersen O, Parkhill J, Weissenbach J; MetaHIT Consortium, Bork P, Ehrlich SD, Wang J. 2010. A human gut microbial gene catalogue established by metagenomic sequencing. *Nature* **464:** 59–65.

73. Vollaard EJ, Clasener HA. 1994. Colonization resistance. *Antimicrob Agents Chemother* **38:** 409–414.

74. Broecker F, Kube M, Klumpp J, Schuppler M, Biedermann L, Hecht J, Hombach M, Keller PM, Rogler G, Moelling K. 2013. Analysis of the intestinal microbiome of a recovered *Clostridium difficile* patient after fecal transplantation. *Digestion* **88:** 243–251.

75. Broecker F, Klumpp J, Schuppler M, Russo G, Biedermann L, Hombach M, Rogler G, Moelling K. 2015. Long-term changes of bacterial and viral compositions in the intestine of a recovered *Clostridium difficile* patient after fecal microbiota transplantation. *Cold Spring Harb Mol Case Stud* **2:** a000448.

76. von Eichel-Streiber C, Boquet P, Sauerborn M, Thelestam M. 1996. Large clostridial cytotoxins–a family of glycosyltransferases modifying small GTP-binding proteins. *Trends Microbiol* **4:** 375–382.

77. Henriques B, Florin I, Thelestam M. 1987. Cellular internalisation of *Clostridium difficile* toxin A. *Microb Pathog* **2:** 455–463.

78. von Eichel-Streiber C, Warfolomeow I, Knautz D, Sauerborn M, Hadding U. 1991. Morphological changes in adherent cells induced by *Clostridium difficile* toxins. *Biochem Soc Trans* **19:** 1154–1160.

79. Krivan HC, Clark GF, Smith DF, Wilkins TD. 1986. Cell surface binding site for *Clostridium difficile* enterotoxin: Evidence for a glycoconjugate containing the sequence Galα1-3Galβ1-4GlcNAc. *Infect Immun* **53:** 573–581.

80. Tucker KD, Wilkins TD. 1991. Toxin A of *Clostridium difficile* binds to the human carbohydrate antigens I, X, and Y. *Infect Immun* **59:** 73–78.

81. Na X, Kim H, Moyer MP, Pothoulakis C, LaMont JT. 2008. gp96 is a human colonocyte plasma membrane binding protein for *Clostridium difficile* toxin A. *Infect Immun* **76:** 2862–2871.

82. Pothoulakis C, Gilbert RJ, Cladaras C, Castagliuolo I, Semenza G, Hitti Y, Montcrief JS, Linevsky J, Kelly CP, Nikulasson S, Desai HP, Wilkins TD, LaMont JT. 1996. Rabbit sucrase-isomaltase contains a functional intestinal receptor for *Clostridium difficile* toxin A. *J Clin Invest* **98:** 641–649.

83. Yuan P, Zhang H, Cai C, Zhu S, Zhou Y, Yang X, He R, Li C, Guo S, Li S, Huang T, Perez-Cordon G, Feng H, Wei W. 2015. Chondroitin sulfate proteoglycan 4 functions as the cellular receptor for *Clostridium difficile* toxin B. *Cell Res* **25:** 157–168.

84. LaFrance ME, Farrow MA, Chandrasekaran R, Sheng J, Rubin DH, Lacy DB. 2015. Identification of an epithelial cell receptor responsible for *Clostridium difficile* TcdB-induced cytotoxicity. *Proc Natl Acad Sci U S A* **112:** 7073–7078.

85. Just I, Wilm M, Selzer J, Rex G, von Eichel-Streiber C, Mann M, Aktories K. 1995. The enterotoxin from *Clostridium difficile* (ToxA) monoglucosylates the Rho proteins. *J Biol Chem* **270:** 13932–13936.

86. Just I, Selzer J, Wilm M, von Eichel-Streiber C, Mann M, Aktories K. 1995. Glucosylation of Rho proteins by *Clostridium difficile* toxin B. *Nature* **375:** 500–503.

87. Qa'Dan M, Ramsey M, Daniel J, Spyres LM, Safiejko-Mroczka B, Ortiz-Leduc W, Ballard JD. 2002. *Clostridium difficile* toxin B activates dual caspase-dependent and caspase-independent apoptosis in intoxicated cells. *Cell Microbiol* **4:** 425–434.

88. Chumbler NM, Farrow MA, Lapierre LA, Franklin JL, Haslam DB, Goldenring JR, Lacy DB. 2012. *Clostridium difficile* Toxin B causes epithelial cell necrosis through an autoprocessing-independent mechanism. *PLoS Pathog* **8:** e1003072.

89. Geric B, Johnson S, Gerding DN, Grabnar M, Rupnik M. 2003. Frequency of binary toxin genes among *Clostridium difficile* strains that do not produce large clostridial toxins. *J Clin Microbiol* **41:** 5227–5232.

90. Gonçalves C, Decré D, Barbut F, Burghoffer B, Petit JC. 2004. Prevalence and characterization of a binary toxin (actin-specific ADP-ribosyltransferase) from *Clostridium difficile*. *J Clin Microbiol* **42:** 1933–1939.

91. Papatheodorou P, Carette JE, Bell GW, Schwan C, Guttenberg G, Brummelkamp TR, Aktories K. 2011. Lipolysis-stimulated lipoprotein receptor (LSR) is the host receptor for the binary toxin *Clostridium difficile* transferase (CDT). *Proc Natl Acad Sci U S A* **108:** 16422–16427.

92. Perelle S, Gibert M, Bourlioux P, Corthier G, Popoff MR. 1997. Production of a complete binary toxin (actin-specific ADP-ribosyltransferase) by *Clostridium difficile* CD196. *Infect Immun* **65:** 1402–1407.

93. Barbut F, Decré D, Lalande V, Burghoffer B, Noussair L, Gigandon A, Espinasse F, Raskine L, Robert J, Mangeol A, Branger C, Petit JC. 2005. Clinical features of *Clostridium difficile*-associated diarrhoea due to binary toxin (actin-specific ADP-ribosyltransferase)-producing strains. *J Med Microbiol* **54(Pt 2):** 181–185.

94. Gerding DN, Johnson S, Rupnik M, Aktories K. 2014. *Clostridium difficile* binary toxin CDT: mechanism, epidemiology, and potential clinical importance. *Gut Microbes* **5:** 15–27.

95. Solomon K. 2013. The host immune response to *Clostridium difficile* infection. *Ther Adv Infect Dis* **1:** 19–35.

96. Akerlund T, Persson I, Unemo M, Norén T, Svenungsson B, Wullt M, Burman LG. 2008. Increased sporulation rate of epidemic *Clostridium difficile* Type 027/NAP1. *J Clin Microbiol* **46:** 1530–1533.

97. Lübbert C, John E, von Müller L. 2014. *Clostridium difficile* infection: guideline-based diagnosis and treatment. *Dtsch Arztebl Int* **111:** 723–731.

98. Spigaglia P. 2016. Recent advances in the understanding of antibiotic resistance in *Clostridium difficile* infection. *Ther Adv Infect Dis* **3:** 23–42.

99. Gerding DN, Muto CA, Owens RC Jr. 2008. Treatment of *Clostridium difficile* infection. *Clin Infect Dis* **46(Suppl 1):** S32–S42.

100. Fekety R, McFarland LV, Surawicz CM, Greenberg RN, Elmer GW, Mulligan ME. 1997. Recurrent *Clostridium difficile* diarrhea: characteristics of and risk factors for patients enrolled in a prospective, randomized, double-blinded trial. *Clin Infect Dis* **24:** 324–333.

101. O'Neill GL, Beaman MH, Riley TV. 1991. Relapse versus reinfection with *Clostridium difficile*. *Epidemiol Infect* **107:** 627–635.

102. Wilcox MH, Spencer RC. 1992. *Clostridium difficile* infection: responses, relapses and re-infections. *J Hosp Infect* **22:** 85–92.

103. Gough E, Shaikh H, Manges AR. 2011. Systematic review of intestinal microbiota transplantation (fecal bacteriotherapy) for recurrent *Clostridium difficile* infection. *Clin Infect Dis* **53:** 994–1002.

104. Johnson S. 2009. Recurrent *Clostridium difficile* infection: a review of risk factors, treatments, and outcomes. *J Infect* **58:** 403–410.

105. Kelly CP, LaMont JT. 2008. *Clostridium difficile*–more difficult than ever. *N Engl J Med* **359:** 1932–1940.

106. Loo VG, Poirier L, Miller MA, Oughton M, Libman MD, Michaud S, Bourgault AM, Nguyen T, Frenette C, Kelly M, Vibien A, Brassard P, Fenn S, Dewar K, Hudson TJ, Horn R, René P, Monczak Y,

Dascal A. 2005. A predominantly clonal multi-institutional outbreak of *Clostridium difficile*-associated diarrhea with high morbidity and mortality. *N Engl J Med* **353:** 2442–2449.

107. Maroo S, Lamont JT. 2006. Recurrent *Clostridium difficile*. *Gastroenterology* **130:** 1311–1316.

108. Nathwani D, Cornely OA, Van Engen AK, Odufowora-Sita O, Retsa P, Odeyemi IA. 2014. Cost-effectiveness analysis of fidaxomicin versus vancomycin in *Clostridium difficile* infection. *J Antimicrob Chemother* **69:** 2901–2912.

109. O'Horo JC, Jindai K, Kunzer B, Safdar N. 2014. Treatment of recurrent *Clostridium difficile* infection: a systematic review. *Infection* **42:** 43–59.

110. Venuto C, Butler M, Ashley ED, Brown J. 2010. Alternative therapies for *Clostridium difficile* infections. *Pharmacotherapy* **30:** 1266–1278.

111. Musher DM, Logan N, Mehendiratta V, Melgarejo NA, Garud S, Hamill RJ. 2007. *Clostridium difficile* colitis that fails conventional metronidazole therapy: response to nitazoxanide. *J Antimicrob Chemother* **59:** 705–710.

112. Basu PP, Shah NJ, Krishnaswamy N, Korapati R, Tang C, Pacana T. 2010. Sequential use of nitazoxanide (NTZ) as a salvage therapy in patient with recurrent mild to moderate *Clostridium difficile* infection (CDI): a prospective, open-label, randomized clinical trial. *Am J Gastroenterol* **105:** S142.

113. Patrick Basu P, Dinani A, Rayapudi K, Pacana T, Shah NJ, Hampole H, Krishnaswamy NV, Mohan V. 2010. Rifaximin therapy for metronidazole-unresponsive *Clostridium difficile* infection: a prospective pilot trial. *Therap Adv Gastroenterol* **3:** 221–225.

114. Jiang ZD, Garey KW, Price M, Graham G, Okhuysen P, Dao-Tran T, LaRocco M, DuPont HL. 2007. Association of interleukin-8 polymorphism and immunoglobulin G anti-toxin A in patients with *Clostridium difficile*-associated diarrhea. *Clin Gastroenterol Hepatol* **5:** 964–968.

115. Aslam S, Hamill RJ, Musher DM. 2005. Treatment of *Clostridium difficile*-associated disease: old therapies and new strategies. *Lancet Infect Dis* **5:** 549–557.

116. WHO technical report. 1989. Requirements for the collection, processing, and quality control of blood, blood components, and plasma derivatives. WHO technical Report Series No 786:Annex 4.

117. Lowy I, Molrine DC, Leav BA, Blair BM, Baxter R, Gerding DN, Nichol G, Thomas WD Jr, Leney M, Sloan S, Hay CA, Ambrosino DM. 2010. Treatment with monoclonal antibodies against *Clostridium difficile* toxins. *N Engl J Med* **362:** 197–205.

118. Dickinson BL, Badizadegan K, Wu Z, Ahouse JC, Zhu X, Simister NE, Blumberg RS, Lencer WI. 1999. Bidirectional FcRn-dependent IgG transport in a polarized human intestinal epithelial cell line. *J Clin Invest* **104:** 903–911.

119. Spiekermann GM, Finn PW, Ward ES, Dumont J, Dickinson BL, Blumberg RS, Lencer WI. 2002. Receptor-mediated immunoglobulin G transport across mucosal barriers in adult life: functional expression of FcRn in the mammalian lung. *J Exp Med* **196:** 303–310.

120. Mostov KE. 1994. Transepithelial transport of immunoglobulins. *Annu Rev Immunol* **12:** 63–84.

121. Schenck LP, Beck PL, MacDonald JA. 2015. Gastrointestinal dysbiosis and the use of fecal microbial transplantation in *Clostridium difficile* infection. *World J Gastrointest Pathophysiol* **6:** 169–180.

122. Fuentes S, de Vos WM. 2016. How to manipulate the microbiota: fecal microbiota transplantation. *Adv Exp Med Biol* **902:** 143–153.

123. Surawicz CM, McFarland LV, Greenberg RN, Rubin M, Fekety R, Mulligan ME, Garcia RJ, Brandmarker S, Bowen K, Borja D, Elmer GW. 2000. The search for a better treatment for recurrent *Clostridium difficile* disease: use of high-dose vancomycin combined with *Saccharomyces boulardii*. *Clin Infect Dis* **31:** 1012–1017.

124. McFarland LV, Surawicz CM, Greenberg RN, Fekety R, Elmer GW, Moyer KA, Melcher SA, Bowen KE, Cox JL, Noorani Z, Harrington G, Rubin M, Greenwald D. 1994. A randomized placebo-controlled trial of *Saccharomyces boulardii* in combination with standard antibiotics for *Clostridium difficile* disease. *JAMA* **271:** 1913–1918.

125. Gerding DN, Meyer T, Lee C, Cohen SH, Murthy UK, Poirier A, Van Schooneveld TC, Pardi DS, Ramos A, Barron MA, Chen H, Villano S. 2015. Administration of spores of nontoxigenic *Clostridium difficile* strain M3 for prevention of recurrent *C. difficile* infection: a randomized clinical trial. *JAMA* **313:** 1719–1727.

126. Kassam Z, Lee CH, Yuan Y, Hunt RH. 2013. Fecal microbiota transplantation for *Clostridium difficile* infection: systematic review and meta-analysis. *Am J Gastroenterol* **108:** 500–508.

127. Eiseman B, Silen W, Bascom GS, Kauvar AJ. 1958. Fecal enema as an adjunct in the treatment of pseudomembranous enterocolitis. *Surgery* **44:** 854–859.

128. van Nood E, Vrieze A, Nieuwdorp M, Fuentes S, Zoetendal EG, de Vos WM, Visser CE, Kuijper EJ, Bartelsman JF, Tijssen JG, Speelman P, Dijkgraaf MG, Keller JJ. 2013. Duodenal infusion of donor feces for recurrent *Clostridium difficile*. *N Engl J Med* **368:** 407–415.

129. Youngster I, Sauk J, Pindar C, Wilson RG, Kaplan JL, Smith MB, Alm EJ, Gevers D, Russell GH, Hohmann EL. 2014. Fecal microbiota transplant for relapsing *Clostridium difficile* infection using a frozen inoculum from unrelated donors: a randomized, open-label, controlled pilot study. *Clin Infect Dis* **58:** 1515–1522.

130. Cammarota G, Masucci L, Ianiro G, Bibbò S, Dinoi G, Costamagna G, Sanguinetti M, Gasbarrini A. 2015. Randomised clinical trial: faecal microbiota transplantation by colonoscopy vs. vancomycin for the treatment of recurrent *Clostridium difficile* infection. *Aliment Pharmacol Ther* **41:** 835–843.

131. Vyas D, Aekka A, Vyas A. 2015. Fecal transplant policy and legislation. *World J Gastroenterol* **21:** 6–11.

132. Schwartz M, Gluck M, Koon S. 2013. Norovirus gastroenteritis after fecal microbiota transplantation for treatment of *Clostridium difficile* infection despite asymptomatic donors and lack of sick contacts. *Am J Gastroenterol* **108:** 1367.

133. Alang N, Kelly CR. 2015. Weight gain after fecal microbiota transplantation. *Open Forum Infect Dis* **2:** ofv004.

134. Petrof EO, Gloor GB, Vanner SJ, Weese SJ, Carter D, Daigneault MC, Brown EM, Schroeter K, Allen-Vercoe E. 2013. Stool substitute transplant therapy for the eradication of *Clostridium difficile* infection: 'RePOOPulating' the gut. *Microbiome* **1:** 3.

135. Leuzzi R, Adamo R, Scarselli M. 2014. Vaccines against *Clostridium difficile*. *Hum Vaccin Immunother* **10:** 1466–1477.

136. Centers for Disease Control and Prevention. 2011. A CDC Framework for Preventing Infectious Diseases. Accessed *via* http://www.cdc.gov/oid/docs/ID-Framework.pdf (2016-03-24).

137. Aronsson B, Granström M, Möllby R, Nord CE. 1985. Serum antibody response to *Clostridium difficile* toxins in patients with *Clostridium difficile* diarrhoea. *Infection* **13:** 97–101.

138. Nakamura S, Mikawa M, Nakashio S, Takabatake M, Okado I, Yamakawa K, Serikawa T, Okumura S, Nishida S. 1981. Isolation of *Clostridium difficile* from the feces and the antibody in sera of young and elderly adults. *Microbiol Immunol* **25:** 345–351.

139. Viscidi R, Laughon BE, Yolken R, Bo-Linn P, Moench T, Ryder RW, Bartlett JG. 1983. Serum antibody response to toxins A and B of *Clostridium difficile*. *J Infect Dis* **148:** 93–100.

140. Libby JM, Jortner BS, Wilkins TD. 1982. Effects of the two toxins of *Clostridium difficile* in antibiotic-associated cecitis in hamsters. *Infect Immun* **36:** 822–829.

141. Kim PH, Iaconis JP, Rolfe RD. 1987. Immunization of adult hamsters against *Clostridium difficile*-associated ileocecitis and transfer of protection to infant hamsters. *Infect Immun* **55:** 2984–2992.

142. Torres JF, Lyerly DM, Hill JE, Monath TP. 1995. Evaluation of formalin-inactivated *Clostridium difficile* vaccines administered by parenteral and mucosal routes of immunization in hamsters. *Infect Immun* **63:** 4619–4627.

143. Ghose C, Kalsy A, Sheikh A, Rollenhagen J, John M, Young J, Rollins SM, Qadri F, Calderwood SB, Kelly CP, Ryan ET. 2007. Transcutaneous immunization with *Clostridium difficile* toxoid A induces systemic and mucosal immune responses and toxin A-neutralizing antibodies in mice. *Infect Immun* **75:** 2826–2832.

144. Siddiqui F, O'Connor JR, Nagaro K, Cheknis A, Sambol SP, Vedantam G, Gerding DN, Johnson S. 2012. Vaccination with parenteral toxoid B protects hamsters against lethal challenge with toxin A-negative, toxin B-positive *Clostridium difficile* but does not prevent colonization. *J Infect Dis* **205:** 128–133.

145. Anosova NG, Brown AM, Li L, Liu N, Cole LE, Zhang J, Mehta H, Kleanthous H. 2013. Systemic antibody responses induced by a two-component *Clostridium difficile* toxoid vaccine protect against *C. difficile*-associated disease in hamsters. *J Med Microbiol* **62(Pt 9):** 1394–1404.

146. Lyerly DM. 1990. Vaccination against lethal *Clostridium difficile* enterocolitis with a nontoxic recombinant peptide of toxin A. *Curr Microbiol* **21:** 29–32.

147. Ward SJ, Douce G, Dougan G, Wren BW. 1999. Local and systemic neutralizing antibody responses induced by intranasal immunization with the nontoxic binding domain of toxin A from *Clostridium difficile*. *Infect Immun* **67:** 5124–5132.

148. Permpoonpattana P, Hong HA, Phetcharaburanin J, Huang JM, Cook J, Fairweather NF, Cutting SM. 2011. Immunization with *Bacillus* spores expressing toxin A peptide repeats protects against infection with *Clostridium difficile* strains producing toxins A and B. *Infect Immun* **79:** 2295–2302.

149. Leuzzi R, Spencer J, Buckley A, Brettoni C, Martinelli M, Tulli L, Marchi S, Luzzi E, Irvine J, Candlish D, Veggi D, Pansegrau W, Fiaschi L, Savino S, Swennen E, Cakici O, Oviedo-Orta E, Giraldi M, Baudner B, D'Urzo N, Maione D, Soriani M, Rappuoli R, Pizza M, Douce GR, Scarselli M. 2013. Protective efficacy induced by recombinant *Clostridium difficile* toxin fragments. *Infect Immun* **81:** 2851–2860.

150. Wang H, Sun X, Zhang Y, Li S, Chen K, Shi L, Nie W, Kumar R, Tzipori S, Wang J, Savidge T, Feng H. 2012. A chimeric toxin vaccine protects against primary and recurrent *Clostridium difficile* infection. *Infect Immun* **80:** 2678–2688.

151. Tian JH, Fuhrmann SR, Kluepfel-Stahl S, Carman RJ, Ellingsworth L, Flyer DC. 2012. A novel fusion protein containing the receptor binding domains of *C. difficile* toxin A and toxin B elicits protective immunity against lethal toxin and spore challenge in preclinical efficacy models. *Vaccine* **30:** 4249–4258.

152. Ghose C, Verhagen JM, Chen X, Yu J, Huang Y, Chenesseau O, Kelly CP, Ho DD. 2013. Toll-like receptor 5-dependent immunogenicity and protective efficacy of a recombinant fusion protein vaccine containing the nontoxic domains of *Clostridium difficile* toxins A and B and *Salmonella enterica* serovar typhimurium flagellin in a mouse model of *Clostridium difficile* disease. *Infect Immun* **81:** 2190–2196.

153. Kyne L, Warny M, Qamar A, Kelly CP. 2001. Association between antibody response to toxin A and protection against recurrent *Clostridium difficile* diarrhoea. *Lancet* **357:** 189–193.

154. Kyne L, Warny M, Qamar A, Kelly CP. 2000. Asymptomatic carriage of *Clostridium difficile* and serum levels of IgG antibody against toxin A. *N Engl J Med* **342:** 390–397.

155. Kuehne SA, Cartman ST, Heap JT, Kelly ML, Cockayne A, Minton NP. 2010. The role of toxin A and toxin B in *Clostridium difficile* infection. *Nature* **467:** 711–713.

156. Drudy D, Harnedy N, Fanning S, O'Mahony R, Kyne L. 2007. Isolation and characterisation of toxin A-negative, toxin B-positive *Clostridium difficile* in Dublin, Ireland. *Clin Microbiol Infect* **13:** 298–304.

157. Kuijper EJ, de Weerdt J, Kato H, Kato N, van Dam AP, van der Vorm ER, Weel J, van Rheenen C, Dankert J. 2001. Nosocomial outbreak of *Clostridium difficile*-associated diarrhoea due to a clindamycin-resistant enterotoxin A-negative strain. *Eur J Clin Microbiol Infect Dis* **20:** 528–534.

158. van den Berg RJ, Claas EC, Oyib DH, Klaassen CH, Dijkshoorn L, Brazier JS, Kuijper EJ. 2004. Characterization of toxin A-negative, toxin B-positive *Clostridium difficile* isolates from outbreaks in different countries by amplified fragment length polymorphism and PCR ribotyping. *J Clin Microbiol* **42:** 1035–1041.

159. Kotloff KL, Wasserman SS, Losonsky GA, Thomas W Jr, Nichols R, Edelman R, Bridwell M, Monath TP. 2001. Safety and immunogenicity of increasing doses of a *Clostridium difficile* toxoid vaccine administered to healthy adults. *Infect Immun* **69:** 988–995.

160. Aboudola S, Kotloff KL, Kyne L, Warny M, Kelly EC, Sougioultzis S, Giannasca PJ, Monath TP, Kelly CP. 2003. *Clostridium difficile* vaccine and serum immunoglobulin G antibody response to toxin A. *Infect Immun* **71:** 1608–1610.

161. Sougioultzis S, Kyne L, Drudy D, Keates S, Maroo S, Pothoulakis C, Giannasca PJ, Lee CK, Warny M, Monath TP, Kelly CP. 2005. *Clostridium difficile* toxoid vaccine in recurrent *C. difficile*-associated diarrhea. *Gastroenterology* **128:** 764–770.

162. Greenberg RN, Marbury TC, Foglia G, Warny M. 2012. Phase I dose finding studies of an adjuvanted *Clostridium difficile* toxoid vaccine. *Vaccine* **30:** 2245–2249.

163. Foglia G, Shah S, Luxemburger C, Pietrobon PJ. 2012. *Clostridium difficile*: development of a novel candidate vaccine. *Vaccine* **30:** 4307–4309.

164. de Bruyn G, Saleh J, Workman D, Pollak R, Elinoff V, Fraser NJ, Lefebvre G, Martens M, Mills RE, Nathan R, Trevino M, van Cleeff M, Foglia G, Ozol-Godfrey A, Patel DM, Pietrobon PJ, Gesser R; H-030-012 Clinical Investigator Study Team. 2016. Defining the optimal formulation and schedule of a candidate toxoid vaccine against *Clostridium difficile* infection: A randomized Phase 2 clinical trial. *Vaccine* **pii:** S0264-410X(16)00339-X.

165. ClinicalTrials.gov identifier: NCT00772343, accessed *via* https://clinicaltrials.gov (2016-03-27).

166. ClinicalTrials.gov identifier: NCT01887912, accessed *via* https://clinicaltrials.gov (2016-03-27).

167. Donald RG, Flint M, Kalyan N, Johnson E, Witko SE, Kotash C, Zhao P, Megati S, Yurgelonis I, Lee PK, Matsuka YV, Severina E, Deatly A, Sidhu M, Jansen KU, Minton NP, Anderson AS. 2013. A novel approach to generate a recombinant toxoid vaccine against *Clostridium difficile*. *Microbiology* **159(Pt 7):** 1254–1266.

168. Sheldon E, Kitchin N, Peng Y, Eiden J, Gruber W, Johnson E, Jansen KU, Pride MW, Pedneault L. 2016. A phase 1, placebo-controlled, randomized study of the safety, tolerability, and immunogenicity of a *Clostridium difficile* vaccine administered with or without aluminum hydroxide in healthy adults. *Vaccine* **pii:** S0264-410X(16)00300-5.

169. ClinicalTrials.gov identifier: NCT02117570, accessed *via* https://clinicaltrials.gov (2016-03-27).

170. ClinicalTrials.gov identifier: NCT02561195, accessed *via* https://clinicaltrials.gov (2016-03-27).

171. ClinicalTrials.gov identifier: NCT01296386, accessed *via* https://clinicaltrials.gov (2016-03-29).

172. ClinicalTrials.gov identifier: NCT02316470, accessed *via* https://clinicaltrials.gov (2016-03-29).

173. Tian JH, Fuhrmann SR, Kluepfel-Stahl S, Carman RJ, Ellingsworth L, Flyer DC. 2012. A novel fusion protein containing the receptor binding domains of *C. difficile* toxin A and toxin B elicits protective immunity against lethal toxin and spore challenge in preclinical efficacy models. *Vaccine* **30:** 4249–4258.

174. Valneva press release 2015-11-30, accessed *via* www.valneva.com/en/investors-media/news/2015 (2016-03-29).

175. Hajj Hussein I, Chams N, Chams S, El Sayegh S, Badran R, Raad M, Gerges-Geagea A, Leone A, Jurjus A. 2015. Vaccines through centuries: major cornerstones of global health. *Front Public Health* **3:** 269.

176. Lopetuso LR, Scaldaferri F, Petito V, Gasbarrini A. 2013. Commensal Clostridia: leading players in the maintenance of gut homeostasis. *Gut Pathog* **5:** 23.

177. Mattos-Guaraldi AL, Moreira LO, Damasco PV, Hirata Júnior R. 2003. Diphtheria remains a threat to health in the developing world–an overview. *Mem Inst Oswaldo Cruz* **98:** 987–993.

178. Adlerberth I, Huang H, Lindberg E, Åberg N, Hesselmar B, Saalman R, Nord CE, Wold AE, Weintraub A. 2014. Toxin-producing *Clostridium difficile* strains as long-term gut colonizers in healthy infants. *J Clin Microbiol* **52:** 173–179.

179. Mulligan ME, Miller SD, McFarland LV, Fung HC, Kwok RY. 1993. Elevated levels of serum immunoglobulins in asymptomatic carriers of *Clostridium difficile*. *Clin Infect Dis* **16(Suppl 4):** S239–S244.

180. Péchiné S, Janoir C, Boureau H, Gleizes A, Tsapis N, Hoys S, Fattal E, Collignon A. 2007. Diminished intestinal colonization by *Clostridium difficile* and immune response in mice after mucosal immunization with surface proteins of *Clostridium difficile*. *Vaccine* **25:** 3946–3954.

181. Sandolo C, Péchiné S, Le Monnier A, Hoys S, Janoir C, Coviello T, Alhaique F, Collignon A, Fattal E, Tsapis N. 2011. Encapsulation of Cwp84 into pectin beads for oral vaccination against *Clostridium difficile*. *Eur J Pharm Biopharm* **79:** 566–573.

182. Ghose C, Eugenis I, Edwards AN, Sun X, McBride SM, Ho DD. 2016. Immunogenicity and protective efficacy of *Clostridium difficile* spore proteins. *Anaerobe* **37:** 85–95.

183. Barnett TC, Lim JY, Soderholm AT, Rivera-Hernandez T, West NP, Walker MJ. 2015. Host-pathogen interaction during bacterial vaccination. *Curr Opin Immunol* **36:** 1–7.

184. Lanis JM, Heinlen LD, James JA, Ballard JD. 2013. *Clostridium difficile* 027/BI/NAP1 encodes a hypertoxic and antigenically variable form of TcdB. *PLoS Pathog* **9:** e1003523.

185. Fagan R, Fairweather N. 2010. Dissecting the cell surface. *Methods Mol Biol* **646:** 117–134.

186. Dingle KE, Didelot X, Ansari MA, Eyre DW, Vaughan A, Griffiths D, Ip CL, Batty EM, Golubchik T, Bowden R, Jolley KA, Hood DW, Fawley WN, Walker AS, Peto TE, Wilcox MH, Crook DW. 2013. Recombinational switching of the *Clostridium difficile* S-layer and a novel glycosylation gene cluster revealed by large-scale whole-genome sequencing. *J Infect Dis* **207:** 675–686.

187. Reeves PR, Hobbs M, Valvano MA, Skurnik M, Whitfield C, Coplin D, Kido N, Klena J, Maskell D, Raetz CR, Rick PD. 1996. Bacterial polysaccharide synthesis and gene nomenclature. *Trends Microbiol* **4:** 495–503.

188. Zhao S, Ghose-Paul C, Zhang K, Tzipori S, Sun X. 2014. Immune-based treatment and prevention of *Clostridium difficile* infection. *Hum Vaccin Immunother* **10:** 3522–3530.

189. Lyerly DM, Bostwick EF, Binion SB, Wilkins TD. 1991. Passive immunization of hamsters against disease caused by *Clostridium difficile* by use of bovine immunoglobulin G concentrate. *Infect Immun* **59:** 2215–2218.

190. Kink JA, Williams JA. 1998. Antibodies to recombinant *Clostridium difficile* toxins A and B are an effective treatment and prevent relapse of *C. difficile*-associated disease in a hamster model of infection. *Infect Immun* **66:** 2018–2025.

191. Lyerly DM, Phelps CJ, Toth J, Wilkins TD. 1986. Characterization of toxins A and B of *Clostridium difficile* with monoclonal antibodies. *Infect Immun* **54:** 70–76.

192. Corthier G, Muller MC, Wilkins TD, Lyerly D, L'Haridon R. 1991. Protection against pseudomembranous colitis in gnotobiotic mice by use of monoclonal antibodies against *Clostridium difficile* toxin A. *Infect Immun* **59:** 1192–1195.

193. Babcock GJ, Broering TJ, Hernandez HJ, Mandell RB, Donahue K, Boatright N, Stack AM, Lowy I, Graziano R, Molrine D, Ambrosino DM, Thomas WD Jr. 2006. Human monoclonal antibodies directed against toxins A and B prevent *Clostridium difficile*-induced mortality in hamsters. *Infect Immun* **74:** 6339–6347.

194. ClinicalTrials.gov identifier: NCT00350298, accessed *via* https://clinicaltrials.gov (2016-04-26).

195. ClinicalTrials.gov identifier: NCT01241552, accessed *via* https://clinicaltrials.gov (2016-04-26).

196. ClinicalTrials.gov identifier: NCT01513239, accessed *via* https://clinicaltrials.gov (2016-04-26).

197. Merck press release 2016-01-27, accessed *via* www.merck.com/newsroom/ (2016-04-27).

198. Shockman GD, Barrett JF. 1983. Structure, function, and assembly of cell walls of gram-positive bacteria. *Annu Rev Microbiol* **37:** 501–527.

199. Hogan CM. 2014. Bacteria. In: The Encyclopedia of Earth, Draggan S, Cleveland CJ (eds.), National Council for Science and the Environment, Washington DC.

200. Brown L, Wolf JM, Prados-Rosales R, Casadevall A. 2015. Through the wall: extracellular vesicles in Gram-positive bacteria, mycobacteria and fungi. *Nat Rev Microbiol* **13:** 620–630.

201. Brown S, Santa Maria JP Jr, Walker S. 2013. Wall teichoic acids of gram-positive bacteria. *Annu Rev Microbiol* **67:** 313–336.

202. Swoboda JG, Campbell J, Meredith TC, Walker S. 2010. Wall teichoic acid function, biosynthesis, and inhibition. *Chembiochem* **11:** 35–45.

203. Naumova IB, Shashkov AS, Tul'skaya EM, Streshinskaya GM, Kozlova YI, Potekhina NV, Evtushenko LI, Stackebrandt E. 2001. Cell wall teichoic acids: structural diversity, species specificity in the genus Nocardiopsis, and chemotaxonomic perspective. *FEMS Microbiol Rev* **25:** 269–284.

204. Percy MG, Gründling A. 2014. Lipoteichoic acid synthesis and function in gram-positive bacteria. *Annu Rev Microbiol* **68:** 81–100.

205. Ganeshapillai J, Vinogradov E, Rousseau J, Weese JS, Monteiro MA. 2008. *Clostridium difficile* cell-surface polysaccharides composed of pentaglycosyl and hexaglycosyl phosphate repeating units. *Carbohydr Res* **343:** 703–710.

206. Bertolo L, Boncheff AG, Ma Z, Chen YH, Wakeford T, Friendship RM, Rosseau J, Weese JS, Chu M, Mallozzi M, Vedantam G, Monteiro MA. 2012. *Clostridium difficile* carbohydrates: glucan in spores, PSII common antigen in cells, immunogenicity of PSII in swine and synthesis of a dual *C. difficile*-ETEC conjugate vaccine. *Carbohydr Res* **354:** 79–86.

207. Reid CW, Vinogradov E, Li J, Jarrell HC, Logan SM, Brisson JR. 2012. Structural characterization of surface glycans from *Clostridium difficile*. *Carbohydr Res* **354:** 65–73.

208. Stortz CA, Cherniak R, Jones RG, Treber TD, Reinhardt DJ. 1990. Polysaccharides from *Peptostreptococcus anaerobius* and structure of the species-specific antigen. *Carbohydr Res* **207:** 101–120.

209. Minnig K, Lazarevic V, Soldo B, Mauël G. 2005. Analysis of teichoic acid biosynthesis regulation reveals that the extracytoplasmic function sigma factor sigmaM is induced by phosphate depletion in *Bacillus subtilis* W23. *Microbiology* **151:** 3041–3049.

210. Hussain M, Heilmann C, Peters G, Herrmann M. 2001. Teichoic acid enhances adhesion of *Staphylococcus epidermis* to immobilized fibronectin. *Microb Pathog* **31:** 261–270.

211. Misawa Y, Kelley KA, Wang X, Wang L, Park WB, Birtel J, Saslowsky D, Lee JC. 2015. *Staphylococcus aureus* colonization of the mouse gastrointestinal tract is modulated by wall teichoic acid, capsule, and surface proteins. *PLoS Pathog* **11:** e1005061.

212. Weidenmaier C, Peschel A. 2008. Teichoic acids and related cell-wall glycopolymers in Gram-positive physiology and host interactions. *Nat Rev Microbiol* **6:** 276–287.

213. Abachin E, Poyart C, Pellegrini E, Milohanic C, Fiedler F, Berche P, Trieu-Cuot P. 2002. Formation of D-alanyl-lipoteichoic acid is required for adhesion and virulence of *Listeria monocytogenes*. *Mol Microbiol* **43:** 1–14.

214. Kristian SA, Datta V, Weidenmaier C, Kansal R, Fedtke I, Peschel A, Gallo RL, Nizet V. 2005. D-alanylation of teichoic acids promotes group A *Streptococcus* antimicrobial peptide resistance, neutrophil survival, and epithelial cell invasion. *J Bacteriol* **187:** 6719–6725.

215. Poxton IR, Byrne MD. 1981. Immunological analysis of the EDTA-soluble antigens of *Clostridium difficile* and related species. *J Gen Microbiol* **122:** 41–46.

216. Poxton IR, Cartmill TD. Immunochemistry of the cell-surface carbohydrate antigens of *Clostridium difficile*. *J Gen Microbiol* **128:** 1365–1370.

217. Jiao Y, Ma Z, Hodgins D, Pequegnat B, Bertolo L, Arroyo L, Monteiro MA. 2013. *Clostridium difficile* PSI polysaccharide: synthesis of pentasaccharide repeating block, conjugation to exotoxin B subunit, and detection of natural anti-PSI IgG antibodies in horse serum. *Carbohydr Res* **378:** 15–25.

218. Willing SE, Candela T, Shaw HA, Seager Z, Mesnage S, Fagan RP, Fairweather NF. 2015. *Clostridium difficile* surface proteins are anchored to the cell wall using CWB2 motifs that recognise the anionic polymer PSII. *Mol Microbiol* **96:** 596–608.

219. Merrigan MM, Venugopal A, Roxas JL, Anwar F, Mallozzi MJ, Roxas BA, Gerding DN, Viswanathan VK, Vedantam G. 2013. Surface-layer protein A (SlpA) is a major contributor to host-cell adherence of *Clostridium difficile*. *PLoS One* **8:** e78404.

220. Davies HA, Borriello SP. 1990. Detection of capsule in strains of *Clostridium difficile* of varying virulence and toxigenicity. *Microb Pathog* **9:** 141–146.

221. Rappuoli R, Black S, Lambert PH. 2011. Vaccine discovery and translation of new vaccine technology. *Lancet* **378:** 360–368.

222. Hawken S, Manuel DG, Deeks SL, Kwong JC, Crowcroft NS, Wilson K. 2012. Underestimating the safety benefits of a new vaccine: the impact of acellular pertussis vaccine versus whole-cell pertussis vaccine on health services utilization. *Am J Epidemiol* **176:** 1035–1042.

223. Astronomo RD, Burton DR. 2010. Carbohydrate vaccines: developing sweet solutions to sticky situations? *Nat Rev Drug Discov* **9:** 308–324.

224. Ada G, Isaacs D. 2003. Carbohydrate-protein conjugate vaccines. *Clin Microbiol Infect* **9:** 79–85.

225. Pollard AJ, Perrett KP, Beverly PC. 2009. Maintaining protection against invasive bacteria with protein-polysaccharide conjugate vaccines. *Nat Rev Immunol* **9:** 213–220.

226. Avery OT, Goebel WF. 1931. Chemo-immunological studies on conjugated carbohydrate-proteins: V. The immunological specificity of an antigen prepared by combining the capsular polysaccharide of type III pneumococcus with foreign protein. *J Exp Med* **54:** 437–447.

227. Ghimire TR. 2015. The mechanisms of action of vaccines containing aluminum adjuvants: an *in vitro* vs *in vivo* paradigm. *Springerplus* **4:** 161.

228. Jones LS, Peek LJ, Power J, Markham A, Yazzie B, Middaugh CR. 2005. Effects of adsorption to aluminum salt adjuvants on the structure and stability of model protein antigens. *J Biol Chem* **280:** 13406–13414.

229. Anish C, Schumann B, Pereira CL, Seeberger PH. 2014. Chemical biology approaches to designing defined carbohydrate vaccines. *Chem Biol* **21:** 38–50.

230. Kuronen T, Peltola H, Nors T, Hague N, Mäkelä PH. 1977. Adverse reactions and endotoxin content of polysaccharide vaccines. *Dev Biol Stand* **34:** 117–125.

231. World Health Organization. 2009. Recommendations to assure the quality, safety and efficacy of pneumococcal conjugate vaccines. Geneva: World Health Organization.

232. Monteiro MA, Ma Z, Bertolo L, Jiao Y, Arroyo L, Hodgins D, Mallozzi M, Vedantam G, Sagermann M, Sundsmo J, Chow H. 2013. Carbohydrate-based *Clostridium difficile* vaccines. *Expert Rev Vaccines* **12:** 421–431.

233. Seeberger PH, Werz DB. 2007. Synthesis and medical applications of oligosaccharides. *Nature* **446:** 1046–1051.

234. Verez-Bencomo V, Fernández-Santana V, Hardy E, Toledo ME, Rodríguez MC, Heynngnezz L, Rodriguez A, Baly A, Herrera L, Izquierdo M, Villar A, Valdés Y, Cosme K, Deler ML, Montane M, Garcia E, Ramos A, Aguilar A, Medina E, Toraño G, Sosa I, Hernandez I, Martínez R, Muzachio A, Carmenates A, Costa L, Cardoso F, Campa C, Diaz M, Roy R. 2004. A synthetic conjugate polysaccharide vaccine against *Haemophilus influenzae* type B. *Science* **305:** 522–525.

235. Adamo R, Romano MR, Berti F, Leuzzi R, Tontini M, Danieli E, Cappelletti E, Cakici OS, Swennen E, Pinto V, Brogioni B, Proietti D, Galeotti CL, Lay L, Monteiro MA, Scarselli M, Costantino P. 2012. Phosphorylation of the synthetic hexasaccharide repeating unit is essential for the induction of antibodies to *Clostridium difficile* PSII cell wall polysaccharide. *ACS Chem Biol* **7:** 1420–1428.

236. Oberli MA, Hecht ML, Bindschädler P, Adibekian A, Adam T, Seeberger PH. 2011. A possible oligosaccharide-conjugate vaccine candidate for *Clostridium difficile* is antigenic and immunogenic. *Chem Biol* **18:** 580–588.

237. Martin CE, Weishaupt MW, Seeberger PH. 2011. Progress toward developing a carbohydrate-conjugate vaccine against *Clostridium difficile* ribotype 027: synthesis of the cell-surface polysaccharide PS-I repeating unit. *Chem Commun* **47:** 10260–10262.

238. Cox AD, St Michael F, Aubry A, Cairns CM, Strong PC, Hayes AC, Logan SM. 2013. Investigating the candidacy of a lipoteichoic acid-based glycoconjugate as a vaccine to combat *Clostridium difficile* infection. *Glycoconj J* **30:** 843–855.

239. Broecker F, Aretz J, Yang Y, Hanske J, Guo X, Reinhardt A, Wahlbrink A, Anish C, Seeberger PH. 2014. Epitope recognition of antibodies against a *Yersinia pestis* lipopolysaccharide trisaccharide component. *ACS Chem Biol* **9:** 867–873.

240. Oberli MA, Tamborrini M, Tsai YH, Werz DB, Horlacher T, Adibekian A, Gauss D, Möller HM, Pluschke G, Seeberger PH. 2010. Molecular analysis of carbohydrate-antibody interactions: case study using a *Bacillus anthracis* tetrasaccharide. *J Am Chem Soc* **132:** 10239–10241.

241. Robbins JB, Kubler-Kielb J, Vinogradov E, Mocca C, Pozsgay V, Shiloach J, Schneerson R. 2009. Synthesis, characterization, and immunogenicity in mice of *Shigella sonnei* O-specific oligosaccharide-core-protein conjugates. *Proc Natl Acad Sci U S A* **106:** 7974–7978.

242. Safari D, Rijkers G, Snippe H. 2012. The future of synthetic carbohydrate vaccines: immunological studies on *Streptococcus pneumoniae* type 14. In: The Complex World of Polysaccharides, Karunaratne DN (ed.), InTech.

243. Benaissa-Trouw B, Lefeber DJ, Kamerling JP, Vliegenthart JF, Kraaijeveld K, Snippe H. 2001. Synthetic polysaccharide type 3-related di-, tri-, and tetrasaccharide-CRM(197) conjugates induce protection against *Streptococcus pneumoniae* type 3 in mice. *Infect Immun* **69:** 4698–4701.

244. Bundle DR, Nycholat C, Costello C, Rennie R, Lipinski T. 2012. Design of a *Candida albicans* disaccharide conjugate vaccine by reverse engineering a protective monoclonal antibody. *ACS Chem Biol* **7:** 1754–1763.

245. Svenson SB, Lindberg AA. 1981. Artificial *Salmonella* vaccines: *Salmonella typhimurium* O-antigen-specific oligosaccharide-protein conjugates elicit protective antibodies in rabbits and mice. *Infect Immun* **32:** 490–496.

246. Anderson PW, Pichichero ME, Insel RA, Betts R, Eby R, Smith DH. 1986. Vaccines consisting of periodate-cleaved oligosaccharides from the capsule of *Haemophilus influenzae* type b coupled to a protein carrier: structural and temporal requirements for priming in the human infant. *J Immunol* **137:** 1181–1186.

247. Pozsgay V, Chu C, Pannell L, Wolfe J, Robbins JB, Schneerson R. 1999. Protein conjugates of synthetic saccharides elicit higher levels of serum IgG lipopolysaccharide antibodies in mice than do those of the O-specific polysaccharide from *Shigella dysenteriae* type 1. *Proc Natl Acad Sci U S A* **96:** 5194–5197.

248. Phalipon A, Costachel C, Grandjean C, Thuizat A, Guerreiro C, Tanguy M, Nato F, Vulliez-Le Normand B, Bélot F, Wright K, Marcel-Peyre V, Sansonetti PJ, Mulard LA. 2006. Characterization of functional oligosaccharide mimics of the *Shigella flexneri* serotype 2a O-antigen: implications for the development of a chemically defined glycoconjugate vaccine. *J Immunol* **176:** 1686–1694.

249. Fernandez C, Sverremark E. 1994. Immune responses to bacterial polysaccharides: terminal epitopes are more immunogenic than internal structures. *Cell Immunol* **153:** 67–78.

250. Tamborrini M, Oberli MA, Werz DB, Schürch N, Frey J, Seeberger PH, Pluschke G. 2009. Immunodetection of anthrose containing tetrasaccharide in the exosporium of *Bacillus anthracis* and *Bacillus cereus* strains. *J Appl Microbiol* **106:** 1618–1628.

251. Anish C, Guo X, Wahlbrink A, Seeberger PH. 2013. Plague detection by anti-carbohydrate antibodies. *Angew Chem Int Ed Engl* **52:** 9524–9528.

252. Broecker F, Anish C, Seeberger PH. 2015. Generation of monoclonal antibodies against defined oligosaccharide antigens. *Methods Mol Biol* **1331:** 57–80.

253. Geissner A, Anish C, Seeberger PH. 2014. Glycan arrays as tools for infectious disease research. *Curr Opin Chem Biol* **18:** 38–45.

254. Muller-Loennies S, Brade L, MacKenzie CR, Di Padova FE, Brade H. 2003. Identification of a cross-reactive epitope widely present in lipopolysaccharide from enterobacteria and recognized by the cross-protective monoclonal antibody WN1 222-5. *J Biol Chem* **278:** 25618–25627.

255. Harris SL, Fernsten P. 2009. Thermodynamics and density of binding of a panel of antibodies to high-molecular-weight capsular polysaccharides. *Clin Vaccine Immunol* **16:** 37–42.

256. Peters T. 2012. A matter of order: how E-selectin makes sweet contacts. *Chembiochem* **13:** 2325–2326.

257. Bundle DR, Young NM. 1992. Carbohydrate-protein interactions in antibodies and lectins. *Curr Opin Struct Biol* **2:** 666–673.

258. Brummell DA, Sharma VP, Anand NN, Bilous D, Dubuc G, Michniewicz J, MacKenzie CR, Sadowska J, Sigurskjold BW, Sinnott B, Young NM, Bundle DR, Narang SA. 1993. Probing the combining site of an anti-carbohydrate antibody by saturation-mutagenesis: role of the heavy-chain CDR3 residues. *Biochemistry* **32:** 1180–1187.

259. Toone EJ. 1994. Structure and energetics of protein-carbohydrate complexes. *Curr Opin Struct Biol* **4:** 719–728.

260. Garcia-Hernandez E, Zubillaga RA, Rojo-Dominguez A, Rodriguez-Romero A, Hernandez-Arana A. 1997. New insights into the molecular basis of lectin-carbohydrate interactions: a calorimetric and structural study of the association of hevein to oligomers of *N*-acetylglucosamine. *Proteins* **29:** 467–477.

261. Garcia-Hernandez E, Hernandez-Arana A. 1999. Structural bases of lectin-carbohydrate affinities: comparison with protein-folding energetics. *Protein Sci* **8:** 1075–1086.

262. Dam TK, Brewer CF. 2002. Thermodynamic studies of lectin-carbohydrate interactions by isothermal titration calorimetry. *Chem Rev* **102:** 387–429.

263. Ladbury JE. 1996. Just add water! The effect of water on the specificity of protein-ligand binding sites and its potential application to drug design. *Chem Biol* **3:** 973–980.

264. Pazur JH, Erikson MS, Tay ME, Allen PZ. 1983. Isomeric, anti-rhamnose antibodies having specificity for rhamnose-containing, streptococcal heteroglycans. *Carbohydr Res* **124:** 253–263.

265. Clément MJ, Fortuné A, Phalipon A, Marcel-Peyre V, Simenel C, Imberty A, Delepierre M, Mulard LA. 2006. Toward a better understanding of the basis of the molecular mimicry of polysaccharide antigens by peptides: the example of *Shigella flexneri* 5a. *J Biol Chem* **281:** 2317–2332.

266. Vyas NK, Vyas MN, Chervenak MC, Johnson MA, Pinto BM, Bundle DR, Quiocho FA. 2002. Molecular recognition of oligosaccharide epitopes by a monoclonal Fab specific for *Shigella flexneri* Y lipopolysaccharide: X-ray structures and thermodynamics. *Biochemistry* **41:** 13575–13586.

267. Sabbatini PJ, Kudryashov V, Ragupathi G, Danishefsky SJ, Livingston PO, Bornmann W, Spassova M, Zatorski A, Spriggs D, Aghajanian C, Soignet S, Peyton M, O'Flaherty C, Curtin J, Lloyd KO. 2000. Immunization of ovarian cancer patients with a synthetic Lewis(y)-protein conjugate vaccine: a phase 1 trial. *Int J Cancer* **87:** 79–85.

268. Kagan E, Ragupathi G, Yi SS, Reis CA, Gildersleeve J, Kahne D, Clausen H, Danishefsky SJ, Livingston PO. 2005. Comparison of antigen constructs and carrier molecules for augmenting the immunogenicity of the monosaccharide epithelial cancer antigen Tn. *Cancer Immunol Immunother* **54:** 424–430.

269. Feng D, Shaikh AS, Wang F. 2016. Recent advance in tumor-associated carbohydrate antigens (TACAs)-based antitumor vaccines. *ACS Chem Biol* **11:** 850–863.

270. Lo-Man R, Bay S, Vichier-Guerre S, Dériaud E, Cantacuzène D, Leclerc C. 1999. A fully synthetic immunogen carrying a carcinoma-associated carbohydrate for active specific immunotherapy. *Cancer Res* **59:** 1520–1524.

271. Grigalevicius S, Chierici S, Renaudet O, Lo-Man R, Dériaud E, Leclerc C, Dumy P. 2005. Chemoselective assembly and immunological evaluation of multiepitopic glycoconjugates bearing clustered Tn antigen as synthetic anticancer vaccines. *Bioconjug Chem* **16:** 1149–1159.

272. Ponader D, Wojcik F, Beceren-Braun F, Dernedde J, Hartmann L. 2012. Sequence-defined glycopolymer segments presenting mannose: synthesis and lectin binding affinity. *Biomacromolecules* **13:** 1845–1852.

273. Ponader D, Maffre P, Aretz J, Pussak D, Ninnemann NM, Schmidt S, Seeberger PH, Rademacher C, Nienhaus GU, Hartmann L. 2014. Carbohydrate-lectin recognition of sequence-defined heteromultivalent glycooligomers. *J Am Chem Soc* **136:** 2008-2016.

274. Wojcik F, O'Brien AG, Götze S, Seeberger PH, Hartmann L. 2013. Synthesis of carbohydrate-functionalised sequence-defined oligo(amidoamine)s by photochemical thiol-ene coupling in a continuous flow reactor. *Chemistry* **19:** 3090–3098.

275. Wojcik F, Lel S, O'Brien AG, Seeberger PH, Hartmann L. 2013. Synthesis of homo- and heteromultivalent carbohydrate-functionalized oligo(amidoamines) using novel glyco-building blocks. *Beilstein J Org Chem* **9:** 2395–2403.

276. Wojcik F. 2014. Sequence-defined oligo(amidoamines): synthesis, carbohydrate functionalization and biomedical applications. PhD thesis, Freie Universität Berlin.

277. Ingale S, Wolfert MA, Gaekwad J, Buskas T, Boons GJ. 2007. Robust immune responses elicited by a fully synthetic three-component vaccine. *Nat Chem Biol* **3:** 663–667.

278. Bai L, Deng S, Reboulet R, Mathew R, Teyton L, Savage PB, Bendelac A. 2013. Natural killer T (NKT)-B-cell interactions promote prolonged antibody responses and long-term memory to pneumococcal capsular polysaccharides. *Proc Natl Acad Sci U S A* **110:** 16097–16102.

279. Cavallari M, Stallforth P, Kalinichenko A, Rathwell DC, Gronewold TM, Adibekian A, Mori L, Landmann R, Seeberger PH, De Libero G. 2014. A semisynthetic carbohydrate-lipid vaccine that protects against *S. pneumoniae* in mice. *Nat Chem Biol* **10:** 950–956.

280. Milstein J, Zaffran M, Kartoglu Ü, Galazka A. 2006. Temperature sensitivity of vaccines. World Health Organization, Geneva.

281. Clapp T, Siebert P, Chen D, Jones Braun L. 2011. Vaccines with aluminum-containing adjuvants: optimizing vaccine efficacy and thermal stability. *J Pharm Sci* **100:** 388–401.

282. Oleksiewicz MB, Nagy G, Nagy E. 2012. Anti-bacterial monoclonal antibodies: back to the future? *Arch Biochem Biophys* **526:** 124–131.

283. Szijártó V, Guachalla LM, Visram ZC, Hartl K, Varga C, Mirkina I, Zmajkovic J, Badarau A, Zauner G, Pleban C, Magyarics Z, Nagy E, Nagy G. 2015. Bactericidal monoclonal antibodies specific to the lipopolysaccharide O antigen from multidrug-resistant *Escherichia coli* clone ST131-O25b:H4 elicit protection in mice. *Antimicrob Agents Chemother* **59:** 3109–3116.

284. Martin CE, Broecker F, Oberli MA, Komor J, Mattner J, Anish C, Seeberger PH. 2013. Immunological evaluation of a synthetic *Clostridium difficile* oligosaccharide conjugate vaccine candidate and identification of a minimal epitope. *J Am Chem Soc* **135:** 9713–9722.

285. Martin CE, Broecker F, Eller S, Oberli MA, Anish C, Pereira CL, Seeberger PH. 2013. Glycan arrays containing synthetic *Clostridium difficile* lipoteichoic acid oligomers as tools toward a carbohydrate vaccine. *Chem Commun* **49:** 7159–7161.

286. Broecker F, Hanske J, Martin CE, Baek JY, Wahlbrink A, Wojcik F, Hartmann L, Rademacher C, Anish C, Seeberger PH. 2016. Multivalent display of minimal *Clostridium difficile* glycan epitopes mimics antigenic properties of larger glycans. *Nat Commun* **7:** 11224.

287. Hewitt MC, Seeberger PH. 2001. Solution and solid-support synthesis of a potential leishmaniasis carbohydrate vaccine. *J Org Chem* **66:** 4233–4243.

288. Hewitt MC, Seeberger PH. 2001. Automated solid-phase synthesis of a branched *Leishmania* cap tetrasaccharide. *Org Lett* **3:** 3699–3702.

289. Anish C, Martin CE, Wahlbrink A, Bogdan C, Ntais P, Antoniou M, Seeberger PH. 2013. Immunogenicity and diagnostic potential of synthetic antigenic cell surface glycans of *Leishmania*. *ACS Chem Biol* **8:** 2412–2422.

290. Yang Y, Oishi S, Martin CE, Seeberger PH. 2013. Diversity-oriented synthesis of inner core oligosaccharides of the lipopolysaccharide of pathogenic Gram-negative bacteria. *J Am Chem Soc* **135:** 6262–6271.

291. Bardotti A, Averani G, Berti F, Berti S, Carinci V, D'Ascenzi S, Fabbri B, Giannini S, Giannozzi A, Magagnoli C, Proiett D, Norelli F, Rappuoli R, Ricci S, Costantino P. 2008. Physicochemical characterisation of glycoconjugate vaccines for prevention of meningococcal diseases. *Vaccine* **26:** 2284–2296.

292. Wenzel T, Sparbier K, Mieruch T, Kostrzewa M. 2006. 2,5-Dihydroxyacetophenone: a matrix for highly sensitive matrix-assisted laser desorption/ionization time-of-flight mass spectrometric analysis of proteins using manual and automated preparation techniques. *Rapid Commun Mass Spectrom* **20:** 785–789.

293. Turula VE Jr, Gore T, Singh S, Arumugham RG. 2010. Automation of the anthrone assay for carbohydrate concentration determinations. *Anal Chem* **82:** 1786–1792.

294. Wu X, Ling CC, Bundle DR. 2004. A new homobifunctional *p*-nitro phenyl ester coupling reagent for the preparation of neoglycoproteins. *Org Lett* **6:** 4407–4410.

295. Skrastina D, Petrovskis I, Lieknina I, Bogans J, Renhofa R, Ose V, Dishlers A, Dekhtyar Y, Pumpens P. 2014. Silica nanoparticles as the adjuvant for the immunisation of mice using hepatitis B core virus-like particles. *PLoS One* **9:** e114006.

296. Ugozzoli M, Laera D, Nuti S, Skibinski DA, Bufali S, Sammicheli C, Tavarini S, Singh M, O'Hagan DT. 2011. Flow cytometry: an alternative method for direct quantification of antigens adsorbed to aluminum hydroxide adjuvant. *Anal Biochem* **418:** 224–230.

297. Zhu D, Huang S, McClellan H, Dai W, Syed NR, Gebregeorgis E, Rausch KM, Mullen GE, Long C, Martin LB, Narum D, Duffy P, Miller LH, Saul A. 2012. Efficient extraction of vaccines formulated in aluminum hydroxide gel by including surfactants in the extraction buffer. *Vaccine* **30:** 189–194.

298. Miles AP, Saul A. 2005. Extraction and characterization of vaccine antigens from water-in-oil adjuvant formulations. *Methods Mol Biol* **308:** 293–300.

299. Koehler G, Milstein C. 1975. Continuous cultures of fused cells secreting antibody of predefined specificity. *Nature* **256:** 495–497.

300. Altschuh D, Björkelund H, Strandgård J, Choulier L, Malmqvist M, Andersson K. 2012. Deciphering complex protein interaction kinetics using Interaction Map. *Biochem Biophys Res Commun* **428:** 74–79.

301. Rodríguez ME, Van der Pol WL, van de Winkel JG. 2001. Flow cytometry-based phagocytosis assay for sensitive detection of opsonic activity of pneumococcal capsular polysaccharide antibodies in human sera. *J Immunol Methods* **252:** 33–44.

302. Romero-Steiner S, Libutti D, Pais LB, Dykes J, Anderson P, Whitin JC, Keyserling HL, Carlone GM. 1997. Standardization of an opsonophagocytic assay for the measurement of functional antibody activity against *Streptococcus pneumoniae* using differentiated HL-60 cells. *Clin Diagn Lab Immunol* **4:** 415–422.

303. Cerquetti M, Serafino A, Sebastianelli A, Mastrantonio P. 2002. Binding of *Clostridium difficile* to Caco-2 epithelial cell line and to extracellular matrix proteins. *FEMS Immunol Med Microbiol* **32:** 211–218.

304. Kovacs-Simon A, Leuzzi R, Kasendra M, Minton N, Titball RW, Michell SL. 2014. Lipoprotein CD0873 is a novel adhesin of *Clostridium difficile*. *J Infect Dis* **210:** 274–284.

305. Naaber P, Lehto E, Salminen S, Mikelsaar M. 1996. Inhibition of adhesion of *Clostridium difficile* to Caco-2 cells. *FEMS Immunol Med Microbiol* **14:** 205–209.

306. Buffie CG, Jarchum I, Equinda M, Lipuma L, Gobourne A, Viale A, Ubeda C, Xavier J, Pamer EG. 2012. Profound alterations of intestinal microbiota following a single dose of clindamycin results in sustained susceptibility to *Clostridium difficile*-induced colitis. *Infect Immun* **80:** 62–73.

307. Lawley TD, Clare S, Walker AW, Goulding D, Stabler RA, Croucher N, Mastroeni P, Scott P, Raisen C, Mottram L, Fairweather NF, Wren BW, Parkhill J, Dougan G. 2009. Antibiotic treatment of *Clostridium difficile* carrier mice triggers a supershedder state, spore-mediated transmission, and severe disease in immunocompromised hosts. *Infect Immun* **77:** 3661–3669.

308. Oyelaran O, McShane LM, Dodd L, Gildersleeve JC. 2009. Profiling human serum antibodies with a carbohydrate antigen microarray. *J Proteome Res* **8:** 4301–4310.

309. Huflejt ME, Vuskovic M, Vasiliu D, Xu H, Obukhova P, Shilova N, Tuzikov A, Galanina O, Arun B, Lu K, Bovin N. 2009. Anti-carbohydrate antibodies of normal sera: findings, surprises and challenges. *Mol Immunol* **46:** 3037–3049.

310. Mantis NJ, Rol N, Corthésy B. 2011. Secretory IgA's complex roles in immunity and mucosal homeostasis in the gut. *Mucosal Immunol* **4:** 603–611.

311. Warny M, Vaerman JP, Avesani V, Delmée M. 1994. Human antibody response to *Clostridium difficile* toxin A in relation to clinical course of infection. *Infect Immun* **62:** 384–389.

312. Adibekian A, Stallforth P, Hecht ML, Werz DB, Gagneux P, Seeberger PH. 2011. Comparative bioinformatics analysis of the mammalian and bacterial glycomes. *Chem Sci* **2:** 337–344.

313. Chen W, Gu L, Zhang W, Motari E, Cai L, Styslinger TJ, Wang PG. 2011. L-rhamnose antigen: a promising alternative to α-gal for cancer immunotherapies. *ACS Chem Biol* **6:** 185–191.

314. Giannini G, Rappuoli R, Ratti G. 1984. The amino-acid sequence of two non-toxic mutants of diphtheria toxin: CRM45 and CRM197. *Nucleic Acids Res* **12:** 4063–4069.

315. Mekada E, Uchida T. 1985. Binding properties of diphtheria toxin to cells are altered by mutation in the fragment A domain. *J Biol Chem* **260:** 12148–12153.

316. Möginger U, Resemann A, Martin C, Parameswarappa S, Govindan S, Wamhoff E, Broecker F, Suckau D, Pereira CL, Anish C, Seeberger PH, Kolarich D. 2016. Cross Reactive Material 197 glycoconjugate vaccines contain privileged conjugation sites. *Sci Rep* **6:** 20488.

317. Buskas T, Li Y, Boons GJ. 2004. The immunogenicity of the tumor-associated antigen Lewis(y) may be suppressed by a bifunctional cross-linker required for coupling to a carrier protein. *Chemistry* **10:** 3517–3524.

318. Scaria J, Suzuki H, Ptak CP, Chen JW, Zhu Y, Guo XK, Chang YF. 2015. Comparative genomic and phenomic analysis of *Clostridium difficile* and *Clostridium sordellii*, two related pathogens with differing host tissue preference. *BMC Genomics* **16:** 448.

319. Kozlowski PA, Cu-Uvin S, Neutra MR, Flanigan TP. 1997. Comparison of the oral, rectal, and vaginal immunization routes for induction of antibodies in rectal and genital tract secretions of women. *Infect Immun* **65:** 1387–1394.

320. Reinhardt A, Yang Y, Claus H, Pereira CL, Cox AD, Vogel U, Anish C, Seeberger PH. 2015. Antigenic potential of a highly conserved *Neisseria meningitidis* lipopolysaccharide inner core structure defined by chemical synthesis. *Chem Biol* **22:** 38–49.

321. Müller-Loennies S, MacKenzie CR, Patenaude SI, Evans SV, Kosma P, Brade H, Brade L, Narang S. 2000. Characterization of high affinity monoclonal antibodies specific for chlamydial lipopolysaccharide. *Glycobiology* **10:** 121–130.

322. Müller-Loennies S, Gronow S, Brade L, MacKenzie R, Kosma P, Brade H. 2006. A monoclonal antibody against a carbohydrate epitope in lipopolysaccharide differentiates *Chlamydophila psitacci* from *Chlamydophila pecorum*, *Chlamydophila pneumoniae*, and *Chlamydophila trachomatis*. *Glycobiology* **16:** 184–196.

323. Brooks CL, Müller-Loennies S, Brade L, Kosma P, Hirama T, MacKenzie CR, Brade H, Evans SV. 2008. Exploration of specificity in germline monoclonal antibody recognition of a range of natural and synthetic epitopes. *J Mol Biol* **377:** 450–468.

324. Geissner A, Pereira CL, Leddermann M, Anish C, Seeberger PH. 2016. Deciphering antigenic determinants of *Streptococcus pneumoniae* serotype 4 capsular polysaccharide using synthetic oligosaccharides. *ACS Chem Biol* **11:** 335–344.

325. Kumagai I, Tsumoto K. 2001. Antigen-antibody binding. *Encyclopedia of Life Sciences*, pp. 1–7, London: Nature.

326. Turnbull WB, Daranas AH. 2003. On the value of c: can low affinity systems be studied by isothermal titration calorimetry? *J Am Chem Soc* **125:** 14859–14866.

327. Pillai S, Dermody K, Metcalf B. 1995. Immunogenicity of genetically engineered glutathione S-transferase fusion proteins containing a T-cell epitope from diphtheria toxin. *Infect Immun* **63:** 1535–1540.

328. Batista FD, Neuberger MS. 1998. Affinity dependence of the B cell response to antigen: A threshold, a ceiling, and the importance of off-rate. *Immunity* **8:** 751–759.

329. Jackson H, Bacon L, Pedley RB, Derbyshire E, Field A, Osbourn J, Allen D. 1998. Antigen specificity and tumour targeting efficiency of a human carcinoembryonic antigen-specific scFv and affinity-matured derivatives. *Br J Cancer* **78:** 181–188.

330. Khurana S, Verma N, Yewdell JW, Hilbert AK, Castellino F, Lattanzi M, Del Giudice G, Rappuoli R, Golding H. 2011. MF59 adjuvant enhances diversity and affinity of antibody-mediated immune response to pandemic influenza vaccines. *Sci Transl Med* **3:** 85ra48.

331. Maynard JA, Maassen CB, Leppla SH, Brasky K, Patterson JL, Iverson BL, Georgiou G. 2002. Protection against anthrax toxin by recombinant antibody fragments correlates with antigen affinity. *Nat Biotechnol* **20:** 597–601.

332. Yang WP, Green K, Pinz-Sweeney S, Briones AT, Burton DR, Barbas CF 3rd. 1995. CDR walking mutagenesis for the affinity maturation of a potent human anti-HIV-1 antibody into the picomolar range. *J Mol Biol* **254:** 392–403.

333. Zahnd C, Spinelli S, Luginbühl B, Amstutz P, Cambillau C, Plückthun A. 2004. Directed *in vitro* evolution and crystallographic analysis of a peptide-binding single chain antibody fragment (scFv) with low picomolar affinity. *J Biol Chem* **279:** 18870-18877.

334. Zahnd C, Sarkar CA, Plückthun A. 2010. Computational analysis of off-rate selection experiments to optimize affinity maturation by directed evolution. *Protein Eng Des Sel* **23:** 175–184.

335. Beyers R, Baldwin M, Dalabih S, Dalabih A. 2014. *Clostridium sordellii* as a cause of fatal septic shock in a child with hemolytic uremic syndrome. *Case Rep Pediatr* **2014:** 237674.

336. Edagiz S, Lagace-Wiens P, Embil J, Karlowsky J, Walkty A. 2015. Empyema caused by *Clostridium bifermentans*: A case report. *Can J Infect Dis Med Microbiol* **26:** 105–107.

337. Wu PH, Lin YT, Lin CY, Lin WR, Chen TC, Lu PL, Chen YH. 2011. *Peptostreptococcus anaerobius* infective endocarditis complicated by spleen infarction. *Am J Med Sci* **342:** 174–176.

338. Gardner EM, Kestler M, Beieler A, Belknap RW. 2008. *Clostridium butyricum* sepsis in an injection drug user with an indwelling central venous catheter. *J Med Microbiol* **57:** 236–239.

339. Haussen DC, Macedo FY, Caperton CV, Zuckerman DC. 2011. *Clostridium subterminale* sepsis in adult acute lymphoblastic leukemia. *Leuk Lymphoma* **52:** 1137–1138.

340. Nizet V, Klein JO. 2011. In: Infectious diseases of the fetus and newborn infant, 7th edition, Wilson CB, Maldonado YA, Nizet V (eds.), pp. 222–275.

341. Schwandner R, Dziarski R, Wesche H, Rothe M, Kirschning CJ. 1999. Peptidoglycan- and lipoteichoic acid-induced cell activation is mediated by toll-like receptor 2. *J Biol Chem* **274:** 17406–17409.

342. Hogendorf WF, Gisch N, Schwudke D, Heine H, Bols M, Pedersen CM. 2014. Total synthesis of five lipoteichoic acids of *Clostridium difficile*. *Chemistry* **20:** 13511–13516.

343. Rescigno M. 2010. Intestinal dendritic cells. *Adv Immunol* **107:** 109–138.

344. Haller Hasskamp J, Zapas JL, Elias EG. 2005. Dendritic cell counts in the peripheral blood of healthy adults. *Am J Hematol* **78:** 314–415.

345. Broecker F, Martin CE, Wegner E, Mattner J, Baek JY, Pereira CL, Anish C, Seeberger PH. 2016. Synthetic lipoteichoic acid glycans are potential vaccine candidates to protect from *Clostridium difficile* infections. *Cell Chem Biol* **23:** 1014–1022.

346. Maraskovsky E, Brasel K, Teepe M, Roux ER, Lyman SD, Shortman K, McKenna HJ. 1996. Dramatic increase in the numbers of functionally mature dendritic cells in Flt3 ligand-treated mice: multiple dendritic cell subpopulations identified. *J Exp Med* **184:** 1953–1962.

347. Morath S, Stadlmaier A, Geyer A, Schmidt RR, Hartung T. 2002. Synthetic lipoteichoic acid from *Staphylococcus aureus* is a potent stimulus of cytokine release. *J Exp Med* **195:** 1635–1640.

348. Pedersen CM, Figueroa-Perez I, Lindner B, Ulmer AJ, Zähringer U, Schmidt RR. 2010. Total synthesis of lipoteichoic acid of *Streptococcus pneumoniae*. *Angew Chem Int Ed Engl* **49:** 2585–2590.

349. Zähringer U, Lindner B, Inamura S, Heine H, Alexander C. 2008. TLR2 - promiscous or specific? A critical re-evaluation of a receptor expressing apparent broad specificity. *Immunobiology* **213:** 205–224.

350. Caux C, Massacrier C, Vanbervliet B, Dubois B, Van Kooten C, Durand I, Banchereau J. 1994. Activation of human dendritic cells through CD40 cross-linking. *J Exp Med* **180:** 1263–1272.

351. Lindblad EB. 2004. Aluminium compounds for use in vaccines. *Immunol Cell Biol* **82:** 497–505.

352. Dong C, Flavell RA. 2001. Th1 and Th2 cells. *Curr Opin Hematol* **8:** 47–51.

353. Brewer JM, Alexander J. 1997. Cytokines and the mechanism of action of vaccine adjuvants. *Cytokines Cell Mol Ther* **3:** 233–246.

354. Peek LJ, Martin TT, Elk Nation C, Pegram SA, Middaugh CR. 2007. Effects of stabilizers on the destabilization of proteins upon adsorption to aluminum salt adjuvants. *J Pharm Sci* **96:** 547–557.

355. Sturgess AW, Rush K, Charbonneau RJ, Lee JI, West DJ, Sitrin RD, Hennessy JP Jr. 1999. *Haemophilus influenzae* type b conjugate vaccine stability: catalytic depolymerization of PRP in the presence of aluminum hydroxide. *Vaccine* **17:** 1169–1178.

356. Petrofsky N, Aguilar JC. 2004. Vaccine adjuvants: current state and future trends. *Immunol Cell Biol* **82:** 488–496.

357. Berzofsky JA, Schechter AN, Kon H. 1976. Does Freund's adjuvant denature protein antigens? EPR studies of emulsified hemoglobin. *J Immunol* **116:** 270–272.

358. Richards RL, Rao M, Vancott TC, Matyas GR, Birx DL, Alving CR. 2004. Liposome-stabilized oil-in-water emulsions as adjuvants: increased emulsion stability promotes induction of cytotoxic T lymphocytes against an HIV envelope antigen. *Immunol Cell Biol* **82:** 531–538.

359. Dailey DC, Kaiser A, Schloemer RH. 1987. Factors influencing the phagocytosis of *Clostridium difficile* by human polymorphonuclear leukocytes. *Infect Immun* **55:** 1541–1546.

360. Tana, Watarai S, Isogai E, Oguma K. 2003. Induction of intestinal IgA and IgG antibodies preventing adhesion of verotoxin-producing Escherichia coli to Caco-2 cells by oral immunization with liposomes. *Lett Appl Microbiol* **36:** 135–139.

361. Fogh J, Trempe G. 1975. New human tumor cell lines. In: Human tumor cells *in vitro*, Fogh J (ed.), pp. 115–159.

362. Garneau JR, Valiquette L, Fortier LC. 2014. Prevention of *Clostridium difficile* spore formation by sub-inhibitory concentrations of tigecycline and piperacillin/tazobactam. *BMC Infect Dis* **14:** 29.

363. Larson HE, Borriello SP. 1990. Quantitative study of antibiotic-induced susceptibility to *Clostridium difficile* enterocecitis in hamsters. *Antimicrob Agents Chemother* **34:** 1348–1353.

364. Lawley TD, Clare S, Deakin LJ, Goulding D, Yen JL, Raisen C, Brandt C, Lovell J, Cooke F, Clark TG, Dougan G. 2010. Use of purified *Clostridium difficile* spores to facilitate evaluation of health care disinfection regimens. *Appl Environ Microbiol* **76:** 6895–6900.

365. Riedel T, Bunk B, Wittmann J, Thürmer A, Spröer C, Gronow S, Liesegang H, Daniel R, Overmann J. 2015. Complete genome sequence of the *Clostridium difficile* type strain DSM 1296T. *Genome Announc* **3:** pii: e01186-15.

366. Rijkers GT, Sanders LA, Zegers BJ. 1993. Anti-capsular polysaccharide antibody deficiency states. *Immunodeficiency* **5:** 1–21.

367. Sarkar S, Salyer AC, Wall KA, Sucheck SJ. 2013. Synthesis and immunological evaluation of a MUC1 glycopeptide incorporated into L-rhamnose displaying liposomes. *Bioconjug Chem* **24:** 363–375.

368. Kitchens RL. 2000. Role of CD14 in cellular recognition of bacterial lipopolysaccharides. *Chem Immunol* **74:** 61–82.

369. Ranoa DR, Kelley SL, Tapping RI. 2013. Human lipopolysaccharide-binding protein (LBP) and CD14 independently deliver triacylated lipoproteins to Toll-like receptor 1 (TLR1) and TLR2 and enhance formation of the ternary signaling complex. *J Biol Chem* **288:** 9729–9741.

370. Soell M, Lett E, Holveck F, Schöller M, Wachsmann D, Klein JP. 1995. Activation of human monocytes by streptococcal rhamnose glucose polymers is mediated by CD14 antigen, and mannan binding protein inhibits TNF-alpha release. *J Immunol* **154:** 851–860.

371. Zelensky AN, Gready JE. 2005. The C-type lectin-like domain superfamily. *FEBS J* **272:** 6179–6217.

372. Tzianabos A, Wang JY, Kasper DL. 2003. Biological chemistry of immunomodulation by zwitterionic polysaccharides. *Carbohydr Res* **338:** 2531–2538.

373. Cobb BA, Wang Q, Tzianabos AO, Kasper DL. 2004. Polysaccharide processing and presentation by the MHCII pathway. *Cell* **117:** 677–687.

374. Rubinstein ND, Mayrose I, Halperin D, Yekutieli D, Gershoni JM, Pupko T. 2008. Computational characterization of B-cell epitopes. *Mol Immunol* **45:** 3477–3489.

375. Petrovsky N, Aguilar JC. 2004. Vaccine adjuvants: current state and future trends. *Immunol Cell Biol* **82:** 488–496.

376. Avci FY, Li X, Tsuji M, Kasper DL. 2011. A mechanism for glycoconjugate vaccine activation of the adaptive immune system and its implications for vaccine design. *Nat Med* **17:** 1602–1609.

377. Berger A. 2000. Th1 and Th2 responses: what are they? *BMJ* **321:** 424.

378. Pilette C, Ouadrhiri Y, Van Snick J, Renauld JC, Staquet P, Vaerman JP, Sibille Y. 2002. IL-9 inhibits oxidative burst and TNF-alpha release in lipopolysaccharide-stimulated human monocytes through TGF-beta. *J Immunol* **168:** 4103–4111.

379. Pilette C, Ouadrhiri Y, Van Snick J, Renauld JC, Staquet P, Vaerman JP, Sibille Y. 2002. Oxidative burst in lipopolysaccharide-activated human alveolar macrophages is inhibited by interleukin-9. *Eur Respir J* **20:** 1198–1205.

380. Wolf JE, Massof SE. 1990. *In vivo* activation of macrophage oxidative burst activity by cytokines and amphotericin B. *Infect Immun* **58:** 1296–1300.

381. Unanue ER. 1984. Antigen-presenting function of the macrophage. *Annu Rev Immunol* **2:** 395–428.

382. Allen PM, Unanue ER. 1984. Antigen processing and presentation by macrophages. *Am J Anat* **170:** 483–490.

383. Kaul D, Ogra PL. 1998. Mucosal responses to parenteral and mucosal vaccines. *Dev Biol Stand* **95:** 141–146.

384. Halliwell B, Aruoma OI. 1991. DNA damage by oxygen-derived species. Its mechanism and measurement in mammalian systems. *FEBS Lett* **281:** 9–19.

385. Knox KW, Wicken AJ. 1973. Immunological properties of teichoic acids. *Bacteriol Rev* **37:** 215–257.

386. Hutton ML, Mackin KE, Chakravorty A, Lyras D. 2014. Small animal models for the study of *Clostridium difficile* disease pathogenesis. *FEMS Microbiol Lett* **352:** 140–149.

387. Uematsu S, Fujimoto K, Jang MH, Yang BG, Jung YJ, Nishiyama M, Sato S, Tsujimura T, Yamamoto M, Yokota Y, Kiyono H, Miyasaka M, Ishii KJ, Akira S. 2008. Regulation of humoral and cellular gut immunity by lamina propria dendritic cells expressing Toll-like receptor 5. *Nat Immunol* **9:** 769–776.

388. Denning TL, Wang YC, Patel SR, Williams IR, Pulendran B. 2007. Lamina propria macrophages and dendritic cells differentially induce regulatory and interleukin 17-producing T cell responses. *Nat Immunol* **8:** 1086–1094.

389. Christ AD, Blumberg RS. 1997. The intestinal epithelial cell: immunological aspects. *Springer Semin Immunopathol* **18:** 449–461.

390. Drudy D, O'Donoghue DP, Baird A, Fenelon L, O'Farrelly C. 2001. Flow cytometric analysis of *Clostridium difficile* adherence to human intestinal epithelial cells. *J Med Microbiol* **50:** 526–534.

391. Tontini M, Berti F, Romano MR, Proietti D, Zambonelli C, Bottomley MJ, De Gregorio E, Del Giudice G, Rappuoli R, Costantino P; Study Group, Brogioni G, Balocchi C, Biancucci M, Malito E. 2013. Comparison of CRM197, diphtheria toxoid and tetanus toxoid as protein carriers for meningococcal glycoconjugate vaccines. *Vaccine* **31:** 4827–4833.

392. Romano MR, Leuzzi R, Cappelletti E, Tontini M, Nilo A, Proietti D, Berti F, Costantino P, Adamo R, Scarselli M. 2014. Recombinant *Clostridium difficile* toxin fragments as carrier protein for PSII surface polysaccharide preserve their neutralizing activity. *Toxins (Basel)* **6:** 1385–1396.

393. Hapfelmeier S, Lawson MA, Slack E, Kirundi JK, Stoel M, Heikenwalder M, Cahenzli J, Velykoredko Y, Balmer ML, Endt K, Geuking MB, Curtiss R 3rd, McCoy KD, Macpherson AJ. 2010. Reversible microbial colonization of germ-free mice reveals the dynamics of IgA immune responses. *Science* **328:** 1705–1709.

394. Mayer M, James TL. 2004. NMR-based characterization of phenothiazines as a RNA binding scaffold. *J Am Chem Soc* **126:** 4453–4460.

395. Case DA, Cheatham TE 3rd, Darden T, Gohlke H, Luo R, Merz KM Jr, Onufriev A, Simmerling C, Wang B, Woods RJ. 2005. The Amber biomolecular simulation programs. *J Comput Chem* **26:** 1668–1688.

396. Kirschner KN, Yongye AB, Tschampel SM, González-Outeiriño J, Daniels CR, Foley BL, Woods RJ. 2008. GLYCAM06: a generalizable biomolecular force field. Carbohydrates. *J Comput Chem* **29:** 622–655.

397. Pettersen EF, Goddard TD, Huang CC, Couch GS, Greenblatt DM, Meng EC, Ferrin TE. 2004. UCSF Chimera–a visualization system for exploratory research and analysis. *J Comput Chem* **25:** 1605–1612.

398. Sigurskjold BW, Altman E, Bundle DR. 1991. Sensitive titration microcalorimetric study of the binding of *Salmonella* O-antigenic oligosaccharides by a monoclonal antibody. *Eur J Biochem* **197:** 239–246.

399. Sigurskjold BW, Bundle DR. 1992. Thermodynamics of oligosaccharide binding to a monoclonal antibody specific for a *Salmonella* O-antigen point to hydrophobic interactions in the binding site. *J Biol Chem* **267:** 8371–8376.

400. Bundle DR, Eichler E, Gidney MA, Meldal M, Ragauskas A, Sigurskjold BW, Sinnott B, Watson DC, Yaguchi M, Young NM. 1994. Molecular recognition of a *Salmonella* trisaccharide epitope by monoclonal antibody Se155-4. *Biochemistry* **33:** 5172–5182.

401. Evans SV, Sigurskjold BW, Jennings HJ, Brisson JR, To R, Tse WC, Altman E, Frosch M, Weisgerber C, Kratzin HD, Klebert S, Vaesen M, Bitter-Suermann D, Rose DR, Young MN, Bundle DR. 1995. Evidence for the extended helical nature of polysaccharide epitopes. The 2.8 Å resolution structure and thermodynamics of ligand binding of an antigen binding fragment specific for α-(2$\rightarrow$8)-polysialic acid. *Biochemistry* **34:** 6737–6744.

402. Harris SL, Craig L, Mehroke JS, Rashed M, Zwick MB, Kenar K, Toone EJ, Greenspan N, Auzanneau FI, Marino-Albernas JR, Pinto BM, Scott JK. 1997. Exploring the basis of peptide-carbohydrate crossreactivity: evidence for discrimination by peptides between closely related anti-carbohydrate antibodies. *Proc Natl Acad Sci U S A* **94:** 2454–2459.

403. Pitner JB, Beyer WF, Venetta TM, Nycz C, Mitchell MJ, Harris SL, Mariño-Albernas JR, Auzanneau FI, Forooghian F, Pinto BM. 2000. Bivalency and epitope specificity of a high-affinity IgG3 monoclonal antibody to the *Streptococcus* group A carbohydrate antigen. Molecular modeling of a Fv fragment. *Carbohydr Res* **324:** 17–29.

404. Nguyen HP, Seto NO, MacKenzie CR, Brade L, Kosma P, Brade H, Evans SV. 2003. Germline antibody recognition of distinct carbohydrate epitopes. *Nat Struct Biol* **10:** 1019–1025.

405. Chames P, Van Regenmortel M, Weiss E, Baty D. 2009. Therapeutic antibodies: successes, limitations and hopes for the future. *Br J Pharmacol* **157:** 220–233.

406. Reichert JM, Rosensweig CJ, Faden LB, Dewitz MC. 2005. Monoclonal antibody successes in the clinic. *Nat Biotechnol* **23:** 1073–1078.

407. Jones PT, Dear PH, Foote J, Neuberger MS, Winter G. 1986. Replacing the complementarity-determining regions in a human antibody with those from a mouse. *Nature* **321:** 522–525.

408. McCafferty J, Griffiths AD, Winter G, Chiswell DJ. 1990. Phage antibodies: filamentous phage displaying antibody variable domains. *Nature* **348:** 552–554.

409. Hoogenboom HR, Chames P. 2000. Natural and designer binding sites made by phage display technology. *Immunol Today* **21:** 371–378.

410. Vaccaro C, Zhou J, Ober RJ, Ward ES. 2005. Engineering the Fc region of immunoglobulin G to modulate *in vivo* antibody levels. *Nat Biotechnol* **23:** 1283–1288.

411. Shearman DJ, Parkin DM, McClelland DB. 1972. The demonstration and function of antibodies in the gastrointestinal tract. *Gut* **13:** 483–499.

412. Green SJ, Brendsel J. 2006. Could the GI tract be a petter portal for antibody therapy? *Gut* **55:** 1681–1682.

413. Mane V, Muro S. 2012. Biodistribution and endocytosis of ICAM-1-targeting antibodies versus nanocarriers in the gastrointestinal tract in mice. *Int J Nanomedicine* **7:** 4223–4237.

414. Alexander J, del Guercio MF, Maewal A, Qiao L, Fikes J, Chesnut RW, Paulson J, Bundle DR, DeFrees S, Sette A. 2000. Linear PADRE T helper epitope and carbohydrate B cell epitope conjugates induce specific high titer IgG antibody responses. *J Immunol* **164:** 1625–1633.